STUDIES ON DETECTION AND DOSIMETRY OF IRRADIATED FOOD BY THERMOLUMINESCENCE (TL) AND ELECTRON PARAMAGNETIC RESONANCE (EPR) SPECTROSCOPY

By

BHASKAR SANYAL

Bhabha Atomic Research Centre, Mumbai

A thesis submitted to the
Board of Studies in Life Science Discipline

In partial fulfillment of requirements
For the degree of

DOCTOR OF PHILOSOPHY

of

HOMI BHABHA NATIONAL INSTITUTE

July, 2011

Homi Bhabha National Institute

Recommendations of the Viva Voce Board

As members of the Viva Voce Board, we certify that we have read the dissertation prepared by Bhaskar Sanyal entitled "Studies on detection and dosimetry of irradiated food by thermoluminescence (TL) and electron paramagnetic resonance (EPR) spectroscopy" and recommend that it may be accepted as fulfilling the dissertation requirement for the Degree of Doctor of Philosophy.

M V Hosur — **Date:** 22/03/2012

Chairman- Dr. M. V. Hosur

A K Sharma — **Date:** 22/03/2012

Guide / Convener- Dr. A. K. Sharma

K V R Murthy — **Date:** 22/03/2012

External Examiner- Dr. K. V. R. Murthy

Y S Mayya — **Date:** 22/03/2012

Member 1- Dr. Y. S. Mayya

M Sheshadri — **Date:** 22/03/2012

Member 2- Dr. M. Sheshadri

V Natarajan — **Date:** 22/03/2012

Member 3- Dr. V. Natarajan

Final approval and acceptance of this dissertation is contingent upon the candidate's submission of the final copies of the dissertation to HBNI.

I hereby certify that I have read this dissertation prepared under my direction and recommend that it may be accepted as fulfilling the dissertation requirement.

Date: 22/03/2012

Place: FTD, BARC, Mumbai

A K Sharma

(Dr. A. K. Sharma)
Research Guide

STATEMENT BY AUTHOR

This dissertation has been submitted in partial fulfillment of requirements for an advanced degree at Homi Bhabha National Institute (HBNI) and is deposited in the Library to be made available to borrowers under rules of the HBNI.

Brief quotations from this dissertation are allowable without special permission, provided that accurate acknowledgement of source is made. Requests for permission for extended quotation from or reproduction of this manuscript in whole or in part may be granted by the Competent Authority of HBNI when in his or her judgment the proposed use of the material is in the interests of scholarship. In all other instances, however, permission must be obtained from the author.

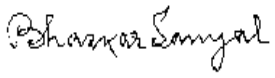

(Bhaskar Sanyal)

DECLARATION

I, hereby declare that the investigation presented in the thesis has been carried out by me. The work is original and has not been submitted earlier as a whole or in part for a degree / diploma at this or any other Institution / University.

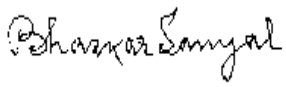

Bhaskar Sanyal

DEDICATIONS

I dedicate this thesis to my beloved wife ***Poulomi*** *who has been a great source of motivation and inspiration.*

I also dedicate this thesis to my ***Ma*** *and* ***Babai*** *for instilling the importance of hard work, sincerity and higher education.*

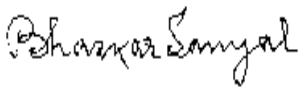

Bhaskar Sanyal

ACKNOWLEDGEMENTS

I wish to thank my research guide **Dr. Arun Kumar Sharma**, Outstanding Scientist, Head, Food Technology Division, Bhabha Atomic Research Centre and Senior Professor, Homi Bhabha National Institute for his constant guidance, suggestions and critical evaluation of the thesis. Without his support this work would not have taken the present shape.

I would like to express my gratitude to all the members of my doctoral committee namely **Dr. M. V. Hosur**, Outstanding Scientist, Solid State Physics Division and Chairman, Doctoral Committee, **Dr. M. Sheshadri**, Head, Radiation Biology and Health Safety Division, **Dr. Y. S. Mayya**, Head, Radiological Physics and Advisory Division and **Dr. V. Natarajan**, Scientific Officer (H), Radiochemistry Division, Bhabha Atomic Research Centre for their suggestions, critical evaluation and continuous encouragement.

My sincere thanks are due to **Dr. S. P. Chawla** and **Dr. R. M. Kadam** for their cooperation, technical help and moral support. I would like to express my gratitude to **Dr. S. K. Gupta** and **Dr. A. K. Debnath** of Technical Physics and Prototype Engineering Division, BARC for their cooperation in SEM / EDX scan of the samples.

My sincere thanks are due to **Dr. A. K. Tyagi**, Chemistry Division, BARC for his cooperation in carrying out XRD of the samples. I am also thankful to **Dr. A. K. Bakshi**, RPAD, BARC for helping in TL studies by preparing TL phosphor.

I take this opportunity to thank all the staff members of FTD for their cooperation.

I am thankful to all my friends for their help and moral support throughout this project.

I am indebted to my parents, my wife **Poulomi**, my son **Arkoprobho** and other family members for their cooperation, encouragement, understanding and moral support needed for completion of this thesis.

.....Bhaskar

CONTENTS

	Page No.
SYNOPSIS	**1 - 17**
LIST OF FIGURES	**18 - 25**
LIST OF TABLES	**26 - 27**
CHAPTER 1 (Introduction)	**28 - 49**
CHAPTER 2 (Literature survey)	**50 - 60**
CHAPTER 3 (Experimental procedures)	**61 - 75**
CHAPTER 4 (Identification of irradiated Basmati rice and soybean)	**76 - 99**
CHAPTER 5 (Identification of irradiated potato, ginger, turmeric and dog feed)	**100 - 122**
CHAPTER 6 (Identification of irradiated cashew nut, shrimp and medicinal plant products)	**123 - 149**
CHAPTER 7 (TL and EPR studies of TL phosphors for food irradiation dosimetry)	**150 - 170**
CHAPTER 8 (Summary & Conclusion)	**171 - 179**
REFERENCES	**180 – 194**
PUBLISHED PAPERS	

SYNOPSIS

Food irradiation is the treatment of food by ionizing radiation. The process involves exposing food, either packaged or in bulk, to carefully controlled doses of ionizing radiation for a specific time to achieve certain desirable objectives. In 1980, A Joint Expert Committee of Food and Agriculture Organization / International Atomic Energy Agency / World Health Organization on Food Irradiation (JECFI) [1] concluded "The irradiation treatment of any food commodity up to an overall average dose of 10 kGy present no toxicological hazard; toxicological testing of foods so treated is no longer required." As a consequence, food irradiation is now legally accepted in many countries.

The need for reliable and routine tests to determine whether or not food has been irradiated has arisen as a result of the progress made in commercialization of the food irradiation technology, increased international trade in irradiated foods, differing regulations relating to the use of the technology in many countries, and consumer demand for clear labeling of the treated food. It is presumed that the availability of such tests would help strengthen national regulations on irradiation of specific foods, and enhance consumer confidence in such regulations. The availability of reliable identification methods would be of assistance in establishing a system of legislative control, and help to achieve acceptance of irradiated foods by consumers. In fact, an International Conference on Acceptance, Control of, and Trade in Irradiated Food held in Geneva in 1988 recommended that "governments should encourage research into methods of detection of irradiated foods so that administrative control of irradiated food, once it leaves the facility, can be supplemented by additional means of enforcement, thus facilitating international trade and reinforcing consumer confidence in the overall process" [2].

The effectiveness of processing of food by ionizing radiation depends on proper delivery of absorbed dose and its reliable measurement. For food destined for international trade, it is of utmost importance that the dosimetry techniques used for dose determination are carried out

accurately and that the process is monitored in accordance with the internationally accepted procedures. Correct application of dosimetry to radiation processing of food is an important issue [3]. Finding a single dosimeter system covering the full range of food irradiation from 10 Gy to 10 kGy is a challenging proposition. External influences such as the temperatures of dose measurement and accuracy in a rather narrow dose range are the other problems that confront dosimetry.

An attempt has been made to study the identification methodology of irradiated foods with commercially relevant doses based on physical methods namely, Thermoluminescence (TL) measurements and Electron Paramagnetic Resonance (EPR) spectroscopy. In case of measurements of absorbed dose, investigations were carried out to understand the mechanism of modified $CaSO_4$ based thermoluminescence phosphors by TL-EPR correlation studies and to find out the efficacy of the phosphor as a food irradiation dosimeter.

Chapter 1 of the thesis introduces the subject of identification of irradiated foods using EPR spectroscopy and TL measurements. Detailed working principles of EPR spectroscopy and TL technique are discussed. Based on the review of available literature on the identification of irradiated foods, it was found that there was an increasing interest in extending the EPR methodology to various types of food. The main problem lies in the instability of the relatively weak radiation specific signals. A negligible change in food commodities after radiation treatment makes the identification of irradiated food an extremely challenging task and the statistical safety margin is rather small. Therefore, one method alone is not reliable enough for the detection of a treatment by ionizing radiation. Thermoluminescence (TL) is a radiation specific phenomenon and a suitable technique for detection of irradiated foods from which inorganic components can be isolated. Food commodities studied for the detection of irradiation are selected from the approved list of food items and allied products for commercial radiation processing in India (Table1).

Evaluation of absorbed dose at low temperatures in frozen or chilled food using a cost effective and simple dosimetry system is also a challenging task. As a consequence there is interest for new dosimetry systems with improved performances. Thermoluminescence dosimeters are widely employed for personnel and environmental dosimetry, but rarely for application at higher doses. In radiation processing of food, a large number of food items namely seafood, Ready to Cook (RTC) fruits and vegetables are required to be processed by ionizing radiation at chilled (0±4ºC) or frozen (-20±2ºC) temperature in the dose range of 1 to 4 kGy.

Consequently, the following problems were identified for investigation in this thesis.

a) Nature of radiation induced paramagnetic centres formed after irradiation with commercially approved radiation dose for foods under study
b) Relaxation behavior and thermal characteristics of the paramagnetic centres to obtain clue of radiation processing with commercially relevant doses after prolonged storage
c) Compositional analysis of the polyminerals isolated from irradiated foods and possibility of employing TL technique to identify them
d) Standardization of the procedure for isolation of inorganic components from foods and TL measurements
e) Understanding TL properties of $CaSO_4$ based phosphor and its efficacy for use as food irradiation dosimeter

Table 1. The food commodities studied

Name of the food	Purpose	Dose (kGy)	
		Min	Max
Potato	Sprout inhibition	0.06	0.15
Ginger, Fresh turmeric	Sprout inhibition	0.03	0.15
Rice	Insect disinfestation	0.25	1.0
Cashew nut	Insect disinfestation	0.25	1.0
Aswagandha, Amla, Turmeric and Guduchi	Microbial decontamination	6.0	14.0
Soybean	Insect disinfestation	0.25	1.0
Shrimp	Shelf-life extension under refrigeration	1.0	3.0
Dog feed	Microbial decontamination	6.0	14.0

Chapter 2 of the thesis presents a review of the literature available on the various aspects of identification of irradiated foods using EPR spectroscopy and TL measurements, and a detailed survey of the available literatures on high dose measurements by TL phosphor.

Several detection methods have been developed for identification of irradiated foods [4]. Among them, EPR spectroscopy and thermoluminescence detection are the two leading techniques. For use in detection, radiation induced EPR signals in food must fulfill several requirements, i.e. they must be stable or fairly stable during the usual storage period of the foodstuff and must be clearly distinguishable from the background signals of the non-irradiated sample [5]. Three European standards for detection of irradiated food by EPR spectroscopy have been released by European Committee of Normalization (CEN) and adopted by Codex Alimenterius Commission as Codex Standards. These pertain to food containing bone [6], cellulose [7] and crystalline sugar [8]. Recently, for extending the applicability of EPR to identify irradiated food, a new approach based on thermal treatment and EPR saturation has been used when the radiation induced signals have disappeared due to long period of time elapsed after treatment [9, 10]. Thermoluminescence (TL) is a radiation

specific phenomenon that arises due to energy stored by trapped charge carriers following irradiation [11]. TL has been tested for detection of spices and herbs and was adopted as a standard method for detecting irradiated foods from which silicate minerals can be isolated [12]. Therefore, extension of TL measurement of inorganic component from irradiated foods assumes importance.

International trade in irradiated food is expanding. Irradiation as a quarantine treatment of fresh fruits and vegetables and as a method to ensure hygienic quality of food of animal origin is increasingly accepted and applied. International trade in these commodities is highly likely in the near future. TL phosphors can be used for dose measurement during food irradiation using simple read out methods [13, 14]. In case of LiF: Mg,Cu,P phosphor, the shifting of intensity maximum towards lower temperature with decreasing temperatures of irradiation was reported by Ramos–Bernel et.al, 2002 [14]. In case of CaSO4: Dy phosphor, it is reported that the thermal treatment in the range of 400 – 700ºC enhances the response of high temperature peak [15]. In order to investigate the role of radiation induced paramagnetic centers in TL glow and the cause of sensitization of low temperature peak, a TL-EPR correlation study was carried out. The thesis describes the results of the studies on the effects of low temperature irradiation of commercial and thermally treated $CaSO_4$: Dy (0.2 mol %) phosphor. Energy transfer mechanism from one dopant (sensitizer) to another (luminescent center) is sometimes used to enhance the sensitivity of a phosphor. Earlier, several researchers have tried to sensitize TL phosphor by co-doping with different rare earth metals [16]. Bi^{3+} is a heavy metal with $7s^2$ electronic configuration and is known for its fluorescence properties [17, 18]. It is an interesting co-dopant ion, capable of transferring energy to rare earth ions such as Eu^{3+} [19]. In view of this, TL-EPR correlation study on gamma irradiated $CaSO_4$:Bi^{3+}, $CaSO_4$:Dy^{3+}, Bi^{3+} was carried out for possible explanation of the observed TL characteristics.

The efficacy of the Bi^{3+} co-doped $CaSO_4$: Dy phosphor to measure food irradiation dose in the range of 1 to 5 kGy was studied.

Chapter 3 of the thesis describes the experimental setup and procedures. Irradiation was carried out using a cobalt-60 irradiator (GC 5000, Board of Radiation and Isotope Technology, Mumbai, India) at FTD, BARC, Mumbai. The determination of the absorbed dose for the calibration of the gamma chamber was carried out using Fricke reference standard dosimeters [20]. The dosimeters were placed throughout the irradiation volume of the chamber and a Dose Uniformity Ratio (DUR = D_{max} / D_{min}) of 1.21 was observed. EPR measurements were performed using a BRUKER EMX spectrometer (BRUKER, Gemany). All spectra were recorded after 3 accumulated scans at the ambient temperature of EPR laboratory (27°C). EPR spectra simulation studies were carried out using WIN EPR and Simfonia programme (BRUKER). In order to determine the electron relaxation behavior of radicals in food samples, the microwave field strength was varied between 0.06 – 50 mW to obtain progressive saturation behavior (PSB). The position of the radiation induced EPR signal was compared with that of the standard 2, 2, diphenyl-1-picrylhydrazyl (DPPH) with g = 2.0032.

For separation of minerals and organic materials from the food, European Standards EN 1788, 1996 was followed. The important procedures involved in sample preparation for TL analysis were standardized. Thermoluminescence analysis was carried out using a TL 1009I Reader (Nucleonix Systems, India). Nitrogen was flushed in the heating chamber to reduce spurious TL arising due to the presence of oxygen. The initial temperature was 40ºC, which was increased to 320ºC by linear heating at a rate of 5ºC/s. After measurement of glow 1, the discs with the deposited mineral were irradiated with a normalization radiation dose followed by TL measurement of glow 2 with the similar instrumental settings. Scanning Electron Microscopy and Energy Dispersive X-ray Spectrometer analysis (SEM/EDX) were carried

out to determine the poly-mineral composition of the isolated minerals. The electron microscopic analysis was done with TESCAN, Czechoslovakia and EDX, INCA x–sisht, Oxford, U.K. with secondary electron detector.

In order to carry out TL–EPR correlation study of TL phosphors (CaSO4: Dy and CaSO4: Dy, Bi), polycrystalline $CaSO_4$:Dy (0.2 mol %) prepared and marketed by Renentech Laboratory Private Ltd, Mumbai, India were used. $CaSO_4:Bi^{3+}$, $CaSO_4:Dy^{3+}$, Bi^{3+} and $CaSO_4:Dy^{3+}$ phosphors were prepared by re-crystallization method following the recipe of Yamahashita [21]. The concentration of Dy was 0.05 mol%, while the concentration of Bi was 0.05, 0.2 and 0.5 mol%. Pre-irradiation thermal treatment of commercial CaSO4: Dy phosphor was carried out using a furnace at 700-900°C. Phosphor were exposed to gamma radiation from a cobalt 60 source at room temperature, chilling temperature (0±4ºC), freezing temperature (-10±2ºC) and liquid nitrogen temperature (-196ºC). Electron Paramagnetic Resonance (EPR) study was carried out using EMX model EPR spectrometer (BRUKER, Germany) with a microwave frequency of 9.42 GHz. EPR spectra were obtained at liquid nitrogen temperature (-196°C) and from room temperature (25°C) to 300°C in step of 50º using in situ nitrogen gas heating assembly BVT 3000 of BRUKER.

Chapter 4 of the thesis presents the identification of irradiated Basmati rice and soybean. Two independent physical methods, EPR spectroscopy and Thermoluminescence (TL) detection were employed for detection of irradiation treatment on Basmati rice. EPR investigation of 0.5 – 2 kGy irradiated rice samples showed a short lived, asymmetric, dose dependent spectrum (g = 2.005), characterized by the radicals of irradiated starch. However, this signal disappeared with time. The present work explores the possibility of identifying irradiated rice by the relaxation characteristics and thermal behavior of the radicals. This study reports for the first time that the differences in microwave saturation behavior of the signal (g = 2.004) in irradiated and non-irradiated rice samples could be an important clue to

identify radiation treatment beyond the period when the radiation specific EPR spectral lines have disappeared. TL investigation involving Scanning Electron Microscopy/Energy Dispersive X ray analysis (SEM/EDX) of the polyminerals isolated from the rice samples allowed to discriminate clearly between irradiated and nonirradiated samples even after a prolonged period of storage.

In order to identify irradiated soybean, samples were exposed to gamma radiation within the commercially permitted dose range 0.25 – 1 kGy, in a step of 0.25 kGy for insect disinfestation of food. Immediately after irradiation EPR spectrum of skin part of soybean showed a triplet signal (g = 2.0046, hyperfine coupling constant hfcc = 3 mT) superimposed on naturally present singlet. These signals were characterized as cellulose and phenoxyl radicals using EPR spectrum simulation technique. Kernel part of the samples exhibited a short-lived, radiation-induced singlet of carbon centered radical superimposed on naturally present sextet signal of Mn^{2+}. A detailed study on relaxation and thermal behavior of induced radicals in skin part were carried out using EPR spectroscopy. The findings revealed that progressive saturation and thermal characteristics of the induced radicals may be the most suitable parameters to distinguish irradiated soybean subjected to radiation dose as low as 0.25 kGy from thermally treated and non-irradiated samples, even after a prolonged period of storage.

Chapter 5 of the thesis presents studies on identification of irradiated potato, ginger, fresh turmeric and dog feed. The identification of irradiated potato of different geographical location was carried out using TL technique. Minerals were isolated from potato by density separation method and characterized by X-Ray diffraction (XRD) technique. The relative abundance of K-feldspars ($KAlSi_3O_8^-$) and quartz (SiO_2) was predominant in potato of all geographical locations under study. These minerals were responsible for TL glow after irradiation. TL glows were recorded from room temperature to 350°C at a heating rate of

5°C/s. The intensities of the glow curves for both nonirradiated and irradiated samples showed significant difference even after a storage period of one month. The ratio of glow 1 / glow 2 for nonirradiated samples was 0.003±0.0005 and for irradiated samples was 0.25±0.052. The results of the present study revealed that isolation of polyminerals from the surface of potato was possible using density separation and TL measurement can clearly differentiate between irradiated and nonirradiated samples. TL investigation on ginger and turmeric with their TL glows before and after irradiation was also carried out. Reirradiation was attempted to obtain the glow in order to confirm the treatment identification.

For identification of irradiated dog feed a detailed analysis of the radiation induced radical species and thermoluminescence measurements of isolated minerals from irradiated samples were carried out. The EPR spectrum of non-irradiated dog feed was characterized by singlet g = 2.0047±0.0003. Irradiated samples exhibited a complex EPR spectrum. During high power (50 mW) EPR spectroscopy, a visible change in the shape of the EPR spectrum was observed and characterized by EPR spectrum simulation technique. An axially symmetric anisotropic signal with $g_{\parallel}$ = 2.0028 and $g_{\perp}$= 1.9976 was identified. However, a negligible change in the matrix of irradiated edible dog chew was observed using EPR spectroscopy. Therefore, thermoluminescence study of the isolated minerals from dog chew was carried out. The composition of the polyminerals was studied using SEM and EDX analysis and a complete verdict on identification of irradiation was possible.

Chapter 6 of the thesis presents the EPR studies on cashew nut, shrimp and medicinal plant products. Cashew nut samples were irradiated at gamma radiation doses 0.25, 0.5, 0.75 and 1 kGy, the permissible dose range for insect disinfestation of food commodities. A weak and short-lived triplet (g = 2.004 and hfcc = 3 mT) along with an anisotropic signal ($g_{\perp}$ =2.0032 and $g_{\parallel}$= 2.000) were produced immediately after irradiation. These signals were assigned to that of cellulose and CO_2^- radical ion. The nature of the free radicals formed during

conventional processing such as thermal treatment was investigated and showed an increase in intensity of the central line (g = 2.0045) similar to that of irradiation. Characteristics of the free radicals were studied by their relaxation and thermal behaviors. The present work explores the possibility of identifying irradiated cashew nut from nonirradiated ones by the thermal behaviors of the radicals beyond the period when the characteristic EPR spectral lines of the cellulose free radicals have essentially disappeared. In addition, this study first time reports that relaxation behavior of the radicals could be a useful tool to distinguish between roasted and irradiated cashew nut.

For detection of irradiation on shrimp, the intestinal grits were isolated from the nonirradiated and irradiated samples by alkaline hydrolysis followed by density separation. For all irradiated samples, the areas under glow 1 were 30 to 35 times higher compared to that of nonirradiated samples. Higher values of glow 1 in irradiated samples have been reported in previous studies on spices and herbs [11]. All irradiated samples were characterized by glow peak at 225°C±6.5°C. Normalization by reirradiation at 1 kGy (glow 2) enhanced the detection results. The ratio of areas for glow 1/glow 2 determined for nonirradiated shrimp was 0.009±0.002, while for irradiated shrimp it was 0.678±0.025. Possibility of identification of irradiated and cooked shrimps at three different temperatures such as 80, 100 and 120°C was also studied. The detection of cooked and irradiated shrimps was successfully done directly from the TL glows of the samples. EPR investigation of the shell isolated from the nonirradiated and irradiated shrimps was also tried. However, no change in EPR spectrum was observed within the commercially important radiation dose 3 – 4 kGy for the irradiation of shrimp using the chitin shell. However, an axially symmetric signal was observed in EPR spectrum of the sample subjected to gamma irradiation at > 8 kGy.

A study on identification of gamma-irradiated medicinal herbs was carried out by investigating radiation induced free radicals produced using EPR spectroscopy. Indian

medicinal herbs namely Aswagandha (*Withania somnifera*), Vairi (*Salacia reticulata*), amla (*Emblica officinalis*), turmeric (*Curcuma longa*) and Guduchi (*Tinospora cordifolia*) exhibited a weak singlet signal at g = 2.005 before irradiation. Aswagandha immediately after radiation treatment revealed a complex EPR spectrum and exhibited change in shape of the spectrum during prolonged storage. Other medicinal herbs did not show any change in shape of EPR spectra after irradiation. Relaxation characteristics and thermal behavior of the induced radicals were studied but no clue of radiation treatment was observed. However, the irradiated spectrum of Aswagandha was characterized by EPR spectrum simulation technique and identified as superposition of two paramagnetic centres. One was carbohydrate radical and the other anisotropic signal ($g_{\parallel}$ = 2.0023 and $g_{\perp}$ = 1.9988) was possibly of CO_2^- radical. The kinetics of the signals were studied and proposed as a new marker for identification of irradiation even after a long storage time.

Chapter 7 of the thesis represents the TL and EPR studies of TL phosphors ($CaSO_4$: Dy and $CaSO_4$: Dy, Bi) to investigate the efficacy in measurement of food irradiation dose.

The effect of sub-ambient temperatures of irradiation and dose response of $CaSO_4$: Dy phosphor was investigated. The irradiation dose in the range of 0.5 to 7 kGy was chosen to meet the requirement of commercial food irradiation at low temperature. Commercially available phosphor showed no significant change in glow curve structure with low temperature of irradiation. In order to enhance the sensitivity of the low temperature glow peak (142°C), the phosphor was subjected to different post preparation thermal treatments at 700 to 900°C. The change in glows and improvement in dose response characteristics were explained by EPR spectroscopy. At sub-ambient temperature of irradiation, the behavior of thermally treated $CaSO_4$: Dy phosphor with increasing dose revealed improved linear response of the low temperature glow peak and could be an efficient dosimetry system for food commodities irradiated at low temperatures.

$CaSO_4$: Dy, $CaSO_4$: (Dy, Bi) and $CaSO_4$: Bi phosphors were prepared through re-crystallization method. Thermoluminescence (TL) characteristics of these phosphor samples were investigated. The radiation induced radical ions formed in these phosphors were investigated using EPR spectroscopy. The main signals observed in both $CaSO_4$: (Dy, Bi) and $CaSO_4$: Bi were identified as SO_4^- (∥), SO_4^- (⊥) and SO_3^- (isotropic) with "g" values 2.023, 2.0089 and 2.004, respectively. In order to understand the TL mechanism, $CaSO_4$: (Dy, Bi) phosphor samples were annealed at temperatures between 100 - 250°C and their EPR spectra were studied. It was observed that EPR signal intensities reduce drastically in 250°C annealed phosphor confirming the role of SO_4^- and SO_3^- types of defect centers in the dosimetric peak. The reduction in the TL sensitivity with increase in Bi^{3+} co-dopant in the phosphor samples was correlated with quenching of TL by Bi^{3+} ions rather than the reduction in the concentration of the above defect centers. An effort was made to use the Bi^{3+} co-doped $CaSO_4$: Dy phosphor for dosimetry of chilled or frozen food during irradiation.

Chapter 8 presents the summary and conclusions of the thesis. Based on the above studies the following conclusions have been made.

a) EPR spectroscopy was useful in identifying irradiated food commodities even after a prolonged storage. Studying thermal behavior and relaxation characteristics of the paramagnetic centres was of particular interests.

b) EPR spectral characteristics also provided clue to radiation treatment in many food commodities even after long storage. However, in case of many food samples detection of radiation treatment was not possible using EPR method alone.

c) TL technique provided promising results even after a long period of storage, but, involved tedious sample preparation protocol.

d) The SEM/EDX study revealed the composition of the isolated mineral from food commodities. TL glow curve structures and the ratio of the TL glows (glow1/ glow 2) were found to be successful tools to identify irradiated foods.

e) Post-preparation thermal treatments of $CaSO_4$: Dy phosphor revealed structural change in TL glow curve, exhibiting increased sensitivity of the low temperature peak. This could be exploited for the dosimetry of irradiated foods at sub-ambient temperatures.

f) The reduction in TL sensitivity and glow curve structure with an increase in Bi concentration in $CaSO_4$: (Dy, Bi) was attributed to the quenching action of Bi^{3+} ions on the TL. The study also suggested that $CaSO_4$: (Dy, Bi) (Bi concentration 0.5 mol %) can be used as a suitable dosimeter in food irradiation dosimetry.

REFERENCES

[1] FAO/IAEA/WHO (1981). Wholesomeness of Irradiated Foods, WHO, Geneva. Technical Report Series No 659.

[2] FAO/IAEA/WHO (1999). Facts about Food Irradiation. International Consultative Group on Food Irradiation (IGCFI).

[3] Bogl K. W., Regulla D. F., Suess M. J. (Eds) (1988). Health Impact, Identification, and Dosimetry of lrradiated Foods. Institut fur Strahlenhygiene des Bundesgesondheitsamtes,

Neuherberg, F.R.G., ISH-Heft-125.

[4] Chung, H. W., Delincee, H., Han, S., Hong, J., Kim, H., Kim, M., Byun, M., Kwon, J. (2004). Trials to identify irradiated chestnut (*Castanea bungena*) with different analytical techniques. *Radiation Physics and Chemistry, 71*, 179-182.

[5] Raffi, J. J., Agnel, J. L., Buscarlet, L. A., Martin, C. C. (1988). Electron spin resonance identification of irradiated strawberries. *Journal of Chemical Society Faraday*, Trans *84*(10), 3359-3362.

[6] European Standard EN 1786 (1997). Foodstuffs-detection of irradiated food containing bone: analysis by electron paramagnetic resonance. Brussels, Belgium: European Committee for Standardization.

[7] European Standard EN 1787 (2000). Foodstuffs-detection of irradiated food containing cellulose: analysis by EPR. Brussels, Belgium: European Committee for Standardization.

[8] European Standard EN 13708 (2001). Foodstuffs-detection of irradiated food containing crystalline sugar: analysis by EPR. Brussels, Belgium: European Committee for Standardization.

[9] Yordanov, N. D., Aleksieva, K., Mansour, I. (2005). Improvement of the EPR detection of irradiated dry plants using microwave saturation and thermal treatment. *Radiation Physics and Chemistry*, *73*, 55-60.

[10] Yordanov, N. D., Gancheva, V. (2000). A new approach for the extension of the identification period of irradiated cellulose containing foodstuffs by EPR spectroscopy. *Applied Radiation and Isotopes*, *52*, 195-198.

[11] Sanderson, D. C. W., Carmichael, L. A., Spencer, J, Q., Naylor, J. (1996). Luminescence detection of shell fish. In C. H. McMurray, Detection methods of irradiated foods, *Cambridge: The Royal Society of Chemistry*, 139-148.

[12] European Standard EN 1788 (2001). Foodstuffs-detection of irradiated food from which silicate minerals can be isolated: method by thermoluminescence. Brussels, Belgium: European Committee for Standardization.

[13] Lewandoski, A.C., Mathur, V.K., (1996). High dose and phototransferred thermoluminescence in CaSO4, Ca SO4: Dy and CaSO4: Tm. Radiat. Prot. Dosim. 66, 213-216.

[14] Ramos-Bernal, S., Cruz, E., Negron-Mendoza, A., Bustos, E., (2002). Irradiation dose determination below room temperature. Radiat. Phys. Chem. 63, 813-815.

[15] Bakshi, A. K., Pradhan, A. S., Srivastava, K., Kolambe, D. H. (2002). New parameters of annealing and re-use of TLDs based on $CaSO_4$: Dy phosphor. Radiat. Prot. Dosimetry 100, 293-296.

[16] Lin, J., Su, Q., Wang, S., Zhang, H., (1996). Influence of crystal structure on the luminescence properties of bismuth (III), europium (III) and dysprosium (III) in Y_2SiO. J. Mater. Chem. 6, 265-269.

[17] Moncorge, R., Boulon, G., Denis, J.P. (1979). Fluorescence Properties of Bismuth doped LaPO4, J. Phys. C: Solid State Phys. 12, 1165-1171.

[18] Murata, T., Mouri, T., (2007). Matrix effect on absorption and Infrared Flurescence properties of Bi ions in Oxide glasses. J. Non-crystalline solids. 353, 2403-2407 [19] Qiang, et al, 1983.

[20] ASTM Standard, E 1026. Standard Practice for Using Fricke Reference Standard Dosimetry System

[21] Yamahashita, T., Nada, N., Omishi, H., Katimura, S. (1968). Calcium sulphate phosphor activated by rare earth. In: Proc. 2nd Int. Conf. on Luminescence Dosimetry, Gatlinburg (Springfield, VA: NTIS) CONF 680920.

List of Publication during Ph.D. work

1. **Bhaskar Sanyal**, S P Chawla, Arun Sharma. **(2011)**. An improved approach to identify irradiated dog feed by electron paramagnetic resonance study and thermoluminescence measurements. Radiation Physics and Chemistry. Vol. 80: pp of 650 – 657.
2. **Bhaskar Sanyal,** V. Natarajan, S. P. Chawla, Arun Sharma. (**2010**). TL and EPR studies of $CaSO_4$: Dy phosphor to investigate its efficacy in measurement of food irradiation dose at sub-ambient temperatures. Radiation Measurements. Vol. 45: pp of 899 – 905.
3. **Bhaskar Sanyal,** Arun Sharma. (**2009**). A new electron paramagnetic resonance method to identify irradiated soybean. Journal of Food Science. Vol. 74 Nr 8: pp of 57-64.
4. **Bhaskar Sanyal,** S. P. Chawla, Arun Sharma. (**2009**). An improved method to identify irradiated rice by EPR spectroscopy and Thermoluminescence measurements. Food Chemistry. Vol. 116 (2): pp of 526 – 534.
5. **Bhaskar Sanyal**, M. G. Sajilata., S. Chatterjee.; R. S. Singhal, P. S. Variyar, M. Y. Kamat, Arun Sharma. (**2008**). Identification of irradiated cashew nut by electron paramagnetic resonance spectroscopy. Journal of Agriculture and Food Chemistry. Vol. 56: pp of 8987-8991.
6. A.K. Bakshi, **Bhaskar Sanyal,** V J Joshi, M K Bhide, V Natarajan and Arun Sharma. (**2011**). EPR-TL correlation studies on Bi co-doped $CaSO_4$: Dy phosphor. Applied Radiation and Isotope**.** 69, pp of 254 – 260.
7. **Bhaskar Sanyal,** S. P. Chawla, Arun Sharma. (**2010**). Thermoluminescence study of isolated minerals from irradiated food. International Symposium on Luminescence Spectrometry (ISLS – 2010), Prague, Czech Republic.
8. **Bhaskar Sanyal,** S. P. Chawla, Arun Sharma. (**2008**). Identification of irradiated potato by thermoluminescence characteristics of isolated minerals. International Food Convention IFCON. 15-19, December. Mysore

LIST OF FIGURES

Figure No.	Figure caption	Page No.
Fig.1	Energy levels for a system with S=1/2 as a function of applied magnetic field. The experimentally detected first-derivative line shape dy/dB is shown.	**46**
Fig.2	Energy-level presentation of the TL process, showing the filling process of electron and hole traps and mechanism, which is responsible for thermally activated luminescence (TL). N= total concentration of electron traps with energy Ee, M= total concentration of hole traps with energy Ep.	**46**
Fig.3	Block diagram of working principle of TL reader, **b)** The aluminum discs fabricated to keep isolated minerals were shown under label 1 and the discs containing isolated minerals from food are shown under label 2, **c)** Experimental set up for TL measurement with nitrogen gas purging system.	**66**
Fig.4	**a)** Block diagram of EPR spectrometer, **b)** experimental set up for EPR spectroscopy for thermal behavior study of the paramagnetic centre. The thermal Dewar flask was installed inside the sample cavity and inlet and outlet nitrogen gas pipes were attached with appropriate greasing to avoid leakage. The gas flow rates and the temperature rise were controlled from an integrated computer.	**70**
Fig.5	EPR spectra of **a)** nonirradiated, **b)** heat treated at 100ºC, 1h, **c)** irradiated (1 kGy) rice samples, and **d)** EPR spectrum of irradiated pure starch.	**83**
Fig.6	**a)** Response of the radiation induced signal intensity of the central line (g = 2.005) with increasing radiation dose, **b)** thermal behavior of the central line of EPR spectrum for nonirradiated, irradiated (after 10 and 90 d) rice samples. Relaxation behavior of main line of non-irradiated and irradiated	**84**

(1 kGy) rice sample, **c)** 10 d after irradiation, **d)** 90 d after irradiation.

Fig.7 Kinetics of the central line of the EPR signal of nonirradiated and irradiated rice samples. **85**

Fig.8 **a)** Scanning Electron Microscopy (SEM) image, **b)** Energy Dispersive X ray (EDX) spectrum of the polyminerals extracted from rice. Feldspar: F and Quartz: Q. **88**

Fig.9 **a)** TL glow of isolated minerals from nonirradiated and irradiated rice, **b)** glow1 and glow 2 of nonirradiated sample and **c)** glow1 and glow 2 of irradiated sample. **88**

Fig.10 EPR spectra of soybean recorded at room temperature **a)** nonirradiated skin part, **b)** 1 d after radiation treatment (1 kGy) of the skin part, **c)** nonirradiated kernel part, and **d)** 1 d after radiation treatment (1 kGy) of the kernel part. **96**

Fig.11 A scheme demonstrating a simulation analysis of experimental EPR spectrum of irradiated (1 kGy) soy bean sample **a)** simulation spectrum of phenoxyl ($C_6H_5O^-$) radical, **b)** simulation spectrum of cellulose radical, **c)** linear combination of the individual spectrum represented in a and b, **d)** experimental spectrum of irradiated sample. **97**

Fig.12 Response of radiation induced signal (g = 2.0046) and dependence of double integral EPR signal intensity evaluated with increasing dose after 2 d of radiation treatment. **98**

Fig.13 **a)** Relaxation characteristics and **b)** thermal behavior of the paramagnetic centres (g = 2.0047) in irradiated (1 kGy) kernel part of soybean after 5 d of radiation treatment. **98**

Fig.14 **a)** Relaxation characteristics of the central singlet of nonirradiated, **99**

thermally treated and irradiated soybean 60 d after radiation treatment. Thermal behavior of skin part of soybean **b)** 1 d after the treatment and c) 60 d after the treatment.

Fig.15 XRD spectra of the isolated minerals from potato of different geographical locations **a)** Bankura, West Bengal, **b)** Midnapore, West Bengal, **c)** Delhi, and **d)** Mumbai. **103**

Fig.16 **a)** TL glow of isolated minerals from nonirradiated and irradiated potato, and **b)** TL glow 1 and glow 2 of the irradiated samples from Bankura district, West Bengal, **c)** TL glow of the isolated minerals from irradiated potato with increasing radiation dose. **104**

Fig.17 TL glow (glow 1) of the isolated minerals from the irradiated and nonirradiated samples of **a)** ginger, and **b)** fresh turmeric. **107**

Fig.18 Glow curve characteristics of glow 1 and glow 2 (normalized with 1 kGy) of the isolated minerals from **a)** nonirradiated ginger, **b)** irradiated (120 Gy) ginger, **c)** nonirradiated fresh turmeric and **d)** irradiated (120 Gy) fresh turmeric. **108**

Fig.19 EPR spectra of nonirradiated (control) and irradiated (7.5 kGy) ready to eat dog feed (granular form) immediately after irradiation recorded with microwave power **a)** 0.63 mW and **b)** 50.2 mW. **112**

Fig.20 Simulation scheme of the EPR spectrum of irradiated dog feed (granular form) **a)** simulated spectrum of phenoxyl radical ion ($C_6H_5O^-$), **b)** simulated spectrum of CO_2^- radical ion and **c)** simulated and experimental spectra of irradiated dog feed. **113**

Fig.21 **a)** Superposition of EPR spectra of irradiated dog feed (granular form) recorded with increasing microwave power. The inset shows progressive **114**

saturation behavior of isotropic signal at g = 2.0052 and anisotropic signal at $g_{\perp}$ = 2.0028 **b)** response of radiation induced signal (g = 2.0052) and the dependence of double integral EPR signal intensity evaluated with increasing dose after 3 d of radiation treatment.

Fig.22 **a)** EPR spectra of nonirradiated (control) and irradiated (7.0 kGy) edible dog chew (stick form) immediately after irradiation recorded with microwave power of 0.63 mW **b)** response of the radiation induced signal (g = 2.00534) and the dependence of double integral EPR signal intensity evaluated with increasing dose after 3 d of radiation treatment. **117**

Fig.23 Time kinetics of nonirradiated and irradiated samples of dog feed during storage **a)** for ready to eat granular form, **b)** edible dog chew stick form. **117**

Fig.24 **a)** Scanning Electron Microscopy (SEM) image, **b)** Energy Dispersive X ray (EDX) spectrum of the poly-minerals extracted from dog chew samples, **c)** TL glows of isolated minerals from nonirradiated (control) and irradiated (10 kGy) edible dog chew (stick form), **d)** response of the TL glows of the isolated minerals with increasing radiation doses from 2.5 to 10 kGy. **121**

Fig.25 TL glow of isolated minerals from dog chew samples **a)** glow 1 and glow 2 (normalized with 1 kGy) of nonirradiated (control) sample and **b)** glow 1 and glow 2 (normalized with 1 kGy) of irradiated (10 kGy) sample. Response of the TL glows during storage for the samples subjected to radiation doses, **c)** 2.5 kGy and **d)** 10 kGy and insets show the behavior of $P_{1height}/P_{2height}$ with increasing time. **122**

Fig.26 Ambient EPR spectra of cashew nut sample **a)** before irradiation, **b)** one day after irradiation (1 kGy). **127**

Fig.27 Response of the radiation induced signal intensity of the central line (g = **127**

2.0044) with increasing radiation dose.

Fig.28 EPR spectra after 1 d of various thermal treatments **a)** without thermal treatment, **b)** subjected to 100°C, 1h and **c)** roasted at 180°C. **128**

Fig.29 Relaxation behavior of main line of nonirradiated, irradiated (1 kGy) and roasted cashew nut **a)** 1 d after irradiation, **b)** after 45 d storage, **c)** thermal behavior of the central line of EPR spectrum for nonirradiated, irradiated (1 kGy) and roasted (180°C) cashew nut samples, **d)** kinetics of the central line of the EPR signal of nonirradiated, irradiated cashew nut samples. **132**

Fig.30 **a)** SEM image, **b)** EDX spectrum of the minerals isolated from the grits of shrimp, **c)** TL glow of the nonirradiated and irradiated samples, d) TL glow with the increasing doses, TL glow 1 and glow 2 of the samples, **e)** irradiated with 1 kGy, and **f)** irradiated with 2 kGy. **136**

Fig.31 **a)** TL glow and **b)** integral TL of the isolated minerals from shrimp of nonirradiated, nonirradiated and cooked, and irradiated and cooked at two different temperatures, **c)** EPR spectra of the nonirradiated and irradiated shrimp shell. **137**

Fig.32 **a)** EPR spectra of nonirradiated, heat treated (100 C, 1 h) and irradiated (7.5 kGy) aswagandha recorded at microwave power attenuation of 25 dB. Inset shows irradiated spectrum at high power (6 dB), **b)** EPR spectrum of irradiated (7.5 kGy) aswagandha after 90 days storage. **144**

Fig.33 Simulation scheme of EPR spectrum of irradiated aswagandha **a)** simulated spectrum of carbohydrate, **b)** simulated spectrum of CO_2^- radical ion, **c)** simulated spectrum of cellulose radical, and **d)** simulated and experimental spectra of irradiated aswagandha. **145**

Fig.34 **a)** Progressive saturation behavior of central EPR signals of nonirradiated, **146**

irradiated aswagandha and CO_2^- radical ion signal, **b)** dose dependence of central EPR line, **c)** time kinetics of nonirradiated and irradiated samples of aswagandha during storage.

Fig.35 EPR spectra of **a)** nonirradiated samples, and **b)** irradiated samples (7.5 kGy) of medicinal herbs, vairi (*Salacia reticulata*), amla (*Emblica officinalis*), turmeric (*Curcuma longa*) and guduchi (*Tinospora cordifolia*). Behaviors of nonirradiated EPR signal (g = 2.0049) and irradiated signal (g = 2.0050) of amla (*Emblica officinalis*) after a storage of 45 days, **c)** with increasing microwave power, and **d)** with increasing temperature. **149**

Fig.36 **a)** Integral TL output of commercial $CaSO_4$: Dy (0.2 mol %) irradiated at chilled (0±4°C), frozen (-10±2°C) and liquid nitrogen temperature (-196°C), **b)** TL response of $CaSO_4$:Dy (0.2 mol %) with increasing gamma dose at 0±4ºC. **157**

Fig.37 **a)** Change in high temperature peak height and low temperature peak height with gamma dose at chilled temperature for commercial $CaSO_4$:Dy (0.2 mol %) without any sensitization treatment, **b)** change in Glow curve structure after post-preparation thermal treatments at 700, 800 and 900°C. **158**

Fig.38 EPR spectra recorded at room temperature with microwave power attenuation 15 db **a)** untreated $CaSO_4$: Dy (0.2 mol %) phosphor, **b)** annealed at 700°C, **c)** annealed at 800°C, and **d)** annealed at 900°C. **159**

Fig.39 EPR spectra recorded at 77°K (-196°C) with microwave power attenuation 15 db **a)** CaSO4: Dy (0.2 mol %) phosphor, **b)** annealed at 700°C, **c)** annealed at 800°C, and **d)** annealed at 900°C. **160**

Fig.40 Response of the EPR signal intensities **a)** SO_3^-, **b)** SO_4^-, and **c)** O_3^- of **161**

untreated and annealed at 700, 800, 900°C CaSO4: Dy phosphor with increasing temperature.

Fig.41 Behavior of the TL response of the commercial and annealed (900°C) CaSO4: Dy phosphor with increasing radiation dose (at 0±4°C) **a)** low temperature peak height, and **b)** high temperature peak height. **162**

Fig.42 **a)** TL glow curves of $CaSO_4$:Dy (0.05mol%), $CaSO_4$:Dy (0.05), Bi (0.05mol%) and $CaSO_4$:Bi (0.05mol%), and **b)** glow curves of $CaSO_4$: Dy, Bi with different concentration of Bi; curve A with Bi: 0.05 mol%, curve B with Bi: 0.2 mol% and curve C with Bi: 0.5 mol%. **167**

Fig.43 **a)** EPR spectra of $CaSO_4$: (Dy, Bi) at (-196°C) with different concentration of Bi, **b)** EPR spectra of $CaSO_4$:Bi at (-196°C) with different concentration of Bi along with DPPH. **168**

Fig.44 EPR spectra of $CaSO_4$: (Dy, Bi) annealed at different temperatures **a)** Bi: 0.05 mol%, **b)** Bi: 0.02 mol %, and **c)** Bi: 0.5 mol%. Variation in peak intensity of sulphoxy radical ions with temperature for $CaSO_4$: (Dy, Bi), **d)** with Bi (0.05mol %), **e)** Bi (0.5mol %), and **f)** Bi (0.2 mol %). **169**

Fig.45 Dose response of $CaSO_4$: Dy, Bi in the dose range 1-5 kGy along with polynomial fit. **170**

LIST OF TABLES

Table No.	Table caption	Page No.
Table 1	Food items approved for radiation processing in India under PFA Act rules.	**32**
Table 2	Some requirements of an identification procedure for irradiated food.	**34**
Table 3	Potential detection methods for irradiated foods, status and products studied.	**35**
Table 4	The food commodities studied.	**49**
Table 5	Spin Hamiltonian parameters of gamma irradiated induced EPR signals observed in soybean (skin part) treated with 1 kGy dose.	**95**
Table 6	Hamiltonian parameters of the EPR signals for irradiated Aswagandha.	**143**
Table 7	Peak height ratio of high temperature peak to low temperature peak with increasing temperatures of pre-irradiation annealing.	**156**

CHAPTER 1

Introduction

Food is one of the basic necessities of life. The rate of increase in world population is much faster than the rate of food production. Therefore, production of more food and at the same time prevention of postharvest food losses is of immense importance. Developing countries of the world face an ever increasing energy crisis and hence cannot afford highly energy intensive food preservation procedures. Food irradiation, with its unique advantages, is emerging as an important method of food preservation. It is being used in more and more countries worldwide to enhance shelf life and to improve hygienic quality of raw or processed food commodities.

Food irradiation is the treatment of food by ionizing radiation. The process involves exposing food, either packaged or in bulk, to carefully controlled amounts of ionizing radiation for a specific time to achieve certain desirable objectives. It is one of the most extensive and thoroughly studied methods of food preservation. In 1980, Joint Expert Committee of Food and Agriculture Organization / International Atomic Energy Agency / World Health Organization on Food Irradiation FAO/IAEA/WHO, 1981 [1] concluded "The irradiation treatment of any food commodity up to an overall average dose of 10 kGy present no radiological, microbiological or toxicological hazard." As a result toxicological testing of foods so treated is no longer required. Food irradiation is now legally accepted in many countries. The ranges of dose commonly employed in various food irradiation applications to achieve different objectives can be classified into three groups.

Low dose applications. Low dose applications typically use a dose range of 10 Gy–1 kGy. These include inhibition of sprouting of bulbs, tubers, rhizomes and root crops by doses in the range 20–150 Gy. Physiological processes such as ripening and senescence of fruits and vegetables can be delayed by doses in range 0.1–1 kGy. Insect disinfestation can be achieved in the dose range 0.2–1 kGy to destroy quarantine insects or for preventing losses caused by

insect pests in stored grains, pulses, cereals, flour, coffee beans, spices, dried fruits and nuts, dried fishery products.

Medium dose applications. Applications at medium dose levels range between 1 – 10 kGy where, radiation enhances the keeping quality of certain foods through a substantial reduction in the number of spoilage causing micro-organisms and elimination of pathogens. Fresh meat and seafood, as well as vegetables and fruits, may be exposed to such treatments depending on the product.

High dose applications. Applications of ionizing radiation at high dose levels ranging from 10 - 100 kGy is employed to destroy microorganisms to achieve either commercial or total sterility. For example commercial sterility is achieved in spices by processing in the range of 10 - 30 kGy. Radiation sterilization in the dose range 25 - 70 kGy extends the shelf life of precooked or enzyme inactivated food products in hermetically sealed containers almost indefinitely at ambient temperature. High doses for sterilization of these products are usually delivered at very low temperature.

Approval of food irradiation in India and abroad

After the endorsement of safety of irradiated food by a joint FAO/IAEA/WHO Expert Committee on Food Irradiation (JECFI) in 1980, another group of experts was constituted by WHO in 1994 and the committee again reviewed the wholesomeness data available till then and validated the earlier conclusion. In 1998 one more expert group constituted by WHO/FAO/IAEA affirmed the safety of food irradiated to doses above 10 kGy. In view of these recommendations the Codex Committee on Food Standards of the Codex Alimentarius Commission has also revised in 2003 the Codex General Standard for Irradiated Foods that sets standards for process foods world-wide. In 1994 Government of India amended Prevention of Food Adulteration Act (1954) Rules and approved irradiation of onion, potato and spices for domestic market. Additional items were approved in April, 1998 and in May

2001 (Table 1). In 2004 the government amended plant protection and quarantine measures. Laws and regulations enacted under the Atomic Energy Act enforced by the Atomic Energy Regulatory Board, an independent body, govern operations of irradiators used to process non-food products, such as medical supplies as well as food. Many medical product irradiators are operating in India and around the world. The plants that must be approved by the government before construction and operation are subject to regular inspection, safety audits, and other reviews to ensure that they are safely and properly operated. Only those foods approved under the Prevention of Food Adulteration (PFA) Act rules can be irradiated and sold in domestic market.

Table 1. Food items approved for radiation processing in India under PFA Act rules

Name of the food	Purpose	Dose (kGy)*	
		Min	Max
Onion	Sprout inhibition	0.03	0.09
Potao		0.06	0.15
Ginger, garlic		0.03	0.15
Shallots (Small onion)		0.03	0.15
Mango	Disinfestation (Quarantine)	0.25	0.75
Rice, Semolina (rawa), Whole wheat flour (atta) and maida	Insect disinfestation	0.25	1.00
Raisins, figs and dried dates		0.25	0.75
Pulses		0.25	1.00
Dried sea-foods		0.25	1.00
Meat and meat products including chicken	Shelf-life extension and pathogen control	2.50	4.00
Fresh sea-foods	Shelf-life extension under refrigeration	1.00	3.00
Frozen sea-foods	Pathogen control	4.00	6.00
Spices	Microbial decontamination	6.00	14.00
*Gray (Gy) is SI unit of energy absorbed (1 Joule/kg) by food from ionizing radiation			

Identification of irradiated food

The need for reliable and routine methods to establish whether food has been irradiated or not arose as a result of the progress made in commercialization of food irradiation in many countries, increased international trade in irradiated foods, differing regulations relating to the use of the technology in many countries, and consumer demand for labeling of the treated product. It is envisaged that the availability of such methods would help strengthen national regulations on irradiation of specific foods, and enhance consumer confidence in such regulations. The availability of reliable identification methods would be of assistance in establishing a system of legislative control, and help achieve acceptance of irradiated foods by consumers. In fact, an International Conference on Acceptance, Control of, and Trade in Irradiated Food held in Geneva in 1988 recommended that "governments should encourage research into methods of detection of irradiated foods so that administrative control of irradiated food once it leaves the facility can be supplemented by an additional means of enforcement, thus facilitating international trade and reinforcing consumer confidence in the overall process" [2]. Originally, it was envisaged that one method applicable to all foods could be developed, but it is now accepted fact that no single method can effectively serve the wide range of food likely to be treated with ionizing radiation and several techniques will need to be actually developed. Many of the changes occurring in food products during irradiation treatment are similar to those induced by other processes, such as cooking and canning, hence in order to develop methods for identification of irradiated foods, it has to fulfill several technical criteria as shown in Table 2 [3]. In practice, it is difficult to fulfill all the requirements of an ideal method. A number of different techniques based on physical, chemical and biological changes occurring in irradiated food have been investigated in order to establish their potential as detection methods. Their current status and the products studied are shown in Table 3.

Table 2. Some requirements of an identification procedure for irradiated food

Technical criteria	
Discrimination	The parameter measured in the irradiated food should be absent in non-irradiated food. Radiation induced response should be distinct and separable
Specificity	Should not be induced by other food processing methods and storage
Applicability	Applicable throughout the dose range relevant to the irradiation of the food tested
Robustness	Insensitive or predictable response for: variation in radiation parameters (dose rate, temperature, gaseous environment etc.); presence of other food components; further processing
Independence	Should not require samples of the non-irradiated food from the particular batch tested
Reliability	Reproducible, accurate, validated
Stability	Throughout storage life
Dose-dependent proof in court	Estimation of the absorbed dose
Confidence	No falsification possible
Practical criteria	
Practicability	Simple, low cost, small sample size, rapid, non-destructive, no complicated instruments, applicable to wide range of foods, easy to standardized and cross calibrate

Reproduced from McMurray et al, 1996 [3]

Table 3. Potential detection methods for irradiated foods, status and products studied

	Method	**Product / status**
	Physical	
1	Electron Paramagnetic Resonance (EPR)	Food containing bone, cellulose, crystalline sugar
2	Thermoluminescence (TL)	Food from which silicate minerals can be isolated
3	Phtostimulated luminescence (PSL)	Foods like spices, herbs, shell fish
4	Impedance	Potato
5	Viscometry	Black and white pepper, cinnamon, allspice
	Chemical	
1	Hydrocarbons	Food containing fat
2	2-alkylcyclobutanone	Food containing fat
3	Gas evolution (H_2, CO)	Frozen shellfish, frozen chicken, peppercorns
4	Peroxides	Pork, Chicken
5	O-tyrosine	Shellfish, chicken
	Biological	
1	Germination	Citrus fruit, cherries, apples, grains
	DNA	
1	Comet assay	Chicken, pork, fish, shellfish, fruits and vegetables
2	Mitochondrial DNA	Chicken and beef, king prawns, trout
	Microbiological	
1	DEFT / APC	Spices, herbs, chicken
2	LAL	Microbiological screening for irradiated food like chicken
	Immunological	
1	Dihydrothymidine	Grains
2	Protein	Egg white

Based on Stevenson & Stewart, 1995 [4]

Food Irradiation Dosimetry

With the increasing recognition and application of irradiation as a sanitary and phytosanitary treatment of food based on the provisions of the Agreement on Application of Sanitary and Phytosanitary Measures of the World Trade Organization, international trade in irradiated food is expected to expand. Therefore, it is essential that a proper dosimetry system is employed to ensure compliance of trade in irradiated food with national and international standards. The effectiveness of processing of food by ionizing radiation depends on proper delivery of absorbed dose and its reliable measurement. For food destined for international markets, it is of utmost importance that the dosimetry techniques used for dose determination are carried out accurately and that the process is monitored in accordance with the internationally accepted procedures. Correct application of dosimetry to radiation processing of food is important [5]. Some studies are concerned with finding a single dosimeter system covering the full range of food irradiation from 10 Gy to 10 kGy. Other studies are devoted to the problems of external influences such as temperature and to the problem of increasing accuracy with which rather a narrow dose ranges can be reliably measured. In all the various guidelines and standards developed for food irradiation, the activities of principal concern are process validation and process control. The objectives of such formalized procedures are to establish documentary evidence that the irradiation process has achieved the desired results. Industrial radiation processing such as irradiation of foodstuffs and sterilization of healthcare products are both highly regulated, in particular with regard to the absorbed dose. In addition, dosimetry is necessary for scaling up processes from the research level to the industrial level. Thus, accurate dosimetry is indispensable.

The main focus of this study is to improve methodologies based on physical principles, namely, Electron Paramagnetic Resonance spectroscopy (EPR) and Thermoluminescence

(TL) techniques, in the fields of identification of irradiated foods and food irradiation dosimetry.

Electron Paramagnetic Resonance (EPR) Spectroscopy

EPR is a non-destructive spectroscopic technique used to detect and/or identify paramagnetic centres in a complex matrix such as food. The paramagnetic centres are characterized by the presence of at least one unpaired electron and can be atoms, molecules or molecular ions. An important category is radicals in solids, characterized by one unpaired electron. When a paramagnetic system is placed in a magnetic field, its energy levels split (Zeeman splitting). Radicals have two low-lying Zeeman levels corresponding to the ground state (Fig. 1). Spectroscopy in general involves measurement and interpretation of energy differences, the knowledge of which gives insight into the identity, microscopic structure and dynamics of the system under study. This energy difference ΔE can be measured because, as can be shown in quantum mechanics, electromagnetic radiation incident on a sample will be absorbed if

$$\Delta E = h\nu \qquad \text{(Eq. 1)}$$

Where, h is the Planck's constant and ν is the frequency of the radiation. The quantity $h\nu$ is, then, the energy of the incident radiation (photon or quantum).

The absorption of energy results in a transition of the system from the lower energy state to the higher energy state. In conventional spectroscopy, the frequency ν is varied (swept), and, at certain values corresponding to ΔE in Eq. (1), absorption peaks will occur, giving rise to what is called an (absorption) spectrum. A wide range of frequencies can be used to perform different types of spectroscopy (e.g., IR, UV, NMR spectroscopy). In EPR experiments, microwave radiation (ν in the gigahertz range, 10^9 s^{-1}) is used.

The g- value

EPR becomes particularly relevant when the magnetic spins are embedded in crystal lattice. The spectra then reflect the magnetic interactions in solids and the coupling of magnetism to

crystal fields and lattice vibrations. The simplest EPR system is a single electron in a vacuum. Due to the intrinsic magnetic moment of the electron the energy of the two levels, for the parallel or anti-parallel alignments, with respect to the applied magnetic field, becomes non-degenerate and dependent on the external magnetic field (Fig 1). The resonance is detected when the energy difference between the two spin states equals the energy of the applied photons (Eq 2). The ratio between magnetic field and microwave frequency or spectroscopic splitting factor (g) is given by

$$\Delta E = g_e \mu_B B_0 = h\nu \qquad \text{(Eq. 2)}$$

$$g_e = h\nu / \mu_B B_0 \qquad \text{(Eq. 3)}$$

Where, B_0 is the field of maximum absorbance, usually determined by the zero crossing in the first derivative (field modulated) spectra; μ_B is the Bohr magneton; h is Planck's constant and ν is microwave frequency. For an electron in vacuum $g_e = 2.00232$

Knowledge of the g-factor can give information about a paramagnetic center's electronic structure. An unpaired electron responds not only to a spectrometer's applied magnetic field B_0, but also to any local magnetic fields of atoms or molecules. The effective field (B_{eff}) experienced by an electron is thus written as

$$B_{eff} = B_0 (1 - \sigma) \qquad \text{(Eq. 4)}$$

where σ includes the effects of local fields (σ can be positive or negative). Therefore, the $h\nu = g_e\mu_B B_{eff}$ resonance condition (above) is rewritten as follows

$$h\nu = g_e \mu_B B_{eff} = g_e \mu_B B_0 (1 - \sigma) \qquad \text{(Eq. 5)}$$

The quantity $g_e (1 - \sigma)$ is denoted g and called simply the g-factor, so that the final resonance equation becomes

$$h\nu = g \mu_B B_0 \qquad \text{(Eq. 6)}$$

This last equation is used to determine g in an EPR experiment by measuring the field and the frequency at which resonance occurs. If g does not equal g_e the implication is that the ratio of

the unpaired electron's spin magnetic moment to its angular momentum differs from the free electron value. Since an electron's spin magnetic moment is constant (approximately the Bohr magneton), then the electron must have gained or lost angular momentum through spin-orbit coupling. Because the mechanisms of spin-orbit coupling are well understood, the magnitude of the change gives information about the nature of the atomic or molecular orbital containing the unpaired electron. For most of organic radicals and radical ions, unpaired electrons have orbital angular momentum (L) close to zero and the total electron angular momentum quantum number (J) is pretty much the spin quantum number (S). As a result, their g-values are close to 2. Situation becomes much more complicated with transition metals. Not only they have large L's and S's, but these values depend on the surrounding electric fields of ligands.

In principle, EPR spectra can be generated by either varying the photon frequency incident on a sample while holding the magnetic field constant, or doing the reverse. In practice, it is usually the frequency which is kept fixed. A collection of paramagnetic centers, such as free radicals, is exposed to microwaves at a fixed frequency. By increasing an external magnetic field, the gap between the energy states $m_s = +1/2$ and $m_s = -1/2$ is widened until it matches the energy of the microwaves, as represented by the double-arrow in the diagram above. At this point the unpaired electrons can move between their two spin states. Since there are typically more electrons in the lower state, due to the Maxwell-Boltzmann distribution, there is a net absorption of energy, and it is this absorption which is monitored and converted into a spectrum.

Maxwell-Boltzmann distribution

In practice, EPR samples consist of collections of many paramagnetic species, and not single isolated paramagnetic centers. If the population of radicals is in thermodynamic equilibrium, its statistical distribution is described by the Maxwell-Boltzmann equation:

$$n_{upper} / n_{lower} = \exp (E_{upper} - E_{lower}) / kT = \exp (-\Delta E / kT) = \exp (-h\nu / kT) \quad \text{(Eq. 7)}$$

Where n_{upper} is the number of paramagnetic centers occupying the upper energy state, k is the Boltzmann constant, and T is the temperature in kelvins. At 298 K, X-band microwave frequencies ($\nu \approx 9.75$ GHz) give $n_{upper} / n_{lower} \approx 0.998$, meaning that the upper energy level has a smaller population than the lower one. Therefore, transitions from the lower to the higher level are more probable than the reverse, which is why there is a net absorption of energy. The sensitivity of the EPR method is defined by the minimum number of detectable spins N_{min}. This depends on the photon frequency ν according to

$$N_{min} = k_1 V / Q_0 k_f \nu^2 P^{1/2} \quad \text{(Eq. 8)}$$

Where k_1 is a constant, V is the sample's volume, Q_0 is the unloaded quality factor of the microwave cavity (sample chamber), k_f is the cavity filling coefficient, and *P* is the microwave power in the spectrometer cavity. In other words, the higher the spectrometer frequency the lower the detection limit (N_{min}), and hence the greater sensitivity.

Hyperfine coupling

Since the source of an EPR spectrum is a change in an electron's spin state, it might be thought that all EPR spectra would consist of a single line. However, the interaction of an unpaired electron, by way of its magnetic moment, with nearby nuclear spins, results in additional allowed energy states and, in turn, multi-lined spectra. In such cases, the spacing between the EPR spectral lines indicates the degree of interaction between the unpaired electron and the perturbing nuclei. The hyperfine coupling constant (hfcc) of a nucleus is directly related to the spectral line spacing and, in the simplest of cases, is essentially the spacing itself.

Two common mechanisms by which electrons and nuclei interact are the Fermi contact interaction and dipolar interaction. The former applies largely to the case of isotropic interactions (independent of sample orientation in a magnetic field) and the latter to the case

of anisotropic interactions (spectra dependent on sample orientation in a magnetic field). Spin polarization is a third mechanism for interactions between an unpaired electron and a nuclear spin, being especially important for π-electron organic radicals, such as the benzene radical anion. The symbols "a" or "A" are used for isotropic hyperfine coupling constants while "B" is usually employed for anisotropic hyperfine coupling constants. For a radical having M equivalent nuclei, each with a spin of I, the number of EPR lines expected is 2MI + 1. As an example, the methyl radical, CH_3, has three ^1H nuclei each with I = 1/2, and so the number of lines expected is 2MI + 1 = 2(3) (1/2) + 1 = 4.

In real systems, electrons are normally not solitary, but are associated with one or more atoms. As a result of this there are several important consequences:

1. An unpaired electron can gain or lose angular momentum, which can change the value of its g-factor, causing it to differ from g_e. This is especially significant for chemical systems with transition-metal ions.
2. If an atom with which an unpaired electron is associated has a non-zero nuclear spin, then its magnetic moment will affect the electron. This leads to the phenomenon of hyperfine coupling, analogous to J-coupling in NMR, splitting the EPR resonance signal into doublets, triplets and so forth.
3. Interactions of an unpaired electron with its environment influence the shape of an EPR spectral line. Line shapes can yield information about, for example, rates of chemical reactions.
4. The g-factor and hyperfine coupling in an atom or molecule may not be the same for all orientations of an unpaired electron in an external magnetic field. This anisotropy depends upon the electronic structure of the atom or molecule (e.g., free radical) in question, and so can provide information about the atomic or molecular orbital containing the unpaired electron.

EPR spectrum line shape

The line shape of an EPR signal is an output of several complex factors. It may be affected by the so-called homogeneous and inhomogeneous broadening. Homogeneous broadening can be properly described only in terms of quantum mechanics. According to the Heisenberg uncertainty principle, it is related to the life times of the energy levels involved in the transitions. These life times are determined by the energy exchange between the unpaired electrons (spin system) on the one hand and the environment (lattice) on the other, or simply between the spins themselves. These two processes are characterized by the spin–lattice (T1) and spin–spin (T2) relaxation times, respectively. For organic radicals, T1 and T2 are in the ranges of 10^{-3} - 10^{-1} and 10^{-7} - 10^{-5} s, respectively. The spin–spin relaxation time of the CO_2^- radical in tooth enamel estimated from pulsed EPR measurements is in the range 500–640 ns [6]. The inhomogeneous broadening is partly due to unresolved (super) hyperfine interactions.

Thermoluminescence (TL)

Thermoluminescence is a thermally stimulated emission of light from an insulator or a semiconductor following the previous absorption of energy from ionizing radiation. The thermoluminescence process can be understood in terms of the band structure model of insulators. In a pure insulator there are two relevant energy bands: (i) an almost completely filled valence band and (ii) an almost empty conduction band. The two energy bands are separated by a forbidden gap, which means that between these two bands there are no electronic energy levels. Transitions of electrons between the valence band and the conduction band are allowed and they produce “free” electrons in the conduction band and “free” holes in the valence band. The energy difference between the two bands is denoted by the band-gap energy Eg (Fig. 2).

Imperfections in the crystal, associated with impurities and/or lattice defects may create new localized energy levels in the forbidden band gap. The positions of the energy levels depend

on the nature of the imperfections/defects and the host lattice. Some of these defects are capable of trapping an electron or a hole. Therefore, the centers are referred to as electron or hole traps and after trapping an electron or hole the new defects are called trapped electron or trapped hole centers, respectively. The most simple trapped electron center is the F-center, which is an anion vacancy in the crystal lattice after it has trapped an electron. The name 'F-center' is derived from the German word 'Farbe', which means color. When the concentration of F-centers is sufficient, the crystal absorbs sufficient light in a limited frequency range and as a result, the crystal is colored. To maintain electro-neutrality of the crystal, for each electron, which is trapped at an electron trap a hole is produced, which might be trapped at a hole trap.

TL mechanism

The complexity of the TL mechanism arises from the multi-stage nature of the conversion from the initial energy imparted by the radiation field to the final energy liberated as TL photons. These conversions occur in three stages.

a) Absorption of energy from the radiation field via the capture of charge carriers at defect trapping centres accompanied by possible creation or alteration of radiation induced-defects which participate or compete with the TL process. The various defects which have captured the charge carrier of either sign can serve as trapping centre (TCs), luminescence centre (LCs) or competitive centre (CCs). The rate filling of these types of centre is an important topic in TL phenomena.

b) Absorption of thermal energy in non-isothermal annealing (glow curve heating) which liberates the charge carriers and can also bring about changes in the trapping structures and/or their spatial correlations. Each centre is associated with thermal activation energy (E) and "attempt-to-escape" frequency which determine the rate of de-trapping. These parameters are

especially important in the modeling of the kinetics of the "traffic" of the charge carriers as the sample is first disturbed and then returns to thermal equilibrium.

c) Dissipation of thermal and radiant energy via diffusion of the charge carriers through the crystal lattice followed by recombination, a certain fraction of which results in TL photons. Recombination can occur via charge carrier diffusion in the conduction band which can be viewed as a "de-localized" or long range mechanism or by "germinate" recombination i.e., via recombination between a locally trapped electron-hole pair.

TL phosphor material

The emission of light when certain solids are warmed, generally to a temperature lower than that needed to provoke visible incandescence. Two characteristics of thermoluminescence distinguish it from incandescence. First, the intensity of thermoluminescent emission does not remain constant at constant temperature, but decreases with time and eventually ceases altogether. Second, the spectrum of the thermoluminescence is highly dependent on the composition of the material and is only slightly affected by the temperature of heating. If a thermoluminescent material emits both thermoluminescence and incandescent light at some temperature of observation, the transient light emission is the thermoluminescence and the remaining steady-state emission is the incandescence. The transient nature of the thermoluminescent emission suggests that heating merely triggers the release of stored energy previously imparted to the material. Supporting this interpretation is the fact that after the thermoluminescence has been reduced to zero by heating, the sample can be made thermoluminescent again by exposure to one of a number of energy sources: x-rays and gamma rays, electron beams, nuclear particles, ultraviolet light, and, in some cases, even short-wave visible light (violet and blue). A thermoluminescent material, therefore, has a memory of its earlier exposure to an energizing source, and this memory is utilized in a

number of applications. Many natural minerals are thermoluminescent, but the most efficient materials of this type are specially formulated synthetic solids (phosphors).

In addition to special sites capable of emitting light (luminescent centres), the basic mechanism of light emission from the phosphors is that they have centres that can trap electrons or holes when these are produced in the solid by ionizing radiation. The luminescent center itself is often the hole trap, and the electron is trapped at another center, although the reverse situation can also occur. In the former case, if the temperature is low and the energy required to release an electron from a trap (the trap depth) is large, electrons will remain trapped and no luminescence will occur. If, however, the temperature of the phosphor is progressively raised, electrons will receive increasing amounts of thermal energy and will have an increased probability of escape from the traps. Freed electrons may then go over to luminescent centers and recombine with holes trapped at or near these centers. The energy liberated by the recombination can excite the luminescent centers, causing them to emit light.

Radiation dosimeters based on thermoluminescence are widely used for monitoring integrated radiation exposure in nuclear power plants, hospitals, and other installations where high-energy radiations are likely to be encountered. The key elements of the dosimeters, thermoluminescent phosphors with deep traps, can store some of the energy absorbed from these radiations for very long periods of time at normal temperatures and release it as luminescence on demand when appropriately heated. The brightness (or light sum) of the luminescence is a measure of the original radiation dose. There are several TL phosphors used to measure ionizing radiation such as lithium fluoride, calcium sulphate doped with dysprosium, lithium fluoride doped with magnesium, copper and phosphorous.

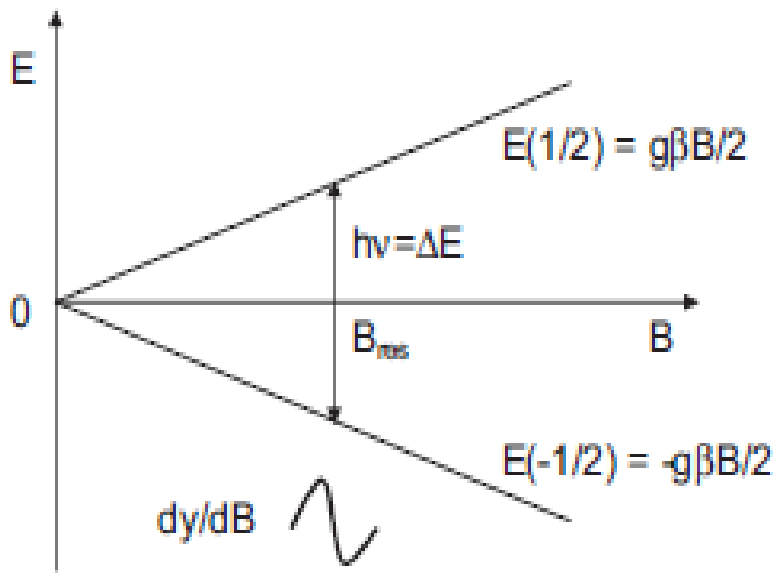

Fig.1. Energy levels for a system with S=1/2 as a function of the applied magnetic field. The experimentally detected first-derivative line shape dy/dB is also shown.

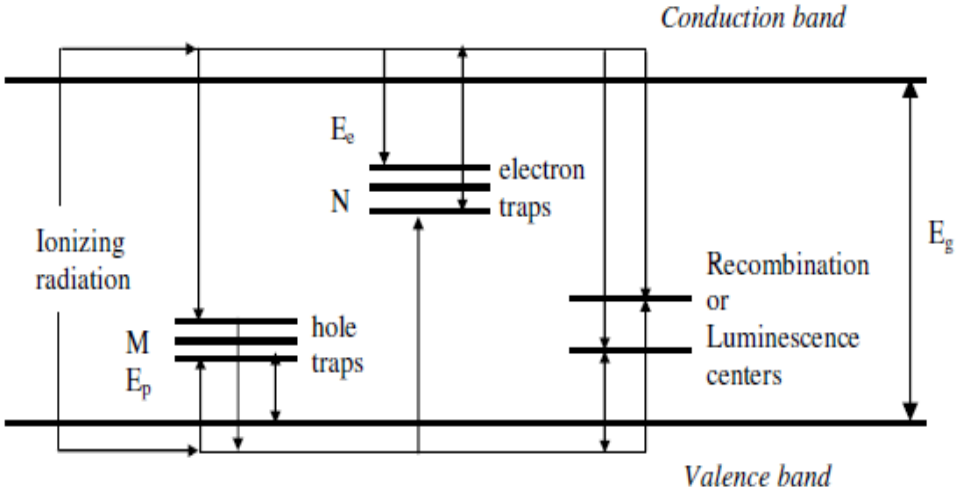

Fig.2. Energy-level presentation of the TL process, showing the filling process of electron and hole traps and mechanism, which is responsible for thermally activated luminescence (TL). N= total concentration of electron traps with energy Ee, M= total concentration of hole traps with energy Ep.

Aims and objectives

A large number of detection techniques are being developed for testing an increasing variety of food products. Newly emerging techniques must be assessed for their suitability for field application. In case of irradiated foods improved qualitative detection is often of greater relevance than quantitative dose estimation [7], mainly due to the self-controlling nature of food irradiation. Higher doses may cause unacceptable sensory changes and higher costs for the radiation treatment. Whereas, a certain minimum dose is necessary to achieve the desired objective (e.g. say Salmonella eradication in chicken,). Possibly, a posteriori detection of treatment and possible dose estimation may enforce Good Irradiation Practice (GIP) [8]. However, effective dosimetry and process control at the radiation facility must be an absolute priority for the enforcement of GIP.

Based on the review of available literature on identification of irradiated foods, it was felt that there is an increasing interest in extending the EPR methodology to various types of food. The main problem lies in the instability of the relatively weak radiation specific signals. A negligible change in food commodities after radiation treatment makes the identification of irradiated food an extremely challenging task and the statistical margin is rather small. Therefore, one method alone is not reliable enough for detection of a treatment by ionizing radiation. Thermoluminescence (TL) is a radiation specific phenomenon and a suitable technique for detection of irradiated foods from which inorganic components can be isolated. An attempt has been made to study the identification methodology for irradiated foods with commercially relevant doses based on physical techniques namely, Thermoluminescence (TL) measurements and Electron Paramagnetic Resonance (EPR) spectroscopy. Table 4 shows the food commodities chosen for study from the list of food and allied products approved for commercial radiation processing in India.

The effectiveness of processing of food by ionizing radiation depends on proper delivery and reliable measurement of the absorbed dose. It is extremely important for food destined for international markets that the dosimetry is carried out accurately and that the process is monitored in accordance with the internationally accepted protocols and procedures. The evaluation of absorbed dose at low temperatures in frozen or chilled food using a cost effective and simple dosimetry system is a challenging task. Therefore, there is an interest for the development of new dosimetry systems with improved performance. Thermoluminescence dosimeters are widely employed for personnel and environmental dosimetry, but rarely for application at higher doses. In radiation processing of food, a large number of food items namely seafood, fruits and vegetables are required to be processed by ionizing radiation at chilled (0±4ºC) or frozen (-20±2ºC) temperature in the dose range of 1 to 4 kGy. In view of these, investigations were carried out to understand the mechanism of modified $CaSO_4$ based thermoluminescence phosphors by TL-EPR correlation studies and to find out the efficacy of the phosphors as food irradiation dosimeters.

The following objectives were identified for investigation in this thesis.

a) Study the nature of radiation induced paramagnetic centres formed after exposure of food to commercially recommended doses of gamma radiation (Table 4).
b) Investigation of relaxation behavior and thermal characteristics of the paramagnetic centres for detection of radiation processed foods after prolonged storage.
c) Compositional analysis of polyminerals isolated from irradiated foods and the possibility of employing TL technique to identify stored irradiated foods.
d) Standardization of the process of isolation of inorganic components of irradiated foods and their TL measurements.
e) Studies to understand the TL properties of a phosphor and its suitability as a food irradiation dosimeter both at ambient and sub-ambient temperatures.

Table 4. The food commodities studied

Name of the food	Purpose	Dose (kGy)	
		Min	Max
Potato	Sprout inhibition	0.06	0.15
Ginger, Fresh turmeric	Sprout inhibition	0.03	0.15
Rice	Insect disinfestation	0.25	1.00
Cashew nut	Insect disinfestation	0.25	1.00
Aswagandha (*Withania somnifera*), Vairi (*Salacia reticulate*), Amla (*Emblica officinalis*), Turmeric (*Curcuma longa*) and Guduchi (*Tinospora cordifolia*)	Microbial decontamination	6.00	14.0
Soybean	Insect disinfestation	0.25	1.00
Shrimp	Shelf-life extension under refrigeration	1.00	3.00
Dog feed	Microbial decontamination	6.00	14.0

CHAPTER 2

Literature Survey

This chapter focuses on the present status of identification of irradiated foods by EPR spectroscopy and TL techniques. In addition available literature on high dose measurements by TL phosphor is also discussed.

Presents status of identification of irradiated foods using EPR spectroscopy

There are only a limited number of papers dealing with the influence of higher doses of ionizing radiation on the changes in the structure, physical, chemical or biochemical properties of foods preserved by radiation processing. Use of gamma radiation in food processing and aspects related to safety, nutritional and organoleptic properties have been reviewed in detail by Desrosiers, M. F. 1996, Raffi *et al*., 2000, Delincée, H. 2002 [9, 10, 11]. Korkmaz & Polat, 2000 [12] reported identification of irradiated durum wheat using EPR spectroscopy and studied the kinetics of radiation induced radicals. Nonirradiated wheat samples exhibited a weak, single-line EPR signal originating from a radical of unknown structure. Irradiation produced two more radicals identified as hydroxyalkyl and aldehydalkyl radicals. All the radicals followed a complicated kinetics. In another report Korkmaz & Polat, 2001 [13] studied the identification of irradiated red pepper using EPR spectroscopy. Nonirradiated sample also exhibited a weak single EPR line and attributed it to the existence of a radical with partially resolved structure, g varying from 2.0043 to 2.0047 and peak to peak line width (ΔB_{pp}) from 1.5 to 2 mT. This radical was proposed to be derived from a membrane-bound semiquinone. Raffi *et al*, 2000 [10] also reported that nonirradiated samples of all studied plants exhibited a very weak EPR singlet line characterized with g = 2.0050±0005. In case of spices and herbs, the experimental spectra of nonirradiated (reference) samples were characterized by one stable narrow EPR signal (g = 2.0022, ΔB_{pp} ~ 1 mT) typical for the semiquinone radicals produced by the oxidation of plant polyphenolics [14, 15, 16].

Identification of irradiated cellulose containing foods by EPR spectroscopy

The gamma radiation treatment of plant products containing cellulose leads to generation of a three-line EPR signal, characterized by a g-value of 2.0060±0.0005 and hyperfine splitting at about 3.00±0.05 mT attributed in literature to 'cellulosic' radical [17, 18, 16]. The application of gamma radiation leads to changes in chemical structure of spice matrices, producing new types of paramagnetic species analogous for all investigated spice species. Simulation of EPR spectra obtained for black pepper samples revealed the formation of three paramagnetic species, i.e. the triplet and doublet assigned to 'carbohydrate' radical structures and the typical three-line 'cellulosic' signal [15, 16]. In case of fruits, it is reported that the cellulose free radicals are generated by gamma irradiation [19]. In case of irradiated red pepper as reported by Korkmaz & Polat [13], a doublet or triplet EPR signal was present only in irradiated samples. However, as the singlet signal in case of nonirradiated sample was almost at the center of the low-field and high-field peaks of radiation induced signal, it was reported that these minor peaks are part of a triplet. The presence of radiation induced triplet signal was assumed to be generated from a molecule present in large amount in the medium and this molecule could be cellulose, hemi-cellulose or lignin. In relation to the formation of paramagnetic species upon gamma radiation processing of food, EPR spectroscopy represents a unique detection technique for their characterization and investigation. In EN 1787:2000, [20] CEN proposed the EPR method for detection of foods containing irradiated cellulose. This European Standard EN 1787 has been validated for pistachio shells, paprika powder and strawberry seeds of fresh strawberry. Satellites in the seeds of fresh fruits have been observed for fresh strawberries (EN 1787), as also for the seeds of sherry, raspberry, red currant, gooseberry [21] and even for other fruits like black berry, mulberry, figs, melon and prunes [19, 21]. For the purpose of post-radiation identification of cellulose-containing foods, the presence of this signal was accepted as a marker of the gamma radiation treatment. In recent

time Yordanov & Aleksieva, 2009 [22] showed the results of EPR study on fresh fruits like whole pulp of pear, apple, peach, apricot, avocado, kiwi and mango. In order to remove water from nonirradiated and irradiated samples the pulp of fresh fruits was dried by two different drying processes. The results obtained with both drying procedures were compared. All samples under study showed a singlet EPR line with g = 2.0048±0005 before irradiation. Irradiation gave rise to typical ‘‘cellulose-like’’ EPR spectrum featuring one intensive line with g = 2.0048±0.0005 and two very weak satellite lines situated at 3 mT left and right to the central line. Only mango samples showed a singlet line after irradiation. The satellite lines were measurable for less than 17 days of storage. The reported results unambiguously showed that the presence of satellite lines in the EPR spectra could be used for identification of radiation processing of fresh fruits.

Identification of irradiated food containing bone by EPR spectroscopy

Onderdelinden & Strackee, 1974 [23] suggested that EPR spectroscopy had the potential as a method for detection of irradiated food containing bone. It has been shown that nonirradiated bone gave a weak broad signal, which increased in magnitude if bone was ground to powder [24]. This method can be utilized in meat industry. In radiation-treated food such as bone tissue, two prevailing types of paramagnetic species have been observed. One is derived from bone collagen and the other due to structural defects in the crystalline fractions of minerals present in bone such as hydroxyapatite [$Ca_{10}(PO_4)_6$ $(OH)_2$] [25, 26]. The first paramagnetic species is slowly decayed by atmospheric oxygen, while the second species is extremely stable at room temperature during years of storage. The characteristic signal generated during irradiation of bone is due to CO_3^{1-}, CO_3^{3-}, and CO_2^{1-} ions that are trapped in the hydroxyapatite matrix [27, 28, 29]. The signal patterns produced during irradiation in all bones are the same, thus it is evident that EPR can be used for qualitative detection of irradiated foods containing bone. Further, the intensity of the EPR signal increases linearly

with the applied dose [30] and the relationship holds when corrected with standard ash, calcium, or phosphorus content. With chicken, the observed EPR signal intensity was found to be varying depending on the age of the chicken and which bone was monitored. These differences were assumed due to variation in the crystallinity of the bone [31, 32, 33]. Dodd *et al*, 1985 [34] and Goodman *et al*, 1989 [35] have demonstrated that ESR spectroscopy can also be used for irradiated crustaceans using signals induced in the exoskeleton or shell because they have very low moisture content. Desrosiers 1989 [36] and Stewart *et al*, 1994 [37] reported that the aragonite or calcite minerals in shells were responsible for signal production. The EPR spectra produced by crustaceans are dependent on species and geographical origin of prawn and shrimp [38]. European standards for detection of irradiated food containing bone by EPR spectroscopy has been released by European Committee of Normalization (CEN) and adopted by Codex Alimenterius Commission as Codex Standards. EN 1786, 1997 [39].

Identification of irradiated foods containing crystalline sugar by EPR spectroscopy

EPR investigation of fresh fruits were first focused on the detection of those parts of fruits, which have less water content for example seed, stalk, skin, stone and peel. These parts of fruits are solid and have very low water content, so that the gamma radiation induced radicals are stable and can be detected by EPR. The spectra of nonirradiated hard plant tissue samples show a singlet line with a g-value varying from 2.0040 to 2.0047. Sometimes, a six-line spectrum of Mn^{2+} is also recorded. The above signals are also present in the EPR spectra of irradiated samples, where the amplitude of the natural singlet increases after irradiation and the intensity of the Mn^{2+} sextet is radiation independent. A further promising application of EPR spectroscopy is the analysis of foods containing crystalline sugar. Although for some dehydrated fruits a multi component EPR spectrum with a total signal width corresponding to a magnetic field strength of 7±1 mT allows unequivocal identification of irradiated samples

like mango, papaya, fig, and raisin. Some other fruits seem `inactive' and do not give the expected spectra [40]. For nonirradiated samples, both single and multi component spectra have been observed, but the signal width was less than 7 mT. More information about the behavior of various dehydrated fruits upon irradiation seems desirable. European standards for detection of irradiated food containing crystalline sugar by EPR spectroscopy has been released by European Committee of Normalization (CEN) and adopted by Codex Alimenterius Commission as Codex Standards [41]. However, it was observed that the EPR intensity of the paramagnetic centres induced by ionizing radiation gradually decreased with storage time and the rate of disappearance depended on temperature, humidity, presence of oxygen and on some other factors. Therefore, improved approach based on EPR spectroscopy was felt extremely necessary for identification of irradiated foods [42, 43, 44].

Present status of identification of irradiated foods using TL technique

Thermoluminescence (TL) analysis is one of the more specific methods for identification of irradiated foods. It is based on the physical changes in minerals (from sand and dust) which are concomitant in many food products. Silicate minerals are able to store the energy imparted by radiation. Heat stimulation releases some of this stored energy in the form of light. A thermoluminescence reader measures the amount of light which is emitted during controlled heating [45]. Over the last fifty years, thermoluminescence (TL) has developed into a powerful methodology with many different applications such as a) radiation dosimetry, including clinical applications, e.g. therapeutical treatment of cancer patients; b) age determination in archaeology and geology; c) mineral prospecting, e.g. for uranium sources; d) study of meteorites and lunar material; and e) solid-state defect structure analysis [46, 47, 48, 49, 50, 51].

An early application of thermoluminescence related to food was described by Chadwick and Oosterheert in 1967, who measured the thermoluminescence of tomato seeds irradiated at liquid nitrogen temperature with X rays at 0.05 - 1 kGy [52]. To use thermoluminescence as detection method for irradiated food was first proposed by Heide and Bogl in 1984. They suggested detecting the radiation treatment of spices and herbs by investigating whole samples. A few mg of spice was heated in a commercial TL reader - usually employed for dosimetry - and the light emission recorded as a function of increasing temperature of the spice sample [53]. This led to the idea that spices and herbs themselves may exhibit thermoluminescence. In some inter-laboratory studies [54], large inter-sample variations were observed. However, in 1989, Sanderson *et al*, [55] reported that the origin of luminescence is the contaminating minerals (sand and dust) in the spice samples.

Thermoluminescence (TL) has been studied as a detection technique for various foods and specifically for the detection of irradiated spices and herbs. In 1993, Pinnioja reported that irradiated foods can be detected by thermoluminescence (TL) of contaminating minerals. Altogether about 300 lots of herbs, spices, berries, mushrooms and seafood were studied by the TL method. Irradiated herbs and spices were easily differentiated from nonirradiated ones two years after irradiation at a 10 kGy dose. The mineral composition of spices, herbs and seafood were also studied. In case of seafood, variable mineral composition was reported. While calcite was suitable for the TL analysis, aragonite and smectite gave unreliable results [56]. In 1995, Khan *et al*, [57] studied eight types of spices and herbs and their mixtures of Asian origin for detection of irradiation treatment using TL of insoluble minerals contaminant adhering to the samples. The integrated TL intensities were found to be much higher compared to the nonirradiated samples. In 2005, Marchioni *et al*, [58] studied the possibility of detection of irradiated ingredients included low quantity in nonirradiated food matrix. The authors have developed an enzymatic hydrolysis method for the extraction of silicate minerals

and bone fragments. Even for food containing a mixture of two ingredients spices and mechanically recovered meat, it was possible to detect and identify them simultaneously. In case of identification of irradiated potato, Kwon et al, 2002 [59] investigated thermoluminescence (TL) characteristics for minerals, which were separated from potato irradiated at 0 - 1 kGy of different origins of production in Korea. The glow curve of irradiated samples at 0.05 - 1 kGy peaked at approximately 200°C with high intensity, but that of nonirradiated potato was observed at approximately 300°C with low intensity. Discrimination between irradiated (more than 0.05 kGy) and nonirradiated samples was possible just on the basis of the first glow curve. In 2000, Soika and Delincee [60] studied thermoluminescence technique to detect radiation processing of foods which were contaminated with sand or dust. Silicate minerals were isolated, their radiation-induced luminescence was measured and compared to the thermoluminescence from a second measurement after exposure to a defined radiation dose (normalization). Evaluation of the first and corresponding second glow curve revealed that their shapes depend on the type of minerals in the mixture. TL technique to identify irradiated foods are also reported in case of shellfish [61], traditional foods containing salt [62], and white ginseng powder [63], irradiated anchovy and chestnut [64].

High dose measurements using TL phosphor

Thermoluminescence (TL) involves light emission from solids (insulators and semiconductors) upon heating and is labeled as luminescence. Efficient TL materials have a high concentration of traps provided by structural defects and impurities. Not all the numerous known TL phosphors are suitable for radiation dosimetry. For dosimetric purposes, a thermoluminescent phosphor is expected to show the features including a relatively simple glow curve, with the temperature of the main peak at around 200°C; high sensitivity, which

consists of both high efficiency of light emission and low threshold dose, high resistance against environmental factors such as humidity, solvents, optical fading and long-term stability of the stored information [65]. Amongst the various TL phosphors, rare earth doped $CaSO_4$ thermoluminescent materials are widely used in radiation dosimetry [66, 67]. Because of their high sensitivity and stability of response in adverse climatic conditions, they are widely used in personal dosimetry and environmental monitoring [68, 69]. In India $CaSO_4$: Dy phosphor based TLD badges [70] are in use for countrywide personnel monitoring programme. Similarly, a large number of reports are available where TL phosphors are being used for radiation dosimetry, mainly for low dose measurements, suitable for radiation protection and personnel monitoring [71, 72, 73]. A review of thermoluminescence properties of calcium fluoride, calcium sulphate and calcium carbonate was reported by Sunta, 1984 [74]. TL glow peaks were appeared in a wide temperature range for all the samples starting from liquid nitrogen temperature -196°C to 650°C. The most intense glow peak which appeared in the temperature region of 200 – 250°C is usually exploited in TL dosimetry. A comparative study of low dose measurements with $CaSO_4$: Dy, $CaSO_4$: Tm and $CaSO_4$: Dy Teflon dosimeters was reported by Lakshmann & Jose, 1993 [75]. It was reported that the detection threshold of CaSO4: Dy phosphor was lower than that of Teflon discs because of less spurious TL from the powder. Higher sensitivity and other dosimetric properties of $CaSO_4$: Tm such as reduced intensity of fast fading low temperature peak at 100°C and reduced spurious TL were confirmed. In 1988, trap level spectroscopy of $CaSO_4$: ^{241}Am was reported by Natarajan *et al* [76]. In this study the paramagnetic radical ions produced as a result of internal α irradiation and external γ irradiation in $CaSO_4$:^{241}Am were identified by electron paramagnetic resonance (EPR) and their role in the thermally stimulated reactions leading to thermally stimulated luminescence (TSL) was identified. It was found that Am^{3+} acts as the luminescent centre for all the glow peaks observed. In self-irradiated samples as

well as in samples γ irradiated at room temperature, SO_4^-, SO_3^- and O_3^- radicals were observed whereas the additional radical O^- was observed when the samples were irradiated at -196°C (77°K). The destruction of the SO_4^- radical ion was found to be responsible for the most intense glow peak at 133°C (406°K).

Very few reports on application of TL phosphor for high dose measurements, especially at ambient or sub-ambient temperatures, for food irradiation applications are available. It is reported that TL phosphors can be used for dose measurement during food irradiation using simple read out methods [77, 78]. A few such studies are being discussed here. The primary result of Ramos–Bernel *et al*, 2002 suggested a linear response to both dosimeters namely, LiF:Mg, Cu, P and CaSO4:Dy, when irradiated at low temperature and low doses. Higher doses follow a quadratic fit. The glow-curves for the crystals under study showed an intensity maximum shift toward lower temperature values in comparison with the sample irradiated at room temperature. This shift is very pronounced for LiF:Mg, Cu, P. Characterization of nonlinearities in the dose dependence of thermoluminescence phosphors was reported by Chen and McKeever, 1994 [79]. In this study the authors mentioned that nonlinearities in dose dependence often occurs in TL phosphor and includes sublinearity, usually when there is an approach to saturation in the dose dependence, as well as supralinearity, also termed superlinearity in literature. In case of CaSO4: Dy phosphor, post preparation annealing at a higher temperature is of particular interest in order to optimize the thermal treatment to obtain maximum TL sensitivity. It is reported that the thermal treatment in the range of 400 – 700ºC enhances the response of high temperature peak [80] for use of the phosphor in dosimetry for personnel monitoring. Recently, Hernandez-Medina et al., 2009 [81], studied the behavior of $CaSO_4$ doped with Dy as a function of irradiated dose and irradiation temperature. The important findings of the study were that, a slight shift in the maximum response peak at different values compared with the sample irradiated at room temperature occurred. If the

temperature decreases from room temperature to liquid nitrogen temperature, the TL response also decreases considerably. However, they found a linear dose response up to 400 Gy when irradiated at sub-ambient temperature. In 1999, high dose measurements using $CaSO_4$: Dy phosphor was reported by Mathur *et al* [82]. Their investigations showed that the range of high dose measurements can be increased by an order of magnitude by increasing the concentration of dysprosium in $CaSO_4$:Dy. A further increase in high dose measurements was possible by considering the ratio of two high temperature peaks. As the ratio of two peaks is an intrinsic property of the material, it was expected that the initial calibration of these dosimeters may not be required. This could be advantageous at very high doses where calibration of the dosimeters is quite problematic. Use of thermoluminescence peaks higher than 300°C also made this technique appropriate for high dose measurements at high temperatures.

Energy transfer mechanism from one dopant (sensitizer) to another (luminescent center) is sometimes used to enhance the sensitivity of a phosphor. Earlier several researchers have tried to sensitize TL phosphor by co-doping with different rare earth metals [83]. Moncorge *et al*, 1979 and Murata & Mouri, 2007 [84, 85] reported that the most important co-doped phosphor is $CaSO_4$:Dy^{3+}, Ce^{3+}, where the emission from Ce^{3+} in the region 306 – 324 nm overlaps with the Dy^{3+} excitation and in turn, it enhances its TL emission. It is also reported that Bi^{3+} co-dopant ion with $7s^2$ electronic configuration was capable of transferring energy to rare earth ions such as Eu^{3+} [86].

Hence, the above discussion suggested that further research and development is required for exploitation of EPR and TL techniques for detection of food irradiation treatment and their field applications. These studies would not only provide useful scientific information but also strengthen hands of regulatory agencies in checking compliance in commercial food irradiation.

CHAPTER 3

Experimental procedures

Studies on identification of irradiated food using TL technique

Identification of irradiated food samples namely rice, potato, ginger, fresh turmeric, shrimp, and dog feed were carried out using thermoluminescence (TL) technique. The selection of the food samples for TL studies was based on the possibility of separation of associated inorganic components from the samples. The working principle of the TL reader associated with the experiments, measurement of absorbed dose, procedures for isolation of inorganic components, sample preparation and TL measurements were standardized.

Working principle of TL reader

TL readers work by heating the TL materials and measuring the light output from the photon emissions via de-excitation of electrons trapped in the forbidden band of the crystals. The TL material is placed on a planchet which is heated via a thermocouple. The light emission is focused through a filter or wave shifter which serves to convert the emitted photon wave frequency to a visible spectrum photon which can then be collected in a photomultiplier tube (PMT). The PMT output (current) is then integrated over a set integration range. Fig. 3a is a block diagram of the basic working of a TLD reader. The TLD reader used in this work is Nucleonix TL reader Model 1009I. A photomultiplier tube is used to convert visible photons emitted from the TL material to an electrical signal. The photons interact with the photocathode, where the energy from the photons is absorbed into the photocathode material and is transferred to an electron. The freed electron migrates to and escapes from the surface of the photocathode. Subsequent electrons are then accelerated into the first dynode. The dynode material is designed such that energy deposited by an incident electron will result in the emission of more than one electron from the surface of the dynode. Photomultiplier tubes have about 10 dynodes. After multiplication through the dynode stages, the electrons are collected by the anode and the electrical signal is processed.

Samples procurement and preparation

The food samples of rice, shrimp, potato, ginger, fresh turmeric and dog feed were procured from the local market. The samples were repacked into polyethylene bags (250 g) and subdivided into three to five lots. One served as nonirradiated (control) and the others were exposed to gamma radiation at the recommended doses of radiation approved for commercial processing.

Sample irradiation

Irradiation was carried out either at ambient temperature (27±2°C) for the food samples like rice, potato, ginger, fresh turmeric and dog feed or at chilled temperature (0±4°C) for shrimp. In case of chilled temperature irradiation, the sample was placed inside a Dewar flask containing crushed ice to achieve sub-ambient temperature. The irradiation was carried out using a cobalt-60 irradiator (GC 5000**,** Board of Radiation and Isotope Technology, Mumbai, India) at BARC, Mumbai.

Dosimetry

Determination of the absorbed dose rate of the irradiator was carried out using Fricke reference standard dosimeters [87]. Since, the dose rate of the gamma chamber is changing with the decay of the source activity, the dose rate was determined before irradiation of each food samples. The distribution of the absorbed dose within the irradiation volume of the gamma chamber was found out by fixing 9 numbers of Fricke dosimeters throughout the cylindrical irradiation chamber filled with food equivalent medium. All the Fricke vials were put inside the Perspex buildup cap of thickness 4 mm to achieve charge particle equilibrium required for gamma radiation (average energy 1.25 MeV) from the cobalt-60 source. The uniformity in absorbed dose distribution was measured by the ratio of the maximum absorbed dose (D_{max}) to the minimum absorbed dose (D_{min}). The ratio D_{max} / D_{min} is known as Dose Uniformity Ratio (DUR). A DUR of 1.21 was obtained for the irradiation volume used for the

experiments. Finally, the food samples packed in sealed polyethylene bags were exposed to radiation for calculated time obtained from the dose rate and DUR of the gamma chamber in the respective dose ranges like 0.25 to 1 kGy for rice, 2 to 4 kGy for shrimp, 0.1 to 0.2 kGy for potato, ginger and fresh turmeric and 5 to 10 kGy for dog feed. In order to reconfirm the actual absorbed dose in the food samples a set of chemical dosimeters, Fricke to measure the dose of 0.25 kGy and alanine-EPR dosimeters [88] to measure doses ranging from 0.5 to 1 kGy, were also irradiated along with the samples. A variation in absorbed dose with respect to the desired dose was observed within ± 3%.

Sample preparation for TL measurements

For TL measurements it was essential to isolate natural mineral contaminants of the various commodities. The methodology for isolation of inorganic contaminants associated with food samples was standardized based on the European Standards EN 1788, 1996 [45]. The method has two main steps.

a) Alkaline hydrolysis. In cases of shrimp and dog feed, the samples were subjected to alkaline hydrolysis. Alkaline hydrolysis was carried out to recover the intestinal grits from the shrimp and the inorganic component present in the dog chew samples. Around 100 g of both nonirradiated and irradiated samples were taken, treated with 500 ml alcoholic NaOH (1 N) and heated for 2 h at 80ºC with occasional stirring. The supernatant was decanted and the samples were allowed to cool. Samples were then diluted with double distilled water and left to settle. The supernatant was decanted off. The mineral residue was washed three times with double distilled water and then subjected to a density separation procedure.

For the food samples like rice and potato the inorganic component was isolated with the help of ultrasonication for 10 to 15 min.

b) Density separation. In order to make sure that the extracted samples were free from any organic impurity, a solution of sodium polytungstate ($Na_6W_{12}O_{39} * H_2O$, density 2 g/ml) was

added. The samples were subjected to ultrasonication in a bath sonicator for 5 min followed by centrifugation at 1000 g for 2 min. The organic material floating on the top of the polytungstate solution was removed. The bottom layer was washed three times with double distilled water. After total removal of water, 2 ml of acetone was added. The minerals in acetone were transferred to clean and weighed aluminum discs (diameter 9.0 mm; thickness 0.4 mm, fabricated at workshop, FTD, BARC) with the help of Pasteur pipette, as shown in Fig. 3b. The discs containing minerals were stored overnight at 50ºC.

Standardization of TL measurement technique

The discs containing minerals of control and irradiated samples were weighed to determine the quantity of minerals deposited. Thermoluminescence analyses were carried using TL 1009I Reader (Nucleonix Systems Pvt. Ltd., India). Nitrogen was flushed in the heating chamber to reduce spurious TL arising due to the presence of oxygen. The experimental setup is shown in Fig. 3c. The initial ambient temperature was increased to 300ºC by linear heating at a rate of 5ºC/s. After measurement of glow 1, the discs with the deposited mineral were reirradiated with a normalization radiation dose of 1 kGy followed by TL measurement of glow 2 with the similar instrumental settings as described above. The samples were separated and analyzed in triplicate under similar laboratory and instrumental conditions. The irradiated and non-irradiated samples were stored in dark under the normal laboratory conditions at ambient temperature (27±2°C) until further use.

In order to characterize the isolated polyminerals from food samples, scanning electron microscopy with energy dispersive X-ray spectrometer analysis (SEM/EDX) and X-ray diffraction analysis were carried out. The electron microscopic analysis was done with TESCAN, Czechoslovakia and EDX, INCA x – sisht, Oxford, U. K. with secondary electron detector. XRD studies were carried out by a Philips instrument at room temperature.

a)

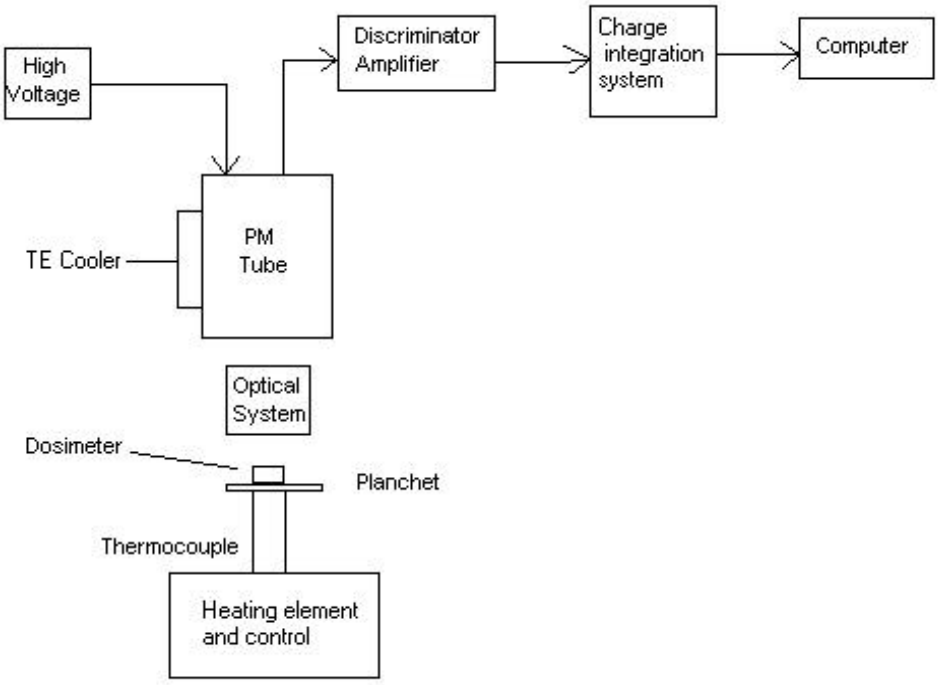

b)

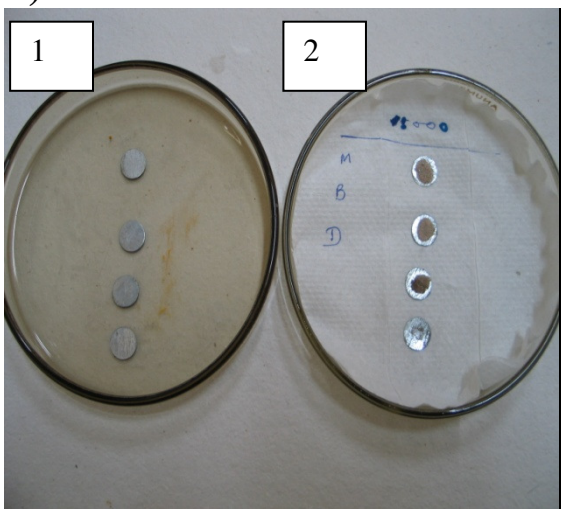

c)

Fig. 3. a) Block diagram of working principle of TL reader [89], **b)** the aluminum discs fabricated to keep isolated minerals were shown under label 1 and the discs containing isolated minerals from food are shown under label 2, **c)** experimental set up for TL measurement with the nitrogen gas purging system.

Identification of irradiated food using EPR spectroscopy

Feasibility to extend the application of EPR spectroscopy to identify various irradiated food samples was investigated. The commodity studies included cashew nut, soybean, rice, shrimp and allied products like dog feed and medicinal plant products were studied. The sample preparation for EPR spectroscopy, irradiation and the experimental parameters of the EPR spectrometer were standardized.

Working principle of EPR spectrometer

A block diagram for a typical EPR spectrometer is shown in Fig. 4a. The radiation source usually used is called a klystron. Klystron is a vacuum tube known to be stable high power microwave source which has low-noise and high sensitivity. A majority of EPR spectrometers operate at approximately 9.5 GHz, which corresponds to about 32 mm. The radiation may be incident on the sample continuously (i.e., continuous wave, abbreviated cw) or pulsed. The sample is placed in a resonant cavity which admits microwaves through an iris. The cavity is located in the middle of an electromagnet and helps to amplify the weak signals from the sample. Numerous types of solid-state diodes are sensitive to microwave energy and absorption lines can be detected when the separation of the energy levels is equal or very close to the frequency of the incident microwave photons. In practice, most of the external components, such as the source and detector, are contained within a microwave bridge control. Additionally, other components, such as an attenuator, field modulator, and amplifier, are also included to enhance the performance of the instrument.

Irradiation and sample preparation

The food samples and allied products were procured from a local market. The samples were subdivided into three to five lots in polyethylene bags of capacity around 200 g. One served as nonirradiated (control) and the others were irradiated at recommended radiation doses approved for commercial radiation processing. Irradiation of all the food samples and other

products selected for the studies was carried out at ambient temperature (27±2°C) except for shrimp which was irradiated at chilled temperature (0±4°C) using a cobalt-60 irradiator (GC 5000**,** Board of Radiation and Isotope Technology, Mumbai, India) at BARC, Mumbai. The determination of the absorbed doses and standardization of the irradiation procedures were similar as explained earlier. In case of soybean, the skin and kernel parts of irradiated and nonirradiated (control) samples were separated. The skin part was chopped and the kernels were cut into fine pieces of approximate length of 1.5 mm in order to transfer into 2-mm quartz capillary tubes for EPR spectroscopy. In case of the other samples, both the irradiated and nonirradiated whole samples were ground, smashed, cut or chopped into granule and powder forms. The samples of desired dimensions were then packed with gentle tapping to a length of 25.4 mm (active length) of the 2-mm quartz capillary tubes. The weights of the samples were determined and found in the range of 60 ± 4 mg.

Standardization of EPR spectrometer operational parameters

EPR measurements were performed using BRUKER EMX spectrometer (BRUKER, Germany). All the spectra were recorded at ambient temperature (25±2°C) of EPR laboratory after 3 accumulated scans.

Operating conditions of the EPR spectrometer were standardized as under:

Centre field 348 mT, scan range 20 mT for narrow scan and 100 mT for wide scan, microwave power 0.253 mW, microwave frequency 9.66 GHz, modulation frequency 100 kHz, receiver gain 4 X 10^4 and time constant 20.48 ms. The position of the radiation–induced EPR signal was compared with that of the standard 2, 2, diphenyl-1-picrylhydrazyl (DPPH) with g = 2.0032 (Sigma Chem. Co. USA).

In order to determine the electron relaxation behavior of radicals in food samples using EPR spectrometer, the microwave field strength was varied between 0.06 – 50 mW to obtain progressive saturation behavior (PSB). Field modulation was operated at 100 kHz. All the

EPR measurements were done at ambient temperature. In case of thermal behavior study of the paramagnetic centres, the thermal Dewar flask was installed inside the sample cavity and the nitrogen gas pipes for gas injection and suction were attached with appropriate greasing to avoid leakage. The experimental setup was made as per the requirement of the BVT-3000 accessory of BRUKER, Germany. The gas flow rates and the temperature rise were controlled from the integrated computer. Heating of the samples from room temperature to 302°C (575°K) in a step of 20° was carried out using nitrogen gas within the EPR spectrometer. The accuracy in heating temperature was within ±3°. The experimental set up is depicted in Fig.4b. EPR spectra simulation studies were carried out using WIN EPR and Simfonia programme (BRUKER). The EPR spectrum having multiple components was evaluated as a linear combination of the individually simulated EPR spectra. The relative concentration of the individual paramagnetic species was evaluated from the contribution of the individual simulation to experimental spectrum by double integration. The correlation of the simulated and experimental spectra was determined by the respective correlation coefficient (R^2).

a)

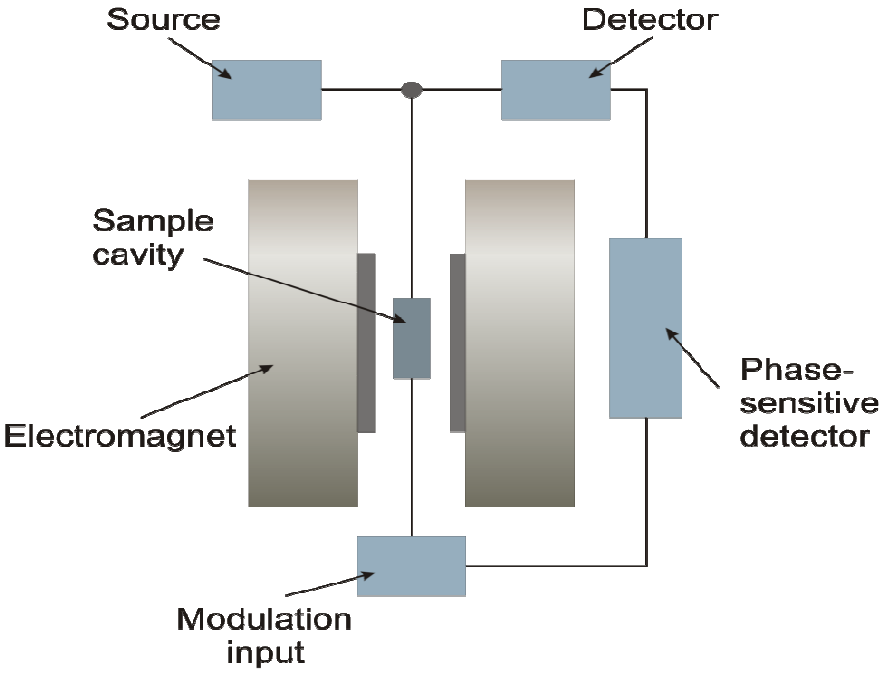

b)

Fig. 4. a) Block diagram of EPR spectrometer, **b)** experimental set up for EPR spectroscopy for thermal behavior study of the paramagnetic centre. The thermal Dewar flask was installed inside the sample cavity and inlet and outlet nitrogen gas pipes were attached with appropriate greasing to avoid leakage. The gas flow rates and the temperature rise were controlled from an integrated computer.

Studies on assessment of TL phosphors for food irradiation dosimetry

Two TL phosphors namely $CaSO_4$: Dy and $CaSO_4$:(Dy, Bi) were investigated to understand their efficacy to measure radiation doses in food irradiation dose range. The experimental methods associated with these studies are represented below.

Studies on $CaSO_4$: Dy phosphor

Polycrystalline $CaSO_4$:Dy (0.2 mol %) phosphor prepared and marketed by Renentech Laboratory Private Ltd, Mumbai, India, was used in the present study. The concentration (0.2 mol %) of dysprosium was chosen, because of its commercial availability and improved sensitivity. The powder was divided into two parts of 100 mg each. One part was subjected to thermal treatments to modify the TL properties and to exploit the TL emission suitable for the measurements of high radiation doses used in food irradiation practice. The other part was studied without any treatments to understand the changes in TL properties after thermal treatments.

Radiation treatment

The first part of the sample without any further treatment was exposed to gamma radiation from a cobalt-60 source at room temperature and at low temperatures. The temperature chosen for the study were -10±2ºC (Frozen) and 0±4ºC (Chilled). The samples were also exposed at liquid nitrogen temperature (-196ºC). The powdered phosphor was kept in a glass tube inside a Dewar flask and irradiated with cobalt-60 gamma radiation in a gamma chamber (GC 5000, Board of Radiation Isotope Technology, India, dose rate 6.5 kGy/h). The dose was calibrated with Fricke reference standard dosimeters [87] as explained earlier. The irradiation temperature was controlled by ice for chilled temperature, two parts of ice and one part of salt for frozen temperature. The freezing mixture of ice and salt was kept inside Dewar flask for insulation and the temperature was monitored using a laboratory thermometer. Initially, the temperature of the freezing mixture went below -10°C within 3 min and was able to maintain

the frozen temperature -10±2°C for a period of around 20 min. The dose response was measured using three aliquots from the same batch of the phosphor.

Thermal treatment

The second part was divided into three lots and each lot was subjected to different thermal treatments in the temperature range 700 – 900ºC in a furnace with a precision of temperature ± 3ºC followed by gamma irradiation at 0.1 kGy in chilled temperatures to study the intensity of EPR spectra. The dose response in terms of integral TL output was studied for untreated and thermally sensitized phosphors in the dose range of 0.5 - 7 kGy at chilled and frozen temperatures.

TL measurement

The irradiation response was analyzed using a thermoluminescence reader (Nucleonix Systems Pvt. Ltd., India) with a linear heating rate of 2ºC/s from ambient temperature to 300ºC. Neutral density filters (Melles Griot BV, Netherland) of optical densities 3 and transmittance 0.01 % were used to avoid saturation of photo multiplier tube (PMT). The peak height is vertical length of the peak tip from the temperature axis measured directly from the glow curve [82, 73]. Control and irradiated phosphors were stored in a dark place under normal laboratory conditions when they were not in use. Entire study was carried out using the same batch of $CaSO_4$: Dy phosphor to avoid inter-batch uncertainty.

EPR analysis

EPR study was carried out using EMX model EPR spectrometer (BRUKER, Germany) with a microwave frequency of 9.42 GHz. EPR spectra were obtained at liquid nitrogen temperature (-196°C) and from room temperature (25°C) to 300°C in step of 50º using in situ nitrogen gas heating assembly BVT 3000 of BRUKER. The samples were irradiated at 2 kGy dose at 0±3°C before taking the EPR spectra. Recording parameters were 338.2 mT central field, 0.1 mT modulation amplitude and 10.20 ms time constant with microwave power attenuation 15

dB. EPR sensitivity was measured by peak to peak amplitude [88, 90]. DPPH with g value 2.0036 was taken as reference for the EPR spectra.

Studies on $CaSO_4$: (Dy, Bi) phosphor

$CaSO_4$: Dy phosphor is well known for its high thermoluminescence (TL) sensitivity and stability to environmental variation. Energy transfer mechanism from one dopant (sensitizer) to another (luminescent center) is sometimes used to modify the sensitivity of a phosphor. The role of Bi^{3+} co-dopant in the matrix of $CaSO_4$: Dy phosphor to measure the food irradiation dose was studied.

Preparation of the phosphor

$CaSO_4$:Bi^{3+}, $CaSO_4$: (Dy^{3+}, Bi^{3+}) and $CaSO_4$:Dy^{3+} phosphors were prepared by recrytallization method following the recipe of Yamahashita [91]. The raw materials, $CaSO_4$: $2H_2O$, Bi_2O_3 and Dy_2O_3, were used in sulphuric acid medium. The concentration of Dy was 0.05 mol%, while the concentration of Bi in $CaSO_4$: (Dy, Bi) sample was 0.05, 0.2 and 0.5 mol%. After preparation, the phosphors were washed with double distilled water and dried at 100°C. The phosphors were further annealed at 700°C for 2 h in presence of N_2 in a furnace capable to attain a maximum temperature of 1100°C.

In order to confirm the presence of Bi in the $CaSO_4$: (Dy, Bi) samples prepared during the experiment, EDXRF study was carried out. $CaSO_4$: (Dy, Bi) (Bi- 0.2 mol%) was analyzed using Jordan Valley EDXRF spectrometer (EX 3600 M) having Rhodium as excitation source and Si (Li) as detector of energy measurement capability in the range of 1 – 40 keV in air. The powdered sample was transferred to polythene cups with a thin mylar film at the bottom in the sample chamber. The characteristic X-ray peaks of Bi, Dy, Ca and S were observed in the spectrum. In case of Bi, L_α and $L_ß$ were found at 10.84 and 10.73 keV. For Dy, the L_α and

$L_{ß}$ were at 6.50 and 6.46 keV. In case of Ca and S, K_{α} and $K_{ß}$ x-rays were observed at 3.69, 4.01 and 2.31, 2.46 keV, respectively.

TL measurements

Phosphor samples were exposed to a gamma radiation dose of 1 Gy from a cobalt-60 teletherapy machine and the TL glow curves were recorded 24 h after irradiation on a TL reader having a photo multiplier tube (PMT) with S-11 response (M/s Nucleonix Systems Pvt. Ltd, India). The glow curve was recorded from 40 -300°C with a heating rate of 5°C/s.

EPR spectroscopy

EPR study was carried out using EMX model EPR spectrometer (BRUKER, Germany) with a microwave frequency of 9.42 GHz. EPR spectra were obtained at liquid nitrogen temperature (-196°C) and at room temperature (25°C). The samples were irradiated at 2 kGy gamma dose in a gamma chamber (GC 5000, Board of Radiation Isotope Technology, India, dose rate 6.5 kGy/h) before recording their EPR spectra. Recording parameters were 338.2 mT central field, 0.1 mT modulation amplitude and 10.2 ms time constant with microwave power attenuation of 15 dB. EPR sensitivity was measured by peak to peak amplitude. 2, 2-diphenyl-1-picrylhydrazyl (DPPH) with g value 2.0036 was taken as reference for the EPR spectra.

Food irradiation dosimetry

It was observed that highly sensitive TL phosphors such as CaSO4: Dy exhibit intense TL output after exposure to radiation doses used in food irradiation practice and caused PMT saturation. However, the phosphor $CaSO_4$: (Dy, Bi) exhibited reduced sensitivity after incorporation of co-dopant Bi^{3+}, and the same could be exploited to measure food irradiation doses. Therefore, $CaSO_4$: (Dy, Bi) with Bi concentration 0.2 and 0.5 mol% were chosen to study their efficacy in food irradiation dosimetry. The phosphor in powder form was irradiated in a glass tube inside a Dewar flask with cobalt-60 gamma radiation in a gamma chamber (GC 5000, Board of Radiation Isotope Technology, India, dose rate 6.5 kGy/h). The

dose was calibrated with a Fricke reference standard dosimeter [87]. The phosphors were irradiated in the dose range of 1 to 5 kGy, which is recommended for commercial irradiation of chilled or frozen food for microbial decontamination and preservation. The irradiation response was analyzed by a TL reader as stated in the earlier paragraph. Neutral density filters (Melles Griot BV, Netherland) of optical densities 3 and transmittance 0.01 % were also used to prevent saturation of PMT. The peak height measured was vertical length of the peak tip from the temperature axis measured directly from the glow curve. Control and irradiated phosphors were stored in a dark place under ambient conditions, when they were not in use. Entire study was carried out using the same batch of the phosphor to avoid inter-batch uncertainty.

CHAPTER 4

Identification of irradiated

Basmati rice and Soybean

Identification of irradiated Basmati rice

Rice is an important cash crop and staple food for many countries. It has high nutritive value and the quality is governed by varietal differences and climatic conditions. The eating quality of rice has long been ascribed to its starch. Starch accounts for 95 % of the dry matter in milled rice grain [92]. Insect infestation during storage is a major problem of rice, resulting in economic losses. Irradiation is increasingly being recognized as an effective technology to reduce post-harvest losses and improve quality. Irradiated (0.25 – 1 kGy) Basmati rice, a high value fragrant rice of India, did not exhibit insect infestation during a storage period of 6 months, at room temperature that varied between 27°C to 33°C and relative humidity between 59 % and 87 %, while the control (nonirradiated) samples were spoiled due to infestation. During sensory evaluation, no significant difference was found between the acceptability of irradiated and nonirradiated (control) rice [93]. These results are significant in view of the high export potential of Basmati rice and the losses attributed to infestation.

In the present work, two independent physical methods were employed. A detailed study of the radical species produced by gamma irradiation of rice has been carried out by EPR saturation and thermal behavior to distinguish between treated and nontreated samples. In addition, characterization of the extracted minerals from the rice sample and the possibility of TL technique to identify irradiated and nonirradiated samples have been examined.

Identification using EPR spectroscopy

Fig. 5a, shows the EPR signal of nonirradiated rice samples exhibiting a weak singlet characterized by g = 2.0049 ± 0.0004 and ΔB_{pp} = 1.3 mT, centered around 346.1 mT. DPPH with g = 2.0032 was used as a reference to calculate the g values of the radicals. Similar singlet EPR line has been reported for other food commodities such as fresh strawberry [36, 34], grapes [36], black pepper [94]. The g value obtained for nonirradiated rice sample compares well with those reported in literature [95, 58]. The origin of these free radicals

responsible for the EPR signal is not clear. Several reports have suggested these free radicals to be those of semi-quinones produced by the oxidation of plant polyphenolics [96] or lignin [97, 98]. In order to validate a method for identifying irradiation, free radicals produced by other processing techniques such as heating (thermolysis) must be distinguished from those produced by irradiation. Fig. 5b shows the EPR signal of the rice sample subjected to thermal treatment at 100ºC for 1 h. The heat energy did not induce any specific change in the EPR spectrum. However, the intensity of the singlet (g = 2.0049) was observed to reduce by about 20 %.

Fig. 5c shows a complex spectrum immediately after irradiation (1 kGy) of rice samples with an increase in signal intensity of the existing weak singlet (g = 2.005). Similar observations were also reported by Raffi *et al*, [10], where the intense signal was noticed in the spectrum of irradiated spices. Irradiation was reported to be responsible for the relatively high intensity increase. As depicted in spectrum c, the exposure to gamma radiation leads to change in rice matrix, producing two new types of paramagnetic species. One pair of intense satellite lines at a distance of 6 mT from each other and the other less intense pair of lines situated at a distance of 2.6 mT from each other. The starch accounts for 95 % of the dry matter in milled rice grain [92]. In order to characterize this radiation specific signal, EPR spectrum of pure starch sample irradiated with 1 kGy dose of gamma radiation was investigated as depicted in Fig. 5d. Irradiated starch exhibited similar signals as that of irradiated rice. This 'sugar-like' spectrum, originated from the radiation treatment of polysaccharides is considered to be an unambiguous evidence of the radiation treatment of the sample under investigation and recommended for the detection of irradiated foods in EN 13708 standards. The same has been validated for irradiated skin of raisins and figs containing considerable amount of polysaccharides in the form of sugar [41]. These radiation specific signals observed in the rice matrix were not particularly stable and disappeared after 3 - 4 days with considerable decrease

in intensity of the central singlet (g = 2.005) to a level that was similar to that of nonirradiated specimen. The instability in signal intensity means that the detection of irradiated rice by EPR spectroscopy has a limitation. The effect of increasing radiation dose from 0.5 – 2 kGy on the spectra of rice samples was studied. The relative intensity of the central line was observed to be significantly related to the radiation dose as shown in Fig. 6a. The measurement was performed 2 days after irradiation. The dotted line represents a linear fit, Y = aD + b with a = 79.5, b = 3.5 and each point representing the mean value of four samples.

Thermal behavior of EPR signal

The small life time of the radiation induced radicals such as cellulose and 'sugar-like' strongly limits the applicability of the EPR analysis for detection of some irradiated food. This is the case with rice samples under investigation where the procedure based on EPR sugar-like signal [41] cannot be used beyond 2 - 3 days of radiation treatment. Therefore, alternative methods based on EPR are desirable. Thermal behavior of the EPR signal was investigated in order to distinguish the irradiated rice samples from natural samples. Nonirradiated and irradiated samples were subjected to in situ heating from 27 to 275°C in steps of 50°C prior to EPR spectra recording. Fig. 6b shows the thermal behavior of the nonirradiated and irradiated rice samples after a storage period of 10 and 90 days. The intensity of the central singlet of the irradiated rice after 10 days of storage exhibited a monotonous decrease in signal intensity up to 125ºC followed by almost unchanged behavior up to 275ºC. Whereas, 90 d stored samples, both nonirradiated and irradiated (90 d) showed sharp fall in intensity of the central singlet up to 50ºC followed by slow increase up to 150ºC. However, temperature increase beyond 150°C lead to an increase in signal intensities in both the cases. This could probably be due to the decomposition of the samples and formation of new thermally induced radicals. A decline in EPR signal of irradiated allspice sample has recently been reported by Polovka *et al,* [99]. Yordanov & Gancheva [43] proposed that EPR

analysis of the central peak of spices that had undergone thermal treatment before and relatively long time after irradiation could be a tool for detection of irradiation. But, the present investigation revealed that a complete thermal behavior of the singlet signal of rice samples can give a clue of radiation processing only after a storage period of 10 days. The thermal behavior of the singlet of irradiated and nonirradiated rice samples after a long period of storage exhibited similar characteristics making the identification of irradiated rice sample difficult.

Progressive saturation behavior (PSB) of EPR signal

The electron relaxation behavior of radicals in the rice was studied. The microwave field strength was varied from 0.063 to 50 mW to obtain progressive saturation behavior (PSB). The effect of saturation is manifested by continuous nonlinear increase of EPR signal intensity with square root of microwave power ($P_{MW}^{½}$), reaching a maximum followed by a decrease with the simultaneous increase of EPR line width. Fig. 6c shows the PSB of the central line of nonirradiated and irradiated (1 kGy) samples 10 d after radiation treatment. For the radicals of nonirradiated rice sample a comparatively faster saturation at microwave power around 6 mW followed by a decrease in signal intensity in a monotonic fashion was observed. This saturation behavior revealed the characteristics of organic radicals with a large relaxation time. Whereas, the radicals of irradiated rice sample exhibited saturation at microwave power at around 20 mW. As depicted in Fig. 6d, even after a storage period of 90 days, the relaxation behavior of nonirradiated rice sample exhibited early saturation of central singlet in comparison with the irradiated sample, similar to their behavior noticed 10 days after radiation treatment. The EPR detection of irradiated dry food using microwave saturation has been proposed by Yordanov *et al,* [100]. In this method curves of saturation of nonirradiated and irradiated plants vs. $P_{MW}^{1/2}$ were studied and nonirradiated samples showed saturation at microwave power higher than 15 mW, whereas, irradiated sample exhibited early

saturation at microwave power of around 8 mW. But, in the present study, nonirradiated rice samples exhibited early saturation even after a storage period of 90 days and revealed a significant difference in saturation behavior from irradiated rice samples.

Time kinetics study of EPR signal

Different factors, including humidity, temperature, light intensity, exposure to air and structure of food matrix influence the behavior of induced radicals during storage of the sample before and after irradiation and thereby, restrict the time interval after irradiation during which detection is possible. The fading kinetics of the radiation induced radicals give information on the time interval after which identification of the irradiated samples was possible. Marked decrease in the concentration of free radicals in irradiated foods with time has been reported by many authors [43, 10, 101]. In order to avoid these variations all the samples were kept inside the EPR measurement tube under normal laboratory condition. Kinetics of nonirradiated and irradiated samples was monitored up to 12 weeks after radiation treatment. The radiation induced paramagnetic species identified as starch radical was observed to be stable up to 48 – 72 h after irradiation in the matrix of rice. Therefore, application of EN 1787 and EN 13708 Standards were not possible as a method of detection. Fig. 7 shows the fading characteristics of nonirradiated and irradiated rice samples throughout the storage period of 90 d. The results can be well fitted by a bi-exponential decay described by the following equation:

$$y = y_0 + A_1 \exp(- t/T_1) + A_2 \exp(- t/T_2)$$

where, y represents the EPR signal intensity of the central line. Typical parameter values of the curve for the sample treated with 1 kGy radiation dose obtained with a nonlinear least squares fitting procedure were $y_0 = 10.35$, $A_1 = 38.5$, T_1 (days) = 3, $A_2 = 19.25$ and T_2 (days) = 15. As the EPR signals of cellulose or ‘sugar-like’ signals required by the European Standards were not visible in rice samples after prolonged storage, the application of protocol

EN 1787 or EN 13708 was not possible. However, the rate of EPR saturation of natural radicals in nonirradiated rice in comparison with the radiation induced radicals could be used as a tool to identify irradiated rice.

a)

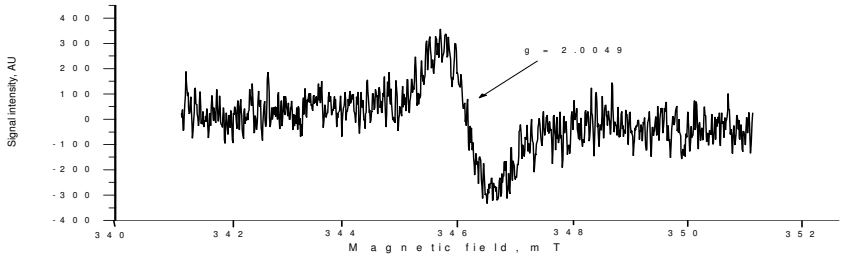

b)

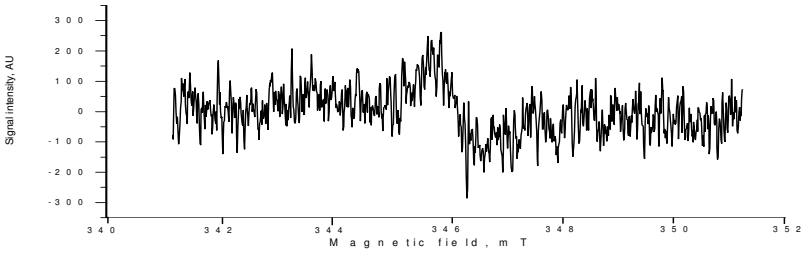

c)

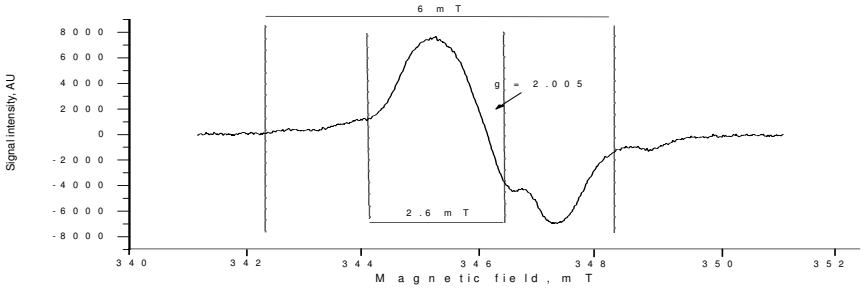

d)

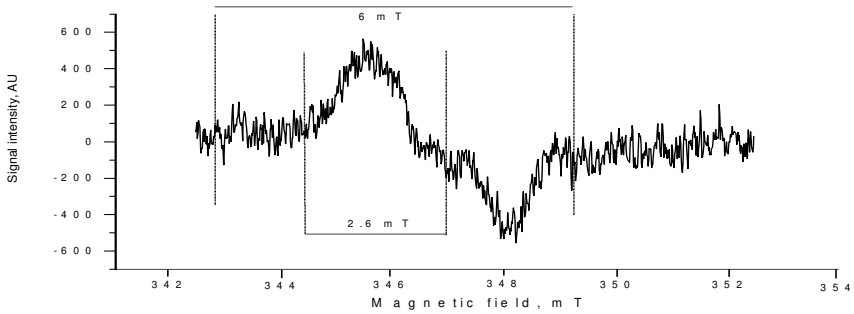

Fig. 5. EPR spectra of **a)** nonirradiated, **b)** heat treated at 100ºC, 1h, **c)** irradiated (1 kGy) rice samples and **d)** EPR spectrum of irradiated pure starch.

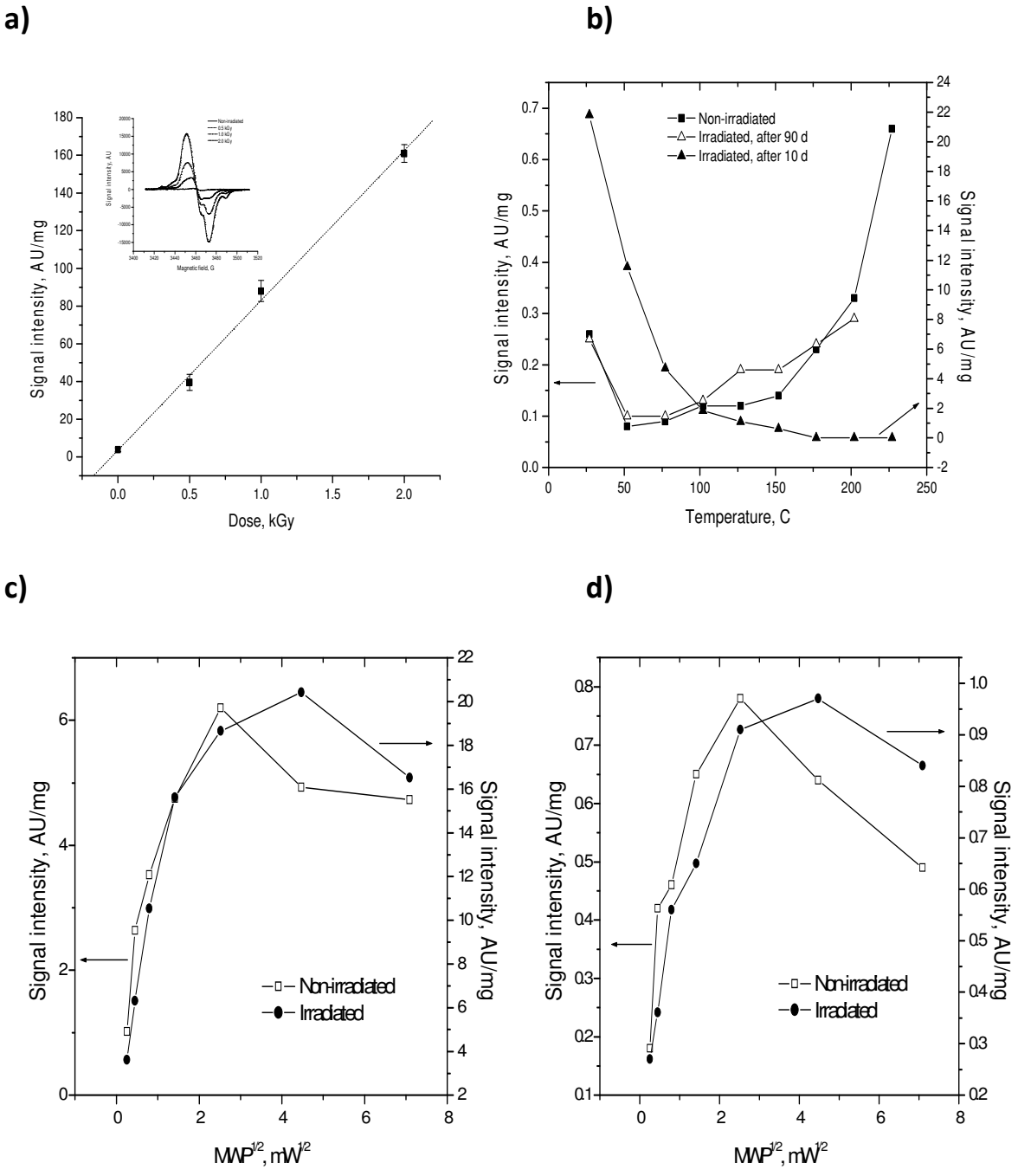

Fig. 6. a) Response of the radiation induced signal intensity of the central line (g = 2.005) with increasing radiation dose, **b)** thermal behavior of the central line of EPR spectrum for nonirradiated, irradiated (after 10 and 90 d) rice samples. Relaxation behavior of main line of nonirradiated and irradiated (1 kGy) rice sample **c)** 10 d after irradiation, **d)** 90 d after irradiation.

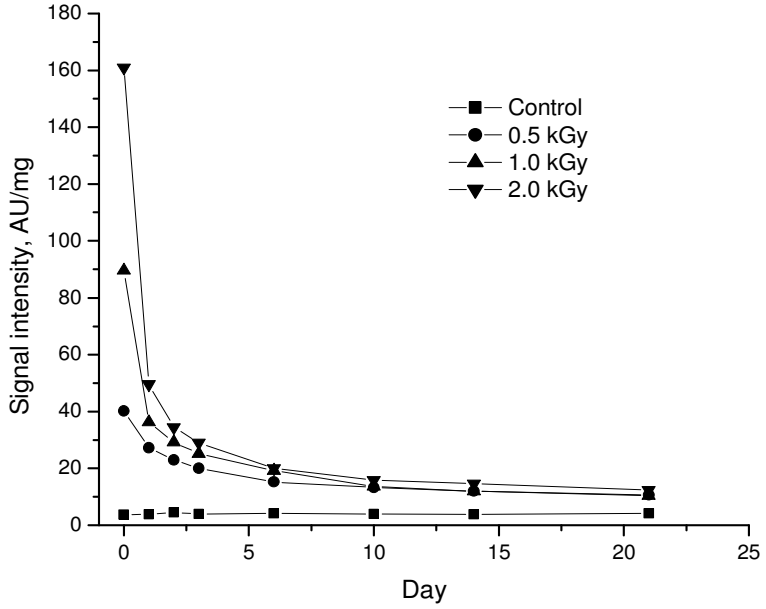

Fig. 7. Kinetics of the central line of the EPR signal of nonirradiated and irradiated rice samples.

Identification by thermoluminescence measurements

TL method is applicable for detection of irradiated foods from which silicate minerals can be isolated [45]. Therefore, investigation on the composition of the isolated minerals from rice samples was of paramount importance to assess the possibility of employing TL for identification of irradiated rice. In view of this, the composition of the separated polyminerals from rice sample was studied using scanning electron microscopy (SEM) and energy dispersive X ray spectrometer (EDX) analysis. The results of these qualitative studies were interesting to examine the relative abundance of polyminerals. Fig. 8a shows the SEM image of the extracted polyminerals from the rice sample revealing the morphology. Fig. 8b shows the EDX spectrum of polyminerals which mainly composed of quartz (SiO_2) and K-feldspars ($KAlSi_3O_8^-$) with a higher abundance of quartz (about 59.6 %) than K-feldspars (20.7 %). Apart from quartz and feldspar, traces of FeO (4.0 %), Na_2O (4.1 %), CaO (11.1%) were also identified. Using X-ray diffraction (XRD) similar patterns of mineral composition have been reported for herbs and spices such as oregano, mint and sage [102], paprika [103], potato [59]. TL response after radiation treatments is mainly responsible for quartz and feldspar component of the polyminerals isolated from the food samples [104].

Fig. 9a shows the TL intensities of glow curves for separated polyminerals from the nonirradiated and irradiated rice samples 10 d after radiation treatment. In case of irradiated sample the glow curve was characterized by a low temperature peak at about 184±4ºC and a high temperature peak at about 282±5ºC. The position of glow peak for nonirradiated sample through all temperature ranges was not clear. However, low level natural radioactivity exhibited TL signal because of deep traps around 295ºC. The yield of the polyminerals on each disc was in the range of 0.5 – 0.6 mg. The areas of glow curves for irradiated samples were 190 to 300 times more than the area from the nonirradiated samples. Higher values of TL glow (Glow 1) in irradiated samples have been reported in previous studies on spices and

herbs [105] and chestnut [64]. Glow peak temperatures at about 207ºC for irradiated anchovy and 192ºC for irradiated chestnut have been reported [64]. Therefore, discrimination between irradiated and nonirradiated rice samples was possible on the basis of the shape of the first glow curve from the separated polyminerals. Normalization of results by reirradiation with a dose of 1 kGy enhanced the reliability of the detection results. Fig. 9 b and c show the comparison of reirradiation glow curves (glow 2) with respect to first glow curves (glow 1) for nonirradiated and irradiated samples, respectively. The reirradiation glow curves (glow 2) were characterized by a glow peak at 168±4ºC and a higher temperature shoulder at 278ºC. The differences of the peak temperatures observed between glow 1 and 2 attributed to the time difference elapsed between irradiation and analysis because low energy trapped electrons were released during storage. Glow 2 was recorded 1 d after exposing to the normalization dose, whereas, samples were stored for several days after irradiation prior to the analysis of glow 1. The ratio of areas for first glow curve to second glow curve (glow 1/glow 2) determined for nonirradiated samples was 0.002±0.023, while for irradiated sample 0.69±0.085. Higher values of ratio of areas for glow 1/glow 2 in irradiated rice samples are in good agreement with the European Standard EN 1788, 1997. TL glow of the irradiated samples were recorded after 65 days of storage in dark with normal laboratory conditions and around 20 % fading in TL glow intensity was observed with clear discrimination from the TL glow of the nonirradiated samples. Therefore, it was possible to discriminate clearly between irradiated and nonirradiated rice samples by the shape of the first TL glow and comparing the TL ratios (glow 1/glow 2).

a) **b)**

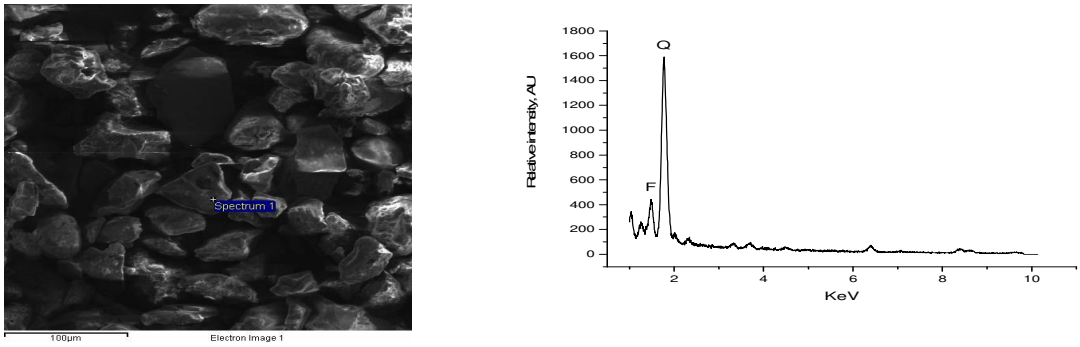

Fig. 8 a) Scanning Electron Microscopy (SEM) image, **b)** Energy Dispersive X ray (EDX) spectrum of the polyminerals extracted from rice. Feldspar: F and Quartz: Q.

a) **b)**

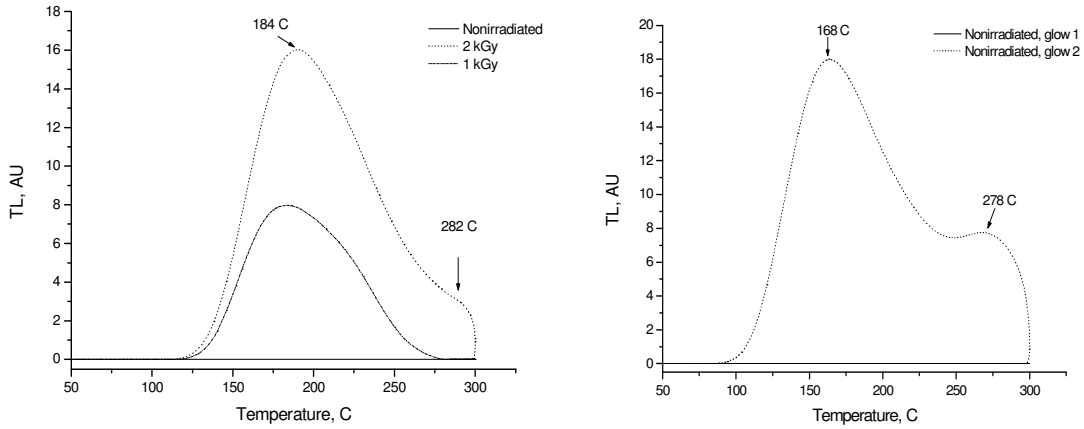

c)

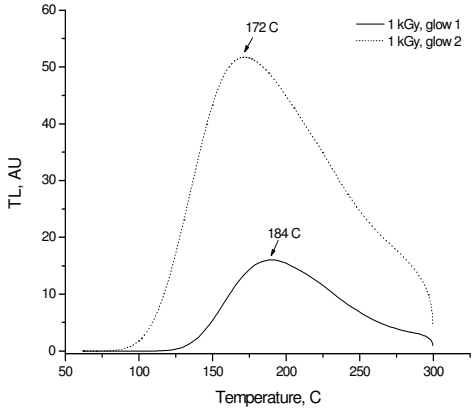

Fig. 9. a) TL glows of isolated minerals from nonirradiated and irradiated rice, **b)** glow1 and glow 2 of nonirradiated sample, and **c)** glow1 and glow 2 of irradiated sample.

Identification of irradiated Soybean

Soybean (Glycine max) is a rich source of nutrition and bioactive phytochemicals. The nutritional quality of soybean has long been ascribed to its high protein and oil content accounting for 40 and 20% of its dry weight, respectively. The remainder consists of carbohydrate 35% and ash 5%. [106]. Insect infestation during storage is a major problem, resulting in economic losses. Irradiation is increasingly being recognized as an effective technology to reduce post-harvest losses and improve quality. Irradiation effects are minimum and similar to those produced by conventional food processing methods, such as heating and freezing [10]. Moreover, a low radiation dose in the range of 0.25 to 1 kGy for insect disinfestation is delivered for commercial irradiation of soybean, making the identification of irradiated product an extremely challenging task.

The main objective of this study was to identify irradiated soybean with commercially approved radiation dose (0.25 to 1 kGy) for the purpose of insect disinfestation, particularly after prolonged storage. Skin and kernel parts of soybean were studied separately using EPR spectroscopy. Stable radiation induced signal identified in the skin part was characterized by EPR spectrum simulation technique. In addition to that a detailed study of EPR saturation characteristics and thermal behavior of the induced radicals were carried out to distinguish between treated and nontreated samples, when the satellite lines due to cellulose have presumably disappeared due to prolonged storage.

EPR spectroscopy to identify irradiated soybean

Skin and kernel parts of nonirradiated and irradiated soybean were separated and EPR spectroscopy was carried out. Fig. 10a shows the EPR spectra recorded using a broad magnetic field sweep width (100 mT) of skin part of soybean before radiation treatment. A singlet EPR signal at g = 2.0046±0.0004 centered around 347.8 mT was observed. This g value obtained compared well with those reported in literature [107, 34, 108]. Fig. 10 b shows

the EPR spectrum 1 d after the radiation treatment with dose 1 kGy of the skin part with an increase in signal intensity of the existing weak singlet (g = 2.0046) by a factor of 7. Irradiation was explained to be responsible for the relatively high intensity increase. The exposure to gamma radiation leads to another paramagnetic species (triplet signal) at the same g value as that of nonirradiated samples with hyperfine coupling constant (hfcc) 3 mT. In order to characterize the radiation induced signals in skin part of irradiated soybean, EPR spectra simulation studies were carried out using WIN EPR and Simfonia programme (BRUKER). The detailed simulation scheme of EPR spectra of the skin part of soybean irradiated with a dose of 1 kGy is depicted in Fig. 11a – d and their spin Hamiltonian parameters ($g_{\perp}$, $g_{\parallel}$, $A_{\perp}$, $A_{\parallel}$; ΔB_{pp}) used in simulation are summarized in Table 5. The spectrum as depicted in Fig. 11c was simulated as a linear combination of the individual signals represented in Fig. 10a and b ($R^2 = 0.968$). Simulation of EPR spectra obtained from irradiated skin revealed the formation of two paramagnetic species, one was singlet signal attributed to phenoxyl radical ($C_6H_5O^-$) ion and the other was triplet signal of cellulose radicals. The signal attributed to cellulose radical was induced by the ionizing radiation as a consequence of the cleavage of cellulose polymer chain. Korkmaz & Polat, 2001 [13] have reported similar observation for gamma irradiated red pepper.

EPR spectra of the kernel part of nonirradiated and irradiated soybean were carried out using similar experimental parameters as that of the skin part. Fig. 10c shows the EPR spectrum of nonirradiated kernel depicting a sextet signal at g = 2.0046 with hyperfine interaction of hfcc = 9.4 mT. This signal was attributed to Mn^{2+} ion. Existence of Mn^{2+} has also been reported for ground black pepper and wheat flour [15]. Fig. 10d shows the EPR spectrum of irradiated (1 kGy) soybean kernel part. A sharp and intense EPR singlet at g = 2.0047 was observed superimposed on the sextet signal of Mn^{2+}. This radiation-induced signal was attributed to carbon centered organic radical. Similar observation has been reported by Oliveria *et al*, 2007

[106] and proposed it as a marker of radiation treatment. However, this radiation specific signal observed in the matrix of kernel part was not particularly stable and disappeared after 10 - 12 d to a level that was similar to that of nonirradiated specimen, exhibiting only the sextet signal of Mn^{2+}. The instability in signal intensity indicates that the detection of irradiated soybean by EPR spectroscopy of kernel part is limited.

Dose dependent response of EPR signal

The effect of increasing radiation dose from 0.25 – 1 kGy on the spectra of skin part of soybean samples was studied. The triplet signal of cellulose for 1 kGy irradiated sample was more prominent in comparison with the sample exposed to 0.25 kGy dose and was visible up to 50 d of storage. But, the sample irradiated with a minimum dose of 0.25 kGy, the radiation specific triplet was visible up to 35 d. The integral intensities of the EPR signals were obtained by double integration of the spectrum and the integral intensity of the central line and was observed to be significantly related to the radiation dose as shown in Fig. 12. The measurement was performed 2 d after irradiation. The dotted line represents a polynomial fit, $Y = aD^2 + bD + c$ with $a = -2.55 \times 10^6$, $b = 3.49 \times 10^6$ and $c = 5.29 \times 10^5$, and each point wass the mean value of three samples.

Relaxation and thermal behavior of EPR signal

Characterization of the free radicals, naturally present or induced by radiation was essential for the investigation of radiation treatment. In view of this, two independent techniques based on EPR were employed, one was to study the electron relaxation behavior and the other was thermal characteristic of the EPR signals. In order to determine the electron relaxation behavior of the radicals in soybean, we varied the microwave field strength from 0.063 to 50 mW to obtain progressive saturation behavior (PSB). Fig. 13a shows the PSB of the central line ($g = 2.0047$) and Mn^{2+} signal of irradiated (1 kGy) soybean kernel part five days after radiation treatment. A comparatively faster saturation with microwave power around 6 mW

followed by a decrease in the signal intensity in a monotonic fashion was observed for the radiation induced signal in kernel. However, the PSB of Mn^{2+} signal showed a monotonous increase in signal intensity without any saturation confirming the characteristics of paramagnetic centre of inorganic origin and short relaxation time. Fig. 13b shows the behavior of the organic and inorganic signals in the matrix of kernel with increasing temperature from 27 to 177°C. The intensity of the central singlet (g = 2.0047) exhibited a sharp fall in signal intensity up to 52ºC followed by almost unchanged behavior up to 127ºC. However, temperature increase beyond 127°C lead to an increase in signal intensity probably as a result of phase transition of the organic matrix and formation of new thermally induced radicals. Whereas, in case of inorganic signal of Mn^{2+} a monotonous decrease was observed in signal intensity up to 147°C without further increase with temperature.

The most important objective of identification of irradiated food is to trace the signal, which is originated only because of radiation treatment. In order to validate a method for identifying irradiation, free radicals produced by other processing techniques such as heating (thermolysis) must be distinguished from those produced by irradiation. In view of this, whole soybean was subjected to thermal treatment at 100ºC for 1 h and EPR spectrum of skin part was recorded. The heat energy did not induce any specific change in the EPR spectrum. However, the intensity of the singlet (g = 2.0046) similar to that of nonirradiated sample was observed. In order to distinguish nonirradiated, irradiated and thermally treated soybean samples, a detailed investigation of the paramagnetic centres of skin part were carried out by PSB studies and thermal characteristics after storage period of 60 d. Fig. 14a showed that a comparatively faster saturation at microwave power of 6 mW followed by a decrease in signal intensity in monotonic fashion was observed for thermally induced radicals. This saturation behavior revealed the characteristics of organic radicals with a large relaxation time. But both the non-irradiated and irradiated (0.25 and 1 kGy) samples exhibited similar behavior of

microwave saturation at around 20 mW. Therefore, EPR analysis by PSB of the radicals may not be a useful method to distinguish irradiated soybean sample. However, faster EPR saturation of thermally induced radicals in comparison with the radiation-induced radicals could be used as a tool to distinguish between irradiated and heated soybean.

In order to address the problem of detection of irradiated soybean thermal behavior of the EPR signal was investigated. Nonirradiated, irradiated and thermally treated samples were subjected to in situ heating from 27 to 177°C. Fig. 14b shows the thermal behavior of the central singlet for nonirradiated, irradiated and thermally treated samples 1 d after heat and radiation treatments. With the increase in temperature from 27 to 127°C, the central lines of nonirradiated and thermally treated samples exhibited a slow fall, but, that of irradiated samples showed a sharp fall of about 84 %. However, temperature increase beyond 152°C lead to an increase in EPR signal intensities in all the cases. Fig. 14c shows the thermal characteristics of the same samples after a storage period of 60 d. Samples irradiated with doses 1 and 0.25 kGy exhibited a sharp fall in signal intensities of 60 and 55 %, respectively. Whereas, nonirradiated sample showed slower fall in signal intensity of around 34 % up to a temperature of 152ºC. These results are in agreement with the proposal of Yordanov & Gancheva [43] that, EPR analysis of the central peak in case of spice samples, that had undergone thermal treatment relatively long time after irradiation, could be used as a tool for detection of irradiation.

Time kinetics of EPR signal

The time interval after which identification of the irradiated samples is possible was evaluated by the fading kinetics of the radiation induced radicals. In case of kernel part, the EPR singlet at g = 2.0047 was visible with a marked decrease in intensity up to 15 d of radiation treatment. However, for skin part of the sample received 1 kGy dose, the radiation specific triplet signal of cellulose was visible almost throughout the storage time. But, for the sample

irradiated with 0.25 kGy dose, triplet signal was distinguishable only for a time period of about 30 d. Decrease in the concentration of free radicals in irradiated spices with time have been reported by many authors [43, 10, 101]. Therefore, application of EN 1787 Standard was not possible as a method of detection for the samples irradiated with a minimum dose of 0.25 kGy and stored beyond 30 d. The application of protocol EN 1787 was not possible as the EPR signals of cellulose required by the European Standards were not visible in soybean sample after a prolonged storage. Therefore, temperature profiles of the respective samples depicting the thermal behavior of the gamma induced EPR signal represented a valuable tool for the assessment of previous radiation treatment.

Table 5. Spin Hamiltonian parameters of gamma irradiated induced EPR signals observed in soybean (skin part) treated with 1 kGy dose.

Origin of EPR signal	g- value	Hyperfine splitting (mT)	ΔB_{pp} (mT)
Phenoxyl (O^-) radical	2.0040	0.00	0.9
Cellulose	$g_\perp = 2.0040$	$A_\perp = 3$	1
	$g_\parallel = 2.0032$	$A_\parallel = 1.8$	

a)

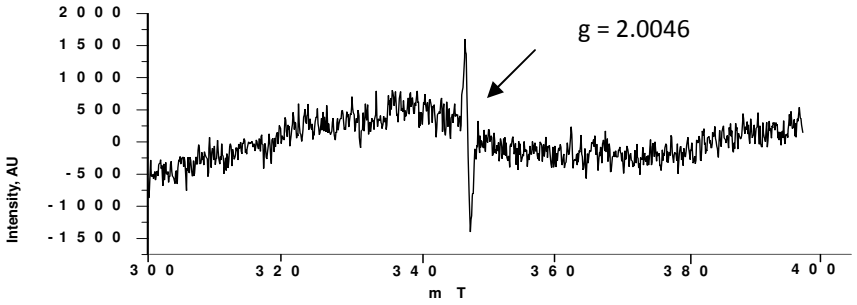

b)

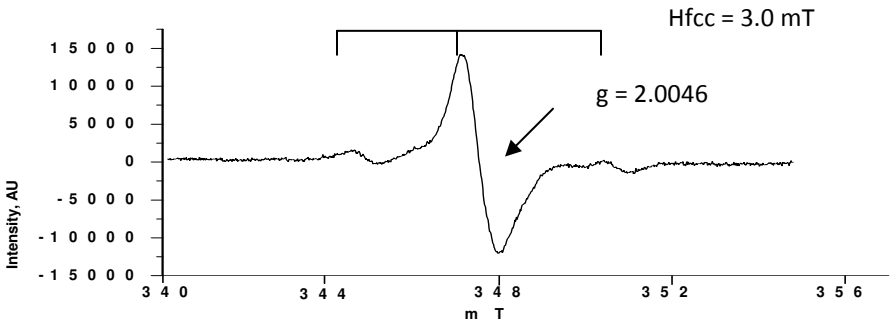

c)

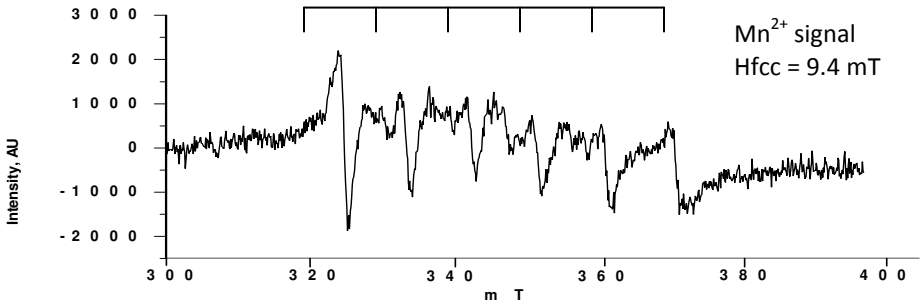

d)

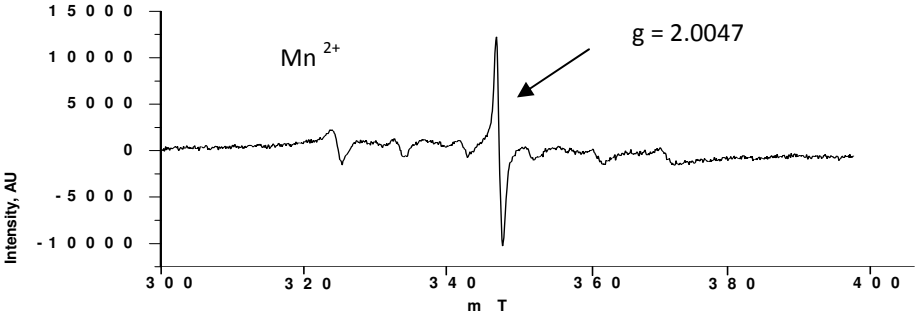

Fig. 10. EPR spectra of soybean recorded at room temperature **a)** nonirradiated skin part, **b)** 1 d after radiation treatment (1 kGy) of the skin part, **c)** nonirradiated kernel part, and **d)** 1 d after radiation treatment (1 kGy) of the kernel part.

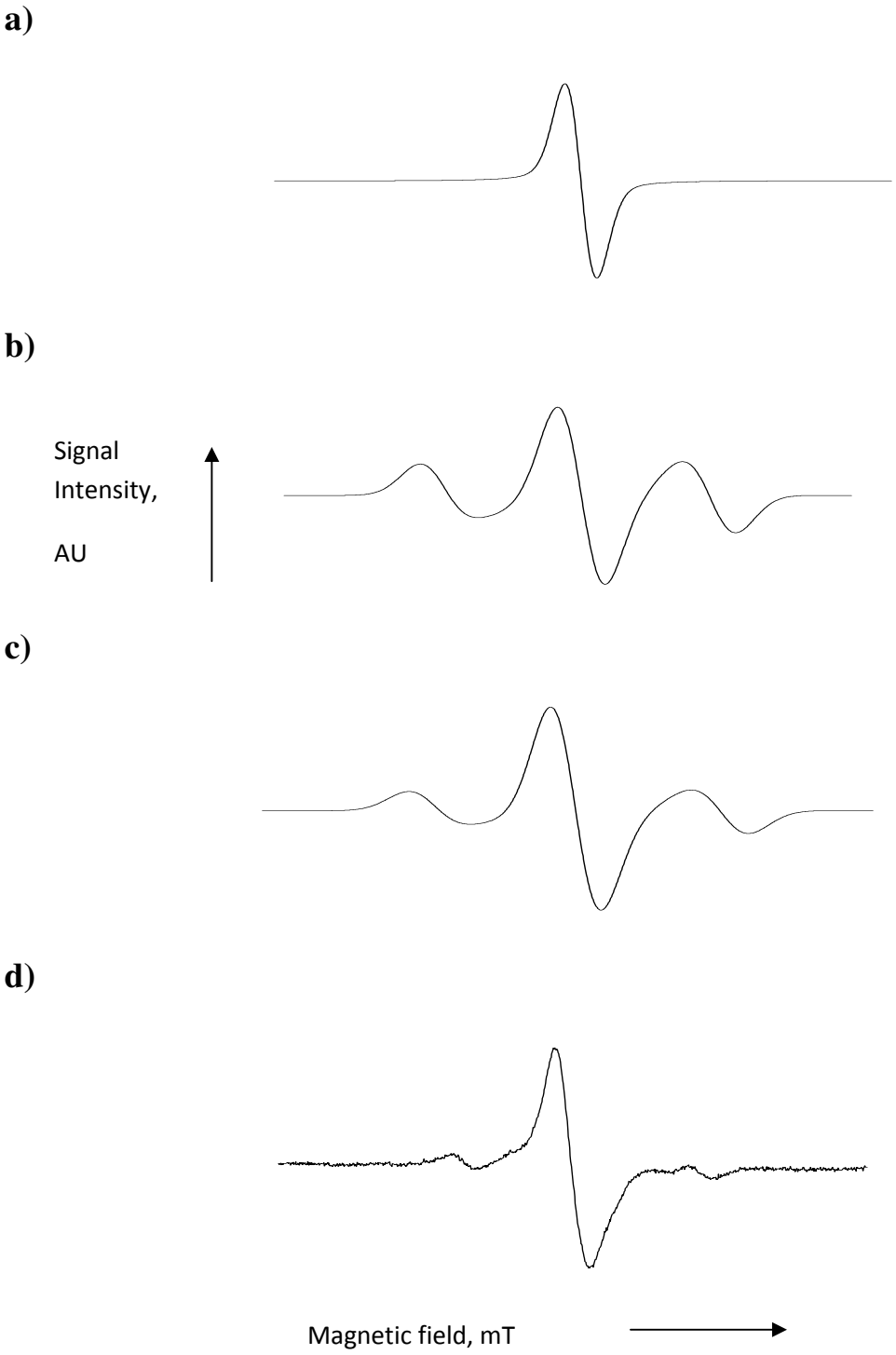

Fig. 11. A scheme demonstrating a simulation analysis of experimental EPR spectrum of irradiated (1 kGy) soy bean sample **a)** simulation spectrum of phenoxyl ($C_6H_5O^-$) radical, **b)** simulation spectrum of cellulose radical, **c)** linear combination of the individual spectrum represented in a and b, **d)** experimental spectrum of irradiated sample.

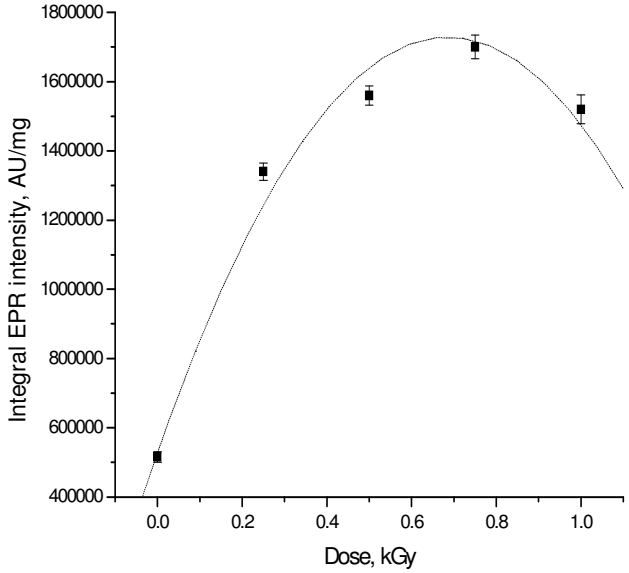

Fig. 12. Response of the radiation induced signal (g = 2.0046) and the dependence of double integral EPR signal intensity evaluated with increasing dose after 2 d of radiation treatment.

a) **b)**

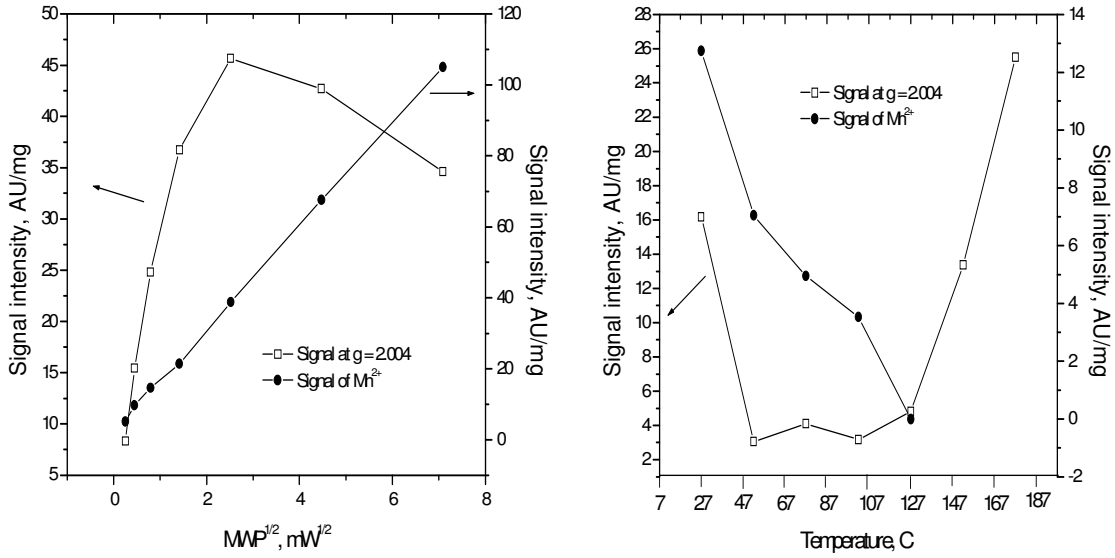

Fig. 13. a) Relaxation characteristics and **b)** thermal behavior of the paramagnetic centres (g = 2.0047) in irradiated (1 kGy) kernel part of soybean after 5 d of radiation treatment.

a)

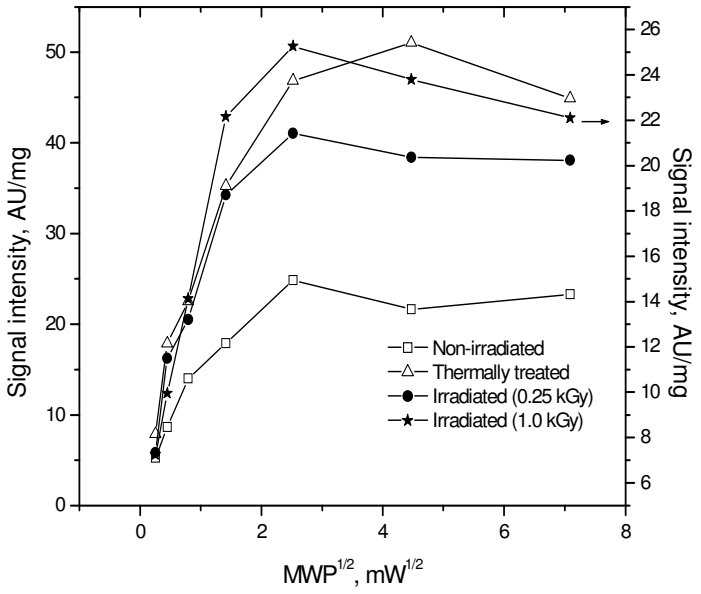

b) **c)**

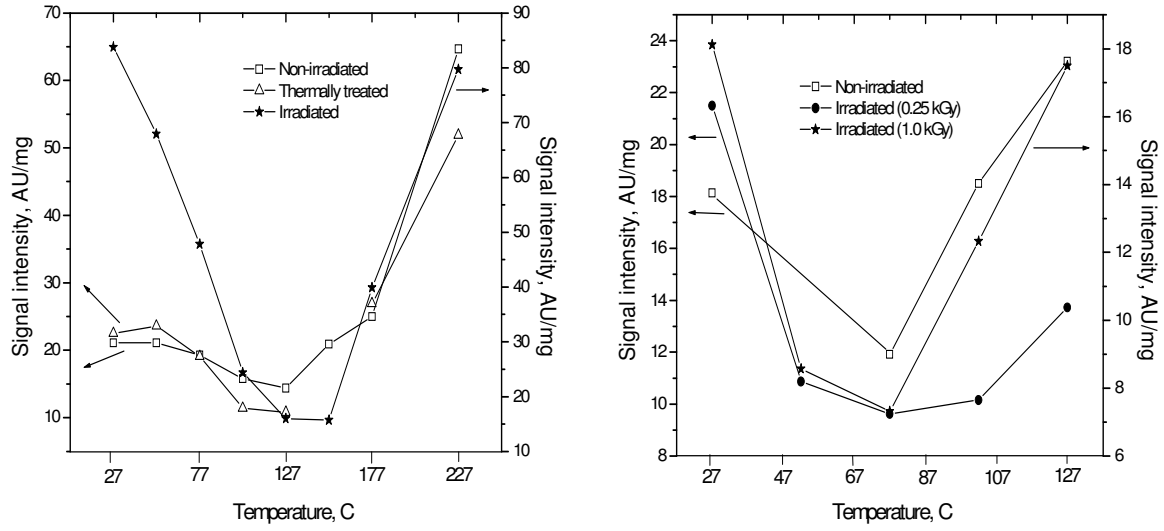

Fig. 14. a) Relaxation characteristics of the central singlet of nonirradiated, thermally treated and irradiated soy bean 60 d after radiation treatment. Thermal behaviors of skin part of soybean **b)** 1 d after the treatments and **c)** 60 d after the treatments.

CHAPTER 5

Identification of irradiated

Potato, Ginger, Fresh turmeric and Dog feed

Identification of irradiated potato using TL technique

The objective of the study was to identify potato of different geographical locations in India irradiated to sprout inhibiting dose, using TL characteristics of the isolated minerals. Potato (Chandramukhi) from two different districts, Bankura and Midnapore of West Bengal and markets of metro cities of Delhi and Mumbai were procured. The samples from each location were divided into three lots. One lot was kept as nonirradiated (control) and the remaining lots were irradiated with gamma radiation doses of 100 and 250 Gy. Minerals were isolated from both the nonirradiated and irradiated potatoes by density separation method. Characterization of the isolated minerals was carried out by X-Ray diffraction (XRD) technique to know the composition. XRD spectra of the isolated minerals from four different geographical locations are shown in Fig. 15 a – d. The XRD analysis of the polyminerals separated from potato showed that the relative abundance of K-feldspars ($KAlSi_3O_8^-$) and quartz (SiO_2) were predominant. However, a little variation in polymineral composition was observed with different origins of production. Similar patterns of mineral composition by X-ray diffraction (XRD) have been reported in herbs and spices such as oregano, mint and sage [102] and potato of South Korea [59]. TL response after radiation treatment is mainly responsible for quartz and feldspar component of the polyminerals isolated from food samples [104]. These findings revealed the possibility of using TL technique to identify irradiated potato.

TL glows were recorded from room temperature to 350°C at a heating rate of 5°C/s. The intensities of the glow curves for both the nonirradiated and irradiated samples showed significant difference even after a storage period of one month. Around 86 fold increases in TL glow (glow 1) of irradiated samples in comparison with nonirradiated ones was observed. Fig. 16 exhibited the TL glow of the irradiated and nonirradiated samples isolated from the potato procured from Bankura district of West Bengal after a storage period of 38 days. In all the cases, the glow curves (Glow 1) of irradiated samples were characterized by peak

temperature at around 204°C, whereas, the position of glow 1 for control sample through all temperature ranges was not clear. However, a small hump was observed at around 345°C, probably, because of the deep traps due to the presence of low level natural radioactivity in the environment.

Normalization dose of 250 Gy was delivered to all the samples and TL glow (glow 2) was measured with similar experimental settings. The reirradiation glow curve (glow 2) was characterized by a glow peak at 175ºC as depicted in Fig. 16b. The differences of the peak temperatures observed between glow 1 and 2 are attributed to the time difference elapsed between irradiation and analysis because of low energy trapped electrons released during storage. The ratio of glow 1 / glow 2 for nonirradiated samples of all the geographical locations was 0.003±0.0005 and for irradiated samples it was 0.25±0.052. Higher values of ratio of areas for glow 1/glow 2 in irradiated potato samples are in good agreement with the European Standard EN 1788, 1996 [45]. In order to study the effects of increasing dose on the polyminerals, the potato samples were irradiated with 100, 250, 500 and 1000 Gy doses. Minerals were isolated from the potatoes by standardized density separation method to study the TL response. An increase in integral TL was observed with the increasing dose as depicted in Fig. 16c.

The results of the present study revealed that isolation of polyminerals from the surface of potato is possible using density separation and TL measurement can clearly differentiate between irradiated and nonirradiated samples. The reirradiation step improved the reliability of the detection results of TL.

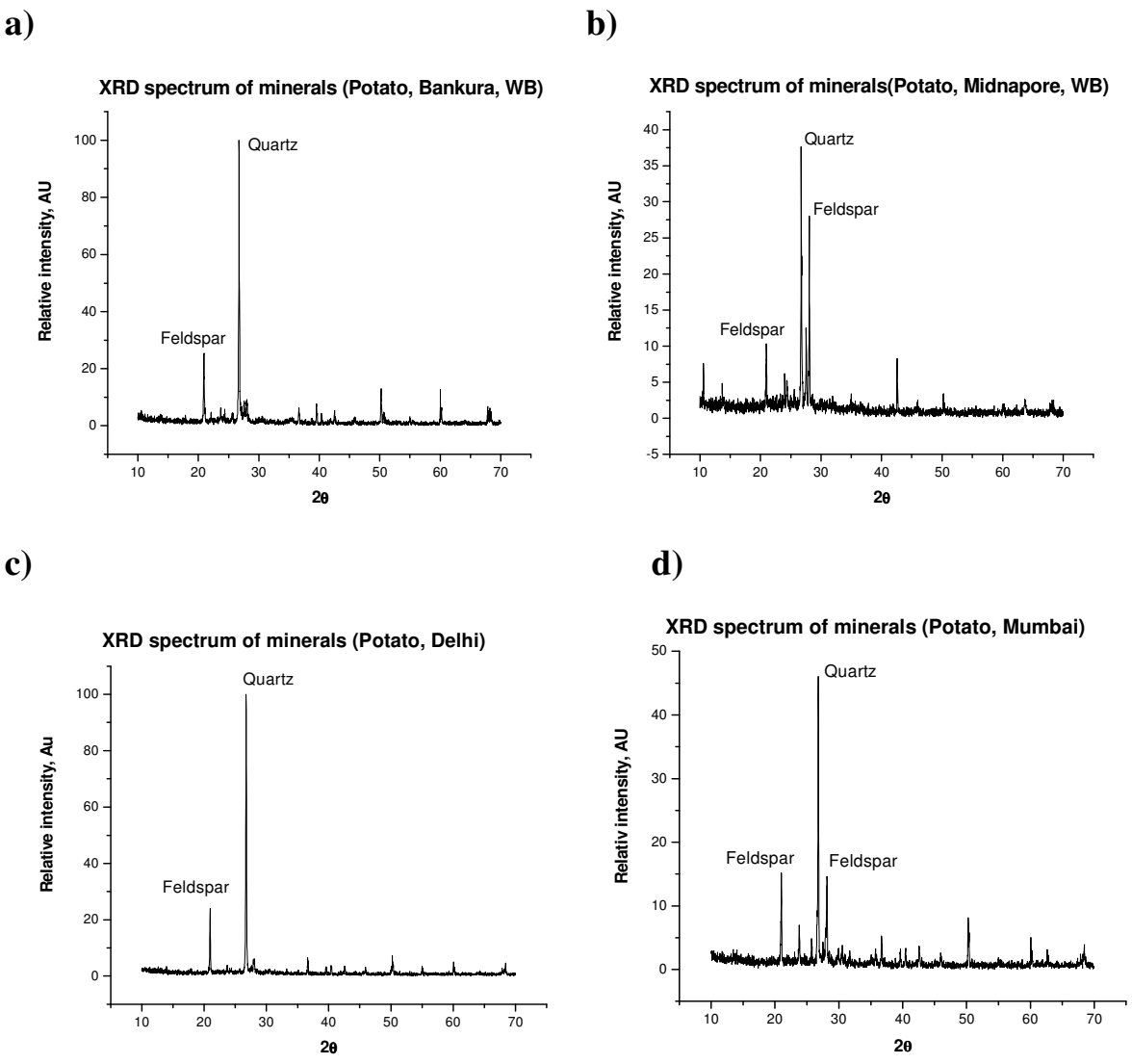

Fig. 15. XRD spectra of the isolated minerals from the potato of different geographical locations **a)** Bankura, West Bengal, **b)** Midnapore, West Bengal, **c)** Delhi and **d)** Mumbai.

a) **b)**

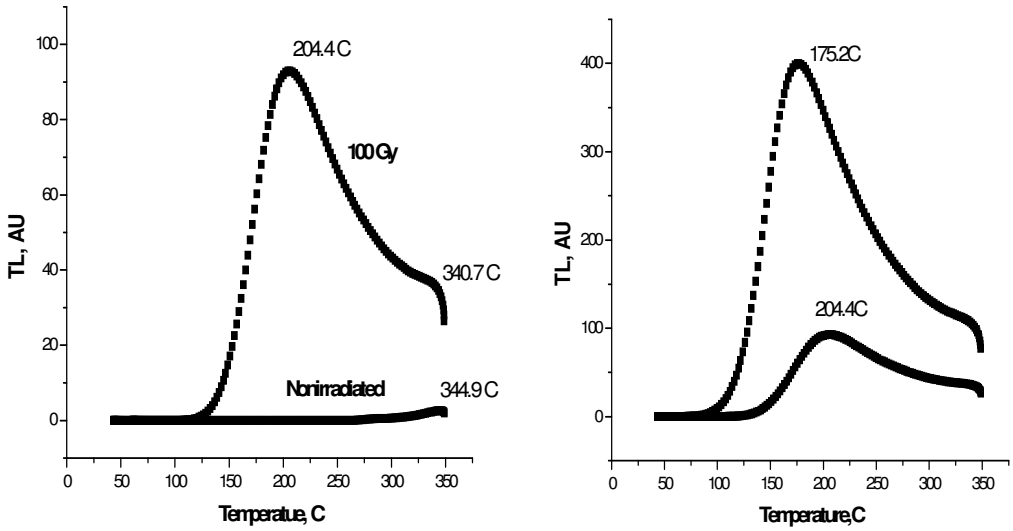

c)

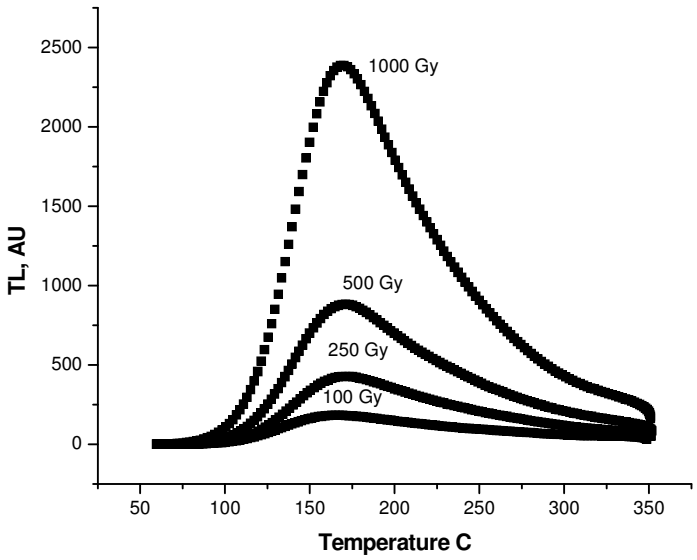

Fig. 16. a) TL glow curves of isolated minerals from nonirradiated and irradiated potato and **b)** TL glow 1 and glow 2 of the irradiated samples from Bankura district, West Bengal, **c)** TL glow curves of the isolated minerals from irradiated potato with increasing radiation dose.

Identification of irradiated ginger and fresh turmeric using TL technique

Identification of irradiated ginger (*Zingiber officinale*) and fresh turmeric (*Curcuma longa*) were studied using TL technique. Ginger and fresh turmeric were procured from a local market in Mumbai and distributed into three lots. One lot was kept as nonirradiated (control) and the remaining lots were irradiated with gamma radiation doses of 80 and 120 Gy. Minerals were isolated from both the nonirradiated and irradiated samples by density separation method. TL glow curves were recorded by heating the isolated minerals from room (27±2°C) temperature to 330°C at a heating rate of 5°C/s. The integral TL and the intensities of the glow peaks for both the nonirradiated and irradiated samples showed significant difference even after a storage period of one month. Around 50 fold increase in integral TL glow (glow 1) in irradiated ginger and around 20 fold increase in glow (glow 1) in case of irradiated fresh turmeric were observed in comparison with their respective nonirradiated samples. Fig. 17a and b show the TL glow curves of the irradiated and nonirradiated minerals isolated from ginger and fresh turmeric after a storage period of 35 days. In all the cases, the glow curves (Glow 1) of irradiated samples were characterized by a peak at temperature of 225±4°C and a small hump at a high temperature of 330±2°C, whereas, the position of glow curve 1 for control sample through all temperature ranges was not prominent.

Normalization dose of 1 kGy was delivered to all samples and TL glow (glow 2) was measured with similar experimental settings. The reirradiation glow curve (glow 2) for both the nonirradiated and irradiated samples isolated from ginger were characterized by an intense glow peak at 152±4°C and a high temperature hump at around 330°C as depicted in Fig. 18a and b. The reirradiation glow curve characteristic (glow 2) of the inorganic minerals isolated from the nonirradiated and irradiated fresh turmeric were also characterized by an intense glow peak at 152±4°C. In addition two more weak peaks were identified at 226±3°C and 331±1°C as shown in Fig. 18 c and d confirming the polyminerals nature of the isolated

samples. The differences in the peak temperatures observed between glow 1 and 2 were attributed to the time difference elapsed between irradiation and analysis. The low temperature peak of glow 2 at around 155°C in all the samples was recorded immediately after reirradiation dose of 1 kGy. The peak temperature suggested that this peak was responsible for shallow trapped electrons and was not stable during prolonged storage. Glow 1 (Fig. 17a, b) for all the samples were recorded after a period of one month, and therefore, a stable peak at around 225°C was observed. The ratio of glow 1 / glow 2 for nonirradiated ginger and fresh turmeric was negligibly small (0.00002). Whereas, in case of irradiated (80 Gy) ginger and fresh turmeric the same was measured as 0.02±0.0011 and 0.02±0.002, respectively. The glow curve structure (glow 2) of reirradiated samples confirmed the inorganic nature of the sample material. The higher values of glow1 / glow 2 in irradiated samples endorsed the effective detection of radiation treatment in good agreement with the European Standard EN 1788, 1996 [45]. In all the cases the higher dose of irradiation at 120 Gy exhibited increased level of TL output. The results of the present study revealed that isolation of polyminerals from the surface of ginger and fresh turmeric was possible using density separation, and TL measurement can clearly differentiate between irradiated and nonirradiated samples. The reirradiation step improved the reliability of the detection results of TL.

a)

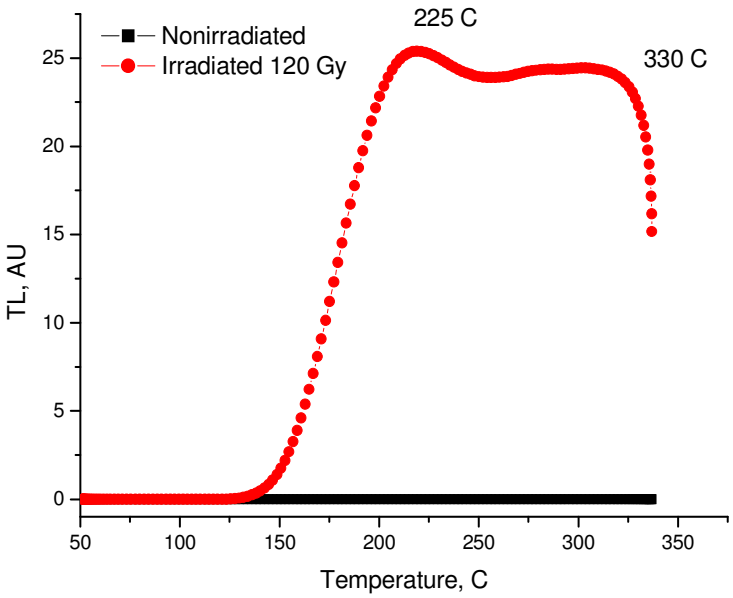

b)

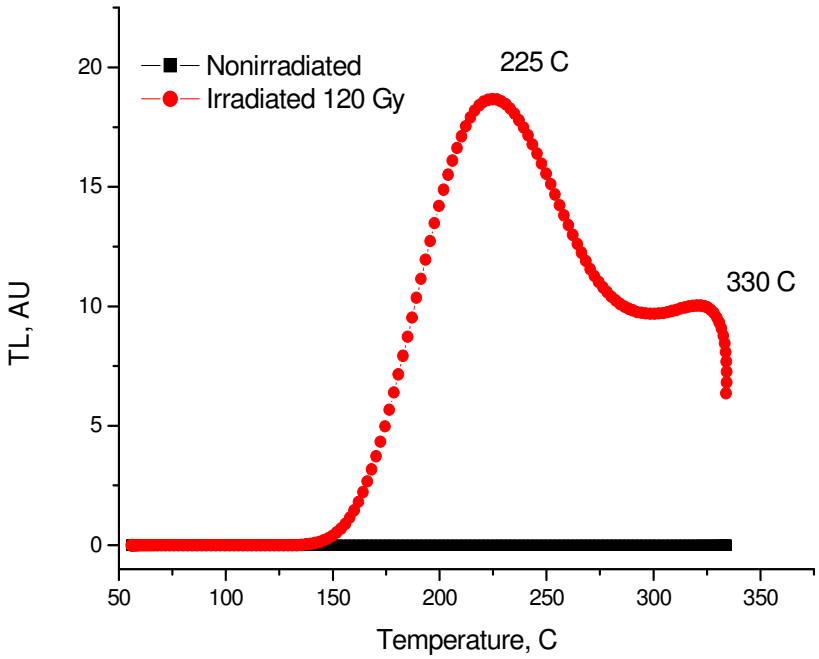

Fig. 17. TL glows (glow 1) of the isolated minerals from the irradiated and nonirradiated samples of **a)** ginger and **b)** fresh turmeric.

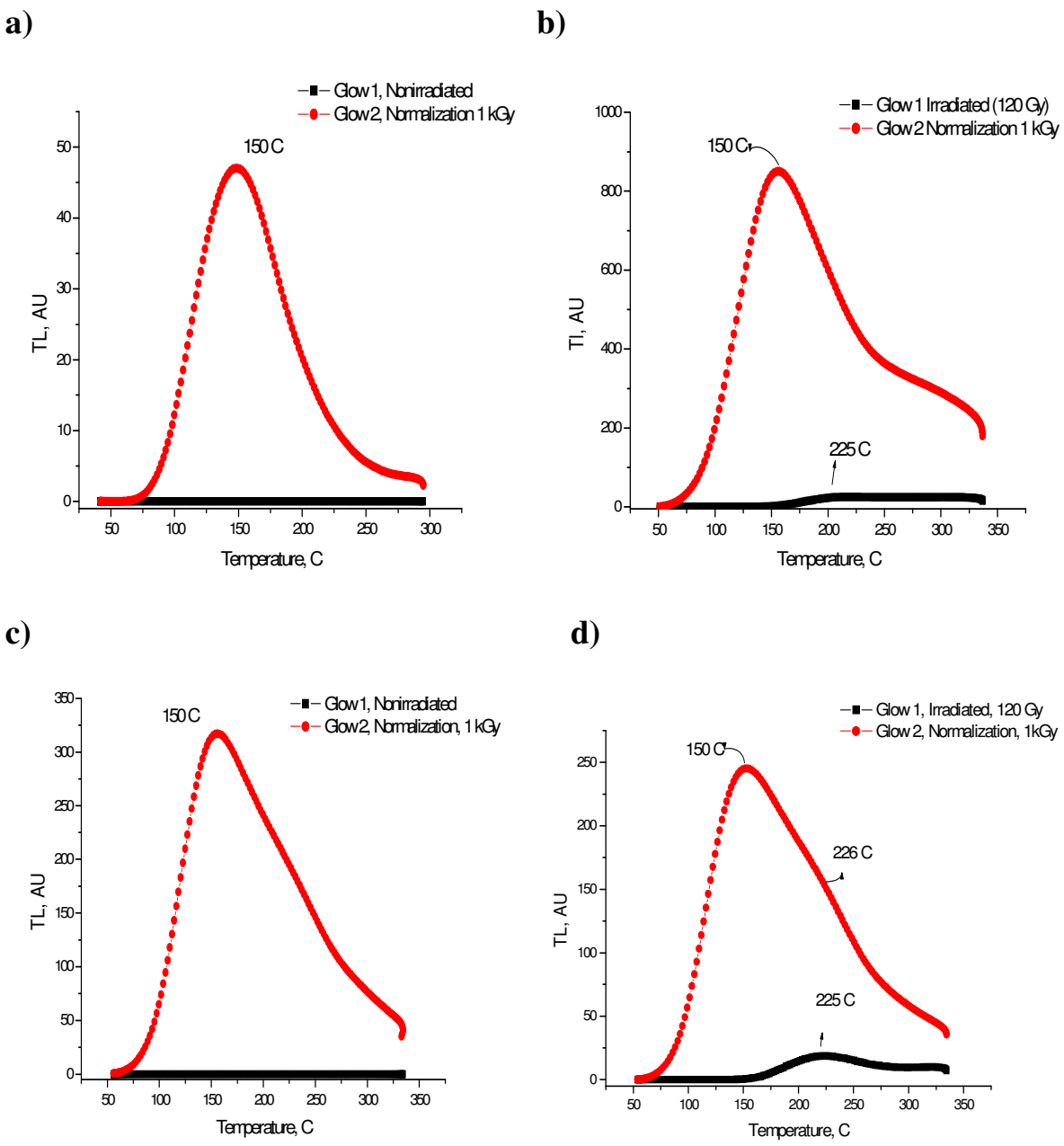

Fig. 18. Glow curve characteristics of glow 1 and glow 2 (normalized with 1 kGy) of the isolated minerals from **a)** nonirradiated ginger, **b)** irradiated (120 Gy) ginger, **c)** nonirradiated fresh turmeric, and **d)** irradiated (120 Gy) fresh turmeric.

Identification of irradiated dog feed

Exposure to ionizing radiation is an effective microbial disinfection process for animal feed. It is currently used in many countries for dog chew to control pathogens namely *Salmonella.* The irradiation of poultry feed for control of *Salmonella* is also approved by FDA in US. In India, commercial radiation processing of animal feed is carried out for microbial decontamination with an average dose of 7 kGy. Pet food manufacturers use dietary fiber sources from grains, fruits and vegetables, celluloses, gums, and other sources. The main ingredients normally include cereal and cereal byproducts, meat and poultry industry waste, vegetable byproducts, proteins, vegetable oils, iodized salt, essential vitamins and minerals. In the present work, a detailed study of the radical species produced by gamma radiation in two varieties of dog feeds, namely, ready-to-eat granular form and edible dog chew in stick form has been carried out by EPR spectroscopy. The thermoluminescence technique has also been employed for confirmation of identification of radiation treatment of the samples. In addition, characterization of the extracted minerals from the edible dog chew samples was carried out for TL studies and the requirement of independent detection methods to give reliable identification of the irradiated samples has been established.

EPR spectroscopy on granular dog feed

Fig. 19 a depicts the EPR spectra recorded with microwave power 0.253 mW of nonirradiated and irradiated samples of granular form ready to eat dog feed. The EPR spectrum of nonirradiated sample was characterized by a singlet with g = 2.0047±0.0003 and ΔB_{pp} = 0.810 mT. These free radicals were of semiquinones produced by the oxidation of polyphenolics [96] or lignin [97, 98]. Immediately after the radiation treatment of the sample at 7.5 kGy dose, a complex and broad EPR spectrum was observed with an increase in signal intensity of the existing weak singlet (g = 2.0052±0.0002). Increase in line width (ΔB_{pp}) of the EPR signal from 0.766 to 1.311 mT could probably be attributed to the induction of multiple

paramagnetic centres in the matrix of dog feed. As shown in Fig. 19a, both nonirradiated and irradiated EPR spectra recorded with low microwave power of 0.253 mW, did not show any radiation specific signal. However, when the same samples were subjected to high microwave power of 50 mW, a visible change in the shape of the EPR spectrum was observed in case of irradiated sample as depicted in Fig. 19 b. The signal characterized by g = 2.0052 exhibited reduction in signal amplitude and an axially symmetric anisotropic signal with $g_{\perp}$ = 2.0028 and $g_{\parallel}$= 1.9976 was identified. In order to characterize the radiation induced signal, EPR spectra simulation studies were carried out using WIN EPR and Simfonia programme (BRUKER). The detailed simulation scheme of EPR spectra of ready-to-eat granular form dog feed irradiated with a dose of 7.5 kGy is depicted in Fig. 20 a – c. Fig. 20 c exhibits the superposition of experimental and simulated spectra. The simulated spectrum was a linear combination of the individual signals represented in Fig. 20 a and b (R^2 = 0.962). Simulation of EPR spectra revealed the formation of two paramagnetic species. The isotropic signal was attributed to phenoxyl radical ion ($C_6H_5O^{\cdot}$). The other anisotropic signal was probably because of $CO_2^{\cdot-}$ radical ion formed due to breakdown of the fatty acid which is one of the major constituents of the chicken meat associated with ready-to-eat dog feed. The spin Hamiltonian parameters used to simulate phenoxyl radical ion were g = 2.0052 and ΔB_{pp} = 0.86 mT and for anisotropic $CO_2^{\cdot}$ radical ion, $g_{\perp}$ = 2.0028, $g_{\parallel}$ = 1.9976 and ΔB_{pp} = 0.30 mT. The g values obtained compare well with those reported in literature [109, 58]. The anisotropic signal of $CO_2^{\cdot}$ observed at 50 mW power was stable throughout the storage period of 90 d and could be considered as a marker for radiation treatment. In order to further reconfirm the nature of these radical species, their electron relaxation behavior was studied. Fig. 21a exhibits the EPR spectra recorded with a narrow scan width of 4 mT and exhibited the behavioral change in signal amplitudes of both the isotropic and anisotropic signals with the variation of the microwave field strength from 0.063 to 50 mW. The inset in Fig. 21a

shows the progressive saturation behavior (PSB) of the signals. The EPR signal at g = 2.0052 showed comparatively faster saturation at microwave power of 20 mW followed by decrease in signal intensity by monotonic fashion. The microwave saturation characteristics of these radicals suggested that they were possibly of organic origin with large relaxation time. However, the PSB of CO_2^- radical ion signal showed a monotonous increase in signal intensity without any saturation confirming the characteristics of paramagnetic centre of inorganic origin and short relaxation time. The integral intensities of the EPR signals were obtained by double integration of the spectrum and the integral intensity of the central line was observed to be significantly related to the radiation dose as shown in Fig. 21b. The integral intensity showed saturation above 7.5 kGy radiation dose. The measurements were performed 2 d after irradiation.

a)

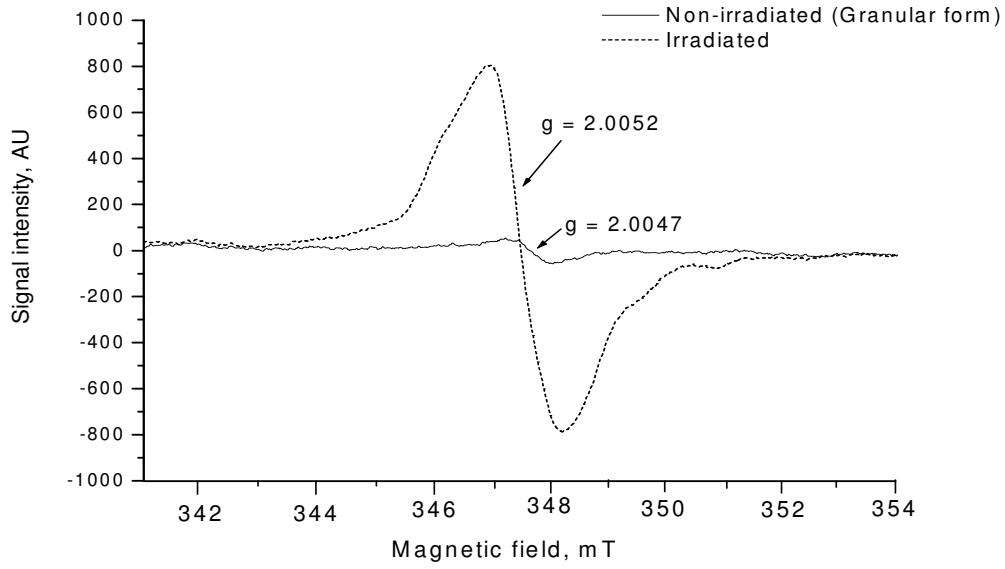

b)

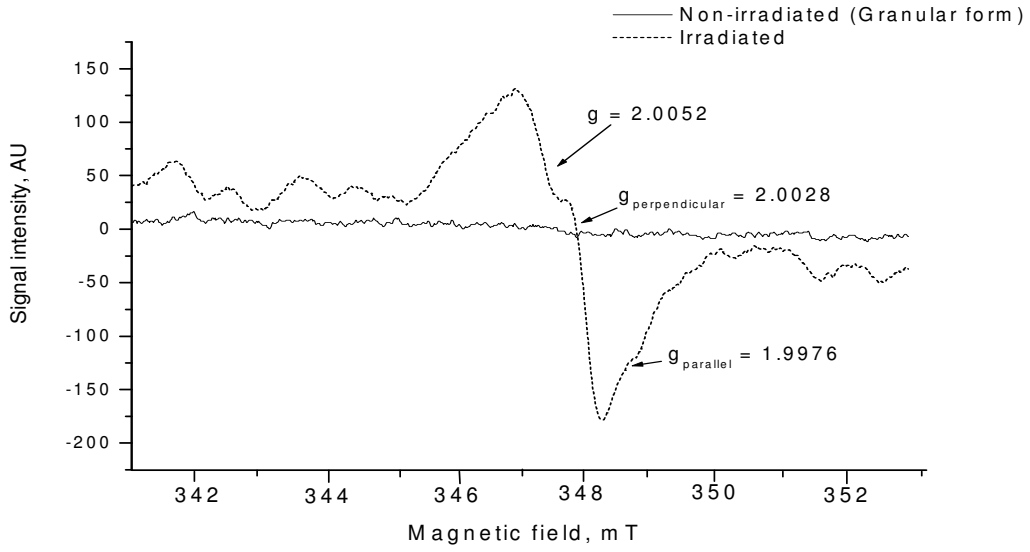

Fig. 19. EPR spectra of nonirradiated (control) and irradiated (7.5 kGy) of ready to eat dog feed (granular form) immediately after irradiation recorded with microwave power **a)** 0.63 mW and **b)** 50.2 mW.

a)

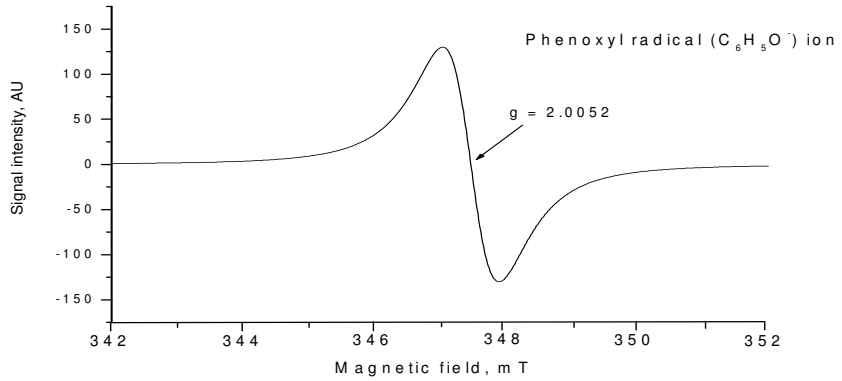

b)

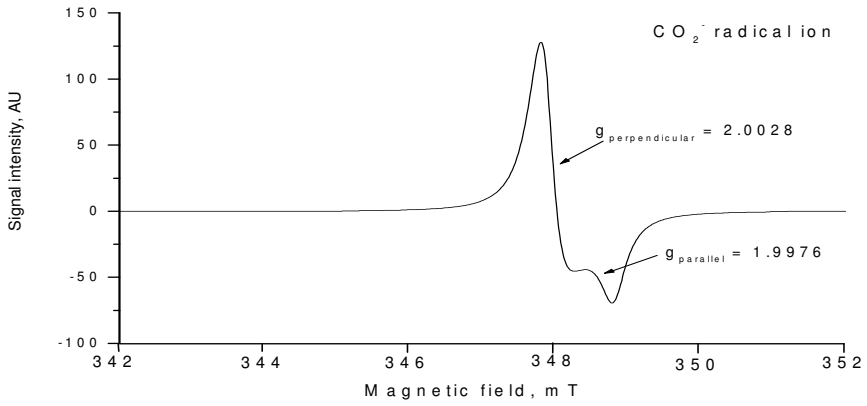

c)

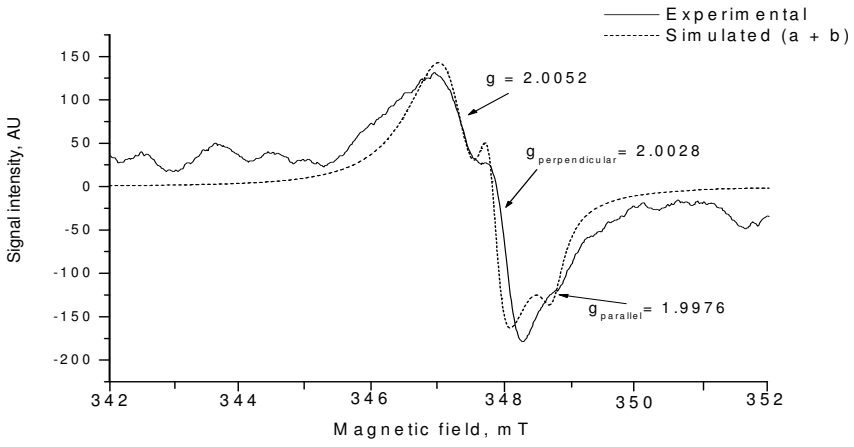

Fig. 20. Simulation scheme of the EPR spectrum of irradiated dog feed (granular form) **a)** simulated spectrum of phenoxyl radical ion ($C_6H_5O^-$), **b)** simulated spectrum of CO_2^- radical ion, and **c)** simulated and experimental spectra of irradiated dog feed.

a)

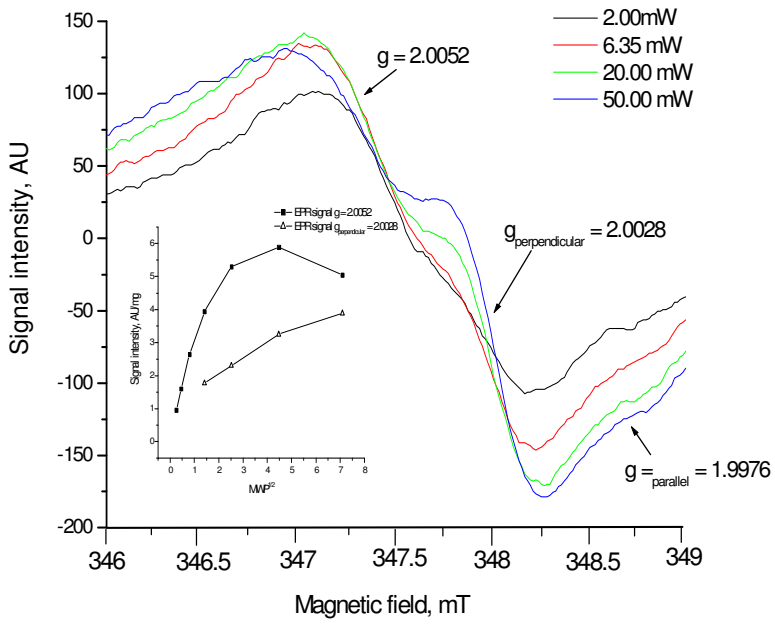

b)

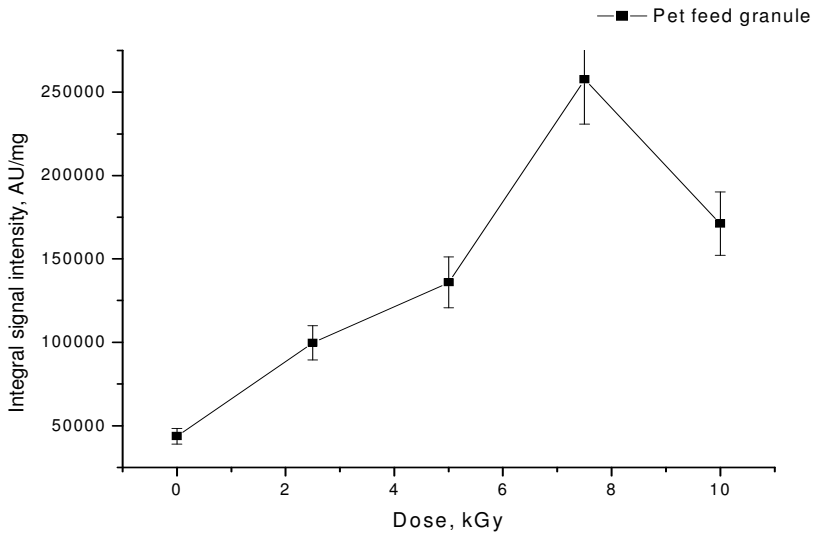

Fig. 21. a). Superposition of EPR spectra of irradiated dog feed (granular form) recorded with increasing microwave power. The inset shows the progressive saturation behavior of the isotropic signal at g = 2.0052 and anisotropic signal at $g_{\perp}$ = 2.0028, **b)** response of the radiation induced signal (g = 2.0052) and the dependence of double integral EPR signal intensity evaluated with increasing dose after 3 d of radiation treatment.

EPR spectroscopy on gamma irradiated edible dog chew

Fig. 22a depicts the EPR spectra of nonirradiated and irradiated dog chew (stick form) recorded at microwave power of 0.253 mW. Both the nonirradiated and irradiated samples were characterized by an isotropic signal g = 2.0034. No radiation specific signal was observed in irradiated sample. However, the signal amplitude of the isotropic signal increased with radiation treatment. The high power EPR spectra also did not provide any clue of radiation specific EPR line for this sample. A negligible change in edible dog chew after radiation treatment makes the identification of irradiated material an extremely challenging task. Therefore, European standards for detection of irradiated food by EPR spectroscopy released by European Committee of Normalization (CEN), namely food containing bone [EN 1786, 1997], cellulose [EN 1787, 2000] and crystalline sugar [EN 13708, 2001] cannot be employed to identify irradiated dog chew. In view of this, the electron relaxation behavior of radicals was studied. The inset in Fig. 22a shows the PSB of the central line of nonirradiated and irradiated (7.5 kGy) samples 90 d after radiation treatment. For the radicals of nonirradiated sample a continuous increase in signal intensity was observed with increasing microwave power, without any sign of saturation, revealing the inorganic nature of the paramagnetic centre. Whereas, in case of irradiated sample, a faster saturation at microwave power of 6 mW, followed by a decrease in signal intensity in a monotonic fashion was observed. This saturation behavior revealed the characteristics of organic radicals. The results of the present study are in good agreement with the EPR detection of irradiated dry food using microwave saturation as proposed by Yordanov *et al,* [100]. The integral intensities of the EPR signals were obtained by double integration of the spectrum and the integral intensity of the central line was observed to be significantly related to the radiation dose as shown in Fig. 22b. The measurements were performed 2 d after radiation treatment.

The time interval after which identification of the irradiated sample is possible was evaluated by the fading kinetics of the radiation induced radicals. In order to avoid background variations all samples were kept inside the EPR measurement tube under normal laboratory conditions. Fig. 23a shows the time kinetics of nonirradiated ($g = 2.0047$) and irradiated ($g = 2.0052$, $g_{\perp} = 2.0028$) dog feed granules monitored up to 75 d after radiation treatment. In case of isotropic signal because of the organic radicals, a fast decrease in signal intensity was observed. Whereas, the anisotropic signal, because of $CO_2^{\cdot -}$ radical ion observed at high microwave power, showed slower reduction in signal intensity and was stable during prolonged storage. Fig. 23b depicts the behavior of the EPR signal ($g = 2.0034$) of the nonirradiated and irradiated samples of edible dog feed during storage.

a) **b)**

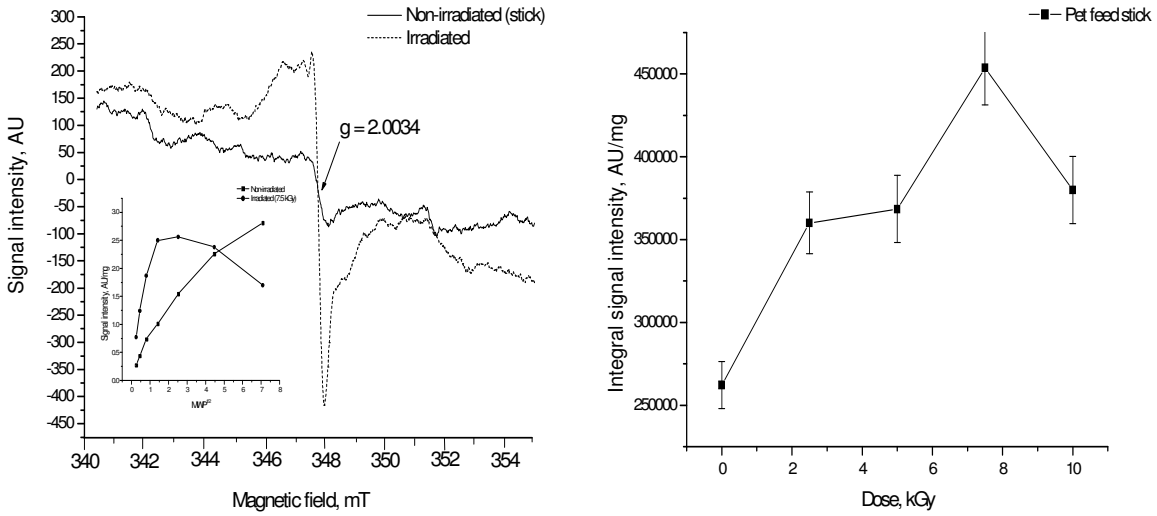

Fig. 22. a) EPR spectra of nonirradiated (control) and irradiated (7 kGy) of edible dog chew (stick form) immediately after irradiation recorded with microwave power of 0.63 mW, **b)** response of the radiation induced signal (g = 2.00534) and the dependence of double integral EPR signal intensity evaluated with increasing dose after 3 d of radiation treatment.

a) **b)**

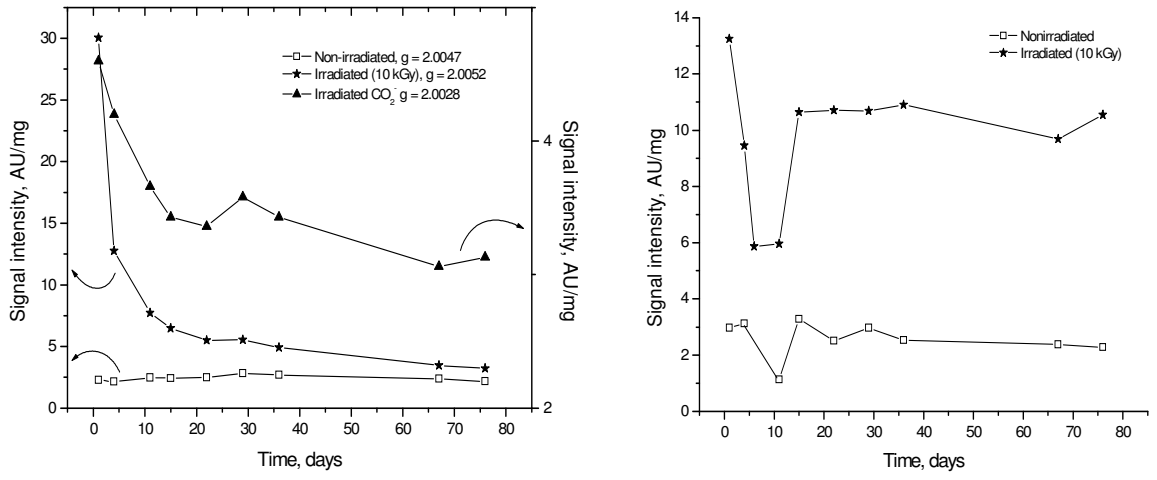

Fig. 23. Time kinetics of nonirradiated and irradiated samples of dog feed during storage **a)** for ready to eat granular form, **b)** edible dog chew stick form.

Thermoluminescence measurements of irradiated edible dog chew

A negligible change in the matrix of edible dog chew samples after radiation treatment makes the identification process using EPR spectroscopy a challenging task. However, the alternative approach based on relaxation behavior of the radiation induced paramagnetic centres provided a clue to radiation treatment. In order to give a reliable result thermoluminescence study of the nonirradiated and irradiated edible dog chew was carried out. Investigation on the composition of the isolated minerals from the edible dog chew sample was carried out using scanning electron microscopy (SEM) and energy dispersive X ray spectrometer (EDX) analysis to assess the possibility of employing TL method for the identification of the irradiated sample. The results of these qualitative studies were interesting to examine the relative abundance of polyminerals. Fig. 24a shows the SEM image of the extracted polyminerals. Fig. 24b shows the EDX spectrum and weight percentage of the major constituents namely calcium (Ca), silicon (Si) and iron (Fe). Calcium being the major component of meat bone associated with the edible dog chew may be responsible for TL signal. Silicon in the form of quartz and aluminum as feldspar are the other two important contributors of TL in this sample.

Fig. 24c shows the TL intensities of glow curves for separated polyminerals from the nonirradiated and irradiated edible dog chew 7 days after radiation treatment. In case of irradiated sample the glow curve was characterized by a low temperature peak at about 213±3°C and a high temperature peak at about 303±5°C. The low temperature peak height ($P_{1height}$) and high temperature peak height ($P_{2height}$) represented the TL intensities at the corresponding glow peak temperatures. No glow peak through the entire temperature range was identified for nonirradiated sample. However, low level natural radioactivity exhibited TL signal because of deep traps around 303°C. The areas under the glow curves for irradiated sample (10 kGy) were 55 times more than the areas under the nonirradiated sample. Higher

values of TL glow (Glow 1) in irradiated samples have been reported in previous studies on spices and herbs [105], chestnut [64]. Therefore, on the basis of the shape of the first glow curve from the separated polyminerals, discrimination between irradiated and nonirradiated samples was possible. Fig. 24d exhibits the dose dependent response of the TL glows of the isolated polyminerals from the edible dog chew. An increase in intensities ($P_{1height}$) of the low temperature peak (213°C) with increasing dose was observed. Normalization of results by re-irradiation with a dose of 1 kGy enhanced the reliability of the detection results. Fig. 25a and b show the comparison of reirradiation glow curves (glow 2) with respect to first glow curves (glow 1) for nonirradiated and irradiated samples, respectively. The reirradiation glow curves (glow 2) were characterized by three glow peaks. The first peak was at 148±3°C, the second and the third peaks were at 213±2°C and 306±5°C, respectively. The differences of the peak temperatures observed between glow 1 and 2 attributed to the time difference elapsed between irradiation and analysis. Glow 2 was recorded 1 d after the normalization doses, whereas, samples were stored for several days after irradiation prior to the analysis of glow 1. In case of nonirradiated sample the ratio of glow 1 / glow 2 was 0.035±0.003, while for the samples irradiated at doses 2.5, 5, 7.5 and 10 kGy the ratios were found to be 0.930±0.012, 2.169±0.25, 2.48±0.22 and 1.90±0.32, respectively. The higher values of the ratio of areas for glow 1/glow 2 for irradiated samples are in good agreement with the European Standard EN 1788, 1996 [45]. The dog chew samples (irradiated and nonirradiated) were stored for seven months to study the fading kinetics of the TL glows. During prolonged storage the isolation of minerals from nonirradiated and irradiated samples was carried out prior to each TL measurement. Fig. 25c and d exhibit the TL glow curve structures of the 2.5 and 10 kGy irradiated samples, respectively. In both the cases the $P_{1height}$ showed a fast decrease in TL intensity with time, whereas, the $P_{2height}$ revealed slow reduction in intensity. The insets of the figures show the variation of the ratio of $P_{1height}$ to $P_{2height}$ ($P_{1height}$ / $P_{2height}$) with increasing

time and confirmed the fast fading kinetics of $P_{1height}$. However, a clear discrimination between irradiated and nonirradiated edible dog chew samples was possible from the shape of the first TL glow even after a prolonged storage of seven months.

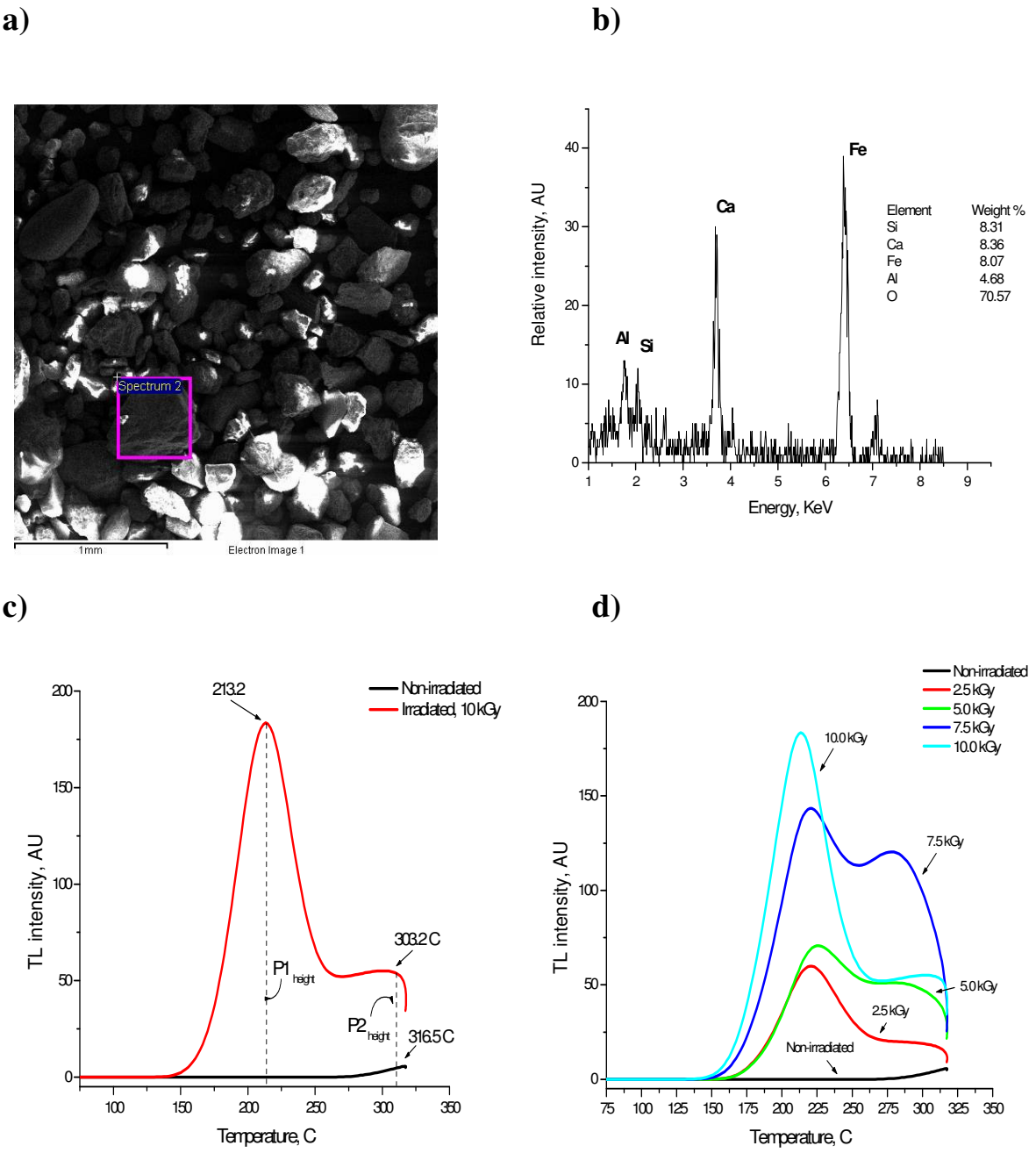

Fig. 24 a) Scanning Electron Microscopy (SEM) image, **b)** Energy Dispersive X ray (EDX) spectrum of the polyminerals extracted from dog chew samples, **c)** TL glows of isolated minerals from nonirradiated (control) and irradiated (10 kGy) edible dog chew (stick form) **d)** response of the TL glows of the isolated minerals with increasing radiation doses from 2.5 to 10 kGy.

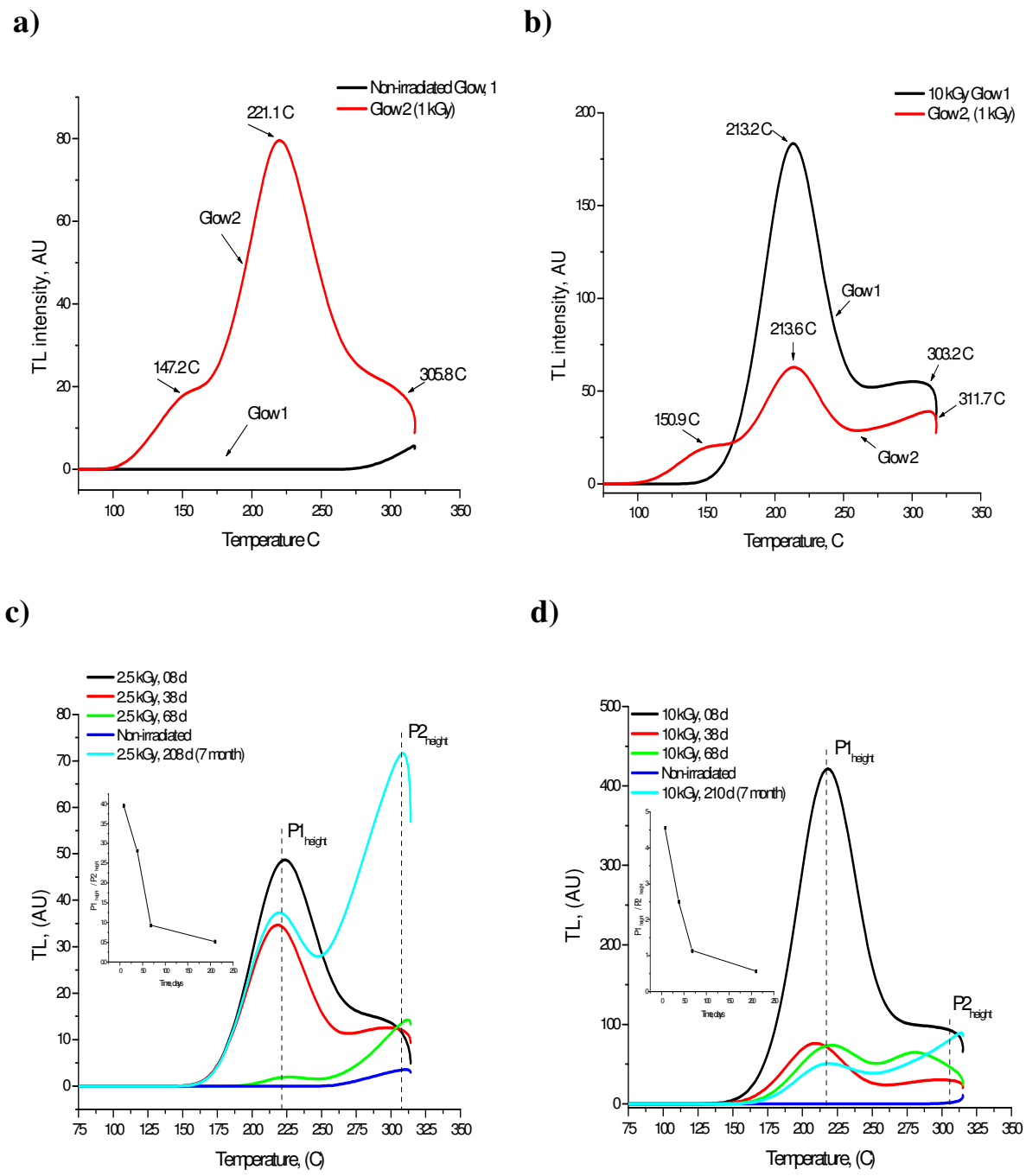

Fig. 25. TL glows of isolated minerals from dog chew samples **a)** glow 1 and glow 2 (normalized with 1 kGy) of nonirradiated (control) sample and **b)** glow 1 and glow 2 (normalized with 1 kGy) of irradiated (10 kGy) sample. Response of the TL glows during storage for the samples subjected to radiation doses **c)** 2.5 kGy and **d)** 10 kGy and insets show the behavior of $P_{1height}/P_{2height}$ with increasing time.

CHAPTER 6

Identification of irradiated

Cashew nut, Shrimp and Medicinal plant products

Identification of irradiated Cashew nut

The nut of the plant, *Anacardium occidentale*, commonly known as cashew is an important cash crop for many countries. The nut has high nutritive value. However, climatic conditions and varietal differences govern quality [110]. The kernel contains approximately 21% protein, 46% fat and 25% carbohydrates. Cashew nut is an important export commodity for India, contributing about 7% of the total export earnings to the national treasury. Insect infestation during storage is a major problem of cashew nut, resulting in economic losses. Irradiation is increasingly being recognized as an effective technology to reduce post-harvest losses and improve quality. Cashew nuts, irradiated at 0.25 kGy or higher doses and stored under ambient conditions showed no insect infestation during storage, while the control nonirradiated samples were spoiled due to infestation [111]. In the present investigation a detailed study of the radical species produced by gamma irradiation of cashew has been carried out. In addition the EPR saturation and thermal behavior to distinguish between treated and nontreated samples by EPR spectroscopy have been examined.

EPR spectroscopy to identify irradiated cashew nut

Spectrum a, Fig. 26 shows the EPR signal of cashew nut samples before irradiation exhibiting a weak and broad singlet characterized by g = 2.0056±0.0004 centered around 347.5 mT. The g value obtained compares well with that reported in literature [43, 10]. In order to characterize the natural signal, EPR spectra of irradiated (1kGy) pure quinone (hydroquinone) was recorded under similar experimental setup. A weak singlet was observed with g = 2.0032 and different from the signal observed in nonirradiated sample. This suggested that, in cashew nut, where the lipid content is more than 40 %, the origin of the singlet could possibly be due to the oxidation of fatty acids [112].

Fig. 26 spectrum b shows a complex spectrum immediately after irradiation (1 kGy) of cashew sample with an increase in signal intensity of the existing weak singlet by a factor of

11. The exposure to gamma irradiation leads to a change in cashew matrix, producing two new types of paramagnetic species. One was identified as a very weak triplet signal probably because of crystalline cellulose [19, 108] superimposed on the natural singlet with a hyperfine coupling constant (hfcc) of 3 mT (Fig. 26, spectrum b). This signal is considered to be an unambiguous evidence of the radiation treatment of sample under investigation and recommended for the detection of irradiated foods in EN 1787 standard (*7*). The same has been validated for pistachio shells by Raffi *et al*, 1992 [113]. Other short lived paramagnetic species with axially symmetric spectrum (Fig. 26, spectrum b) was characterized by an anisotropic g tensor ($g_{\perp}$ = 2.0069 and $g_{\parallel}$ = 2.0000). This signal could possibly be of CO_2^- radical ion formed during the breakdown of fatty acid. The g values obtained compared well with that reported in the literature [109, 58]. This component was not particularly stable and after 2 days had decreased in intensity to a level that was similar to that of nonirradiated specimen. The instability in EPR signal intensity revealed that the detection of fat component by EPR spectroscopy was limited soon after irradiation.

The effects of increasing radiation dose from 0.25 – 1 kGy on the EPR spectra of cashew samples were studied. The radiation induced signal due to CO_2^- radical ion started developing at minimum dose of 0.25 kGy, whereas, signal of cellulose radical was identified at 1 kGy dose. However, the relative intensity of the central line was observed to be significantly related to the radiation dose as shown in Fig. 27. The measurement was performed 3 days after irradiation. The dotted line represents a second order polynomial curve $D = aD^2 + bD + c$ with a = -66.19, b = 119.56 and c = 5.15 and each point representing the mean value of three samples.

Radiation induced radicals formed from fat component of cashew matrix are highly unstable. EPR spectra of irradiated and nonirradiated samples after storage showed similar pattern except for a significant enhancement in the natural signal intensity after irradiation. To

validate a method for identifying irradiation, free radicals produced by other processing techniques such as heating (thermolysis) must be distinguished from those produced by irradiation. Fig. 28, spectra (a) – (c) show the EPR spectra of cashew nut samples subjected to various thermal treatments before and immediately after heating. Only a weak singlet (Fig. 28, spectrum b) similar to the natural signal was observed after thermal treatment of whole sample at 100°C for 1h. Radicals originated due to thermolysis characterized by g = 2.0045 ±0.0005, centered around 347.6 mT. No satellite lines like cellulose and $CO_2^{\cdot-}$ radical ions were observed. The samples subjected to roasting at 180°C showed increased signal intensity (Fig. 28, spectrum c) similar to that of irradiated sample, making detection of radiation treatment of cashew difficult.

a)

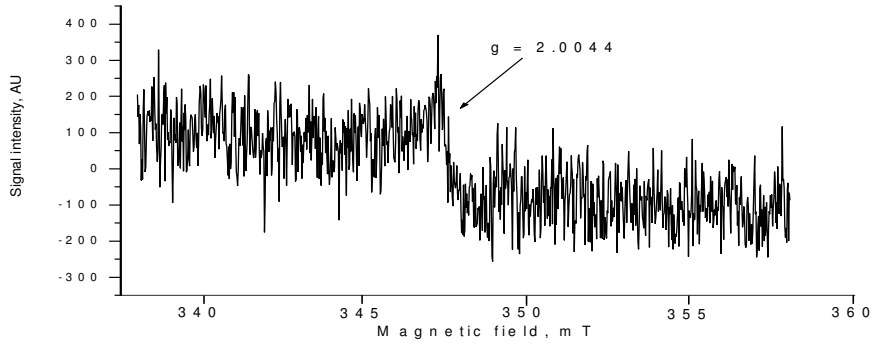

b)

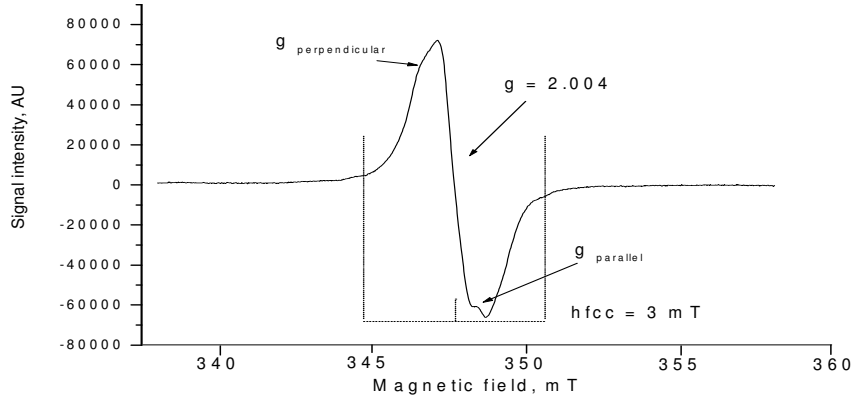

Fig. 26. Ambient EPR spectra of cashew nut sample **a)** before irradiation and **b)** one day after irradiation (1 kGy).

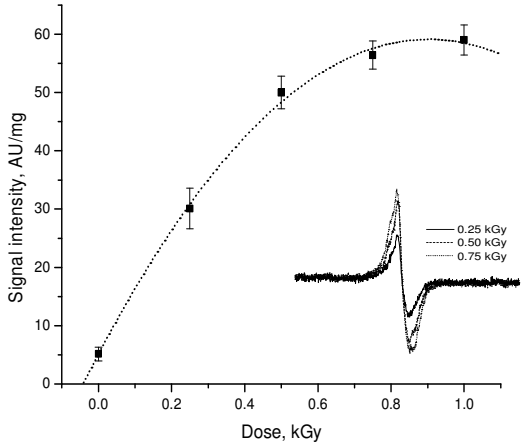

Fig. 27. Response of the radiation induced signal intensity of the central line (g = 2.0044) with increasing radiation dose. Inset shows the EPR spectra with increasing dose.

a)

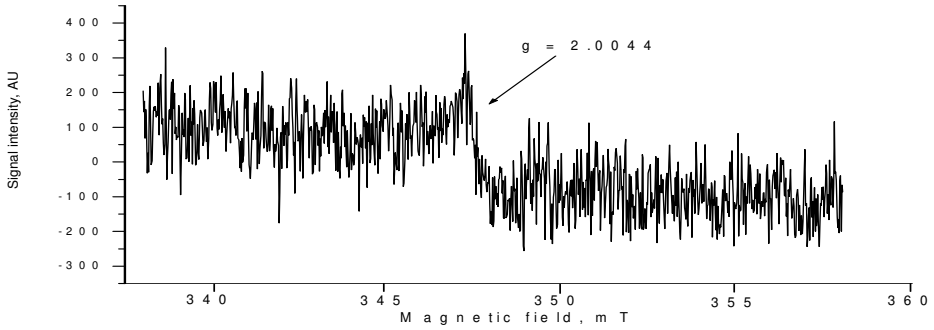

b)

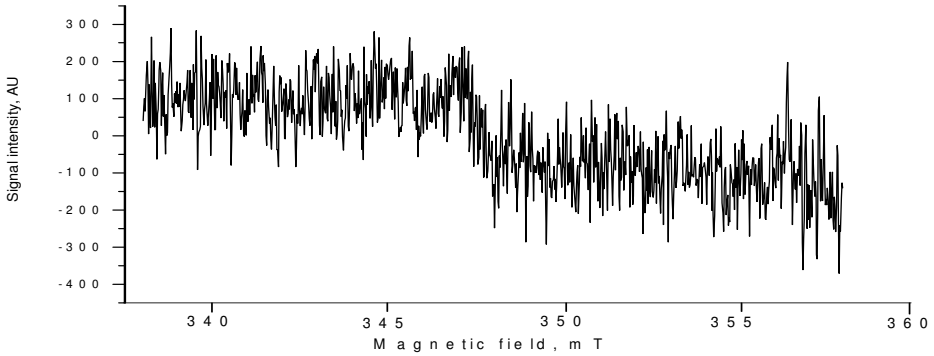

c)

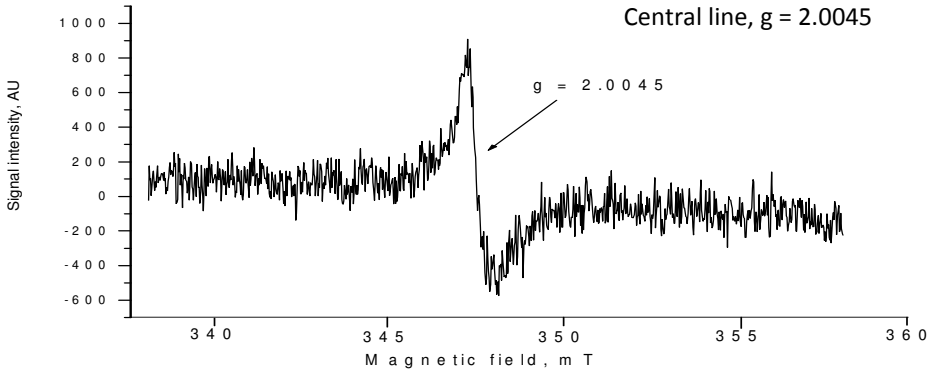

Fig. 28. EPR spectra after 1 d of various thermal treatments **a)** without thermal treatment, **b)** subjected to 100°C, 1h and **c)** roasted at 180°C.

Progressive Saturation Behavior (PSB) of EPR signal

The applicability of the EPR analysis to detect irradiated food is strongly limited by the life time of the radiation induced free radicals such as cellulose radicals. This is the case with cashew nut under investigation, where, the procedure based on EPR cellulose signal cannot be used beyond one day of radiation treatment. Therefore, alternative methods proposed in the European Standard EN 1787 and based on EPR are desirable. Characterization of the free radicals, naturally present, induced by radiolysis or by thermolysis was essential for the investigation to identify different techniques of processing. In order to determine the electron relaxation behavior of radicals in the cashew, progressive saturation behavior (PSB) was studied by varying the microwave field strength between 0.06 – 50 mW. Fig. 29a shows the PSB of the central line of irradiated (1 kGy), roasted (180°C) and nonirradiated samples one day after irradiation and heat treatment. A comparatively faster saturation at microwave power around 6 mW followed by decrease in signal intensity in monotonic fashion was observed for the radicals formed after roasting. This saturation behavior revealed the characteristics of organic radicals with a large relaxation time. Improvement of the EPR detection of irradiated dry food using microwave saturation and thermal treatment has been proposed by Yordonov *et al*, 2005 [100]. In this method curves of saturation of nonirradiated and irradiated plant sample vs. $P_{MW}^{1/2}$ were studied and nonirradiated sample showed saturation at microwave power higher than 15 mW, whereas, irradiated sample exhibited early saturation at microwave power of around 8 mW. In the present study, no significant difference between saturation behavior of nonirradiated and irradiated cashew nut was observed. The central line of the spectra for both nonirradiated and irradiated samples exhibited similar saturation at microwave power around 20 mW revealing shorter relaxation time. As depicted in Fig. 29b the relaxation behavior of nonirradiated, irradiated and roasted samples, even after a storage period of 45 days was almost similar to that of behavior noticed

immediately after irradiation and heat treatment. Therefore, EPR analysis by the saturation behavior of the signals could not be used to distinguish irradiated cashew sample. However, a faster EPR saturation of thermally induced radicals in comparison with the radiation induced radicals could be used as a tool to distinguish between irradiated and roasted cashew.

Thermal behavior of EPR signal

In order to identify the irradiated cashew sample from natural and roasted samples, thermal behavior of the EPR signal was investigated. Nonirradiated, irradiated and roasted samples were subjected to in situ heating from 27 to 187°C. As depicted in Fig. 29c, with the increase of temperature from 27 to 97°C, signal intensities of the central lines of nonirradiated and roasted samples were observed to be almost unchanged, but, that of irradiated samples showed a fast fall of about 50 %. However, temperature increase beyond 152°C lead to an increase in signal intensity in all the cases. A decline of EPR signal of irradiated allspice sample has been reported where Yordanov & Gancheva, 2000 [46] proposed that EPR analysis of the central peak of spices that had undergone thermal treatment before and relatively long time after irradiation could be a tool for detection of irradiation. In order to establish this method, thermal behavior of the samples was investigated after a storage period of six weeks. Nonirradiated, roasted and irradiated samples were subjected to thermal treatment of 100°C for 1h. Irradiated samples showed 39 % reduction in signal intensity, whereas, nonirradiated and roasted samples did not exhibit any significant change in signal intensity. Our results are well in agreement with the proposal of Yordanov & Gancheva, 2000 [43]. The thermal behavior of the gamma induced EPR signal represented a valuable tool for the assessment of previous radiation treatment.

The fading kinetics of the radiation induced radicals give information on the time interval after which identification of the irradiated samples is possible. In order to avoid these variations all samples were kept inside the EPR measurement tube under normal laboratory

conditions. Kinetics of nonirradiated, irradiated and roasted samples were monitored up to 6 weeks after radiation treatment. Both the radiation induced paramagnetic species identified as cellulose radicals and CO_2^- radical ions were observed to be stable up to 24 - 40 h after irradiation in the matrix of cashew nut. Therefore, application of EN 1787 Standard was not possible as a method of detection. However, increased intensity of the central line of the irradiated samples was observed even after several days of irradiation with a clear distinction with respect to nonirradiated samples (Fig. 29d).

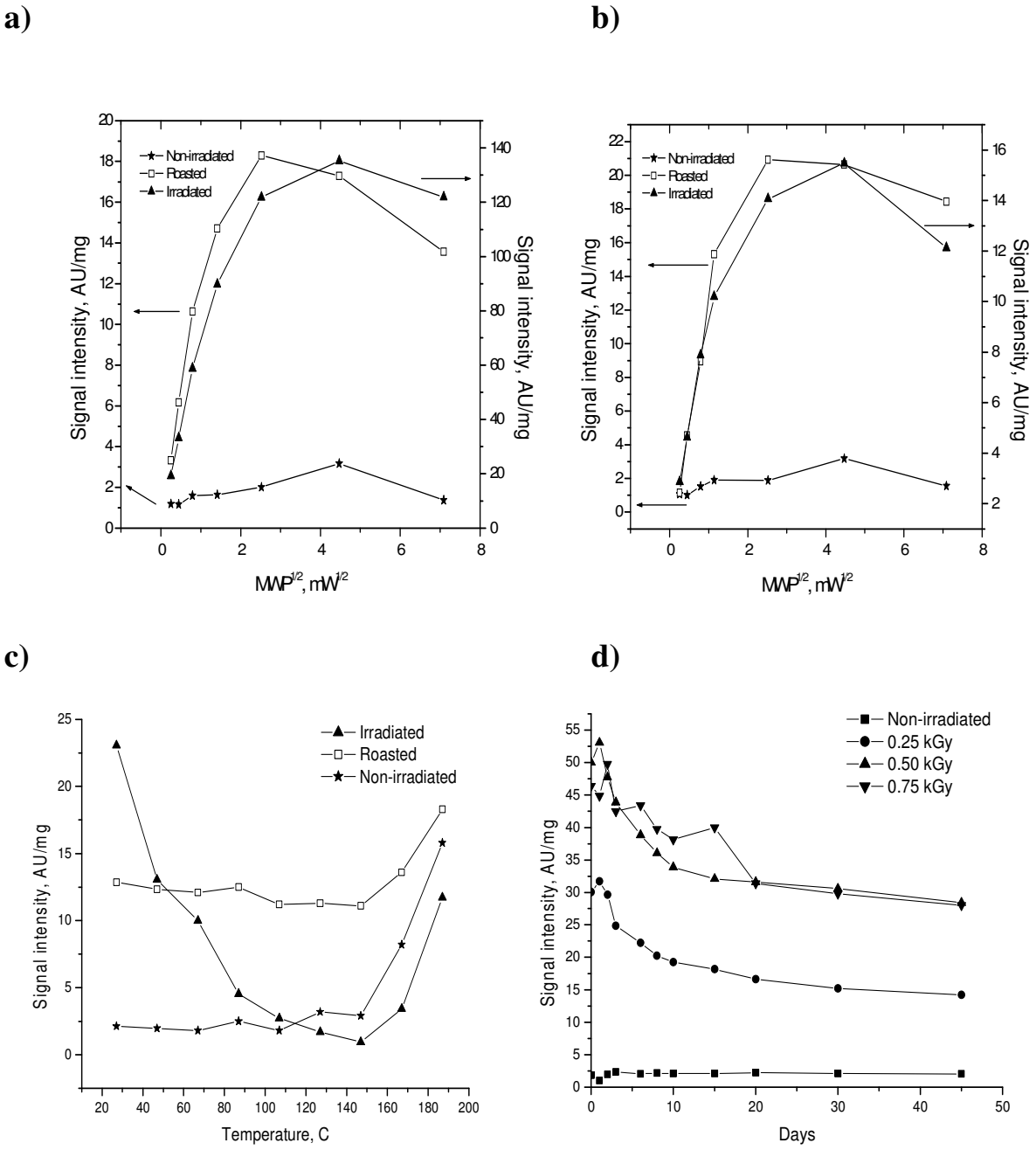

Fig. 29. Relaxation behavior of main line of nonirradiated, irradiated (1 kGy) and roasted cashew **a)** 1 d after irradiation, **b)** after 45 d storage, **c)** thermal behavior of the central line of EPR spectrum for nonirradiated, irradiated (1 kGy) and roasted (180°C) cashew nut samples **d)** kinetics of the central line of the EPR signal of nonirradiated, irradiated cashew nut samples.

Identification of irradiated shrimp

Radiation processing of seafood for preservation and hyginization is approved in India by the Ministry of Health & Family Welfare under PFA Act rules. Shrimps contribute significantly towards seafood export from India. However, many a time our export consignments are rejected due to contamination with pathogens. Radiation processing can play an important role in hyginization of shrimps, thereby, strengthening export of seafood. Response of TL is highly dependent on the geographical and biological variations of irradiated foods. The objective of the present study was to focus on extending the TL method for detection of irradiated shrimps (*Penaeus indicus*) and also to study the efficacy of EPR spectroscopy to identify the same.

Thermoluminescence study to identify irradiated shrimp

The intestinal grits were isolated from the nonirradiated and irradiated shrimps by alkaline hydrolysis followed by density separation. The yield of the minerals on each discs were in the range of 0.2 – 0.3 mg. The composition of the separated polyminerals from the sample was studied using scanning electron microscopy (SEM) and energy dispersive X ray spectrometer (EDX) analysis. Investigation on the composition of the isolated minerals from the intestinal grits of shrimp was important to assess the possibility of employing TL method for the identification of the irradiated sample. The results of these qualitative studies were interesting to examine the relative abundance of polyminerals. Fig. 30a shows the SEM image of the extracted polyminerals revealing the morphology. Fig. 30b shows the EDX spectrum the major constituents namely calcium (Ca) and silicon (Si). Traces of both the elements are probably responsible for TL signal.

Fig. 30 c shows the TL glows of nonirradiated and irradiated samples recorded after a storage period of 45 days. For all irradiated samples, the areas under glow 1 were 30 to 35 times higher compared to that of nonirradiated samples. Higher values of glow 1 in irradiated

samples have been reported in previous studies on spices and herbs [54, 57]. The position of glow 1 for control sample through all temperature ranges was not clear. All irradiated samples were characterized by glow peak at 225°C±6.5° C. Fig. 30d exhibits the response of the integral TL outputs from the irradiated samples with the increasing dose up to 5 kGy. An increase in TL was observed from the samples subjected to increased radiation dose. Normalization by reirradiation at 1 kGy (glow 2) enhanced the detection results by confirming the successful isolation of the inorganic. Fig. 30e and f show the nature of glows (glow 2) obtained for control and irradiated samples and characterized by glow peak at 169.0±15.9°C and a higher temperature shoulder at 306°C probably due to polymineral nature of the samples. The ratio of areas for glow 1/glow 2 determined for nonirradiated shrimp was 0.009±0.002, while for irradiated shrimp it was significantly high at 0.678±0.025. Higher values of ratio of areas for glow 1/glow 2 in irradiated samples are in good agreement with the European Standard EN 1788, 1996 [45].

Thermoluminescence study to identify irradiated shrimp after cooking

Possibility of identification of irradiated shrimp after cooking was also investigated. Four groups of shrimp each of quantity 200 g were prepared. One group was kept as control and the remaining groups were subjected to gamma irradiation at 3 kGy. All the groups (control and irradiated) were heated at 80, 100 and 121°C (Autoclaved) for 15 min. Finally, isolation of polyminerals was carried out before TL measurements. Fig. 31a and b depicted the TL glow curve structures and the integral TL output of the samples isolated from nonirradiated, nonirradiated and cooked, irradiated, irradiated and cooked shrimp. The TL output of the nonirradiated samples after cooking did not show any considerable change. However, the irradiated samples after cooking at 80°C exhibited a minor increase in TL output. However, a decrease in integral TL output with increasing cooking temperatures at 100 and 120°C (Fig. 31b) was also observed. The initial increase in the integral TL output was possibly due to

thermal sensitization of the isolated minerals at low temperature heating (80°C). Decrease in TL output with the increase in cooking temperature was attributed to loss of trapped charge carriers during the cooking process. The glow curve structures of the respective samples showed reduction in glow peak (214°C) intensity with the increase in cooking temperature (Fig. 31a) and at 120°C, the peak completely disappeared due to loss of charge carriers responsible for the glow peak. The TL studies were carried out after a period of one month storage of the samples and the detection of irradiated shrimp even after cooking was possible from the first glow curve of the isolated minerals.

EPR spectroscopy to identify irradiated shrimp

EPR investigation of the shell isolated from the nonirradiated and irradiated shrimps were tried. Shrimps were irradiated with gamma radiation dose of 3 and 8 kGy under chilled conditions. The shell was removed from nonirradiated and irradiated samples and chopped into small pieces to accommodate inside the EPR quartz tube. Fig. 31c shows the EPR spectra of nonirradiated and irradiated samples. Both the nonirradiated and irradiated samples exhibited a singlet signal at g = 2.004 with almost comparable signal intensity. The EPR signal in case of nonirradiated samples may be derived from organic component [9]. No change in spectrum shape was observed after radiation dose (3 kGy) of commercial relevance revealing the limitation of EPR spectroscopy technique to identify irradiated shrimp. However, a higher dose of 8 kGy exhibited enhanced signal intensity and an axially symmetric signal characterized by $g_{\perp} = 2.0046$ and $g_{\parallel} = 1.997$. This signal was similar to CO_2^- radical ion reported in hydroxyapatite matrix. But the structural polysaccharide of shrimp exoskeleton is amino sugar which is a major component of chitin and exhibits similar EPR spectra after irradiation [36].

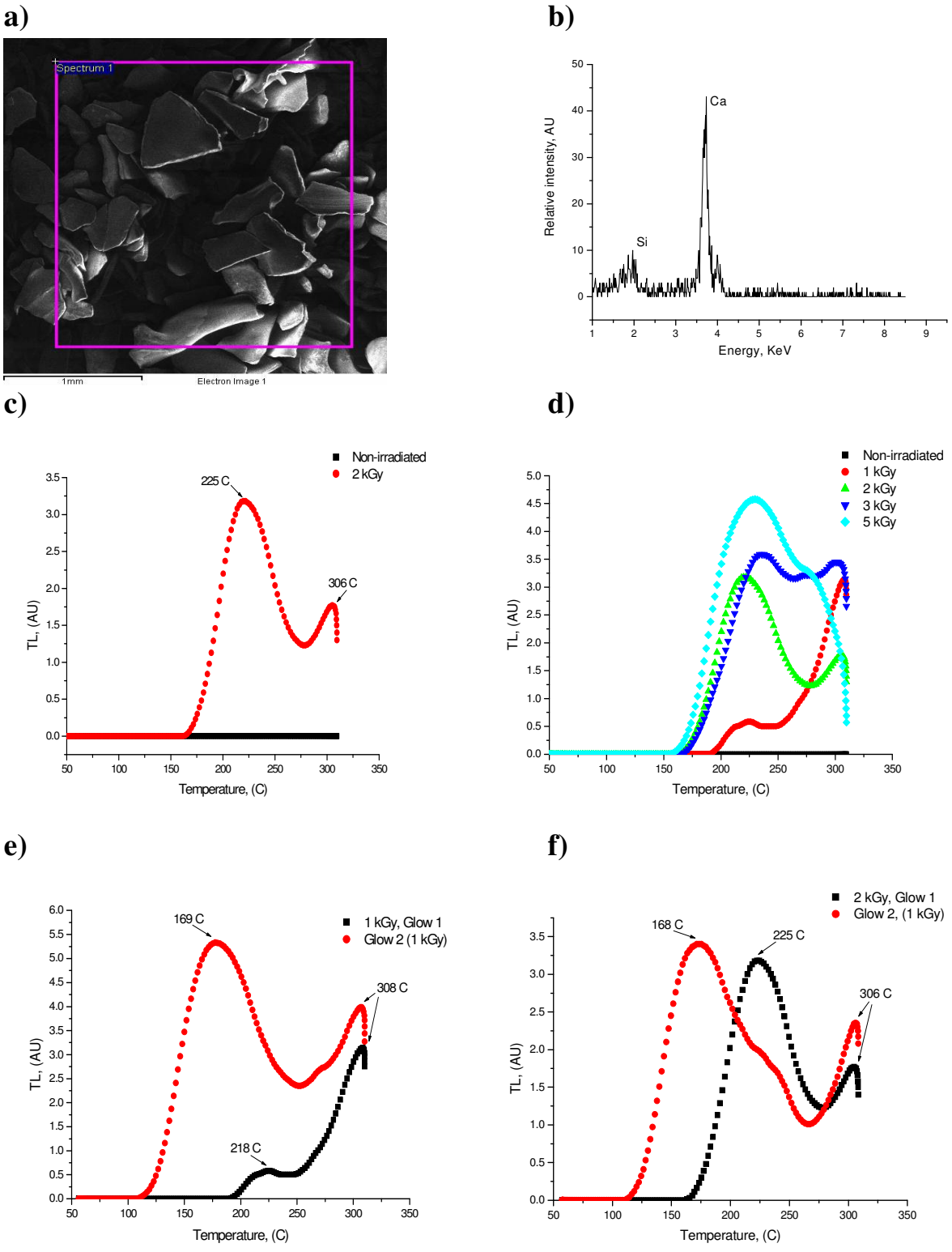

Fig. 30. a) SEM image and **b)** EDX spectrum of the minerals isolated from the grits of shrimp, **c)** TL glows of the non-irradiated and irradiated samples, **d)** TL glows with the increasing doses, TL glow 1 and glow 2 of the samples of **e)** irradiated with 1 kGy and **f)** irradiated with 2 kGy.

a) **b)**

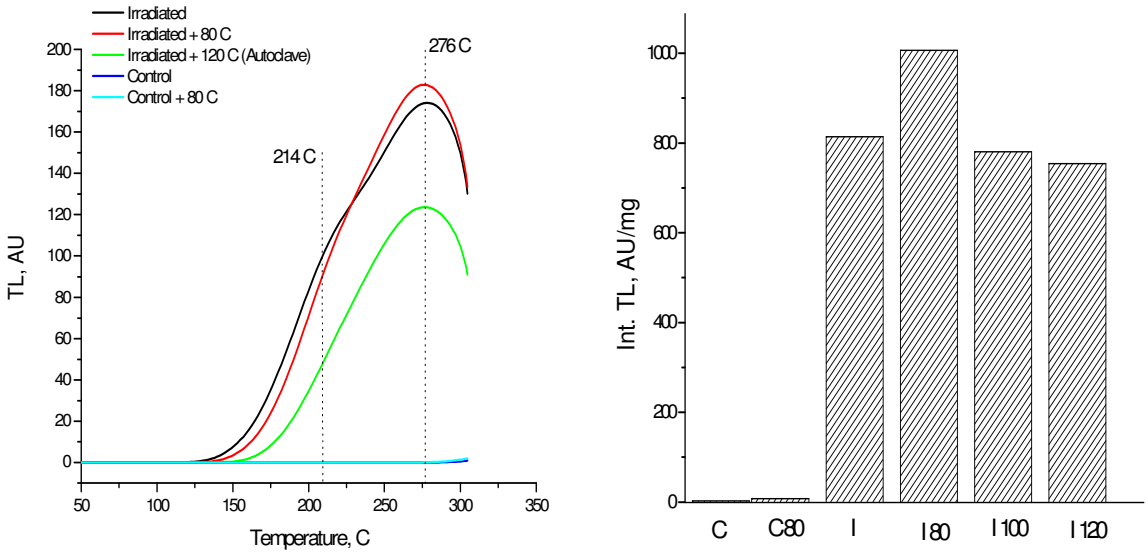

c)

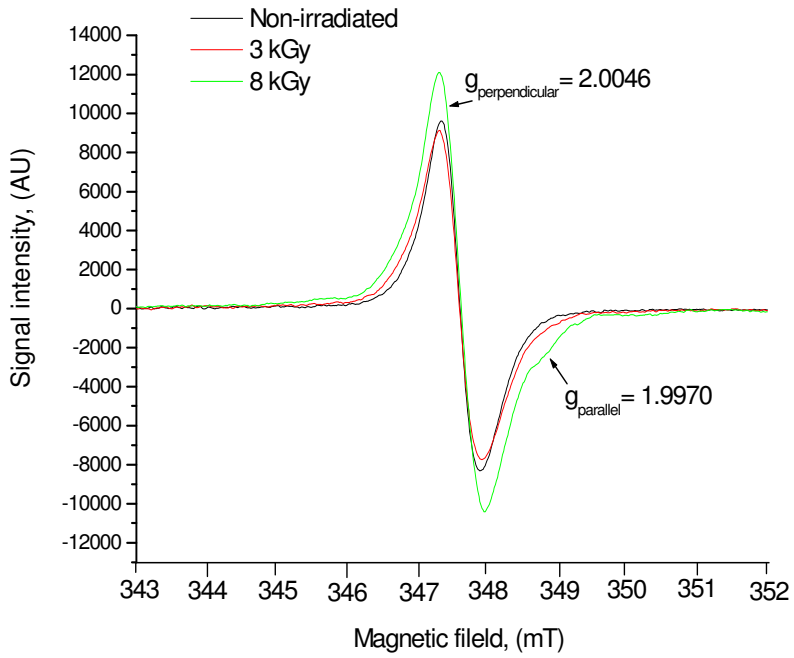

Fig. 31. a) TL glows and **b)** integral TL of the isolated minerals from shrimp of nonirradiated, nonirradiated and cooked and irradiated and cooked at two different temperatures, **c)** EPR spectra of the nonirradiated and irradiated shrimp shell.

Identification of irradiated medicinal plant products

The herbal medicinal plants have been used in traditional medicines since ancient times. Ayurveda and other systems of Indian medicine have identified a number of plants and their components that have curative properties [114]. Worldwide increase in demand of medicinal plant products has been observed because of their effective action without side effects. In addition to this, many times the extraction of biologically active components from plant is more convenient than chemical synthesis. At present phytopharmaceuticals represent a significant part of the world pharmaceutical market [115, 116, 117]. As a matter of fact in recent times, the use of traditional medicines and phytotherapy has become a subject of intense scientific investigation. Therefore, research and development related to identification of medicinal plants, characterization of their biologically active components is gaining interest in many countries. Application of ionizing radiation in preservation of herbal products by microbial decontamination or insect disinfestation is one of the promising options. The radiation technology provides the most effective solution in this regard. The interactions between biological materials and different forms of energy are very complex and depend on the irradiation and post-irradiation conditions.

In this present work, irradiated Indian medicinal plant products, namely aswagandha (*Withania somnifera*), vairi (*Salacia reticulata*), amla (*Emblica officinalis*), turmeric (*Curcuma longa*) and guduchi (*Tinospora cordifolia*) widely used as traditional medicine (http://www.gits4u.com), were studied using EPR spectroscopy. The main objective of this investigation was to identify irradiated medicinal plant products by studying their EPR spectral characteristics during prolonged storage. A detailed study of the radical species produced by gamma irradiation of medicinal plant products has been carried out by EPR saturation and thermal behavior. EPR spectrum simulation was carried out to characterize the radicals to distinguish between treated and nontreated samples.

EPR analysis of aswagandha

Fig. 32a depicts the EPR spectra recorded with microwave power at 0.635 mW of nonirradiated, irradiated and thermally treated (100°C, 1 h) samples of Aswagandha. The EPR spectrum of nonirradiated sample was characterized by a singlet with g = 2.0050±0.0002 and ΔB_{pp} = 0.766 mT. The most important objective of identification of irradiated food is to trace the signal, which originates only because of radiation treatment. In view of this, the samples were subjected to thermal treatment at 100ºC for 1 h and the EPR spectrum showed similar signal at g = 2.0050 that of nonirradiated samples. The heat energy did not induce any specific paramagnetic centre and at the same time the intensity of the signal did not exhibit any considerable change. Immediately after the radiation treatment of the sample at 7.5 kGy dose, a complex EPR spectrum was observed with an increase in signal intensity of the existing weak singlet (g = 2.0050). Irradiation was found to be responsible for this increase. Increase in line width (ΔB_{pp}) of the EPR signal from 0.766 to 0.974 mT could probably be attributed to the induction of multiple paramagnetic centres in the drug matrix. In order to identify the nature of the induced radicals the EPR spectrum of the irradiated sample was recorded at very high microwave power at 50 mW. The inset (Fig. 32a) shows the high power EPR spectrum of the irradiated sample with resolved EPR lines. The signal at g = 2.005 revealed the superposition of radical species of two different groups, one group belonging to radicals of organic origin, exhibited reduction in signal intensity due to the large relaxation time, and the other, may be of inorganic origin, showed increase in signal intensity because of short relaxation characteristics.

In order to study the time kinetics of the irradiated aswagandha, the samples were stored for a period of 90 days. Fig. 32b shows the EPR spectrum of the irradiated (7.5 kGy) sample after a storage of 90 days. The spectrum of the irradiated samples even after a prolonged storage depicted a different spectrum in comparison with the nonirradiated samples. The EPR signal

lines in the spectrum were observed as more resolved and could be characterized by the superposition of two radicals. However, reduction in the intensity of the EPR lines was observed in the spectrum. One signal was characterized by an anisotropic g tensor having $g_{\perp}$ = 2.0044 and $g_{\parallel}$ = 1.9980 appears to originate from radical of inorganic nature. But, the other signals were organic in nature and possibly of the carbohydrate radical and cellulosic radical.

EPR spectrum simulation study

In order to understand the reason for development of prominent EPR lines during prolonged storage, identification of the paramagnetic centres was necessary. In view of this, EPR spectra simulation studies were carried out using WIN EPR and Simfonia programme (Bruker). The detailed simulation scheme of EPR spectra of aswagandha irradiated with a dose of 7.5 kGy is depicted in Fig. 33a – d and their spin Hamiltonian parameters ($g_{\perp}$, $g_{\parallel}$, $A_{\perp}$, $A_{\parallel}$; ΔB_{pp}) used in simulation are summarized in Table 6. Fig. 33d exhibits the superposition of experimental and simulated spectra. The simulated spectrum was a linear combination of the individual signals represented in Fig. 33a, b and c (R^2 = 0.972). Simulation of EPR spectra obtained from irradiated aswagandha also revealed the formation of 3 paramagnetic centres, two signals of organic origin were attributed to carbohydrate radical and cellulosic radical, and the other inorganic signal was anisotropic and similar to the CO_2^- radical ion.

Progressive saturation behavior (PSB) of the EPR signal

The electron relaxation behavior of the radicals was studied in order to reconfirm the origin of these radical species. The microwave power was varied from 0.063 to 50 mW and Fig 34a, shows the progressive saturation behavior (PSB). The EPR signal at g = 2.0050 for irradiated and nonirradiated samples showed comparatively faster saturation at microwave power of 6 mW followed by a decrease in signal intensity in a monotonic fashion. However, the PSB of CO_2^- signal showed a increase in signal intensity without any saturation confirming the characteristics of paramagnetic centre with short relaxation time. In case of aswagandha,

irradiation produced multiple radicals causing line broadening of the EPR signal. However, after prolonged storage, three radicals were identified to be prominent, carbohydrate, cellulose and CO_2^-. The presence of starch as the principal component of the sample and the initial water content may explain the observed differences between the initial and stored spectra of irradiated samples. In case of cereals, water content severely affected the initial spectrum, particularly during irradiation, but the final spectrum was independent of hydration [118, 119]. Starch which is not a simple macromolecule but contains crystalline as well as amorphous fractions could be another one of the important factors responsible for the changed structure of the EPR spectrum during storage. Different initial kinetics observed for cereals and starches may reflect the differences in molecular arrangements in these two fractions [120]. In addition to these, oxygen could play a crucial role in radical kinetics due to its ability in entering easily the reactions with the radiation induced radicals and in transforming them to peroxide radicals having totally different EPR characteristics. The importance of oxygen for signal decay in case of irradiated durum wheat has already been observed by Korkmaz & Polat, 2000 [12].

The effect of increasing dose and time kinetics

The effect of increasing radiation dose from 2.5 – 10 kGy on the spectra of aswagandha samples was studied. The integral intensities of the EPR signal were obtained by double integration of the spectrum and the integral intensity was observed to be significantly related to the radiation dose as shown in Fig. 34b. The measurement was performed 2 d after irradiation. The dotted line represents a linear fit, $y = A + B * x$ with $a = 3.28 \times 10^4$, $b = 8.038 \times 10^3$, and each point is the mean value of three samples.

The time interval after which identification of the irradiated samples is possible was evaluated by the fading kinetics of the radiation induced radicals. Fig. 34c shows the time kinetics of nonirradiated and irradiated samples of aswagandha monitored up to 90 days after radiation

treatment. EPR singlet at g = 2.005 for irradiated sample exhibited an exponential fall in intensity up to 15 days and remained visible throughout the storage period. However, the spectrum exhibited change in shape during storage with visible radiation induced signals. The singlet of nonirradiated sample did not show any characteristic change in spectrum shape and signal intensity. The fading kinetics of the irradiated sample can be well fitted by a bi-exponential decay described by the following equation:

$$y = y_0 + A_1 \exp(-t/T_1) + A_2 \exp(-t/T_2)$$

where, y represents the EPR signal intensity of the central line. Typical parameter values of the curve for the sample treated with 7.5 kGy radiation dose obtained with a non-linear least squares fitting procedure were $y_0 = 13.24$, $A_1 = 18.5$, T_1(days) = 0.4, $A_2 = 48.3$ and T_2 (days) = 5.7. The mathematical representation may be useful to reconstruct the approximate radiation dose received by the unknown irradiated sample after prolonged storage.

Table 6. Hamiltonian parameters of the EPR signals for irradiated aswagandha

EPR signal origin	g value	Hyperfine splitting (mT)	ΔB_{pp} (mT)
Carbohydrate radical	$g_{\perp} = 2.0061$ $g_{\parallel} = 2.0033$	$A_{\perp} = 0.86$ $A_{\parallel} = 0.72$	0.79
CO_2^- radical ion	$g_{\perp} = 2.0044$ $g_{\parallel} = 1.9980$		0.41
Cellulose radical	$g_x = g_y = g_z = 2.005$	$A_{xx} = A_{yy} = 3$, $A_{zz} = 1.5$	0.5

a)

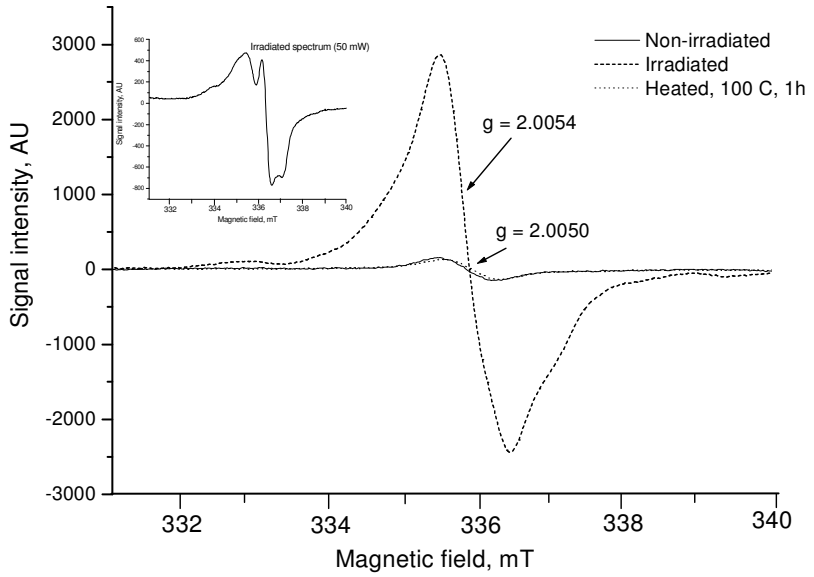

b)

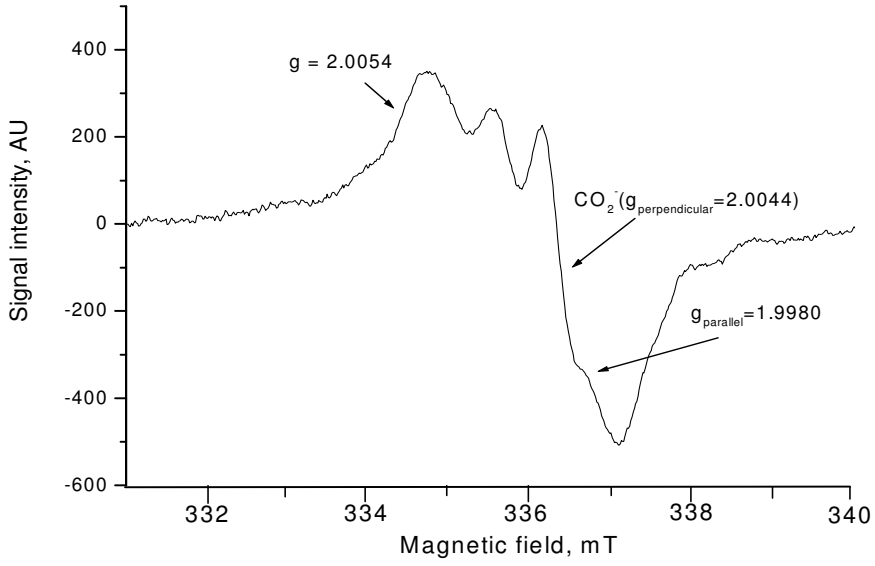

Fig. 32. a) EPR spectra of nonirradiated, heat treated (100 C, 1 h) and irradiated (7.5 kGy) aswagandha recorded at microwave power attenuation of 25 dB. Inset shows Irradiated spectrum at high power (6 dB), **b)** EPR spectrum of irradiated (7.5 kGy) aswagandha after storage of 90 days.

a)

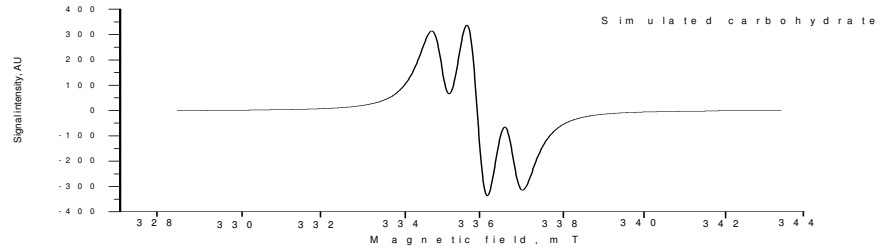

b)

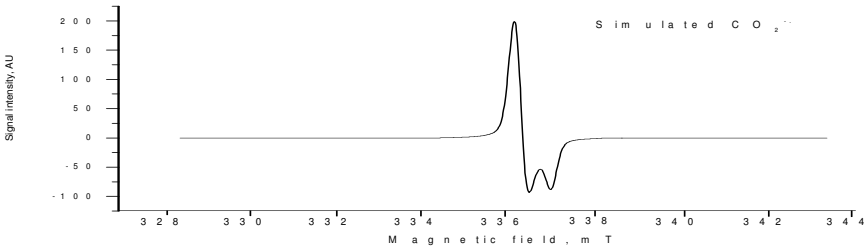

c)

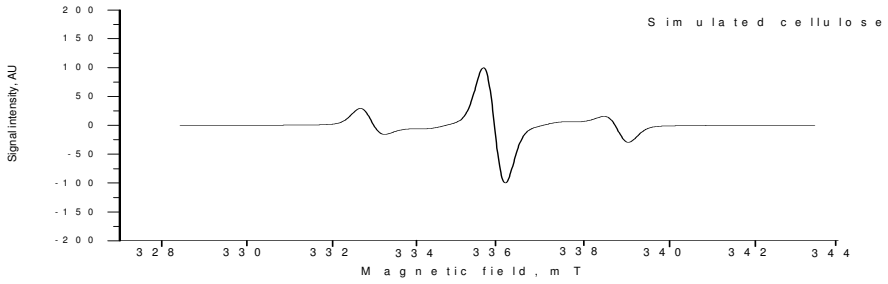

d)

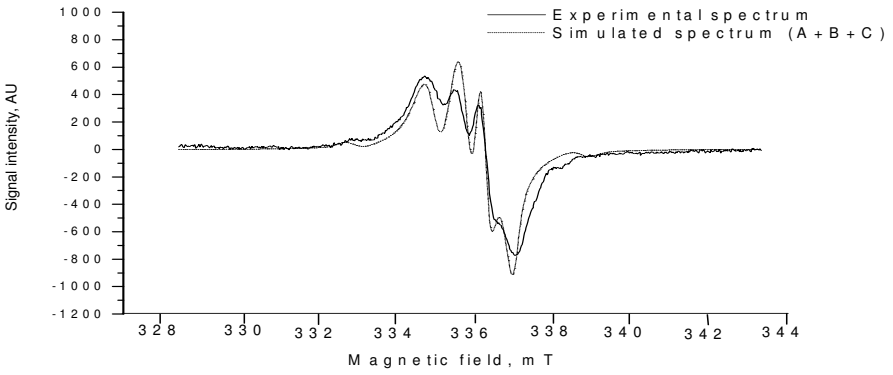

Fig. 33. Simulation scheme of the EPR spectrum of irradiated aswagandha **a)** simulated spectrum of carbohydrate, **b)** simulated spectrum of CO_2^- radical ion, c) simulated spectrum of cellulose radical, and **d)** simulated and experimental spectra of irradiated aswagandha.

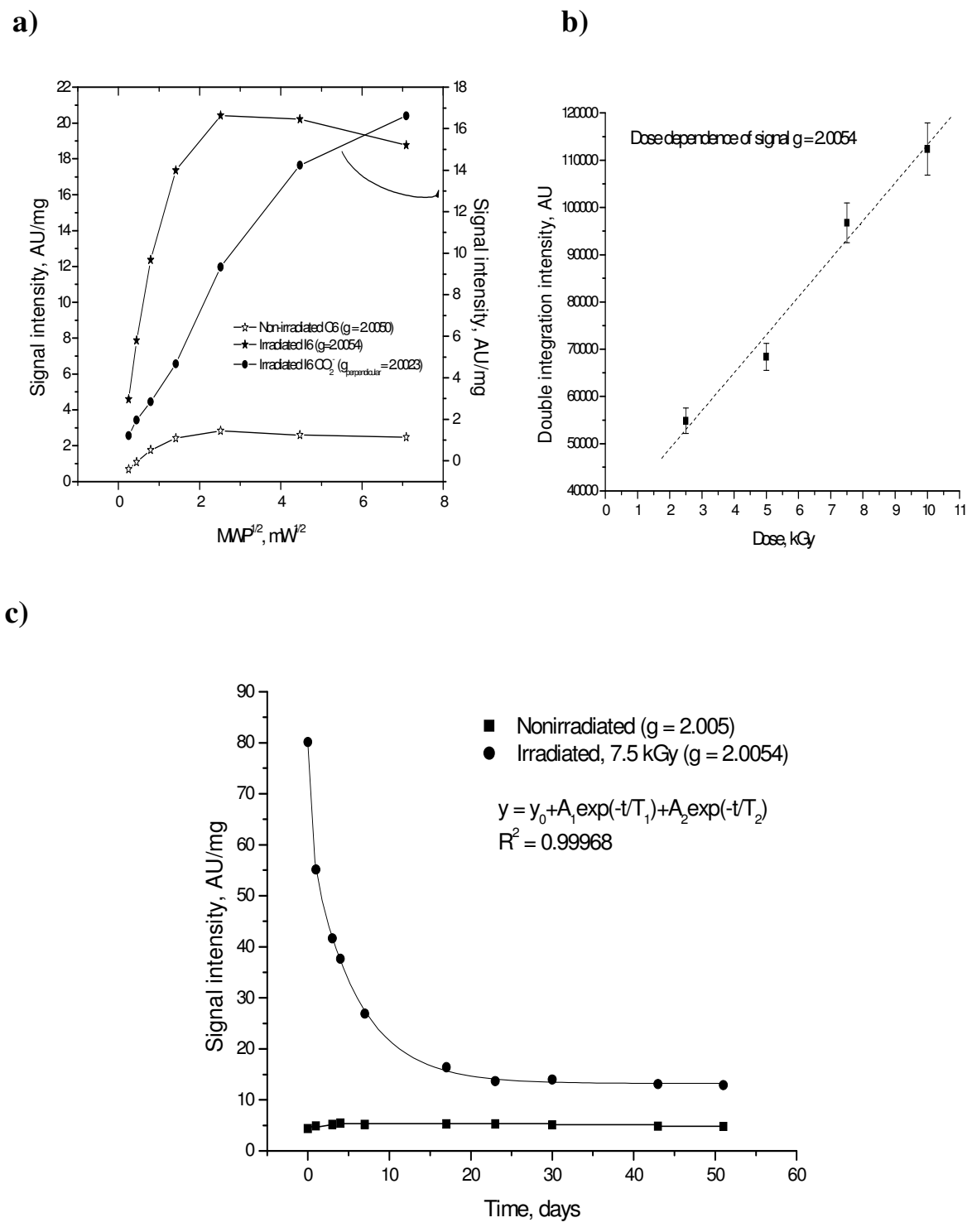

Fig. 34. a) Progressive saturation behaviors of central EPR signals of nonirradiated, irradiated aswagandha and CO_2^- radical ion signal, **b)** dose dependence of integral signal intensity, **c)** time kinetics of nonirradiated and irradiated samples of aswagandha during storage.

EPR analysis of other medicinal plant products

Vairi (*Salacia reticulata*), amla (*Emblica officinalis*), turmeric (*Curcuma longa*) and guduchi (*Tinospora cordifolia*) before and after radiation treatments were studied using EPR spectroscopy. Fig. 35a and b exhibited the EPR spectra of nonirradiated and irradiated (7.5 kGy) samples, respectively. In all the samples, irradiation revealed considerable increase in signal intensity of the EPR lines which were already present in the nonirradiated samples characteriged by g = 2.0050. EPR characteristics of the samples during storage did not reveal any change in spectral shape. Unlike aswagandha no radiation specific signal was detected either immediately after irradiation or after prolonged storage. The application of EN 13708, 2001 [41] for crystalline sugar and EN 1787, 2000 [20] for cellulose was not possible to establish the radiation treatment. In order to address this problem, two independent techniques based on EPR were employed, one was to study the electron relaxation behavior and the other was the thermal characteristic of the EPR signals. All the medicinal herbs under investigation revealed similar EPR characteristics and therefore, the progressive saturation behavior (PSB) and thermal characteristics of the radicals for only amla (*Emblica officinalis*) are shown in Fig. 35c and d. The PSB of the central line (g = 2.005) of nonirradiated and irradiated sample (7.5 kGy) after 45 days of radiation treatment exhibited similar saturation at microwave power of 9 mW. Therefore, EPR analysis by the progressive saturation behavior of the radicals was not useful to distinguish irradiated herbal medicines under investigation, namely vairi, amla, turmeric and guduchi.

In order to address the problem of identification, thermal behavior of the EPR signal was investigated. With the increase in temperature from 27 to 77°C, the central lines of both the nonirradiated and irradiated samples exhibited a slow fall (Fig. 35d). However, temperature increase beyond 77°C lead to an increase in EPR signals intensities in both the cases. The thermal behavior of the nonirradiated and irradiated medicinal plant products exhibited

similar nature limiting the application of EPR spectroscopy to identify radiation treatment after prolonged storage.

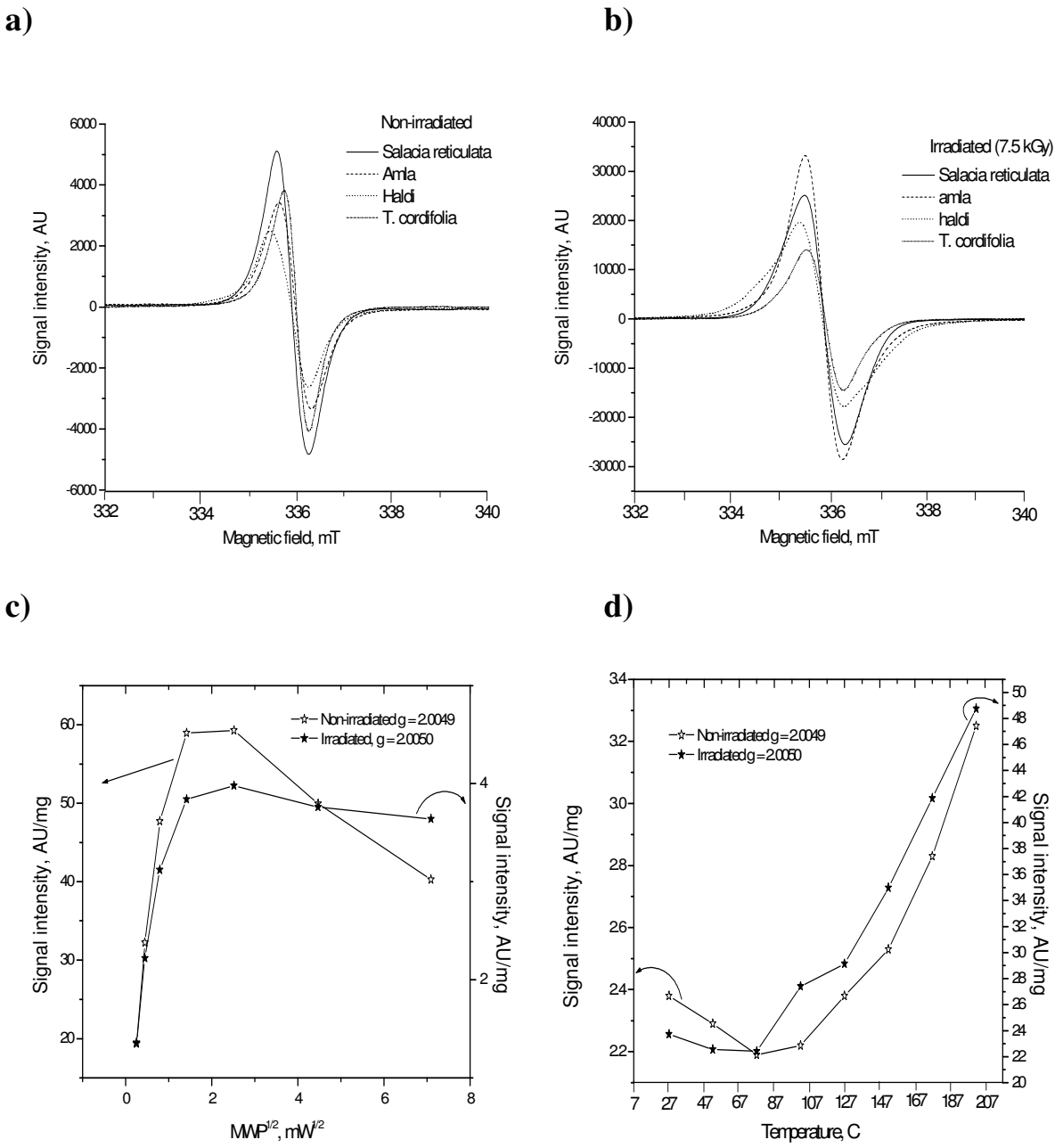

Fig. 35. EPR spectra of **a)** nonirradiated samples **b)** irradiated samples (7.5 kGy) of medicinal herbs, vairi (*Salacia reticulata*), amla (*Emblica officinalis*), turmeric (*Curcuma longa*) and guduchi (*Tinospora cordifolia*). Behavior of nonirradiated EPR signal (g = 2.0049) and irradiated signal (g = 2.0050) of amla (*Emblica officinalis*) after a storage time of 45 days **c)** with increasing microwave power, and **d)** with increasing temperature.

CHAPTER 7

TL and EPR studies of $CaSO_4$: Dy and $CaSO_4$: (Dy, Bi) phosphors for food irradiation dosimetry

Studies on $CaSO_4$: Dy phosphor

Dosimetry is of paramount importance in any quality assurance program for an irradiation facility. The evaluation of absorbed dose at low temperatures in irradiated food using a cost effective and simple dosimetry system is a challenging task. As a consequence there is interest for dosimetry systems with improved performances.

$CaSO_4$: Dy remains one of the most useful and sensitive thermoluminescence dosimeter (TLD) for radiation dosimetry. In case of $CaSO_4$: Dy phosphor for the personal exposure measurements, the dose response of the main TL peak (240ºC) was found to be linear up to 10 Gy [121]. However, supralinear response was reported in the dose range of 10 Gy to 5.0 kGy at room temperature irradiation [122]. For this purpose concentration of dysprosium normally used is 0.1 mol %. With this concentration the saturation of TL response has been attributed to non-availability of trapping centers for trapping the free charges [Mathur *et al*, 1999][82]. However, in this phosphor though the role of dysprosium is to provide recombination centres, it is also indirectly associated with the formation or stabilization of the trapping centres [123]. Therefore, increased concentration (0.2 mol %) of dysprosium was chosen, because of its commercial availability and improved sensitivity. This work was undertaken to study the effects of low temperature irradiation of commercial and thermally treated $CaSO_4$: Dy (0.2 mol %) phosphor. TL and EPR correlation studies were carried out to understand the TL properties of the phosphor after being subjected to pre-irradiation thermal treatments. The irradiation dose in the range of 0.5 to 7 kGy was chosen to meet the requirement of commercial food irradiation at sub-ambient temperature.

Effects of low temperature irradiation of commercial $CaSO_4$: Dy

To evaluate the crystal capacities of irradiated commercial $CaSO_4$: Dy (0.2 mol %), the integral TL (area under the glow) was measured at three different temperatures, chilled (0±4ºC), frozen (-10 ±2ºC) and liquid nitrogen temperature (-196ºC) with two different doses

0.4 and 1 kGy. Recently, Hernandez-Medina *et al*, 2009 [81] showed that annealed (400°C, 1h) samples of CaSO4: Dy exhibited a considerable decrease in response with the decrease of irradiation temperature. But, in our study with commercial phosphor, no significant difference in integral TL was observed with a maximum variation within ± 5% (Fig. 36a). Fig. 36b shows the glow curve structure of $CaSO_4$: Dy (0.2 mol %) irradiated at 0±4ºC. The low temperature and high temperature peaks were observed at 142ºC and 245ºC, respectively, without any structural changes in the glows with respect to the phosphor irradiated at ambient temperature. Low temperature peak (142ºC) was observed to be broad in nature. In case of LiF: Mg,Cu,P phosphor, the shifting of intensity maximum towards lower temperature with decreasing temperatures of irradiation was reported by Ramos–Bernel *e.al*, 2002 [78]. No such shifting was observed in $CaSO_4$: Dy phosphor. However, the peak temperatures shifted towards lower values with the increasing dose.

$CaSO_4$:Dy (0.2 mol %) phosphor was irradiated at 0±4ºC and TL signal response and peak heights at low temperature (142ºC) and high temperature (245ºC) as a function of gamma dose were studied in the dose range of 0.5 to 7 kGy. As shown in Fig. 37a, both the peak heights increased with the dose of radiation. Both the peaks showed a linear response (R= 0.99923) in the range of 0.5 to 1 kGy, limiting the application of this phosphor to measure radiation dose in the range of 3 - 4 kGy, which is normally used in irradiation of food at sub-ambient temperatures. In commercial phosphor supralinear response was observed above 1 kGy with 76.5 % increase in slope with respect to the linear region. As per ISO/ASTM 51956 [122], supralinearity refers to a region where the slope of the response versus dose is greater than that for the linear region. Chen *et al*, 1994 [79] suggested that the term supralinear could be used to describe the property of the measured quantity above the initial linear range. The production of significantly more number of defects at doses above 0.1 kGy may be responsible for the supralinear dose response. Another possible reason for the supraliner

response of the phosphor with increasing radiation dose could be the simultaneous contribution of the completion during excitation as well as heating. Exposure of ionizing radiation may produce trapped electrons and holes at existing impurities along with the defects produced by the process of irradiation itself.

TL and EPR studies of thermally sensitized phosphor

Thermal sensitization technique was employed to enhance the linear response of the CaSO4: Dy phosphor with increasing dose of gamma radiation. Exact determination of TL intensity of the low temperature peak was difficult due to its broad nature. Therefore, use of low temperature peak, as the dosimetry peak was limited unless it was distinguishable and sharp. Commercially available $CaSO_4$: Dy (0.2 mol %) phosphor was subjected to pre-irradiation thermal treatment at 700, 800 and 900ºC for a period of 2 h. As shown in Table 7, the peak height ratio (ratio of high temperature peak to low temperature peak) was observed to decrease sharply with increasing temperature of the thermal treatment, indicating a sharp rise of the low temperature peak intensity. These results were well in conformity with those reported literature [72]. The change in glow curve structures with the annealing temperatures is shown in Fig. 37b. The glow curves recorded from room temperature to 300ºC exhibited high temperature peak at about 245ºC and low temperature peak at about 142ºC. In order to understand the above observations, EPR spectra of the untreated and annealed $CaSO_4$: Dy phosphor were recorded at room temperature 24°C (297°K) and -196ºC (77°K) as shown in Fig. 38a - d and 39a - d. All the spectra recorded at room temperature and -196°C (77°K) exhibited three distinct radicals induced by ionizing radiation. These radicals were centered around 336.1 mT, 336 mT and 334.7 mT with g = 2.0031±0.001, 2.0038±0.0005 and 2.0113±0.0006, respectively. These lines were attributed to SO_3^-, SO_4^- and O_3^- radical ions, respectively. The g values obtained are compared well with those reported in the literature [124, 125, 126, 76, 127, 73]. From Fig. 38 and 39, it is observed that with the increase of

temperature of the pre-irradiation thermal treatment, the intensities of SO_4^- and O_3^- radicals were enhanced. However, the intensity of the SO_3^- did not exhibit any significant change.

In order to investigate the role of radiation induced paramagnetic centers in TL glow and the cause of sensitization of low temperature peak, the thermal behavior of the EPR lines were studied from room temperature to 300°C. Fig. 40a shows the behavior of SO_3^- radical with increasing temperature for all the three samples. In case of commercial phosphor a monotonous decrease up to a temperature of 150°C was observed, whereas, for the samples subjected to 700 and 800°C annealing initial rise of the signal up to 60°C followed by monotonous decrease was exhibited. However, the phosphor annealed at 900°C showed increasing trend throughout the temperature range and probably because of the development of Ca-vacancy defects $(Vca)^{2-}$ at the same position of SO_3^- radical. Similar observation has been reported by Danby *et al*, 1982; Morgan & Stoebe, 1990; Mauricio *et al,* 1996; Bortolin & Onori, 2005 [128, 129, 124, 130]. These results suggested that the paramagnetic center at g = 2.003 either for SO_3^- or for Ca vacancy defects may not be responsible for the enhancement of low temperature peak. Fig. 40b and c show the behavior of SO_4^- and O_3^- radicals with increasing temperature. In case of phosphor annealed at 900°C, the intensities of SO_4^- and O_3^- signals were enhanced in comparison with the other samples. The SO_4^- line showed a sharp fall around 125°C contributing to low temperature peak of the TL glow, whereas, O_3^- line exhibited a monotonous decrease in signal intensity up to 250°C revealing its major contribution to high temperature peak of the TL glow. The behavior of SO_4^- and O_3^- radicals was almost similar to that of phosphor annealed at 900°C. The thermal characteristics of all the paramagnetic centres revealed that SO_4^{--} could be responsible for the enhancement of the low temperature peak intensity.

Fig. 41a and b depict the radiation dose response of the low and high temperature peak heights of the thermally annealed (900°C) CaSO4: Dy phosphor with respect to commercially available phosphor. An increased sensitivity of the low temperature peak with no significant deviation from its linear behavior with increasing dose up to 4 kGy were observed. However, post preparation thermal treatment did not reveal any significant change in the high temperature peak height with increasing dose.

Table 7. Height ratio of high temperature peak to low temperature peak with increasing temperature of pre-irradiation annealing of $CaSO_4$: Dy phosphor

Temperature of thermal treatment (°C, 2h)	**Height ratio of high temp peak to low temp peak**
Without thermal treatment	14.63 ± 0.49
700°	9.91 ± 0.86
800°	7.68 ± 0.50
900°	1.29 ± 0.04

a)

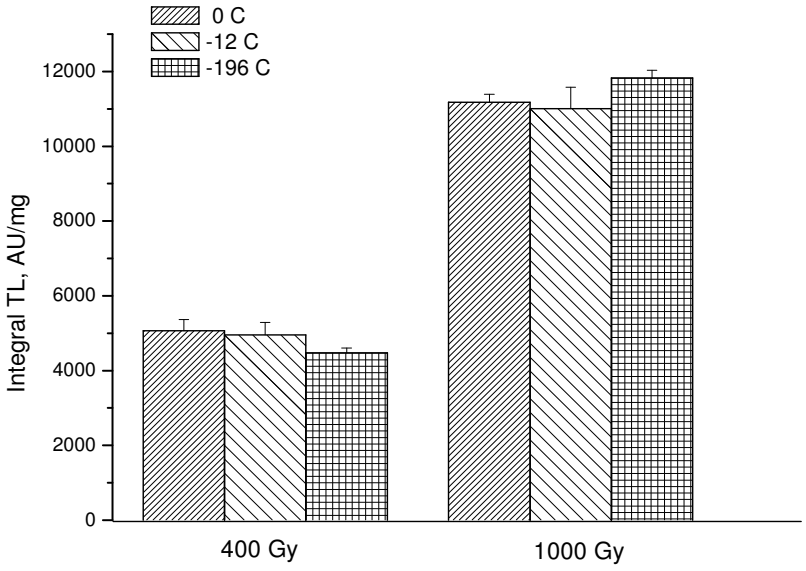

b)

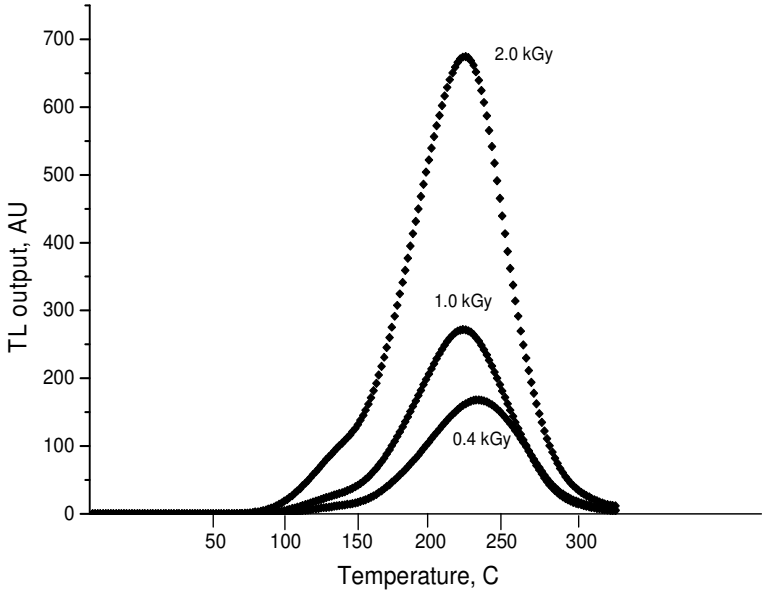

Fig. 36. a) Integral TL output of commercial $CaSO_4$: Dy (0.2 mol %) irradiated at chilled (0±4°C), frozen (-10±2°C) and liquid nitrogen temperature (-196°C), **b)** TL response of $CaSO_4$:Dy (0.2 mol %) with increasing gamma dose at 0±4ºC.

a)

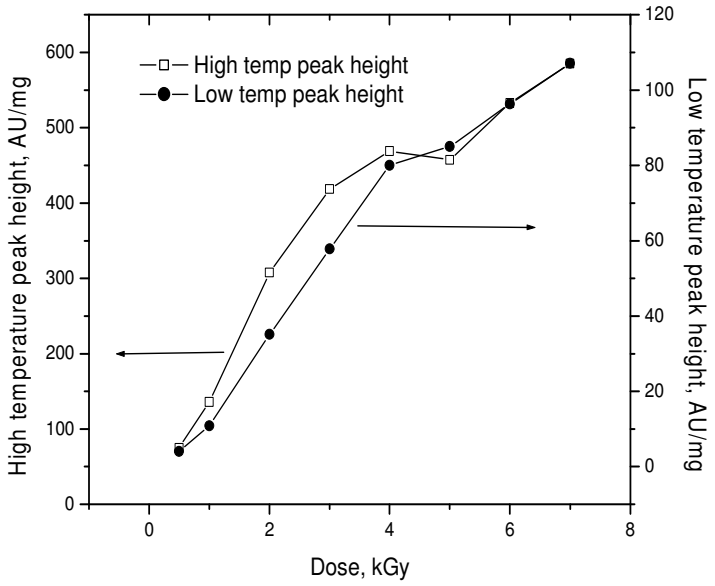

b)

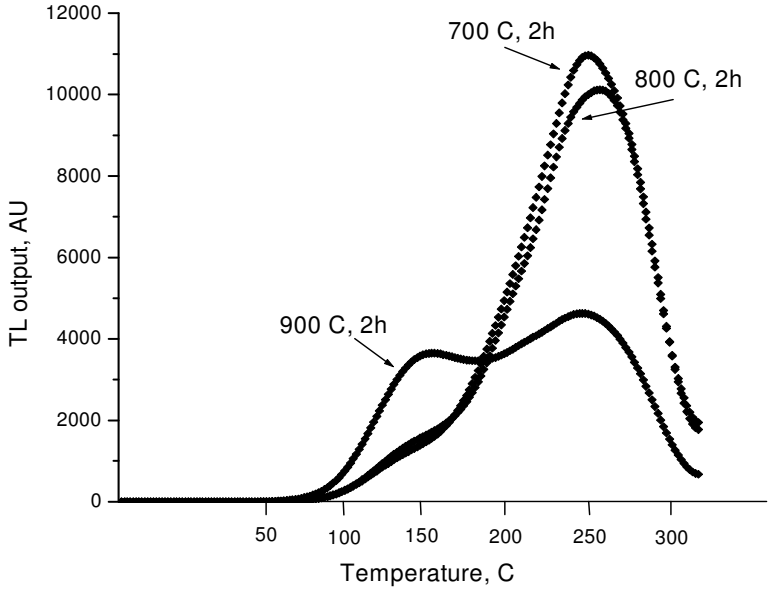

Fig. 37. a) Change in high temperature peak height and low temperature peak height with gamma dose at chilled temperature for commercial $CaSO_4$:Dy (0.2 mol %) without any sensitization treatment, **b)** change in glow curve profile after post-preparation thermal treatments at 700, 800 and 900°C.

a)

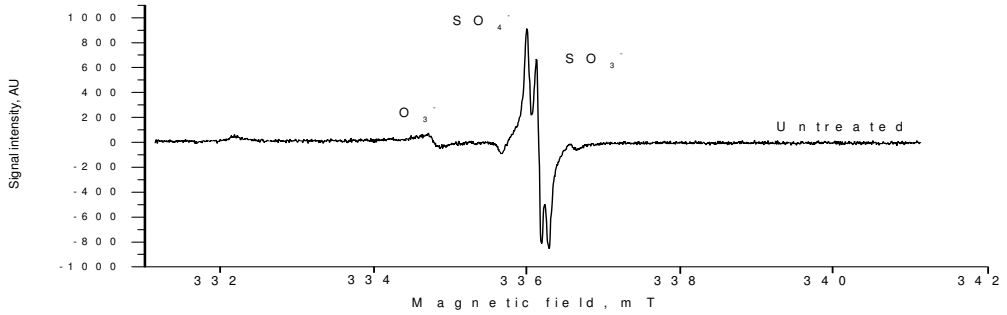

b)

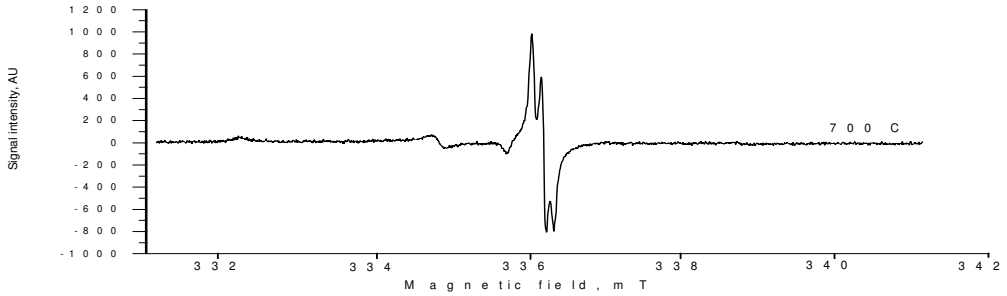

c)

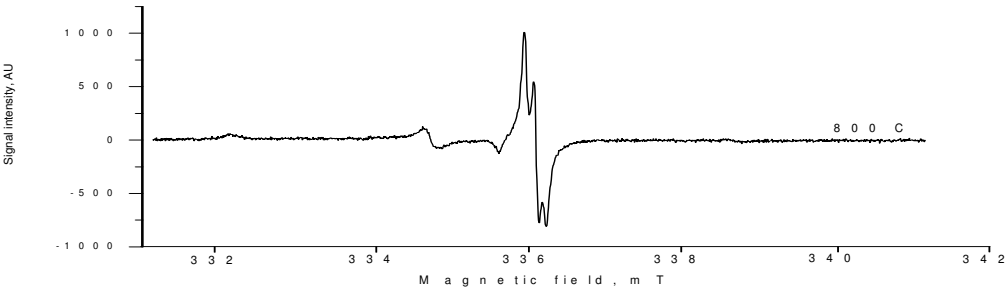

d)

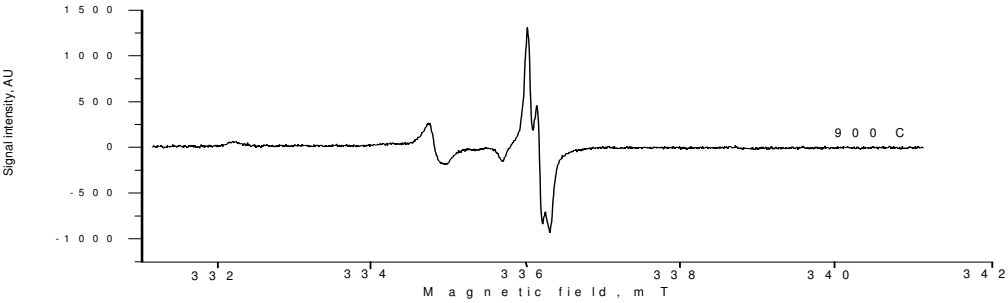

Fig. 38. EPR spectra recorded at room temperature with microwave power of 6.53 mW for **a)** untreated $CaSO_4$: Dy (0.2 mol %) phosphor **b)** annealed at 700°C **c)** annealed at 800°C and **d)** annealed at 900°C.

a)

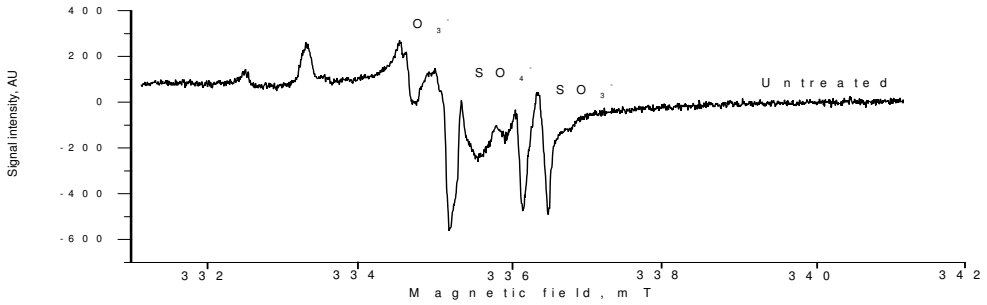

b)

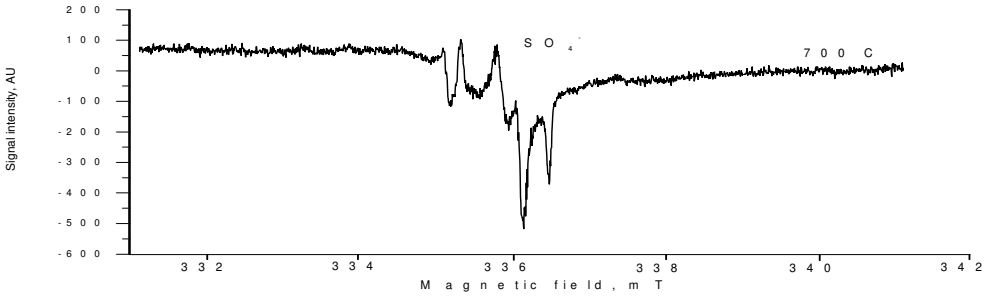

c)

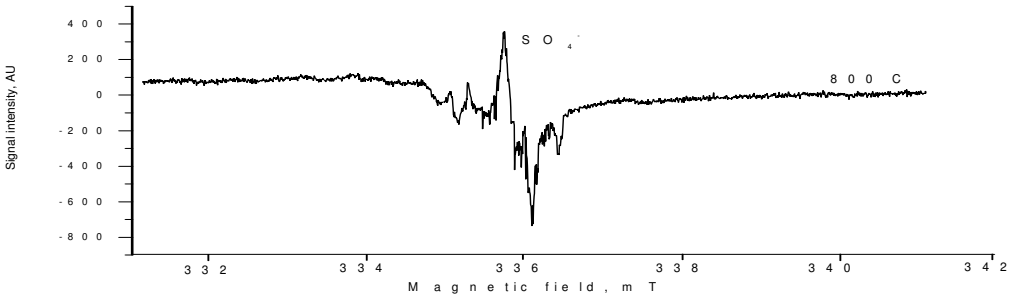

d)

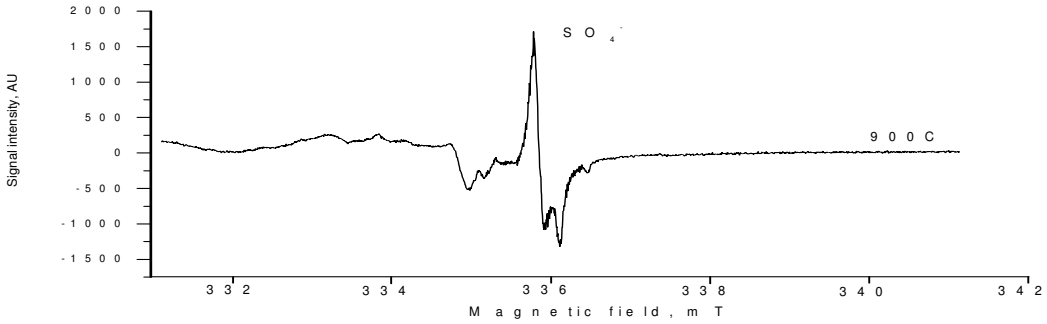

Fig. 39. EPR spectra recorded at 77°K (-196°C) with microwave power of 6.53 mW for **a)** $CaSO_4$: Dy (0.2 mol %) phosphor, **b)** annealed at 700°C, **c)** annealed at 800°C, and **d)** annealed at 900°C.

a)

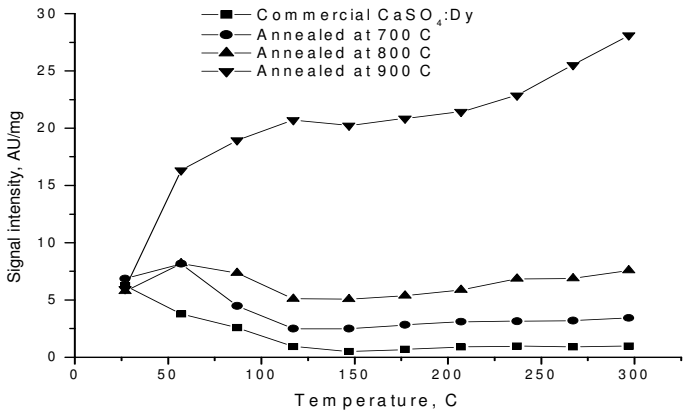

b)

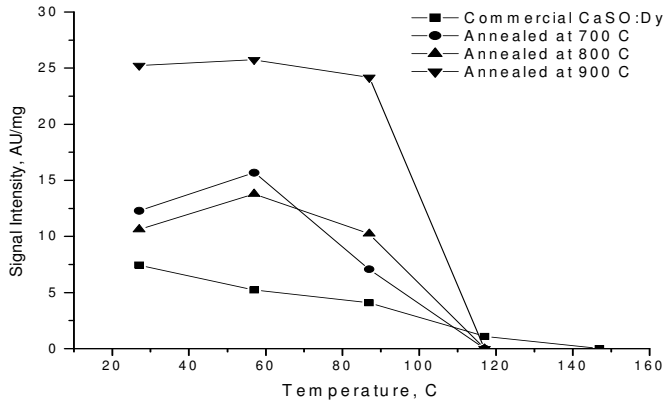

c)

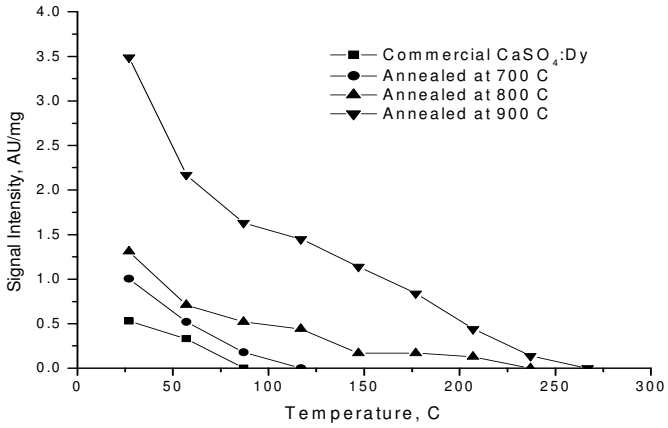

Fig. 40. Response of the EPR signal intensities of **a)** SO_3^-, **b)** SO_4^- and **c)** O_3^- of untreated and annealed at 700, 800, 900°C $CaSO_4$: Dy phosphor with increasing temperature.

a)

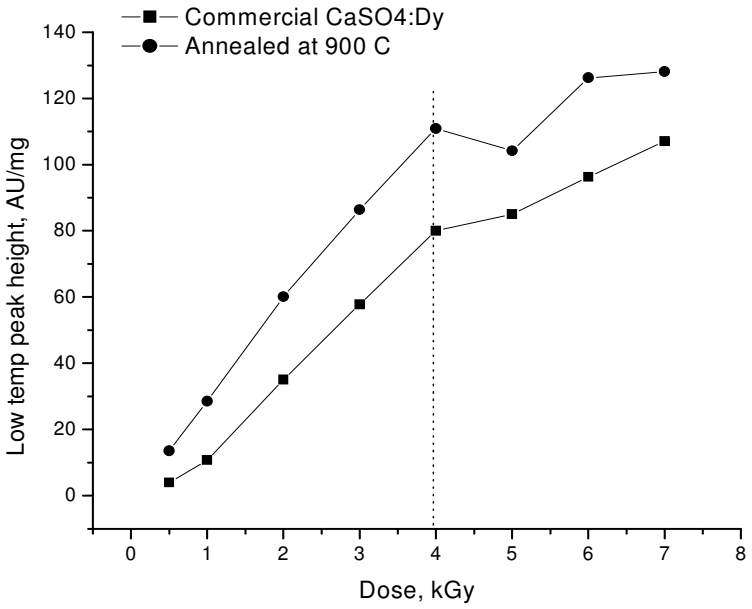

b)

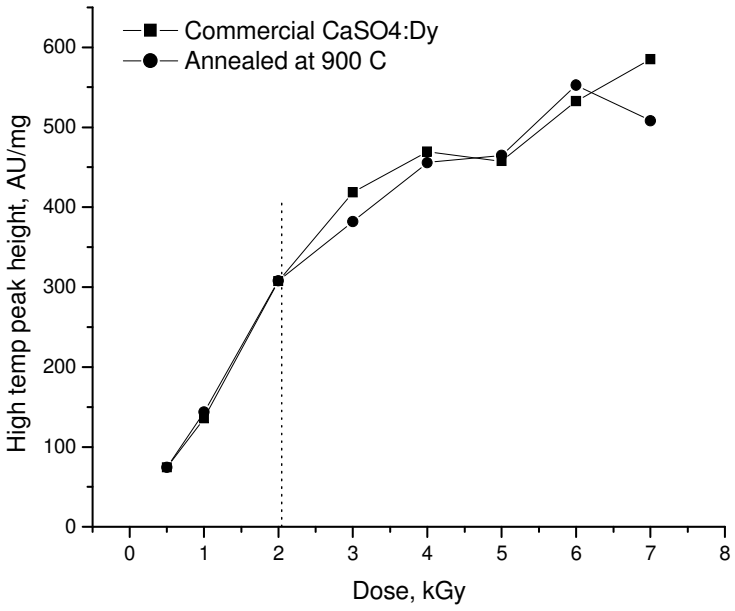

Fig. 41. Behavior of the TL response of the commercial and annealed (900°C) CaSO4: Dy phosphor with increasing radiation dose (at 0±4°C) of **a)** low temperature peak height and **b)** high temperature peak height.

Studies on $CaSO_4$: (Dy, Bi) phosphor

$CaSO_4$: Dy phosphor is well known for its high thermoluminescence (TL) sensitivity and stability to environmental variation. Energy transfer mechanism from one dopant (sensitizer) to another (luminescent center) is sometimes used to enhance the sensitivity of a phosphor. Earlier several researchers have tried to sensitize this phosphor by co-doping with different rare earth metals [84]. The most important co-doped phosphor is $CaSO_4$:Dy^{3+}, Ce^{3+}, wherein, it is reported that the emission from Ce^{3+} in the region 306 – 324 nm overlaps with the Dy^{3+} excitation and in turn enhances its TL emission. Bi^{3+} is a heavy metal with $7s^2$ electronic configuration and is known for its fluorescence properties [84, 85]. It is an interesting co-dopant ion, capable of transferring energy to rare earth ions such as Eu^{3+} [87]. It displays broad intense ultraviolet absorption bands in the wavelength range 230 - 330 nm and a broad emission band, generally in the region 400-600 nm. However, the emission band varies from one host lattice to another. In $CaSO_4$:Bi^{3+}, violet emission around 380 nm ($^3P_0 \rightarrow {}^1S_0$) has been reported at room temperature, while its absorption maximum is around 345 nm [130]. Therefore, it is of interest to examine the TL characteristics of Bi and Dy co-doped $CaSO_4$ phosphor. In the present study we have established the TL properties of Bi^{3+} co-doped $CaSO_4$: Dy in different proportion. Further, we have described the results of electron paramagnetic resonance (EPR) studies on gamma irradiated $CaSO_4$:Bi^{3+}, $CaSO_4$: (Dy^{3+}, Bi^{3+}) and tried to correlate EPR results with the observed TL characteristics for possible explanation. Measurement of high radiation dose using TL phosphor has several advantages. These phosphors can be used for dose measurement during food irradiation using simple read out methods [77, 78]. In view of this, the efficacy of the Bi^{3+} co-doped $CaSO_4$: Dy phosphor to measure the food irradiation dose in the range of 1 to 5 kGy has been investigated.

TL characteristics of the phosphor

Fig. 42a shows the TL glow curve of $CaSO_4$: Dy, $CaSO_4$: (Dy, Bi) and $CaSO_4$: Bi phosphors, which had undergone annealing treatment in N_2 atmosphere at 700°C for 2 h. As such, there is no change in the TL glow curve (peak temperature and shape) of $CaSO_4$: Dy and $CaSO_4$: (Dy, Bi). Glow curve consists of a peak at around 236°C with a lower temperature satellite peak at around 140°C for both $CaSO_4$: Dy and that of $CaSO_4$: (Dy, Bi) (0.05mol %) phosphors. It is clear from Fig. 42a that the TL sensitivity reduced in the presence of Bi co-dopant for $CaSO_4$: Dy phosphor. The TL intensity of $CaSO_4$: Bi was significantly lower than that of $CaSO_4$: Dy as well as $CaSO_4$: (Dy, Bi) phosphors. Its glow curve shape is also different from the other two phosphors. The glow curve has a prominent peak at 130°C and a hump at around 160°C. Fig. 42b shows the glow curve of $CaSO_4$: (Dy, Bi) with varying concentration of Bi. It can be seen that with increasing concentration of Bi, the peak intensity was reduced and peak temperature of the peak at 236°C shifted towards lower temperature side. This indicated that with increasing Bi concentration either Bi^{3+} acts as a quencher of dosimetric TL peak or the concentration of defect centre related to dosimetric peak gets reduced. In case of $CaSO_4$: Bi, it seems Bi is not creating any additional defect centers. The glow curve is characteristic of host lattice [65]. $CaSO_4$: Dy and $CaSO_4$: (Dy, Bi) with Bi concentration 0.05, 0.2 and 0.5 mol % were subjected to thermal treatment at 700°C for 2 h in the inert atmosphere of nitrogen to study the relative TL sensitivity of $CaSO_4$: (Dy, Bi) with varying concentration of Bi with respect to that of $CaSO_4$: Dy phosphor. The relative sensitivity of $CaSO_4$: (Dy, Bi) with Bi concentration 0.05% exhibited a maximum sensitivity of 0.72 with respect to $CaSO_4$: Dy. The sensitivity of $CaSO_4$: Dy was considered as 1. Phosphors having Bi concentrations of 0.2 and 0.5 mol % revealed relative sensitivities of 0.26 and 0.13, respectively.

TL - EPR correlation studies of the phosphor

Fig. 43a shows the EPR spectra of $CaSO_4$: (Dy, Bi) with different concentrations of Bi and irradiated to a gamma dose of 1 kGy. Three prominent peaks were observed with g values 2.023, 2.0089 and 2.004, respectively. Fig. 43b shows the EPR spectra of $CaSO_4$: Bi phosphor samples with different concentration of Bi. In this case also, three lines with g values 2.024, 2.009 and 2.004 were observed. On the basis of earlier reports [126, 76, 124], the three lines were identified as line 1: SO_4^- ($\parallel$), line 2: SO_4^-($\perp$) and line 3: SO_3^- (isotropic). The g values of the signals compared well with those reported in literature. The concentration of theses radical ions [SO_4^- ($\parallel$) and SO_4^- ($\perp$)] decreased with increasing concentration of Bi (Fig. 43a). This indicates that the lowering of TL sensitivity with increasing Bi concentration is attributable to quenching of TL by Bi^{+3} ions rather than reduction in defect concentration.

In order to understand the TL mechanism, $CaSO_4$: (Dy, Bi) phosphor samples were subjected to post irradiation annealing from 150 - 250 °C for 5 min in an air oven and their EPR spectra were recorded. Fig. 44a, b and c show the EPR spectra of $CaSO_4$: (Dy, Bi) samples annealed between 150 - 250°C. EPR signals from traces of Mn^{2+} were also seen in these spectra around the signals from SO_4^- and SO_3^- ions. Mn^{2+} is a natural trace impurity in the starting material used for the preparation of the phosphor. The changes in the EPR line intensities of the radical ions observed in $CaSO_4$: (Dy, Bi) with increasing annealing temperature is depicted in Fig. 44 d, e and f. It may be noted that with increasing annealing temperature the intensity of both SO_4^- and SO_3^- signals is reduced. The temperature of 250^oC was chosen considering the peak temperature of the dosimetric peak of $CaSO_4$: (Dy, Bi). From these figures, it was evident that EPR line intensities of SO_4^- radical ions reduced drastically in 250^oC annealed phosphor as compared to that in nonannealed samples. These results confirmed the role of sulphoxy radical ions, especially SO_4^- radical ion, in the dosimetric peak.

Food irradiation dose measurements

Though different high dose measurement techniques such as alanine-EPR dosimetry system [88], ceric-cerous sulphate dosimetry system [132] are available, they are either expensive and cumbersome or not suitable for low temperature dosimetry, which is required for dosimetry of perishable food commodities like chilled or frozen foods. In this context, thermoluminescence dosimeters are useful as they are cheaper and use a measurement technique. The present investigation showed that the TL sensitivity of $CaSO_4$: (Dy, Bi) phosphor reduced with increasing concentration of Bi^{3+} ion. This property of the phosphor was exploited in the present study for measurement of food irradiation dose. For this purpose involving measurement of high dose, $CaSO_4$: (Dy, Bi) phosphors (Bi concentration 0.2 and 0.5 mol %) was chosen due to its lower TL sensitivity. The phosphors were irradiated using a Cobalt-60 gamma irradiator in the dose range of 1 to 5 kGy, which is recommended for radiation preservation of chilled or frozen food.

Fig. 45 shows the dose response of $CaSO_4$: (Dy, Bi) phosphor samples in the dose range of 1-5 kGy. The dose response of the phosphor with Bi (0.2 mol %) did not reveal well defined relation with increasing radiation dose. However, the dose response of the $CaSO_4$: (Dy, Bi) (0.5 mol %) was well fitted using a second order polynomial (R^2 = 0.99129). The defined response of thermoluminescence characteristics of $CaSO_4$: Dy phosphor with increasing radiation dose in the range of radiation processing of food has already been reported in literature [82]. The response of $CaSO_4$: (Dy, Bi) (0.5 mol %) with increasing dose exhibited saturation beyond 3 kGy. However, the preliminary study revealed a clear trend in the dose response in the higher dose range. Therefore, adequately calibrated $CaSO_4$: Dy phosphors co-doped with 0.5 mol % Bi have the potential for use as a dosimeter in food irradiation dosimetry.

a)

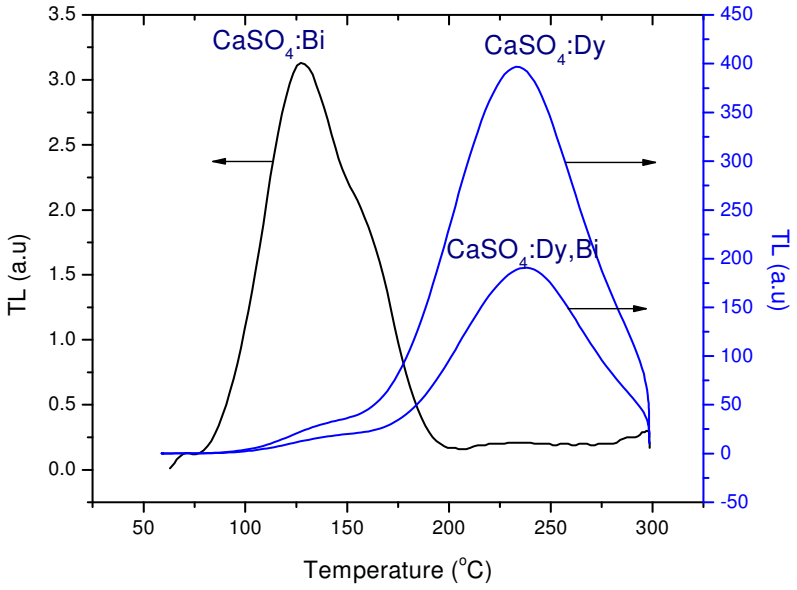

b)

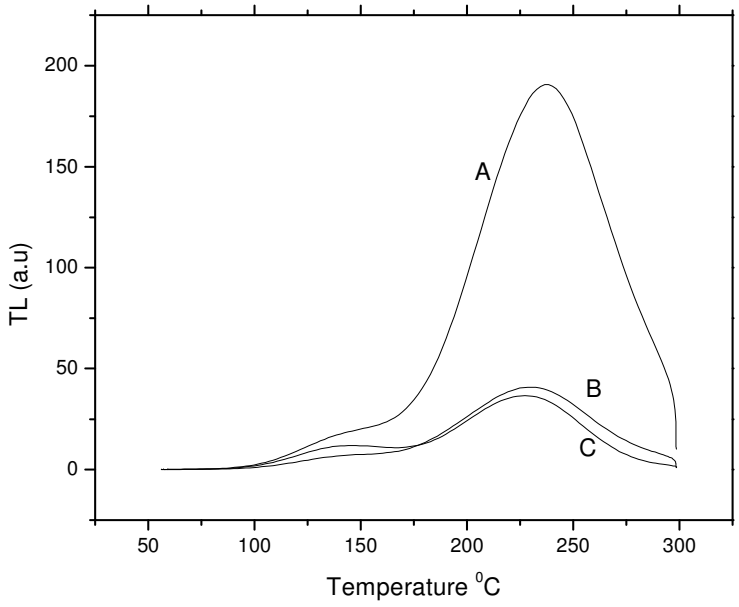

Fig. 42. **a)** TL glow curves of $CaSO_4$:Dy (0.05mol%), $CaSO_4$:Dy (0.05), Bi (0.05mol%) and $CaSO_4$:Bi (0.05mol%) and **b)** glow curves of $CaSO_4$: Dy, Bi with different concentration of Bi; curve A with Bi :0.05 mol%, curve B with Bi:0.2 mol% and curve C with Bi: 0.5 mol%.

a)

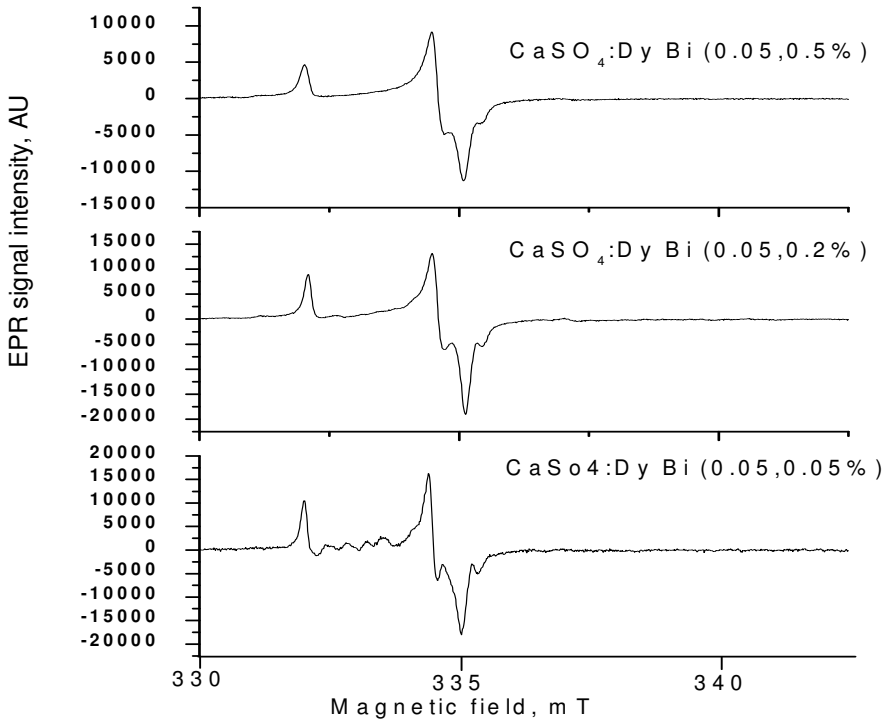

b)

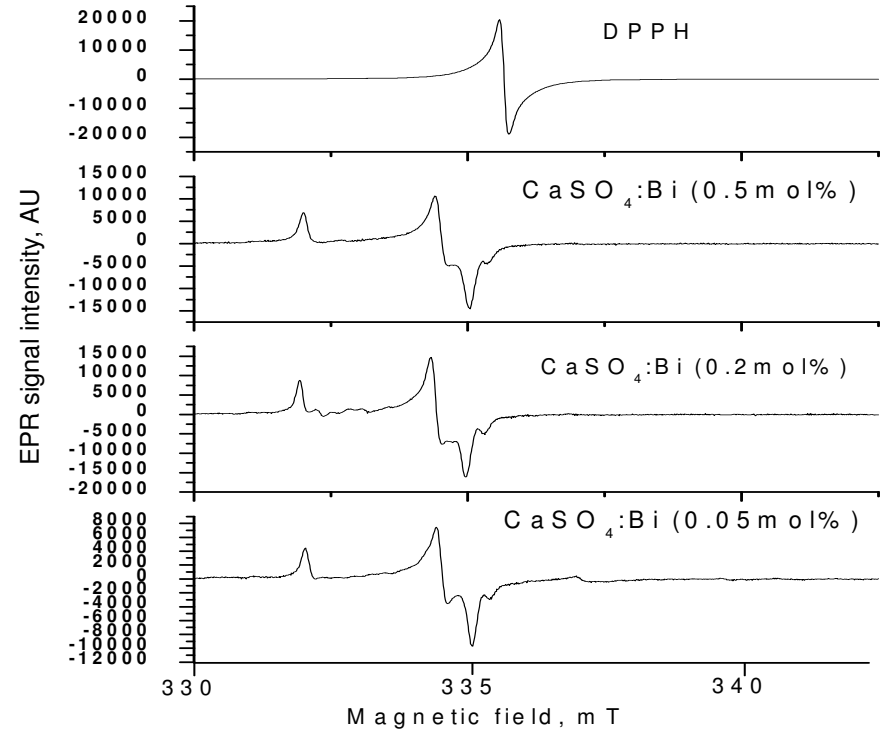

Fig. 43. a) EPR spectra of $CaSO_4$: (Dy, Bi) at (-196°C) with different concentration of Bi **b)** EPR spectra of $CaSO_4$:Bi at (-196°C) with different concentration of Bi along with $DPPH^{\cdot}$.

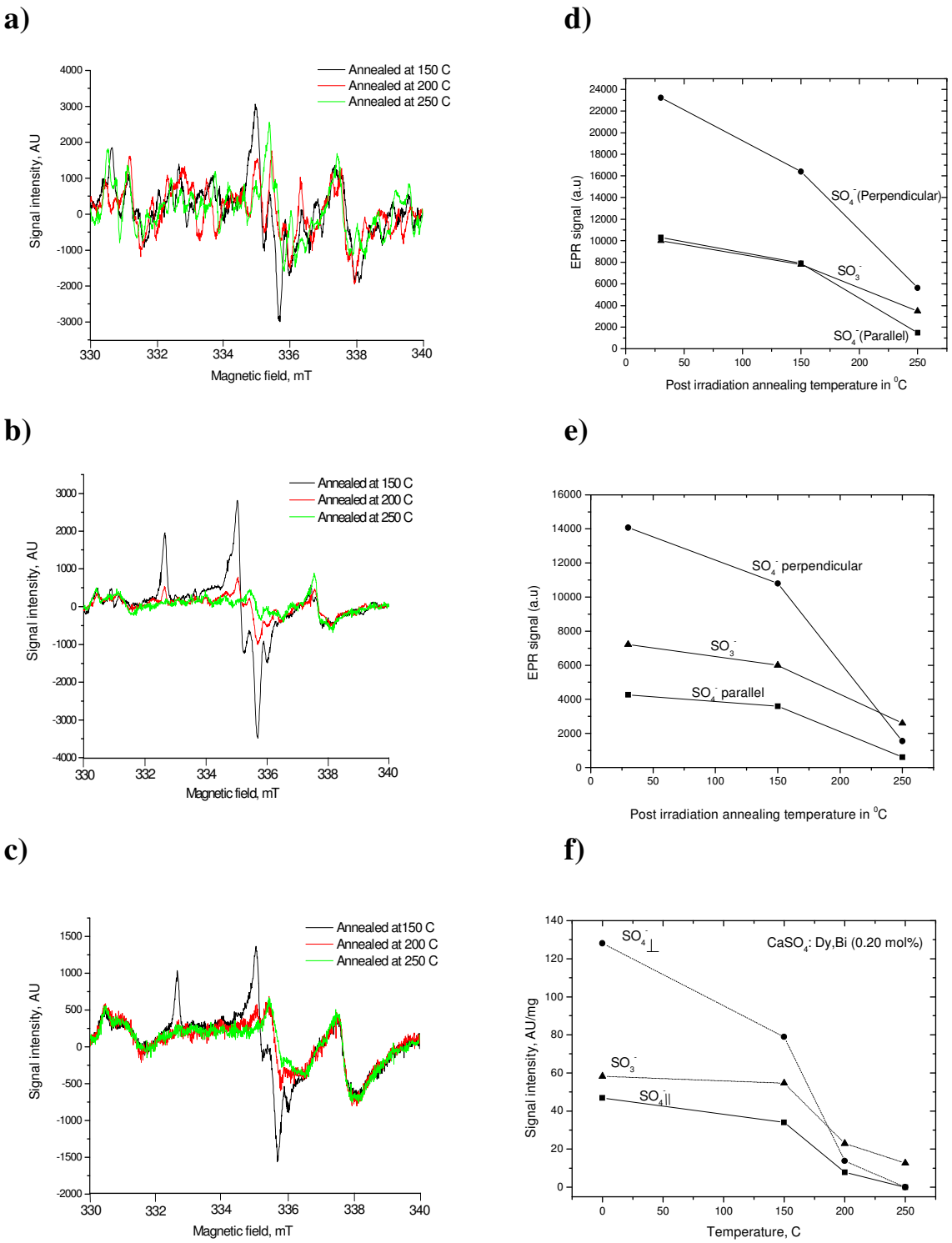

Fig. 44. EPR spectra of $CaSO_4$: (Dy, Bi) undergone annealing at different temperatures **a)** Bi: 0.05 mol%, **b)** Bi: 0.02 mol % and **c)** Bi: 0.5 mol%. Variation in peak intensity of sulphoxy radical ions with temperature for $CaSO_4$: (Dy, Bi) **d)** with Bi (0.05mol %), **e)** Bi (0.5mol %) and **f)** Bi (0.2 mol %).

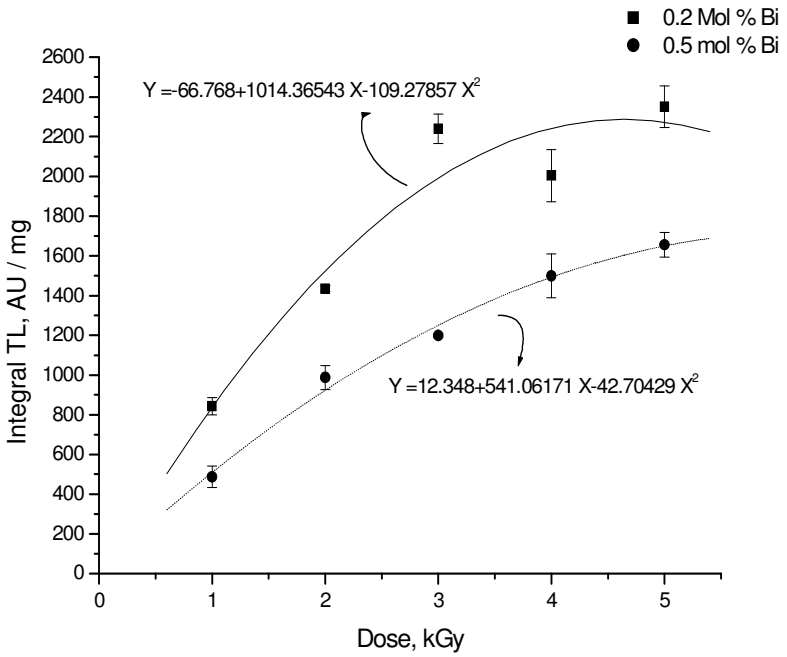

Fig. 45. Dose response of $CaSO_4$: Dy, Bi in the dose range 1-5 kGy along with polynomial fit.

.

CHAPTER 8

Summary and Conclusion

Identification of irradiated foods using TL and EPR techniques

Applications of EPR spectroscopy and thermoluminescence techniques to identify irradiated food from each class of food commodities have been investigated. All studies were focused on detection of foods irradiated with commercially relevant radiation dose. Investigations were carried out to identify irradiated foods after a prolonged storage which is one of the important requirements with practical relevance to radiation processed foods. The extension of feasible application of both the techniques in detection of a wide spectrum of irradiated foods approved for commercial irradiation has been established. Limitations of both the detection methods for various categories of food commodities have also emerged as very useful information. Importance of multiple techniques based on physical principles is therefore required to give a verdict on detection of radiation treatment of foods. The finding on both the detection methods to identify a spectrum of irradiated food commodities studied during this work is summarized below.

Identification of irradiated Basmati rice

Identification of gamma-irradiated Basmati rice was carried out by investigating radiation induced free radicals using electron paramagnetic resonance (EPR) spectroscopy, and thermoluminescence (TL) properties of the isolated polyminerals. In case of EPR spectroscopy, a weak singlet was found in the commercially available rice sample. However, a short lived complex spectrum was observed after radiation treatment attributed to radicals originating from starch. The change in free radical concentration showed a proportional increase with irradiation dose. By increasing the microwave power the line shape of the EPR spectra altered, and in the saturation curves it was possible to identify the irradiated and nonirradiated samples. Further, to distinguish irradiated and nonirradiated rice by EPR, the thermal behavior of the EPR signal was tested by heating the samples up to 187°C before recording the spectra. However, thermal behavior of the EPR signals was unable to identify

irradiated rice samples. TL investigation of the polyminerals isolated from the rice samples were carried out. SEM/EDX analysis revealed the maximum abundance of quartz (SiO_2) in the isolated minerals. TL glow curve structure of irradiated samples showed about 300 times increase in intensity than that of nonirradiated samples. Normalization dose and ratio of the first and second glow (glow 1 / glow 2) confirmed the identification of irradiated samples even after a long period of storage. Identification of radiation treatment after storage of the sample under investigation was not possible by application of any of the European Standards (EN 1787, EN 17083) for EPR spectroscopy. The TL technique adopted in this study provided promising results even after a long period of storage.

Identification of irradiated Soybean

Identification of gamma-irradiated soybean was carried out by investigating radiation induced free radicals using EPR spectroscopy. The skin part of nonirradiated, commercially available soybean exhibited a weak singlet signal, but in kernel part, a sextet signal of Mn^{2+} was identified. Immediately after radiation treatment a triplet signal was observed in skin part and characterized by simulation technique as cellulose radicals. Kernel part exhibited a singlet after irradiation and observed to be stable for 15 d. EPR spectra of kernel and skin parts of the samples were monitored for a period of 60 d and it was concluded that EPR analysis of the skin part of the samples is suitable for detection of irradiated soybean. It was also found that sample irradiated with a maximum dose of 1 kGy could be identified by the cellulose radical signal as per the European Standard EN 1787 up to a period of 50 d. But, the sample irradiated with a minimum dose of 0.25 kGy could be differentiated from nonirradiated (control) only up to a period of 30 d. These observations clearly showed that application of EN 1787 was not possible to identify soybean samples irradiated with this minimum dose of 0.25 kGy after a prolonged storage. In order to address this limitation, relaxation characteristics and thermal behavior of the radicals were studied. A full thermal profile of the

radicals after a prolonged storage time exhibited an important clue to radiation treatment. The relaxation characteristics of the radicals were revealed as a useful technique to identify thermally treated samples from nonirradiated and irradiated soybean.

Identification of irradiated potato, ginger and turmeric

The objective of the study was to identify irradiated potato of different geographical locations in India using TL characteristics of the isolated minerals. Identification of irradiated ginger and fresh turmeric was also studied using TL technique. Characterization of the isolated minerals from potato of various geographical locations was carried out by X-Ray diffraction (XRD) technique. The XRD analysis of the polyminerals showed that the relative abundance of K-feldspars ($KAlSi_3O_8^-$) and quartz (SiO_2) were predominant. However, a little variation in polymineral composition was observed with different origin of production. Normalization dose of 250 Gy was delivered to all the samples and TL glow (glow 2) was measured with the similar experimental settings. The ratio of glow 1 / glow 2 for nonirradiated polyminerals samples isolated from potato of all the geographical locations was 0.003±0.0005 and for irradiated samples it was 0.25± 0.052, thus clearly identifying the irradiated stored samples.

In case of ginger and fresh turmeric the integral TL and the intensity of the glow peaks for both the nonirradiated and irradiated samples showed significant difference even after a prolonged storage. Around 50 folds increase in TL glow (glow 1) in irradiated ginger, and around 20 folds increase in glow (glow 1) in case of irradiated fresh turmeric was observed in comparison with their respective nonirradiated samples. The samples were then exposed to a normalization dose of 1 kGy and the TL glow (glow 2) was measured. The glow curve shape (glow 2) of reirradiated samples not only confirmed inorganic nature of luminescent substances but also the higher value of glow1 / glow 2 ratio in irradiated samples endorsing the effective detection of radiation treatment.

The results of the present study revealed that isolation of polyminerals from the surface of potato, ginger and fresh turmeric was possible using density separation and TL measurement could clearly differentiate between irradiated and nonirradiated samples. The reirradiation step improved the reliability of the detection results of TL.

Identification of irradiated dog feed

Identification of gamma-irradiated dog feed was carried out by investigating radiation induced free radicals using EPR spectroscopy, and studying TL properties of the isolated polyminerals. EPR spectroscopy was useful to identify the irradiated ready to eat granular dog feed even after a prolonged storage. However, in case of edible dog chew sample detection of radiation treatment was not possible using EPR method alone. TL measurements of edible dog chew were employed to detect the irradiated sample. The SEM/EDX study revealed the composition of the isolated minerals. TL technique provided promising results even after a long period of storage, but, involved tedious sample preparation protocol. TL glow curve shapes and the ratio of the TL glow (glow1/ glow 2) emerged as a successful tool to identify irradiated dog chews even after a prolonged storage.

Identification of irradiated cashew nut

Free radicals in gamma-irradiated cashew nut were investigated by EPR spectroscopy. The change in free radical concentration showed a proportional increase with irradiation dose. A weak singlet was found in the commercially available cashew nut. However, two distinct but short lived signals were identified as cellulose and CO_2^- radical ion in irradiated sample. By increasing the microwave power, the line shape of EPR spectra altered and in saturation curves it was possible to identify the irradiated and roasted samples. However, radicals present naturally were not distinguishable from the irradiated signal by the respective relaxation behavior. Thermal behavior of the radicals after storage clearly showed the distinction between naturally present and radiation induced radicals. Identification of

irradiation treatment after storage of the sample under investigation was not possible by the application of protocol EN 1787. However, irradiated cashew nut could be distinguished from nonirradiated samples after a long period of storage by the thermal behavior of the EPR signals. In addition this report for the first time proposes a method to distinguish between irradiated and roasted sample by studying the relaxation characteristics of the induced radicals.

Identification of irradiated shrimp

TL technique was employed to identify irradiated shrimp. The intestinal grits were isolated from the nonirradiated and irradiated shrimps by alkaline hydrolysis followed by density separation. SEM image of the extracted polyminerals revealed the morphology and the EDX spectrum showed the major constituents as Calcium (Ca) and Silicon (Si). Traces of both the elements may be responsible for the TL signal. In case of irradiated samples, the areas under glow 1 were 30 to 35 times higher compared to that of nonirradiated one even after a prolonged storage. The ratio of areas for glow 1/glow 2 determined for nonirradiated shrimp was 0.009±0.002, while for irradiated shrimp 0.678±0.025, respectively. Possibility of identification of irradiated shrimp after cooking was also investigated. The TL studies were carried out after a period of one month storage after irradiation, and detection of irradiated shrimp, even after cooking, was possible from the first glow curve of the isolated minerals. EPR spectroscopy of the shell isolated from the nonirradiated and irradiated shrimps was also carried out. No change in spectrum shape was observed after radiation dose (3 kGy) of commercial relevance, revealing the limitation of EPR spectroscopy technique to identify irradiated shrimp.

Identification of irradiated medicinal plant products

Identification of gamma-irradiated medicinal herbs was carried out by investigating free radicals using EPR spectroscopy. Indian medicinal herbs namely aswagandha (*Withania*

somnifera), vairi (Salacia reticulata), amla (Emblica officinalis), haldi (Curcumin longa) and Guduchi (Tinospora cordifolia) exhibited a weak singlet signal before irradiation. Radiation treatment leads to increase in signal intensity in all the samples without any radiation specific signal in case of Vairi, amla, haldi and Guduchi. Therefore, the application of protocol EN 1787 and EN 13708, 2001 was not possible as the EPR signals of cellulose and crystalline sugar required by the European Standards were not visible in these samples after a prolonged storage. The relaxation characteristics and the thermal behavior of the radicals were studied, but, no clue to radiation treatment was found after prolonged storage. However, irradiated aswagandha exhibited a broad radiation-specific signal immediately after irradiation. High power EPR measurement resolved the spectrum revealing identifiable EPR lines. A time kinetics study of the induced radicals revealed a change in the shape of the EPR spectrum during storage with distinguishable radiation specific signals. The present study revealed a weak but stable radiation induced cellulosic radical signal along with a complex superposition of carbohydrate and CO_2^- type paramagnetic centres in aswagandha. In addition, a high-power EPR measurement may be used as an improved approach to detect an irradiated sample even after prolonged storage.

Studies on food irradiation dosimetry using TL phosphor

Measurement of radiation dose during radiation processing of dose is of paramount importance for commercial radiation processing facilities. Perishable food commodities need irradiation at sub-ambient temperatures where chemical dosimeters normally used for dose measurements cannot be used. Solid state dosimeters like TL phosphors are one of the suitable solutions for sub-ambient dose measurements. The efficacy of the $CaSO_4$ based phosphors namely, $CaSO_4$: Dy and $CaSO_4$: (Dy, Bi) were studied to address this problem. The results of the investigation suggested that the TL phosphors which are normally used to

measure occupational exposure dose need specific physical treatments like thermal sensitization or incorporation of co-dopant. TL – EPR correlation studies were carried out to establish the possibility of using these phosphors in food irradiation dosimetry as summarized below.

TL – EPR correlation studies on $CaSO_4$: Dy phosphor

$CaSO_4$: Dy phosphor exhibited reproducible dose response characteristics after irradiation at sub-ambient temperatures (0±4°C and -10 ±2ºC) in the range of 0.1 to 7 kGy with the onset of supralinearity above 1 kGy. Post-preparation thermal treatments revealed structural change in glow curve exhibiting increased sensitivity of the low temperature peak. Peak sensitization characteristics and the dose response behavior of the peaks of annealed phosphor could be explained based on the observation from the EPR studies. Phosphor subjected to post preparation thermal treatment of 900ºC exhibited saturation of low temperature peak at more than 4 kGy and may be most suitable for the dosimetry for food irradiation carried out at sub-ambient temperatures in the dose range of 0.5 to 4 kGy.

TL – EPR correlation studies on $CaSO_4$: (Dy, Bi) phosphor

EPR studies on gamma irradiated $CaSO_4$: (Dy, Bi) and $CaSO_4$: Bi phosphors samples revealed the presence of SO_4^- and SO_3^- defect centres. The reduction in TL sensitivity and glow curve structure with increase in Bi concentration in $CaSO_4$: (Bi, Dy) is attributed to the quenching action of Bi^{3+} ions on the TL rather than the change in concentration of SO_4^- and SO_3^- related defect centres. The role of SO_4^- and SO_3^- radical ions was identified by analyzing the EPR of $CaSO_4$: (Dy, Bi) samples subjected to post irradiation annealing up to 250ºC. The study also suggested that $CaSO_4$: (Dy, Bi) (0.5 mol %) could be used as a suitable dosimeter in food irradiation dosimetry.

Based on these studies on detection of irradiated food and food irradiation dosimetry the important conclusions drawn are:

a) EPR spectroscopy could be utilized to identify irradiated food commodities even after a prolonged storage. Thermal behavior and relaxation characteristics of the paramagnetic centres are useful tools in identification.

b) EPR spectral characteristics could also provide clue to radiation treatment in many food commodities, even after long storage, when different levels of microwave power were used. However, in case of many food samples detection of radiation treatment was not possible using EPR method alone.

c) In order to give a verdict on detection of radiation treatment for complicated food matrices, employment of more than one detection method was of immense importance. TL technique provided promising results even after a long period of storage, but, involved tedious sample preparation protocol.

d) TL glow curve shapes and the ratio of the TL glow (glow1/ glow 2) were successful tools to identify irradiated foods. The SEM/EDX study could reveal the composition of the isolated mineral from food commodities.

e) For the dosimetry of irradiated foods at sub-ambient temperatures, post-preparation thermal treatments of $CaSO_4$: Dy phosphor revealed structural change in TL glow curve exhibiting increased sensitivity of the low temperature peak that could be usefully exploited for low temperature dosimetry.

f) Reduction in TL sensitivity and glow curve structure with increase in Bi concentration in $CaSO_4$: (Dy, Bi) was attributed to the quenching action of Bi^{3+} ions on the TL. The study also suggested that $CaSO_4$: (Dy, Bi) (Bi concentration 0.5 mol %) could be used as a suitable dosimeter in food irradiation dosimetry.

REFERENCES

[1] FAO/IAEA/WHO (1981). Wholesomeness of Irradiated Foods, WHO, Geneva. Technical Report Series No 659.

[2] FAO/IAEA/WHO (1999). Facts about Food Irradiation. International Consultative Group on Food Irradiation (IGCFI).

[3] McMurray, C. H., Stewart, E. M., Gray, R. and Pearce, J., (Eds) (1996). Detection methods of irradiated foods. pp. 14-19, Royal Society of Chemistry, Cambridge, UK.

[4] Stevenson M. H., Stewart E. M. (1995). Identification of irradiated food: the current status. Radiation Physics & Chemistry, 46, pp. 653.

[5] Bogl, K. W., Regulla, D. F., Suess, M. J. (Eds) (1988). Health Impact, Identification, and Dosimetry of lrradiated Foods. Institut fur Strahlenhygiene des Bundesgesondheitsamtes, Neuherberg, F.R.G., ISH-Heft-125.

[6] Grun, R..,Kohno, H.,Tani, A.,Yamanaka, C.,Ikeya, M., Huang, H. P.(1997). Pulsed ESR measurements on fossil teeth. Radiation Measurements. 27 (2), pp. 425–431.

[7] Delincee, H. (1993) `Control of Irradiated Food: Recent Developments in Analytical Detection Methods' in Radiation Physics & Chemistry. 42, pp. 351-357.

[8] Ehlermann, D.A.E. (1996). The Contribution of Analytical Detection Methods to the Enforcement of Good Irradiation Practice' in Detection Methods for Irradiated Foods - Current Status.

[9] Desrosiers, M. F. (1996). Current status of the EPR method to detect irradiated food. Applied Radiation & Isotopes, 47, pp. 1621-1628.

[10] Raffi, J. - Yordanov, N. D. - Chabane, S. - Douifi, L. - Gancheva, V. - Ivanova, S. (2000). Identification of irradiation treatment of aromatic herbs, spices and fruits by electron paramagnetic resonance and thermoluminescence. Spectrochimica Acta A, 56, pp. 409-416.

[11] Delincée, H. (2002). Analytical methods to identify irradiated food - a review. Radiation Physics & Chemistry, 63, pp. 455-458.

[12] Korkmaz, M and Polat, M. (2000). Free radical kinetics of irradiate durum wheat. Radiation Physics & Chemistry, 58, pp. 169-179.

[13] Korkmaz, M and Polat, M. (2001). Radical kinetics and characterization of the free radicals in gamma irradiated red pepper. Radiation Physics & Chemistry, 62, pp. 411–421.

[14] Polovka, M. - Brezová, V. - Staško, A. - Suhaj, M. - Rácová, J. (2005). Oregano investigated by means of EPR spectroscopy. Chemicke Listy Symposia, 99(S), pp. 187-190.

[15] Polovka, M. - Brezová, V. - Staško, A. - Mazúr, M. - Suhaj, M. - Šimko, P. (2006). EPR investigations of gamma-irradiated ground black pepper. Radiation Physics & Chemistry, *75*, pp. 309-321.

[16] Suhaj, M. - Rácová, J. - Polovka, M. - Brezová, V. (2006). Effect of gamma-irradiation on antioxidant activity of black pepper (*Piper nigrum, L.*). Food Chemistry, 97, pp. 696-704.

[17] Delincée, H. - Soika, C. (2002). Improvement of the ESR detection of irradiated food containing cellulose employing a simple extraction method. Radiation Physics & Chemistry, 63, pp. 437-441.

[18] Bayram, G. - Delincée, H. (2004). Identification of irradiated Turkish foodstuffs combining various physical detection methods. Food Control, 15, pp. 81-91.

[19] Raffi, J., Agnel, J. P. L. (1989). Electron spin resonance identification of irradiated fruits. Radiation Physics & Chemistry, 34, 891-894.

[20] European Standard EN 1787. (2000). Foodstuffs-detection of irradiated food containing cellulose: analysis by EPR. Brussels, Belgium: European Committee for Standardization.

[21] Helle, N., Wolbert, U., Linke, B., Ehlers, D., Krueger, K.-E. (1995). Elektronenspinresonanz-spektroskopishe Untersuchung an frischen Fruechten. Z. Lebensm. Unters. Forsch. 201, pp. 355–360.

[22] Yordanov, N. D., Aleksieva, K. (2009). Preparation and applicability of fresh fruit samples for the identification of radiation treatment by EPR. Radiation Physics & Chemistry. Vol. 78 pp. 213 – 216.

[23] Onderdelinden, D., Strackee L. (1974). ESR as a tool for the identification of irradiated material. The identification of irradiated foodstuffs. Luxembourg: Commission of the European Communities. pp 127–40.

[24] Marino, A. A, Becker, R. O. (1968). Mechanically induced free radicals in bone. Nature 218: 468– 9.

[25] Ostrowski, K, Dziedzic-Goclawska, A., Stachowicz, W., Michalik, J. (1974). Accuracy, sensitivity of electron spin resonance analysis of mineral constituents of irradiated tissues. Ann NY Acad Science, 238, pp. 186–201.

[26] Sin, D. W.,Wong, Y., Yao, M. W., Marchioni, E. (2005). Identification and stability study of irradiated chicken, pork, beef, lamb, fish and mollusk shells by electron paramagnetic resonance (EPR) spectroscopy. European Food Research Technology, 221, pp. 684–91.

[27] Serway, R. A., Marshall, S. A. (1967). Electron spin resonance absorption spectra of CO_3^- and CO_3^{3-} molecule-ions in irradiated single-crystal calcite. Journal of Chemistry & Physics, 46(5), pp. 1949–52.

[28] Cevec, P., Schara, M., Ravnik, C. (1972). Electron paramagnetic resonance study of irradiated tooth and enamel. Radiation Research, 51, pp. 581–9.

[29] Gray, R., Stevenson, M. H. (1989). Detection of irradiated deboned turkey meat using electron spin resonance spectroscopy. Radiation Physics & Chemistry, 34, pp. 899–902.

[30] Chawla, S. P., Thomas, P. (2004). Identification of irradiated meat using electron spin resonance spectroscopy: results of blind trials. International Journal of Food Science & Technology, 39, pp. 653–60.

[31] Ostrowski, K., Dziedzic-Goclawska, A., Stachowicz, W. (1980). Stable radiation induced paramagnetic entities in tissue mineral and their use in calcified tissue research. In: Prayor WA, editor. Free radicals in biology 6. London, U.K.: Academic press. pp. 321–44.

[32] Glimcher, M. J. (1984). Recent studies of the mineral phase in bone and its possible linkage in organic matrix by protein-bound phosphate bands. Phil Trans Royal Society B, 304, pp. 479–508.

[33] Gray, R., Stevenson, M. H., Kilpatrick, D. J. (1990). The effect of irradiation dose and age of bird on the ESR signal in irradiated chicken drumsticks. Radiation Physics & Chemistry, 35, pp. 284 – 287.

[34] Dodd, N. J. F., Ley, J. S., Swallow, A. J. (1985). Use of ESR to identify irradiated food. Radiation Physics & Chemistry, 26(4), pp. 451–453.

[35] Goodman, B. A., McPhail, D. B., Duthie, D. M. L. (1989). Electron spin resonance spectroscopy of some irradiated foodstuffs. Journal of Science Food Agriculture, 47, pp. 101–11.

[36] Desrosiers, M. F. (1989). Gamma-irradiated seafoods: identification and dosimetry by electron paramagnetic resonance spectroscopy. Journal of Agriculture & Food Chemistry, 37, pp. 96–100.

[37] Stewart, E. M., Stevenson, M. H., Gray, R. (1994). Use of ESR spectroscopy for the detection of irradiated crustacean. Journal Science Food Agriculture, 65, pp. 191–197.

[38] Stewart, E. M., Kilpatrick, D. J. (1997). An international collaborative blind trial on electron spin resonance (ESR) identification of irradiated crustacean. Journal Science Food Agriculture, 74, pp. 473–484.

[39] European Standard EN 1786. (1997). Foodstuffs-detection of irradiated food containing bone: analysis by electron paramagnetic resonance. Brussels, Belgium: European Committee for Standardization.

[40]. Mischke, J., Helle, N., Linke, B., Schreiber, G. A. and Bogl, K. W. (1994). Electron spin resonance measurements on dried fruit. Carbohydrate composition and ESR signal structure of irradiated fruit. Z Ernahrungswiss, 33, pp. 258 – 266.

[41] European Standard EN 13708. (2001). Foodstuffs-detection of irradiated food containing crystalline sugar: analysis by EPR. Brussels, Belgium: European Committee for Standardization.

[42] Yordanov, N. D., Gancheva, V., Radicheva, M., Hristova, B., Guelev, M., Penchev, P. (1998). Comparative identification of irradiated herbs by the methods of electron paramagnetic resonance and thermoluminescence. Spectrochimica Acta A, 54, pp. 2413-2419.

[43] Yordanov, N. D. - Gancheva, V. (2000). A new approach for extension of the identification period of irradiated cellulose-containing foodstuffs by EPR spectroscopy. Applied Radiation & Isotopes, 52, pp. 1958-198.

[44] Yordanov, N. D., Aleksieva, K. (2004). X- and Q-band EPR studies on fine powders of irradiated plants. New approach for detection of their radiation history by using Q-band EPR spectrometry. Radiation Physics & Chemistry, 69, pp. 59-64.

[45]. EN 1788. (1996). Foodstuffs - Detection of irradiated food from which silicate minerals can be isolated - Method by thermoluminescence. European Committee for Standardization. Brussels [46] McDougall, D. J. (1968). Thermoluminescence of geological materials. London: Academic Press.

[47] Horowitz, Y. S. (1984). Thermoluminescence and thermoluminescent dosimetry. Vol. I-III. Boca Raton, Florida: CRC Press.

[48] McKeever, S. W. S. (1985). Thermoluminescence of solids. Cambridge: University Press.

[49] Aitken, M. J. (1985). Thermoluminescence dating. London: Academic Press.

[50] Krbetschek, M. R., Gotze, J., Dietrich, A. and Trautmann, T. (1997). Spectral information from minerals relevant for luminescence dating. Radiation Measurements, 27, pp. 695-748.

[51]. Botter-Jensen, L. (1997). Luminescence techniques: instrumentation and methods. Radiation Measurements, 27, 749-768.

[52] Chadwick, K. H. and Oosterheert, W. F. (1967). Radiation induced thermoluminescence of tomato seeds at low temperature. In: Egbert, H. G. (Ed), Proc. Symp. Microdosimetry, 13-15. November 1967, Ispra. Brussels: European Communities, EUR-3747, pp. 633-641.

[53] Heide, L. and Bogl, K. W. (1984). Die Messung der Thermolumineszenz *Ein neues Verfahren zur Identi"zierung strahlenbehandelter GewuK rze. Neuherberg: Institut fuK r Strahlenhygiene des Bundesgesundheitsamtes, *ISH-Heft* 58.

[54] Heide, L. and Bogl, K. W. (1988). Routine application of luminescence techniques to identify irradiated spices - a first counter check trial with 7 different research and food control laboratories. In: *Health impact*, *identification and dosimetry of irradiated foods*. Neuherberg: Institut fuK r Strahlenhygiene des Bundesgesundheitsamtes, ISH-Heft 125, 233-244.

[55] Sanderson, D. C. W., Slater, C. and Cairns, K. J. (1989). Detection of irradiated food. Nature, 340, pp. 23-24.

[56] Pinnioja, S. (1993). Suitability of the TL method for the detection of irradiated foods. Radiation Physics & Chemistry, 42, pp. 397 – 400.

[57] Khan, M. H., Delincee, H. (1995). Detection of radiation treatment of spices and herbs of Asian origin using TL of minerals contaminants. Applied Radiation & Isotope, 46, pp. 1071 – 1075.

[58] Marchioni, E., Horvatovich, P., Charon, H., Kuntz, F. (2005). Detection of irradiated ingredients included in low quantity in non-irradiated food matrix. 1. Extraction and ESR

analysis of bones from mechanically recovered poultry meat. Journal of Agriculture & Food Chemistry. *53*, pp. 3769-3773.

[59] Kwon, J. H., Jeong, J., Chung, H. W. (2002). Thermoluminescence characteristics of minerals from irradiated potatoes of different origins of production. Radiation Physics & Chemistry, 63, pp. 415–418.

[60] Soika, C. and Delincee, H. (2000). Thermoluminescence analysis for detection of irradiated food - luminescence characteristics of minerals for different types of radiation and radiation doses. Lebensm.-Wiss. u.-Technol., 33, pp. 431 – 439.

[61] Schreiber, G. A., Hoffmann, A., Helle, N and Bogl, K. W. (1994). Methods for routine control of irradiated food: determination of the irradiation status of shellfish by thermoluminescence analysis. Radiation Physics & Chemistry, 43, pp. 533-544.

[62] Kwon, J. H., Chung, H. W., Byun, M. W. Kang, I. J. (1998). Thermoluminescence detection of Korean traditional foods exposed to gamma and electron-beam irradiation. Radiation Physics & Chemistry, 52, pp. 151-156.

[63] Chung, H. W., Delincée, H., Kwon, J. H. (2000). Photostimulated luminescence-thermoluminescence application to detection of irradiated white ginseng powder, Korean Journal of Food Science & Technology, 32, pp. 265 – 270.

[64] Chung, H. W., Delincee, H., Han, S., Hong, J., Kim, H., Kim, M., Byun, M., Kwon, J. (2004). Trials to identify irradiated chestnut (*Castanea bungena*) with different analytical techniques. Radiation Physics & Chemistry, 71, pp. 179-182.

[65] Manam, J., Das, S., 2008. Thermally stimulated luminescence studies of undoped, Cu- and Mn-doped $CaSO_4$ compounds. Radiation Effects & Defects in Solids, 163, pp. 955-965.

[66] Lakshmanan, A. R. Luminescence in Rare Earth Doped CaSO4 Phosphors. (1999). Progress Material Science, 44, pp. 181–187.

[67] Townsend, P. D. and White, D. R. (1996). Interpretation of Rare Earth Thermoluminescence Spectra. Radiation Protection Dosimetry. 65, pp. 83–88.

[68] Daltro, T. F. L., Campos, L. L., Perez, H. E. (1999). Thermoluminescence dosemeter for equivalent dose assessment in mixed beta and gamma field. Radiation Protection & Dosimetry. 85, pp. 145 – 148.

[69] Morris, N. D. (1996). Personal radiation monitoring & assessment of doses received by radiation workers. Report No. ARL/TR121 (Australian Radiation Laboratory, Melbourne).

[70] Vohra K.G., Bhatt B.C., Bhuwan Chandra., Pradhan A.S., Lakshmanan A.R. and Sastry S.S. (1980). A Personal Dosimeter TLD Badge Based on $CaSO_4$: Dy Teflon TLD Discs. Health Physics, 38, pp. 193-197.

[71] Kassem, M. E. (2003). Environmental studies on X- and g-irradiated LiCsSO4 crystals. Applied Radiation & Isotopes, 59, pp. 129 – 132.

[72] Bakshi, A. K., Pradhan, A. S., Tyagi, A. K., Kher, R. K., Bhatt, B. C. (2006). Correlation of phase transition with the change in TL characteristics in $CaSO_4$: Dy phosphor – effect of thermal treatment. Radiation Protection Dosimetry, 119, pp. 139-142.

[73] Bakshi, A. K., Patwe, S. J., Bhide, M. K., Sanyal, B., Natarajan, V., Tyagi, A. K., Kher, R. K. (2008). Thermoluminescence, ESR and x-ray diffraction studies of CaSO4: Dy phosphor subjected to post preparation high temperature thermal treatment. Journal of Physics D: Appllied Physics, 41, 025402 (8pp).

[74] Sunta, C. M. (1984). A review of thermoluminescence of calcium fluoride, calcium sulphate and calcium carbonate. Radiation Protection Dosimetry, 8, pp. 25 – 44.

[75] Lakshmann, A. R. and Jose, M. T. (1993). Low dose measurements with $CaSO_4$:Dy, $CaSO_4$: Tm, and $CaSO_4$:Dy Teflon dosimeters – a comparative study. Radiation Protection Dosimetry, Vol. 46, pp. 181 – 187.

[76] Natarajan, V., Dalvi, A. G. I., Sastry, M. D. (1988). Trap level spectroscopy of actinide-doped alkaline-earth sulphates: II. $CaSO_4$: ^{241} Am. Journal of Physics C: Solid State Physics, 21, pp. 5913–5922.

[77] Lewandoski, A. C., Mathur, V. K. (1996). High dose and phototransferred thermoluminescence in CaSO4, Ca SO4: Dy and CaSO4: Tm. Radiation Protection Dosimetry, 66, pp. 213-216.

[78] Ramos-Bernal, S., Cruz, E., Negron-Mendoza, A., Bustos, E. (2002). Irradiation dose determination below room temperature. Radiation Physics & Chemistry, 63, pp. 813-815.

[79] Chen, R. and McKeever, S. W. S., (1994). Characterization of nonlinearities in the dose dependence of thermoluminescence. Radiation. Measurements, 23, pp. 667-673.

[80] Bakshi, A. K., Pradhan, A. S., Srivastava, K., Kolambe, D. H. (2002). New parameters of annealing and re-use of TLDs based on $CaSO_4$: Dy phosphor. Radiation Protection Dosimetry, 100, pp. 293-296.

[81] Hernandez-Medina, A., Negron-Mendoza, S., Ramos-Bernal. (2009). Temperature effect during the gamma irradiation of $CaSO_4$: Dy. Radiation Measurements, 45, pp. 586 – 588.

[82] Mathur, V. K., Lewandowski, A. C., Guardala, N. A., Price, J. L. (1999). High dose measurements using thermoluminescence of $CaSO_4$:Dy. Radiation Measurements, 30, pp. 735-738.

[83] Lin, J., Su, Q., Wang, S., Zhang, H. (1996). Influence of crystal structure on the luminescence properties of bismuth (III), europium (III) and dysprosium (III) in Y_2SiO. J. Material Chemistry, 6, pp. 265 - 269.

[84] Moncorge, R., Boulon, G., Denis, J.P. (1979). Fluorescence Properties of Bismuth doped $LaPO_4$. Journal of Physics C: Solid State Physics, 12, pp. 1165-1171.

[85] Murata, T., Mouri, T. (2007). Matrix effect on absorption and Infrared Flurescence properties of Bi ions in Oxide glasses. Journal of Non-crystalline solids. 353, pp. 2403-2407.

[86] Qiang, Su., Barthou, C., Denis, J. P., Pelle, F., Blanzat, B. (1983). Luminescence and energy transfer in Y_2O_3 CO-doped with Bi^{3+} and Eu^{3+} Journal of Luminesence, 28, pp. 1-11.

[87] ASTM Standard, E 1026. Standard Practice for Using Fricke Reference Standard Dosimetry System.

[88] ASTM standard, ISO/ASTM 51607:2004 E. (2004). Standard practice of use of an Alanine-EPR dosimetry system.

[89] Horowitz, Yigal, S. (1984). Thermoluminescence and Thermoluminescent Dosimetry. CRC Press. pp. 10. Boca Raton FL.

[90] Sharaf, M. A., Hassan, G. M. (2004). Radiation induced radical in barium sulphate for ESR dosimetry: a preliminary study. Nuclear. Instuments & Methods Physics Res. B, 225**,** pp. 521–527.

[91] Yamahashita, T., Nada, N., Omishi, H., Katimura, S. (1968). Calcium sulphate phosphor activated by rare earth. In: Proc. 2nd Int. Conf. on Luminescence Dosimetry, Gatlinburg (Springfield, VA: NTIS) CONF 680920.

[92] Martin, M., and Fitzgerald, M. A. (2002). Proteins in rice grains influence cooking properties. Journal of Cereal Science, 36, pp. 285-294.

[93] Sudha Rao, V., Gholap, A. S., Adhikari, H., Madhusudanan, N. P. (2000). Disinfestation of Basmati rice by the use of γ-radiation. International Journal of food Science and Technology, 35, pp. 533-540.

[94] Franco, R. W. A., Martin-Neto, L., Kato, M. S. A., Furlan, G. R., Walder, J. M. M. & Colnago, L. A. (2004). Identification of irradiation treatment in black pepper by electron paramagnetic resonance. International Journal of Food Science and Technology, *39*, pp. 395-401.

[95] Yordanov, N, D., Pachova, Z. (2006). Gamma-irradiated dry fruits an example of wide variety of long-time dependent EPR spectra. Spectrochimica Acta, 63, pp. 891-895.

[96] Scewartz, H. M., Bolton, J. R., Brog, D. C. (Eds). (1972). Biological Applications of Electron Spin Resonance. Wiley, New York.

[97] Maloney, D. R., Tabner, B. J., Tabner, V. A. (1992). An electron spin resonance study of gamma-irradiated fruits. Radiation Physics & Chemistry, 39, pp. 309-314.

[98] Tabner, B. J., Tabner, V. A.(1994). Electron spin resonance spectra of gamma-irradiated citrus fruits skin, skin components and stalks. International Journal of food Science and Ttechnology, 29, pp. 143-152.

[99] Polovka, M., Brezova, V., Simko P.(2007). EPR spectroscopy: A tool to characterize gamma irradiated foods. Journal of Food and Nutrition Research, 46, pp. 75-83.

[100] Yordanov, N. D., Aleksieva, K., Mansour, I. (2005). Improvement of the EPR detection of irradiated dry plants using microwave saturation and thermal treatment. Radiation Physics & Chemistry, 73, pp. 55-60.

[101] Delincee, H. (1998). Detection of food treated with ionizing radiation. Trends in Food Science and Technology, 9, pp. 73-82.

[102] Calderon, T., Correcher, V., Millan, A., Beneitez, P., Rendell, H. M., Larrson, M., Townsend, P. D., Wood, R. A. (1995). New data on thermoluminescence of inorganic dust from herbs and spices. Journal of Physics D: Applied Physics, 28, pp. 415-423.

[103] Correcher, V., Muniz, J. L., Gomez-Ros, J. M. (1998). Dose dependence and fading effect of the thermoluminescence signal in ν-irradiated paprika. Journal of Science and Food Agriculture, 76, pp. 149-158.

[104] Autio, T., Pinnoja, S. (1990). Identification of irradiated foods by the thermoluminescence of mineral contamination. Z. Lebensm. Unters, Forsch. 191, pp.177-180.

[105] Sanderson, D. C. W., Carmichael, L. A., Spencer, J, Q., Naylor, J. (1996). Luminescence detection of shell fish. In C. H. McMurray, Detection methods of irradiated foods, Cambridge: The Royal Society of Chemistry, pp. 139-148.

[106] Oliveira, M. R. R., Quadrado, M. G. O., Mastro, N. L. (2007). Analysis of gamma irradiated soybean components by electron paramagnetic resonance. Proceedings IJM Cancum, Mexico.

[107] Desrosiers, M. F., McLaughlin, W. L. (1989). Examination of gamma irradiated fruits and vegetables by electron spin resonance spectroscopy. Radiation Physics & Chemistry, 34, pp. 895-898.

[108] Bortolin, E, Griffin, E. B., Cruz-Zaragoza, E., De Coste, V., Onori, S. (2006). Electron paramagnetic resonance detection of Mexican irradiated spices. International Journal of Food Science & Technology, 41, pp. 375-382.

[109] Geoffroy, M., Tochon-Danguy, H. J. (1982). ESR identification of radiation damage in synthetic apatites: a study of the carbon-13 hyperfine coupling. Calcio Tisue Int. 34, S99-S102.

[110] Ohler, J. G. (1979). Cashew. Department of Agricultural Research, Royal Tropical Institute, Amsterdam.

[111] Bhattacharjee, P., Singhal, R. S., Gholap, A. S., Variyar, P. S. , Bongirwar, D. R. (2003). Compositional profiles of γ-irradiated cashew nuts. Food Chemistry. 80(2), pp. 151-157.

[112] Ikeya, M., Baffa, O. F., Mascarenhas, S. (1989). Quality assessment of coffee beans with ESR and gamma- irradiation. Applied Radiation & Isotopes. 40, pp. 1219-1222.

[113] Raffi, J., Stevenson, M. H., Kent, M., Thiery, J. M. & Belliardo, J. J. (1992). European intercomparison on electron spin resonance identification of irradiated food stuffs. International Journal of Food Science & Technology. 27, pp. 111-124.

[114] Adhikari S, Priyadarsini K I, Mukherjee T. (2007). Physico-Chemical Studies on the Evaluation of the Antioxidant Activity of Herbal Extracts and Active Principles of Some Indian Medicinal Plants. Journal of Clinical Biochemistry Nutr, 40, pp.174–183.

[115] Kähkönen, M. P., Hopia, A. I., Vuorela, H. J., Rauha, J. P., Pihlaja, K., Kujala, T. S., Heinonen, M. (1999). Antioxidant activity of plant extracts containing phenolic compounds. Journal of Agriculture & Food Chemistry, 47, pp. 3954–3962.

[116] Zheng W, Wang S. Y (2001) Antioxidant activity and phenolic compounds in selected herbs. Journal of Agriculture & Food Chemistry, 49, pp. 5165–5170.

[117] Arora, D. S., Kaur, J (1999) Antimicrobial activity of spices. Int J Antimicrob Agents, 12, pp. 257–262.

[118] Raffi, J. J., Agnel, J. P. L., Thiery, C. J., Frejaville, C. M., Lebe, S. L. R.. (1981). Study of g-irradiated starches derived from different foodstuffs: a way for extrapolating wholesomeness data. Journal of Agriculture & Food Chemistry, 29, pp. 1227-1232.

[119] Raffi, J. J. Agnel, J. P. L. (1983). Influence of the physical structure of irradiated starches on their electron spin resonance spectra kinetics. Journal of Physics Chemistry, 87, pp. 2369 - 2373.

[120] Arthur, Jr., J., Mares, T., Hinojosa, O. (1966). ESR spectra of gamma-irradiated cotton cellulose 1 and 2. Text. Res. J.36, 630.

[121] Campos, L. L. & Lima, M. F., (1986). Dosimetric properties of CaSO4: Dy Teflon pellets produced at IPEN. Radiation Protection & Dosimetry, 14, pp. 333-335.

[122] ASTM Standard, 51956. (2005) (E). Standard practice for use of thermoluminescence dosimetry (TLD) systems for radiation processing.

[123] Stoebe, T. G., Morgan, M. D., (1984). Models of TL trapping and recombination centers. Thermoluminescence and Thermoluminescent Dosimetry1, pp. 19–47.

[124] Mauricio, C. L. P., Bortolin, E. Onori. S. (1996). ESR study of $CaSO_4$: Dy TLD. Radiation Measurements, 26, pp. 639–44.

[125] Sharaf, M. A., Hassan, G. M. (2004). Radiation induced radical in barium sulphate for ESR dosimetry: a preliminary study. Nuclear Instruments Methods Physics Research B, 225, pp. 521–527.

[126] Gupta, N. M., Luthra, J. M., Shankar, J. (1974). Trapping and emission centres in thermoluminescent barium sulphate. Radiation Effects, 21, pp. 151–156.

[127] Seshagiri, T. K., Dalvi, A. G. I., Sastry, M.D. (1988). Trao level spectroscopy of actinide-doped alkaline-earth sulphates:I. $SrSO_4$:^{239}Pu and $CaSO_4$:^{239}Pu. Journal of Physics C: Solid State Physics, 21**,** pp. 5891–5912.

[128] Danby, R. J., Boas, J. F., Calvert, R. L. Pilbrow, J. R., (1982). ESR of thermoluminescence centres in $CaSO_4$ single crystals. Journal of Physics C: Solid State Physics, 15, pp. 2483-2493.

[129] Morgan, M. D., Stoebe, T. G., (1990). The role of Dy in the thermoluminescence of $CaSO_4$. Radiation Protection Dosimetry, 33, pp. 31-33.

[130] Bortolin, E., Onori, S. (2005). Features of EPR dosimetry with CaSO4: Dy phosphor. Applied Radiation & Isotopes, 62, pp. 349-352.

[131] Van der Voort, D., Blasse, G. (1992). Luminescence of CaSO4:Bi^{3+} a small-offset. Journal of Solid State Chemistry, 99 (2), pp. 404-408.

[132] ASTM Standard, ISO/ASTM 51205:2002 (E). (2002). Standard Practice for use of a Ceric-Cerous Sulphate Dosimetry System.

PUBLISHED PAPERS

Provided for non-commercial research and education use.
Not for reproduction, distribution or commercial use.

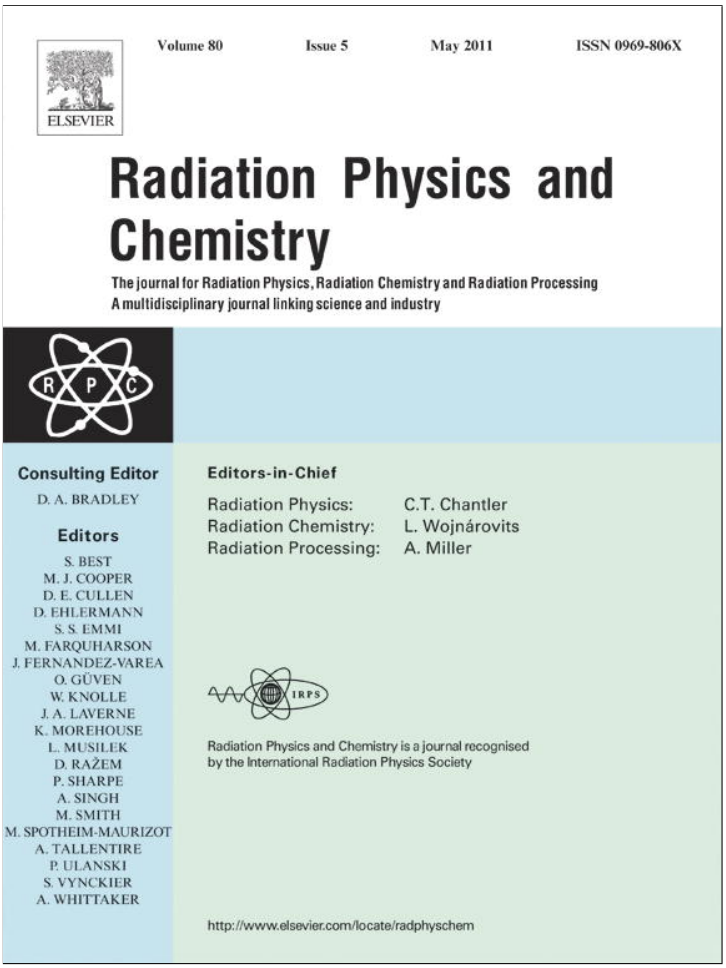

This article appeared in a journal published by Elsevier. The attached copy is furnished to the author for internal non-commercial research and education use, including for instruction at the authors institution and sharing with colleagues.

Other uses, including reproduction and distribution, or selling or licensing copies, or posting to personal, institutional or third party websites are prohibited.

In most cases authors are permitted to post their version of the article (e.g. in Word or Tex form) to their personal website or institutional repository. Authors requiring further information regarding Elsevier's archiving and manuscript policies are encouraged to visit:

http://www.elsevier.com/copyright

Author's personal copy

Radiation Physics and Chemistry 80 (2011) 650–657

Contents lists available at ScienceDirect

Radiation Physics and Chemistry

journal homepage: www.elsevier.com/locate/radphyschem

An improved approach to identify irradiated dog feed by electron paramagnetic resonance study and thermoluminescence measurements

Bhaskar Sanyal *, S.P. Chawla, Arun Sharma

Food Technology Division, Bhabha Atomic Research Centre, Mumbai-400 085, India

ARTICLE INFO

Article history:
Received 4 October 2010
Accepted 28 November 2010
Available online 31 January 2011

Keywords:
Food irradiation
Detection of irradiated foods
EPR
TL
Dog feed

ABSTRACT

In the present study, probably for the first time, a detailed analysis of the radiation induced radical species and thermoluminescence measurements of irradiated dog feed are reported. The EPR spectrum of non-irradiated ready-to-eat dog feed was characterized by singlet $g=2.0047\pm0.0003$. Irradiated samples exhibited a complex EPR spectrum. During high power (50.0 mW) EPR spectroscopy, a visible change in the shape of the EPR spectrum was observed and characterized by EPR spectrum simulation technique. An axially symmetric anisotropic signal with $g_{\parallel}=2.0028$ and $g_{\perp}=1.9976$ was identified. However, a negligible change in the matrix of irradiated edible dog chew was observed using EPR spectroscopy. Therefore, thermoluminescence study of the isolated minerals from dog chew was carried out. The composition of the poly-minerals was studied using SEM and EDX analysis and a complete verdict on identification of irradiation is proposed.

© 2011 Elsevier Ltd. All rights reserved.

1. Introduction

Pet food manufacturers use dietary fiber sources from grains, fruits and vegetables, celluloses, gums, and other sources. The main ingredients normally include cereal and cereal by-products, meat and poultry industry by-products, vegetable by-products, proteins, vegetable oils, iodized salt, essential vitamins and minerals. Therefore, feeds are an important vector of microbial contaminants that can impair both animal health and hamper food trade. Irradiation using ionizing radiation is an effective microbial disinfection process for animal feeds. It is currently used in many countries such as for dog chew to control pathogens namely *Salmonella.* The irradiation of poultry feed for control of *Salmonella* is also approved by FDA in US. In India, commercial radiation processing of animal feed is carried out for microbial decontamination with an average dose of 7.0 kGy.

To facilitate trade in irradiated foods and allied products, regulatory authorities need a reliable method to detect irradiated foods and consequently check compliance with the labeling requirements. In view of the growing interest of the food industry in irradiation technology, development of reliable methods to distinguish between irradiated and non-irradiated food stuffs is essential for the benefit of enforcement agencies.

Several detection methods have been developed for identification of irradiated foods (Sanyal et al., 2009; Chung et al., 2004). Among them, EPR spectroscopy and thermoluminescence detection are the two leading techniques. Three European standards for detection of irradiated food by EPR spectroscopy have been released by European Committee of Normalization (CEN) and adopted by Codex Alimenterius Commission as Codex Standards. These pertain to food containing bone (EN 1786, 1997), cellulose (Protocol EN 1787, 2000) and crystalline sugar (EN 13708, 2001). For use in detection, radiation induced EPR signals in food must fulfill several requirements. The signal must be fairly stable during the usual storage period of the foodstuff and must be clearly distinguishable from the background signals of the non-irradiated sample (Raffi et al., 1988). EPR is a user friendly technique, as the measurement is easy and the sample under test does not require any preparation. There is an increasing interest in extending the EPR methodology to various types of food and allied products. The main problem lies in the instability of the relatively weak radiation specific signals. A negligible change in food commodities after radiation treatment makes identification of irradiated food an extremely challenging task and the statistical safety margin is rather small for a reliable verdict to be given. In addition to that type, state and food constituents become the most important factors to employ the right identification technique. Therefore, one method alone is not reliable enough for the detection of a treatment by ionizing radiation. In view of this, in present work, two independent physical methods were employed. Such a combined approach may be suitable for overcoming certain limitations with detection of irradiated dog feed.

* Corresponding author. Tel.: +91 22 25592533; fax: +91 22 25505151, 25519631.
E-mail address: bhaskar_sanyal@rediffmail.com (B. Sanyal).

0969-806X/$ - see front matter © 2011 Elsevier Ltd. All rights reserved.
doi:10.1016/j.radphyschem.2010.11.014

Author's personal copy

Thermoluminescence (TL) is a radiation specific phenomenon that arises due to energy stored by trapped charge carriers following irradiation (Sanderson et al., 1996). TL has been tested for detection of spices and herbs and was adopted as a standard method for detecting irradiated foods, from which silicate minerals can be isolated (EN 1788, 2001).

In this present work, for the first time, a detailed study of the radical species produced by gamma irradiation in two varieties of dog feeds, namely, ready-to-eat granular form and edible dog chew in stick form has been carried out by EPR spectroscopy. Thermoluminescence measurements have also been employed to give a complete verdict on identification of radiation treatment of the samples. In addition, characterization of the extracted minerals from the edible dog chew samples has been carried out for TL studies and the requirement of independent detection methods to give reliable identification of the irradiated samples has been established.

2. Experimental

2.1. Material

Dog feed (Pedigree, Mars International India Pvt. Ltd.) of two different classes, granular form ready-to-eat sample and edible dog chew stick were procured from a local market. The standard 2,2,diphenyl-1-picrylhydrazyl (DPPH) with $g=2.0032$ was purchased from Sigma Chem. Co., USA. Sodium polytungstate ($Na_6W_{12}O_{39}\cdot H_2O$) was purchased from Fluka, Germany, to prepare a high density solution.

2.2. Irradiation conditions

Irradiation was carried out at ambient temperature (27 ± 2 °C) using a cobalt-60 irradiator (GC-5000, BRIT, Mumbai, dose rate of 5.5 kGy/h) at BARC, Mumbai. The determination of the absorbed dose for the calibration of the gamma chamber was carried out using Fricke reference standard dosimeters (ASTM Standard, E 1026). The dosimeters were placed throughout the irradiation volume of the chamber and a variation of 1.11% in absorbed dose was observed. The dog feed samples were repacked into polyethylene bags (250 g). The packets were subdivided into five lots. One served as control (non-irradiated) and the other four packets were irradiated at 2.5, 5.0, 7.5 and 10.0 kGy doses. The commodity has a shelf life of 10–12 months.

2.3. EPR spectroscopy

The pet feed samples were grounded into fine granules and transferred to 2-mm quartz capillary tubes and packed with gentle tapping to a length of 25.4 mm (active length) and the weight of the sample was determined. The results for the signal intensity of samples were normalized to the packing weight. EPR measurements were performed using a Bruker EMX spectrometer (Bruker, Germany). All spectra were recorded after 3 accumulated scans at the ambient temperature of EPR laboratory (27 °C). EPR spectra simulation studies were carried out using WIN EPR and Simfonia program (Bruker). In order to determine the electron relaxation behavior of radicals in dog feed samples, the microwave field strength was varied between 0.06 and 50 mW to obtain progressive saturation behavior (PSB). Field modulation was operated at 100 kHz. Operating conditions of the EPR spectrometer were as follows: center field 348 mT, scan range 15 mT, microwave power 0.253 mW, microwave frequency 9.66 GHz, modulation frequency 100 kHz, receiver gain 4×10^4 and time constant 40.96 ms. The position of the irradiation-induced EPR signal was compared with that of the standard 2,2,diphenyl-1-picrylhydrazyl (DPPH) with $g=2.0032$ (Sigma Chem. Co., USA). The irradiated and non-irradiated samples were stored inside EPR quartz tube in the normal laboratory conditions at ambient temperature (27 ± 2 °C) until further use.

2.4. Thermoluminescence analysis

For separation of minerals and organic materials from the dog feed (edible dog chew stick), European Standards EN 1788, 1996 was followed. The important procedures involved in sample preparation for TL analysis were as follows.

The solution of sodium polytungstate ($Na_6W_{12}O_{39}\cdot H_2O$) was added to double distilled water to prepare a high density solution (2 g/ml). The samples were subjected to ultrasonication in a bath sonicator for 5 min followed by centrifugation at 1000*g* for 2 min. The organic material floating on the top of the polytungstate solution was removed. The bottom layer was washed three times with double distilled water. After total removal of water, 2 ml of acetone was added. The minerals in acetone were transferred to clean and weighed aluminum discs (diameter 9.0 mm; thickness 0.4 mm) with the help of Pasteur pipette. The discs containing minerals were stored overnight at 50 °C.

The discs containing minerals from control and irradiated samples were weighed to determine the quantity of minerals deposited. Thermoluminescence analysis was carried out using TL 1009I Reader (Nucleonix Systems, India). Nitrogen was flushed in the heating chamber to reduce spurious TL arising due to the presence of oxygen. The initial temperature was 40 °C, which was increased to 320 °C by linear heating at a rate of 5 °C/s. After measurement of glow 1, the discs with the deposited mineral were irradiated with a normalization radiation dose of 1 kGy followed by TL measurement of glow 2 with the similar instrumental settings as described above. The samples were separated and analyzed in triplicate under similar laboratory and instrumental conditions. The irradiated and non-irradiated samples were stored in dark in the normal laboratory conditions at ambient temperature (27 ± 2 °C) until further use.

Scanning electron microscopy and energy dispersive X-ray spectrometer analysis (SEM/EDX) were carried out to determine the poly mineral composition of the isolated minerals. The electron microscopic analysis was done with TESCAN, Czechoslovakia and EDX, INCA x-sisht, Oxford, UK with secondary electron detector.

3. Results and discussion

3.1. Effect of gamma irradiation on ready to eat granular dog feed

Fig. 1a depicts the EPR spectra recorded with microwave power 0.253 mW of non-irradiated and irradiated samples of granular form ready to eat dog feed. The EPR spectrum of non-irradiated sample was characterized by a singlet with $g=2.0047\pm0.0003$ and $\Delta B_{pp}=0.810$ mT. Several reports have suggested these free radicals to be those of semi-quinones produced by the oxidation of polyphenolics (Scewartz et al., 1972) or lignin (Maloney et al., 1992; Tabner and Tabner, 1994). This *g* value obtained compares well with those reported in literature (Desrosiers and McLaughlin, 1989; Dodd et al., 1985; Bortolin et al., 2006). Immediately after the radiation treatment of the sample at 7.5 kGy dose, a complex and broad EPR spectrum was observed with an increase in signal intensity of the existing weak singlet ($g=2.0052\pm0.0002$). Raffi et al. (1992) and Sanyal et al. (2009) also reported similar observations where an intense signal was noticed in the spectrum of irradiated spices and rice, respectively. Irradiation was explained to be responsible for the relatively high signal intensity. Increase in line width (ΔB_{pp}) of the EPR signal from 0.766 to 1.311 mT could probably be attributed to the induction of multiple paramagnetic

Author's personal copy

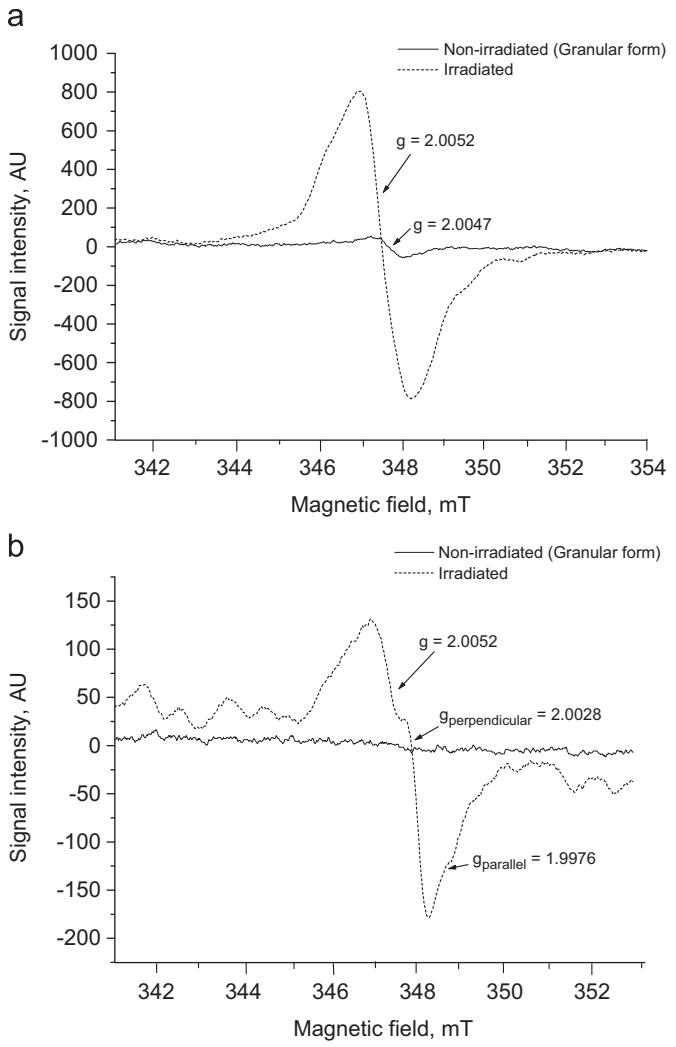

Fig. 1. EPR spectra of non-irradiated and irradiated (7.5 kGy) ready to eat dog feed (granular form) immediately after irradiation recorded with microwave power (a) 0.63 mW and (b) 50.2 mW.

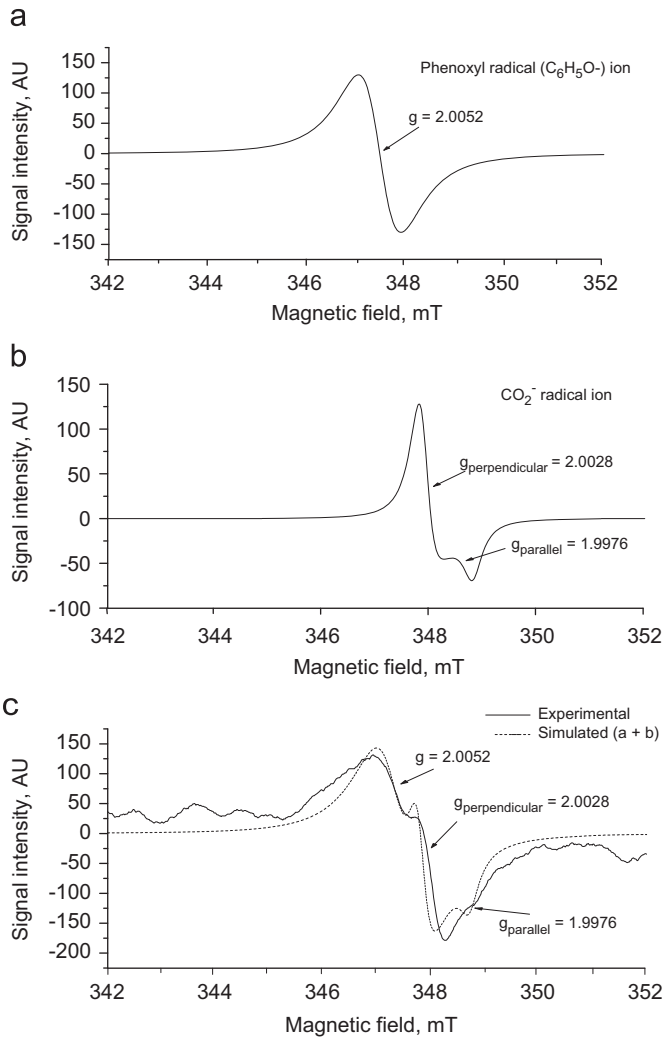

Fig. 2. Simulation scheme of the EPR spectrum of irradiated dog feed (granular form): (a) simulated spectrum of phenoxyl radical ion ($C_6H_5O^-$); (b) simulated spectrum of CO_2^- radical; and (c) simulated and experimental spectra of irradiated dog feed.

centers in the matrix of dog feed. As shown in Fig. 1a, both non-irradiated and irradiated EPR spectra recorded with low microwave power of 0.253 mW, no radiation specific signal was observed. However, when the same samples were subjected to high microwave power of 50 mW, a visible change in the shape of the EPR spectrum was observed in case of irradiated sample as depicted in Fig. 1b. The signal characterized by $g=2.0052$ exhibited reduction in signal amplitude and an axially symmetric anisotropic signal with $g_{\perp}=2.0028$ and $g_{\parallel}=1.9976$ was identified. In order to characterize the radiation induced signal, EPR spectra simulation studies were carried out using WIN EPR and Simfonia program (Bruker). The detailed simulation scheme of EPR spectra of ready-to-eat granular form dog feed irradiated with a dose of 7.5 kGy is depicted in Fig. 2a–c. Fig. 2c exhibits the superposition of experimental and simulated spectra. The simulated spectrum was a linear combination of the individual signals represented in Fig. 2a and b ($R^2=0.962$). Simulation of EPR spectra revealed the formation of two paramagnetic species. The isotropic signal was attributed to phenoxyl radical ion (C_6H_5O-). Similar observation has been reported in our earlier communication on irradiated food (Sanyal et al., 2009). The other anisotropic signal was probably because of CO_2^- radical ion formed due to the breakdown of the fatty acid, which is one of the major constituents of the chicken meat associated with ready-to-eat dog feed. The spin Hamiltonian parameters used to simulate phenoxyl radical ion were $g=2.0052$ and $\Delta B_{pp}=0.86$ mT and for anisotropic CO_2^- radical ion, $g_{\perp}=2.0028$, $g_{\parallel}=1.9976$ and $\Delta B_{pp}=0.30$ mT. The g values obtained are compared well with those reported in literature (Geoffroy and Tochon-Danguy, 1982; Marchioni et al., 2005; Sanyal et al., 2008). The anisotropic signal of CO_2^- radical observed at 50 mW power was stable throughout the storage period of 90 d and could be considered as a marker for radiation treatment. In order to further reconfirm the nature of these radical species, the electron relaxation behavior was studied. Fig. 3a exhibits the EPR spectra recorded with a narrow scan width of 4 mT and exhibited the behavioral change in signal amplitudes of both the isotropic and anisotropic signals with the variation of the microwave field strength from 0.063 to 50 mW. The inset in Fig. 3a shows the progressive saturation behavior (PSB) of the signals. The EPR signal at $g=2.0052$ showed comparatively faster saturation at microwave power of 20 mW followed by decrease in signal intensity by monotonic fashion. The microwave saturation characteristics of these radicals suggested that they were possibly of organic origin with large relaxation time. Similar observations have been reported for organic radical species in irradiated foods (Sanyal and Sharma, 2009; Polovka et al., 2007). However, the PSB

Author's personal copy

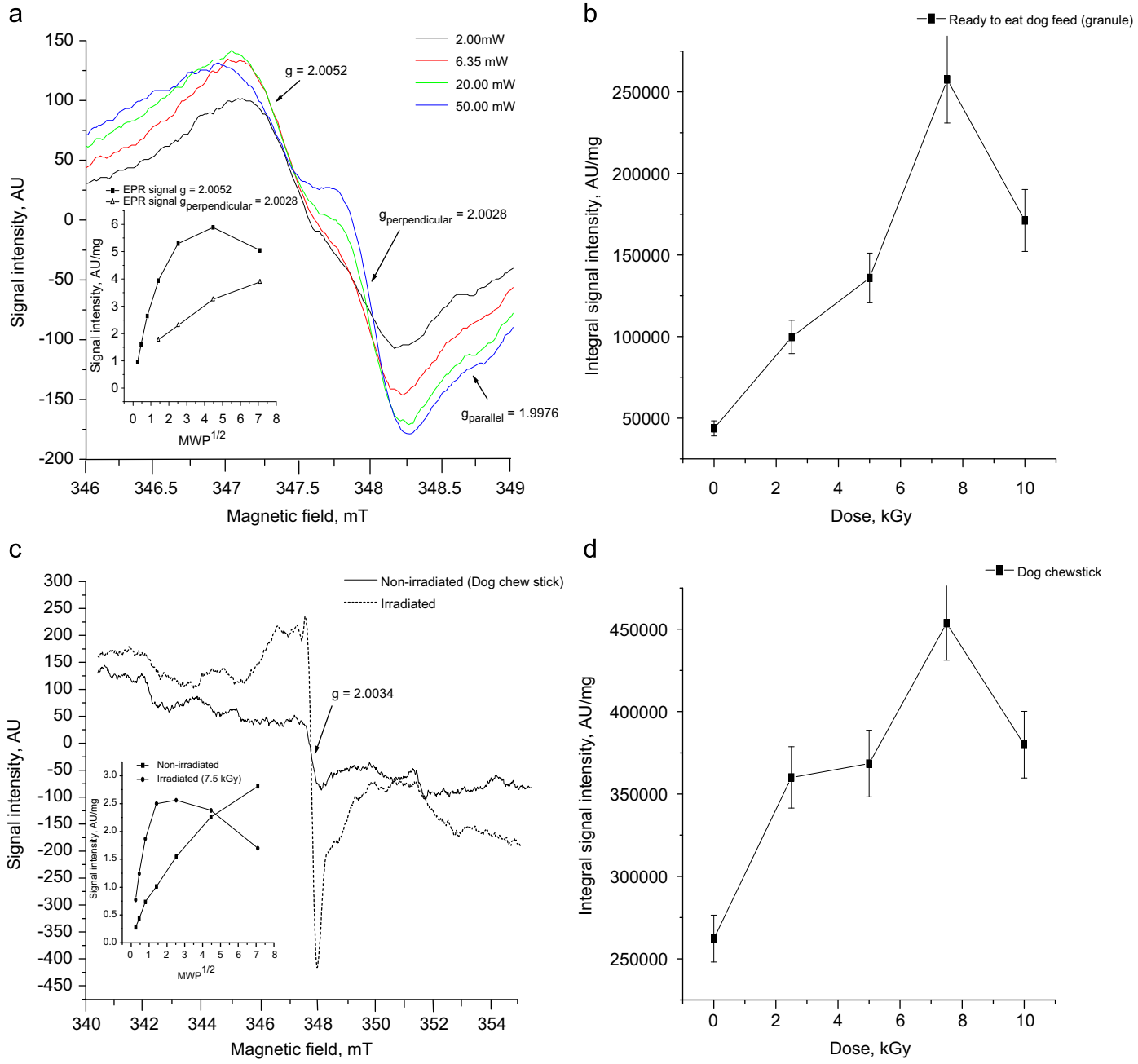

Fig. 3. (a) Superposition of EPR spectra of irradiated dog feed (granular form) recorded with increasing microwave power. The inset shows the progressive saturation behavior of the isotropic (g=2.0052) and anisotropic ($g_{\perp}$=2.0028) signals and (b) response of the double integral of EPR signal (g=2.0052) with increasing dose, (c) EPR spectra of non-irradiated and irradiated (7.5 kGy) edible dog chew after irradiation recorded with 0.63 mW power and (d) response of the double integral of EPR signal (g=2.00534) with increasing dose.

of CO_2^- signal showed a monotonous increase in signal intensity without any saturation confirming the characteristics of paramagnetic center of inorganic origin and short relaxation time. The integral intensities of the EPR signals were obtained by double integration of the spectrum and the integral intensity of the central line was observed to be significantly related to the radiation dose as shown in Fig. 3b. The integral intensity showed saturation above 7.5 kGy radiation dose. The measurement was performed 2 d after irradiation.

3.2. EPR spectroscopy of gamma-irradiated edible dog chew

Fig. 3c depicts the EPR spectra of non-irradiated and irradiated dog chew (stick form) recorded at microwave power of 0.253 mW. Both the non-irradiated and irradiated samples were characterized by an isotropic signal g=2.0034. No radiation specific signal was observed in irradiated sample. However, the signal amplitude increased with radiation treatment. The high power EPR spectra also did not reveal any clue of radiation specific EPR line for this sample. A negligible change in edible dog chew after radiation treatment makes the identification of irradiated food an extremely challenging task. Therefore, European standards for detection of irradiated food by EPR spectroscopy released by European Committee of Normalization (CEN) namely food containing bone (EN 1786, 1997), cellulose (EN 1787, 2000) and crystalline sugar (EN 13708, 2001) cannot be employed to identify irradiated dog chew. Therefore, alternative methods based on EPR are desirable. In view of this, the electron relaxation

Author's personal copy

behavior of radicals was studied. The microwave field strength was varied from 0.063 to 50 mW to obtain progressive saturation behavior (PSB). The effect of saturation is manifested by continuous non-linear increase in EPR signal intensity with $P_{MW}^{1/2}$, reaching a maximum followed by a decrease with the simultaneous increase of EPR line width. The inset in Fig. 3c shows the PSB of the central line of non-irradiated and irradiated (7.5 kGy) samples 90 d after radiation treatment. For the radicals of non-irradiated sample, a continuous increase in signal intensity was observed with increasing microwave power without any sign of saturation revealing the fact of inorganic nature of the paramagnetic center with small relaxation time. Whereas, in case of irradiated sample a faster saturation at microwave power of 6 mW followed by a decrease in signal intensity in a monotonic fashion was observed. This saturation behavior revealed the characteristics of organic radicals with large relaxation time. The results of the present study were in good agreement with the EPR detection of irradiated dry food using microwave saturation as proposed by Yordanov et al. (2005). The integral intensities of the EPR signals were obtained by double integration of the spectrum and the integral intensity of the central line was observed to be significantly related to the radiation dose as shown in Fig. 3d. The measurement was performed 2 d after radiation treatment.

3.3. Time kinetics study of EPR signals

The time interval, after which identification of the irradiated samples is possible was evaluated by the fading kinetics of the radiation induced radicals. Different factors, including humidity, temperature, light intensity, exposure to air and structure of the food matrix influence the behavior of the induced radicals during storage of the sample before and after irradiation and thereby, restrict the time interval after irradiation, during which detection was possible. In order to avoid atmospheric variations all the samples were kept inside the EPR measurement tube in normal laboratory conditions. Fig. 4a shows the time kinetics of non-irradiated (g=2.0047) and irradiated (g=2.0052, $g_{\perp}$=2.0028) ready-to-eat dog feed samples monitored up to 75 d after radiation treatment. In case of isotropic signal because of organic radicals, a fast decrease in signal intensity was observed. Whereas, the anisotropic signal because of CO_2^- radical observed at high microwave power showed slower reduction in signal intensity and was stable for prolonged storage. Fig. 4b depicts the behavior of the EPR signal (g=2.0034) of the non-irradiated and irradiated samples of edible dog chews during storage. Decrease in the concentration of free radicals in irradiated spices with time has been reported by many authors (Sanyal et al., 2008, 2009; Yordanov and Gancheva, 2000; Raffi et al., 2000; Delincee, 1998).

3.4. Thermoluminescence measurements of irradiated edible dog chew

A negligible change in the matrix of edible dog chew samples after radiation treatment makes the identification process using EPR spectroscopy an extremely challenging task. However, the alternative approach based on relaxation behavior of the radiation induced paramagnetic centers gave a clue to radiation treatment. In order to give a reliable verdict thermoluminescence study of the non-irradiated and irradiated edible dog chew was carried out. TL method is applicable for the detection of irradiated foods, from which silicate minerals can be isolated (EN 1788, 2001). Therefore, investigation on the composition of the isolated minerals from the edible dog chew sample was important to assess the possibility of employing TL method for the identification of the irradiated sample. In view of this, the composition of the

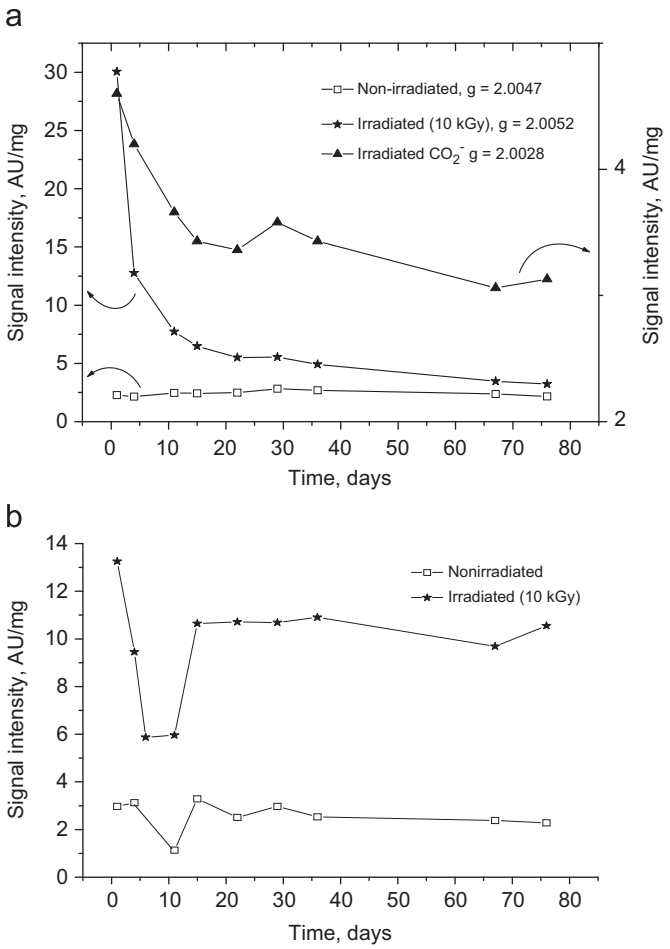

Fig. 4. Time kinetics of non-irradiated and irradiated samples of dog feed during storage (a) for ready to eat granular form and (b) edible dog chew stick form.

separated poly-minerals from the sample was studied using scanning electron microscopy (SEM) and energy dispersive X-ray spectrometer (EDX) analysis. The results of these qualitative studies were interesting to examine the relative abundance of poly-minerals. Fig. 5a shows the SEM image of the extracted poly-minerals revealing the morphology. Fig. 5b shows the EDX spectrum and weight percentage of the major constituents namely calcium (Ca), silicon (Si) and iron (Fe). Calcium being the major component of meat bone associated with the edible dog chew may be responsible for TL signal. Silicon in the form of quartz and aluminum as feldspar are other two important contributors of TL in this sample. It has been reported that the composition of isolated minerals from food commodities like rice, spices and herbs are mainly composed of quartz (SiO_2) and K-feldspars ($KAlSi_3O_8^-$) (Sanyal et al., 2009; Autio and Pinnoja, 1990; Calderon et al., 1995; Correcher et al., 1998; Kwon et al., 2002).

Fig. 5c shows the TL intensities of glow curves for separated poly-minerals from the non-irradiated and irradiated edible dog chew 7 days after radiation treatment. In case of irradiated sample, the glow curve was characterized by a low temperature peak at about 213 ± 3 °C and a high temperature peak at about 303 ± 5 °C. The low temperature peak height ($P_{1\text{height}}$) and high temperature peak height ($P_{2\text{height}}$) represent the TL intensities at the corresponding glow peak temperatures. No glow peak through all temperature ranges was identified for non-irradiated sample. However, low level natural radioactivity exhibited TL signal because of deep traps around 303 °C. The yield of the

Author's personal copy

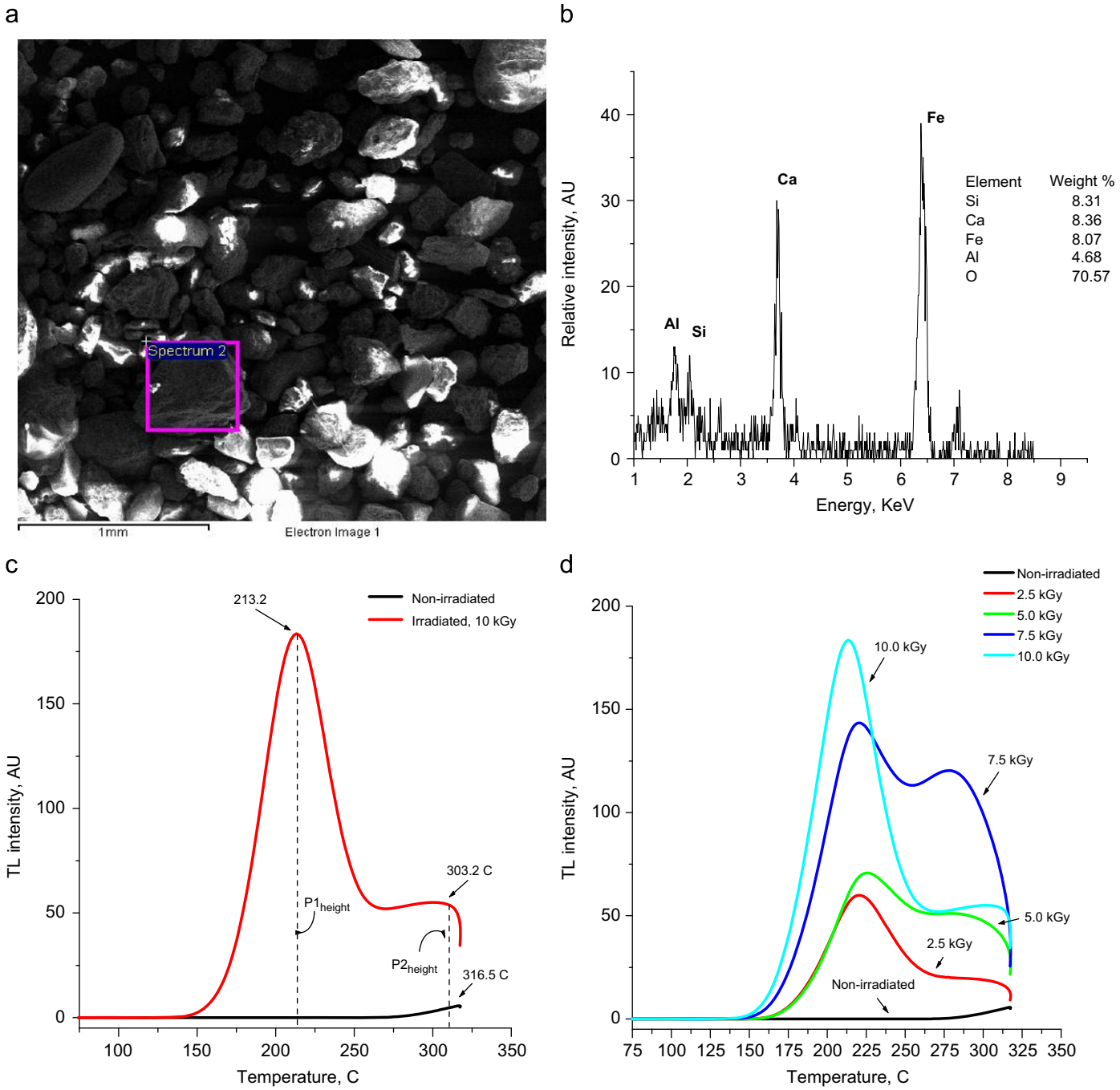

Fig. 5. (a) Scanning electron microscopy (SEM) image and (b) energy dispersive X-ray (EDX) spectrum of the poly-minerals isolated from dog chew samples, (c) TL glows of isolated minerals from non-irradiated and irradiated (10 kGy) edible dog chew and (d) response of the TL glows with increasing radiation doses.

poly-minerals on each discs was 5.0 ± 2 mg. The areas of glow curves for irradiated sample (10 kGy) were 55 times more than the area from the non-irradiated sample. Higher values of TL glow (glow 1) in irradiated samples have been reported in previous studies on spices and herbs (Sanderson et al., 1996), chestnut (Chung et al., 2004) and rice (Sanyal et al., 2009). Therefore, on the basis of the shape of the first glow curve from the separated poly-minerals, discrimination between irradiated and non-irradiated samples was possible. Fig. 5d exhibits the dose dependent response of the TL glows of the isolated poly-minerals from the edible dog chew. An increase in intensities ($P_{1\text{height}}$) of the low temperature peak (213 °C) with increasing dose was observed. Normalization of results by re-irradiation with a dose of 1 kGy enhanced the reliability of the detection results. Fig. 6a and b shows the comparison of re-irradiation glow curves (glow 2) with respect to first glow curves (glow 1) for non-irradiated and irradiated samples, respectively. The re-irradiation glow curves (glow 2) were characterized by three glow peaks. The first peak was characterized by 148 ± 3 °C, the second and the third peaks were characterized by 213 ± 2 and 306 ± 5 °C, respectively. The differences of the peak temperatures observed between glow 1 and 2 attributed to the time difference elapsed between irradiation and analysis because low energy trapped electrons responsible for the first glow peak (148 °C) were released during storage. Glow 2 was recorded 1 d after the normalization doses whereas samples were stored for several days after irradiation prior to the analysis of glow 1. In case of non-irradiated sample, the ratio was 0.035 ± 0.003, while for irradiated samples such as

Author's personal copy

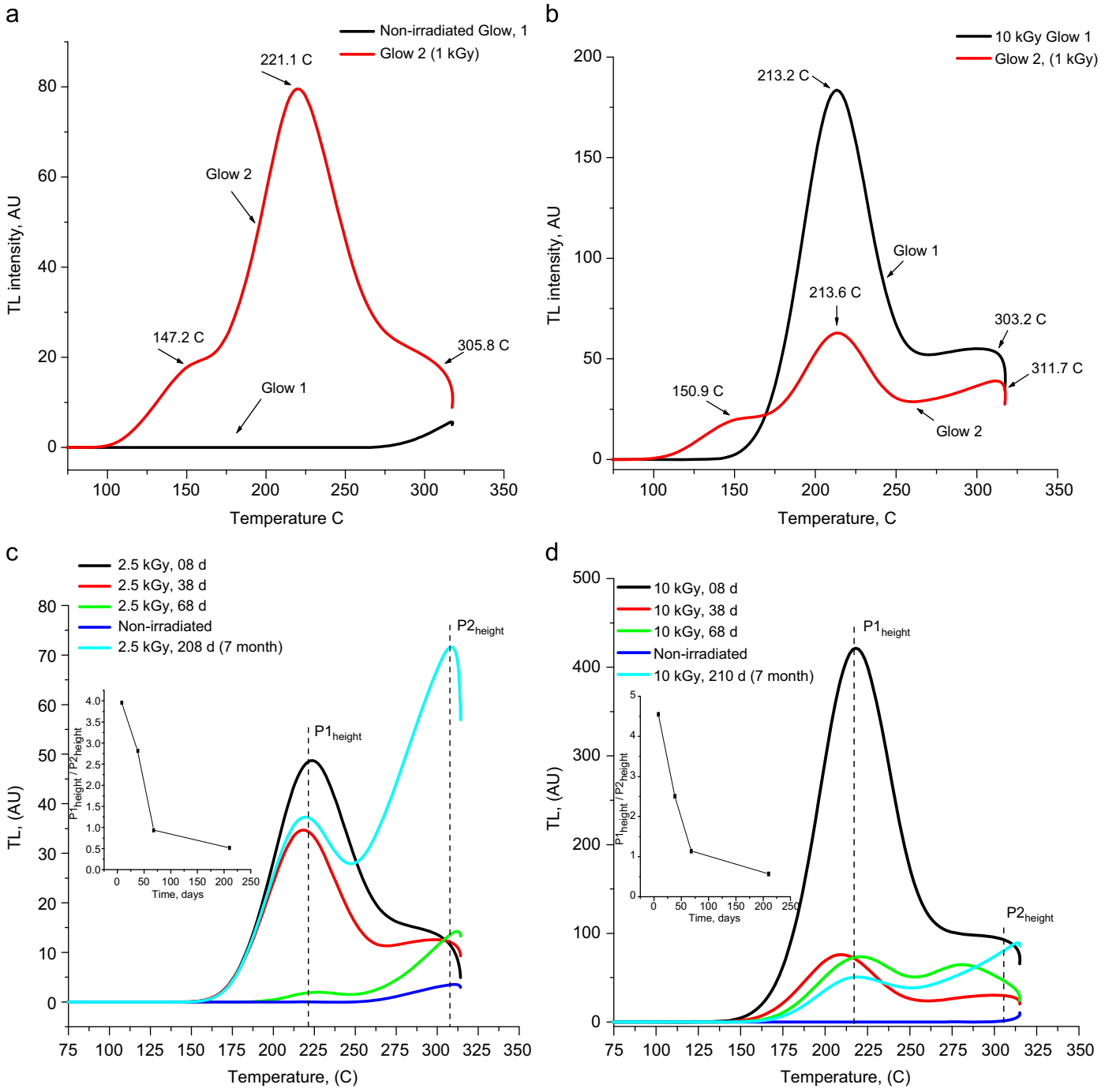

Fig. 6. Glow 1 and glow 2 (normalized with 1 kGy) of (a) non-irradiated and (b) irradiated (10 kGy) dog chew sample. Response of the TL glows during storage for the samples subjected to radiation doses (c) 2.5 kGy and (d) 10.0 kGy. Insets show the behavior of $P_{1height}/P_{2height}$ with increasing time.

2.5, 5.0, 7.5 and 10.0 kGy the ratios were found to be 0.930 ± 0.012, 2.169 ± 0.25, 2.48 ± 0.22 and 1.90 ± 0.32, respectively. The higher values of the ratio of areas for glow 1/glow 2 for irradiated samples are in good agreement with the European Standard EN 1786 (1997). The dog chew samples (irradiated and non-irradiated) were stored for seven months to study the fading kinetics of the TL glows. During prolonged storage the isolation of minerals from non-irradiated and irradiated samples was carried out prior to each TL measurement. Fig. 6c and d exhibit the TL glow curve structures of the irradiated samples 2.5 and 10.0 kGy, respectively. In both the cases the $P_{1height}$ showed a fast decrease in TL intensities with time, whereas, the $P_{2height}$ revealed slow reduction in intensities. The insets of the figures show the variation of the ratio of $P_{1height}$ to $P_{2height}$ ($P_{1height}/P_{2height}$) with increasing time and confirmed the fast fading kinetics of $P_{1height}$. However, a clear discrimination between irradiated and non-irradiated edible dog chew samples was possible from the shape of the first TL glow even after a prolonged storage of seven months.

4. Conclusion

Identification of gamma-irradiated dog feed was carried out by investigating free radicals using electron paramagnetic resonance (EPR) spectroscopy and studying thermo luminescence (TL)

Author's personal copy

properties of the isolated poly-minerals. EPR spectroscopy was useful to identify the irradiated ready-to-eat granular dog feed even after a prolonged storage. However, in case of edible dog chew sample detection of radiation treatment was not possible using EPR method alone. TL measurements of edible dog chew were employed to find out the irradiated sample. The SEM/EDX study revealed the composition of the isolated minerals. TL technique provided promising results even after a long period of storage but, involved tedious sample preparation protocol (Carmichael and Sanderson, 2000). TL glow curve structures and the ratio of the TL glows (glow 1/glow 2) emerged out as successful tool to identify irradiated edible dog chews even after a prolonged storage.

Acknowledgement

The authors are thankful to Dr. S.K. Gupta and Dr. A.K. Debnath of Technical Physics and Prototype Engineering Division, BARC for carrying out SEM/EDX scan of the samples.

References

ASTM Standard, E 1026. Standard Practice for Using Fricke Reference Standard Dosimetry System.

Autio, T., Pinnoja, S., 1990. Identification of irradiated foods by the thermoluminescence of mineral contamination. *Z.* Lebensm. Unters Forsch. 191, 177–180.

Bortolin, E., Butos Griffin, E., Cruz-Zaragoza, E., De Coste, V., Onori, S., 2006. Electron paramagnetic resonance detection of Mexican irradiated spices. Int. J. Food Sci. Technol. 41, 375–382.

Calderon, T., Correcher, V., Millan, A., Beneitez, P., Rendell, H.M., Larrson, M., Townsend, P.D., Wood, R.A., 1995. New data on thermoluminescence of inorganic dust from herbs and spices. J. Phys. D: Appl. Phys. 28, 415–423.

Carmichael, L.A., Sanderson, D.C.W., 2000. The use of acid hydrolysis for extracting minerals from shellfish for thermoluminescence detection of irradiation. Food Chem. 68, 233–238.

Chung, H.W., Delincee, H., Han, S., Hong, J., Kim, H., Kim, M., Byun, M., Kwon, J., 2004. Trials to identify irradiated chestnut (*Castanea bungena*) with different analytical techniques. Radiat. Phys. Chem. 71, 179–182.

Correcher, V., Muniz, J.L., Gomez-Ros, J.M., 1998. Dose dependence and fading effect of the thermoluminescence signal in *v*-irradiated paprika. J. Sci. Food Agric. 76, 149–158.

Delincee, H., 1998. Detection of food treated with ionizing radiation. Trends Food Sci. Technol. 9, 73–82.

Desrosiers, M.F., McLaughlin, W.L., 1989. Examination of gamma irradiated fruits and vegetables by electron spin resonance spectroscopy. Radiat. Phys. Chem. 34, 895–898.

Dodd, N.J.F., Swallow, A.J., Ley, F.J., 1985. Use of ESR to identify irradiated food. Radiat. Phys. Chem. 26, 451.

Geoffroy, M., Tochon-Danguy, H.J., 1982. ESR identification of radiation damage in synthetic apatites: a study of the carbon-13 hyperfine coupling. Calcio Tissue Int. 34, S99–S102.

Kwon, J.H., Jaeyoung, J., Chung, H., 2002. Thermoluminescence characteristics of minerals from irradiated potatoes of different origin of production. Radiat. Phys. Chem. 63, 415–418.

Maloney, D.R., Tabner, B.J., Tabner, V.A., 1992. An electron spins resonance study of gamma-irradiated fruits. Radiat. Phys. Chem. 39, 309–314.

Marchioni, E., Horvatovich, P., Charon, H., Kuntz, F., 2005. Detection of irradiated ingredients included in low quantity in non-irradiated food matrix. 1. Extraction and ESR analysis of bones from mechanically recovered poultry meat. J. Agric. Food Chem. 53, 3769–3773.

Polovka, M., Brezova, V., Simko, P., 2007. EPR spectroscopy: a tool to characterize gamma irradiated foods. J. Food Nutr. Res. 46, 75–83.

Protocol EN 13708, 2001. Detection of Irradiated Food Containing Crystalline Sugar: Analysis by EPR. European Committee for Standardization, Brussels.

Protocol EN 1786, 1997. Detection of Irradiated Food Containing Bone: Analysis by Electron Paramagnetic Resonance. European Committee for Standardization, Brussels.

Protocol EN 1787, 2000. Detection of Irradiated Food Containing Cellulose: Analysis by EPR. European Committee for Standardization, Brussels.

Protocol EN 1788, 2001. Foodstuffs-Detection of Irradiated Food from which Silicate Minerals can be Isolated: Method by Thermoluminescence. European Committee for Standardization, Brussels, Belgium.

Raffi, J.J., Agnel, J.L., Buscarlet, L.A., Martin, C.C., 1988. Electron spin resonance identification of irradiated strawberries. J. Chem. Soc. Faraday Trans. 84 (10), 3359–3362.

Raffi, J., Stevenson, M.H., Kent, M., Thiery, J.M., Belliardo, J.J., 1992. European intercomparison on electron spin resonance identification of irradiated food stuffs. Int. J. Food Sci. Technol. 27, 111–124.

Raffi, J., Yordanov, N.D., Chabane, S., Douifi, L., Gancheva, V., Ivanova, S., 2000. Detection of irradiated aromatic herbs and spices by Electron Paramagnetic Resonance and Thermoluminescence. Spectrochim. Acta 56A, 409–416.

Sanderson, D.C.W., Carmichael, L.A., Spencer, J.Q., Naylor, J., 1996. Luminescence detection of shell fish. In: McMurray, C.H. (Ed.), Detection Methods of Irradiated Foods. The Royal Society of Chemistry, Cambridge, pp. 139–148.

Sanyal, B., Chawla, S.P., Sharma, A., 2009. An improved method to identify irradiated rice by EPR spectroscopy and thermoluminescence measurements. Food Chem. 116 (2), 526–534.

Sanyal, B., Sajilata, M.G., Chatterjee, S., Singhal, R.S., Variyar, P.S., Kamat, M.Y., Sharma, A., 2008. Identification of irradiated cashew nut by electron paramagnetic resonance spectroscopy. J. Agric. Food Chem. 56, 8987–8991.

Sanyal, B., Sharma, A., 2009. A new electron paramagnetic resonance method to identify irradiated soybean. J. Food Sci. 74, N50–N57.

Scewartz, H.M., Bolton, J.R., Brog, D.C. (Eds.), 1972. Biological Applications of Electron Spin Resonance. Wiley, New York.

Tabner, B.J., Tabner, V.A., 1994. Electron spin resonance spectra of gamma-irradiated citrus fruits skin, skin components and stalks. Int. J. Food Sci. Technol. 29, 143–152.

Yordanov, N.D., Aleksieva, K., Mansour, I., 2005. Improvement of the EPR detection of irradiated dry plants using microwave saturation and thermal treatment. Radiat. Phys. Chem. 73, 55–60.

Yordanov, N.D., Gancheva, V., 2000. A new approach for the extension of the identification period of irradiated cellulose containing foodstuffs by EPR spectroscopy. Appl. Radiat. Isot. 52, 195–198.

Provided for non-commercial research and education use.
Not for reproduction, distribution or commercial use.

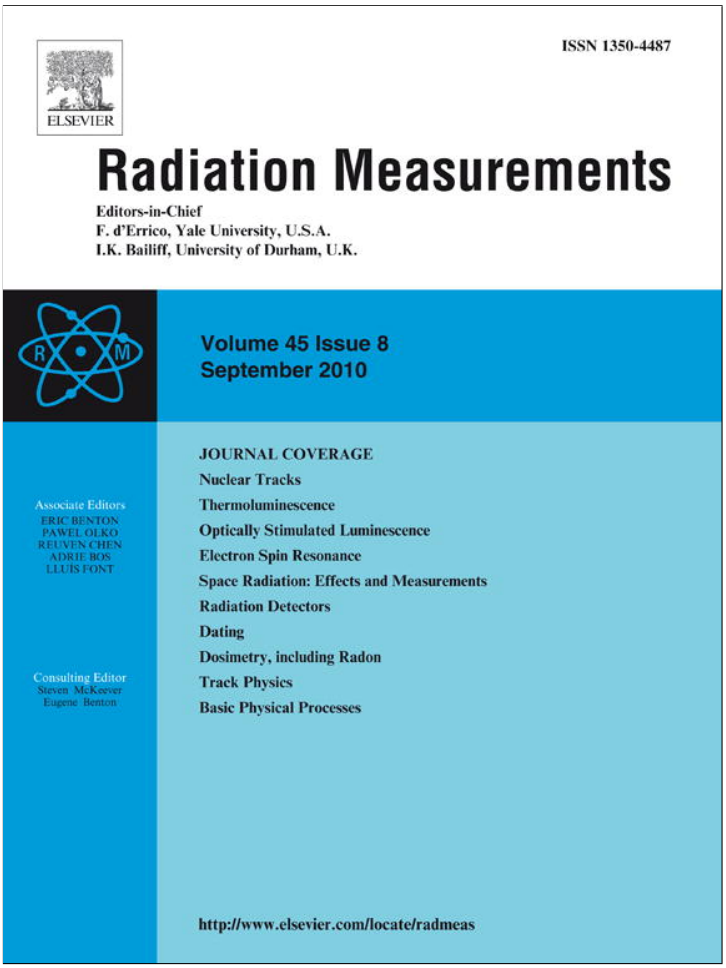

This article appeared in a journal published by Elsevier. The attached copy is furnished to the author for internal non-commercial research and education use, including for instruction at the authors institution and sharing with colleagues.

Other uses, including reproduction and distribution, or selling or licensing copies, or posting to personal, institutional or third party websites are prohibited.

In most cases authors are permitted to post their version of the article (e.g. in Word or Tex form) to their personal website or institutional repository. Authors requiring further information regarding Elsevier's archiving and manuscript policies are encouraged to visit:

http://www.elsevier.com/copyright

Author's personal copy

Radiation Measurements 45 (2010) 899–905

Contents lists available at ScienceDirect

Radiation Measurements

journal homepage: www.elsevier.com/locate/radmeas

TL and EPR studies of $CaSO_4$:Dy phosphor to investigate its efficacy in measurement of food irradiation dose at sub-ambient temperatures

Bhaskar Sanyal [a,*], V. Natarajan [b], S.P. Chawla [a], Arun Sharma [a]

[a] Food Technology Division, Bhabha Atomic Research Centre, Mumbai 400 085, India
[b] Radiochemistry Division, Bhabha Atomic Research Centre, Mumbai 400 085, India

ARTICLE INFO

Article history:
Received 7 December 2009
Received in revised form
24 February 2010
Accepted 7 June 2010

Keywords:
Calcium Sulfate
Irradiation
Thermoluminescence
EPR

ABSTRACT

The effects of sub-ambient temperatures of irradiation and dose response of $CaSO_4$:Dy phosphor was investigated. The irradiation dose in the range 0.5–7.0 kGy was chosen to meet the requirement of commercial food irradiation at low temperature. Commercially available phosphor showed no significant change in glow curve structure with low temperature of irradiation. In order to enhance the sensitivity of the low temperature glow peak (142 °C), the phosphor was subjected to different post-preparation thermal treatments at 700–900 °C. The change in glows and improvement in dose response characteristics were explained by Electron Paramagnetic Resonance (EPR) spectroscopy. At sub-ambient temperature of irradiation, the behavior of thermally treated $CaSO_4$:Dy phosphor with increasing dose revealed improved linear response of the low temperature glow peak and could be an efficient dosimetry system for the food commodities irradiated at low temperatures.

© 2010 Elsevier Ltd. All rights reserved.

1. Introduction

Dosimetry is of paramount importance of any quality assurance program for an irradiation facility. Food irradiation, material testing and other similar applications require accurate means of determination of minimum and maximum doses received by the samples. Thermoluminescence dosimeters are widely employed for personnel and environmental dosimetry, but rarely for application at higher doses. In radiation processing of food, a large number of food items namely sea foods, fruits and vegetables are required to be processed at chilled (0° ± 3 °C) or frozen (−10 ± 4 °C) temperature by ionizing radiation in the dose range 1.0–4.0 kGy. The evaluation of absorbed dose below room temperature in irradiated food using cost effective and simple dosimetry system is a challenging task. As a consequence there is interest for new dosimetry systems with improved performances.

$CaSO_4$:Dy remains one of the most useful and sensitive thermoluminescence dosimeter (TLD) for radiation dosimetry. This phosphor has a wide range of application in dosimetry, such as personnel monitoring, patient dosimetry, environmental monitoring after appropriate correction for energy independence or tissue equivalence. Different high dose measurement techniques are available, but they are either expensive, cumbersome or may not be suitable for low temperature dosimetry, while thermoluminescence dosimeters are cheaper with simple method of measurement.

For the exposure levels in the radiation protection applications range, the dose response of the main TL peak (240 °C) is found to be linear up to 10 Gy (Campos and Lima, 1986). However, supralinear response with dose is reported in the dose range 10 Gy–5.0 kGy at room temperature irradiation (ISO/ASTM 51956). For this purpose concentration of dysprosium normally used is 0.1 mol%. With this concentration the saturation of TL response has been attributed to non-availability of trapping centers for trapping the free charges (Mathur et al., 1999). However, in this phosphor though the role of dysprosium is to provide recombination centers, it is also indirectly associated with the formation or stabilization of the trapping centers (Stoebe and Morgan, 1984). Therefore, increased concentration (0.2 mol%) of dysprosium was chosen, because of its commercial availability and improved sensitivity. It is reported that the thermal treatment of $CaSO_4$:Dy in the range 400–700 °C enhances the response of high temperature peak (Bakshi et al., 2002) for the use of the phosphor in the dosimetry of protection level.

This work was undertaken to study the effects of low temperature irradiation of commercial and thermally treated $CaSO_4$:Dy (0.2 mol%) phosphor. TL and EPR correlation studies were carried out to understand the TL properties of the phosphor after being subjected to pre-irradiation thermal treatments. The irradiation dose in the range 0.5–7.0 kGy was chosen to meet the requirement of commercial food irradiation at sub-ambient temperature.

* Corresponding author. Tel.: +91 22 25592533; fax: +91 22 25505151/25519631.
E-mail address: bhaskar_sanyal@rediffmail.com (B. Sanyal).

1350-4487/$ – see front matter © 2010 Elsevier Ltd. All rights reserved.
doi:10.1016/j.radmeas.2010.06.006

Author's personal copy

2. Experimental procedures

Polycrystalline $CaSO_4$:Dy (0.2 mol%) phosphor prepared and marketed by Renentech Laboratory Private Ltd, Mumbai, India was used in the present study. The powder was divided into two parts of 100 mg each.

2.1. Radiation treatment

The first part of the sample without any further treatment was subjected to gamma radiation from Co^{60} source at room temperature, chilled temperature (0° ± 3 °C), frozen temperature (−10 ± 4 °C) and liquid nitrogen temperature (−196 °C). The phosphor in powder form was irradiated in a glass tube inside a Dewar flask with Co^{60} gamma radiation in a gamma chamber (GC 5000, Board of Radiation Isotope Technology, India, dose rate 6.5 kGy/h). The dose was calibrated with Fricke reference standard dosimeters (ASTM Standard, E 1026). The irradiation temperatures were controlled by ice, ice and salt, and liquid nitrogen (−196 °C). The dose response is measured using three aliquots from the same batch of phosphor.

2.2. Thermal treatment

The second part was divided into three parts and each part was subjected to different thermal treatments in the temperature range 700–900 °C in a furnace with a precision of temperature ±3 °C followed by gamma irradiation of 0.1 kGy at chilled temperatures to study the peak intensities. The dose response was studied for untreated and thermally sensitized phosphors in the dose range 0.5–7.0 kGy at chilled temperature.

2.3. TL measurement

The irradiation response was analyzed by a thermoluminescence reader (Nucleonix Systems Pvt. Ltd. Hyderabad, India) with a linear heating rate of 2 °C per second from room temperature to 300 °C. Neutral density filters (Melles Griot BV, Netherlands) of optical densities 3.0 and transmittance 0.01% were used to avoid saturation of Photo Multiplier Tube (PMT). The peak height is vertical length of the peak tip from the temperature axis measured directly from the glow curve (Bakshi et al., 2008; Mathur et al., 1999). Control and irradiated phosphors were stored in dark place at normal laboratory condition when they were not in use. Entire study was carried out using the same batch of $CaSO_4$:Dy phosphor to avoid inter-batch uncertainty.

2.4. EPR analysis

Electron Paramagnetic Resonance (EPR) study was carried out using EMX model EPR spectrometer (BRUKER, Germany) with a microwave frequency of 9.42 GHz. EPR spectra were obtained at liquid nitrogen temperature (−196 °C) and from room temperature (25 °C) to 300 °C in step of 50° using in situ nitrogen gas heating assembly BVT 3000 of BRUKER. The samples were irradiated at 2.0 kGy gamma dose at 0 ± 3 °C before taking the EPR spectra. Recording parameters were 3382 G central field, 1.0 G modulation amplitude and 10.20 ms time constant with microwave power attenuation 15 dB. EPR sensitivity was measured by peak-to-peak amplitude (ASTM standard, 51607:2004 E; Sanyal et al., 2009; Sharaf and Hassan, 2004). DPPH with g value 2.0036 was taken as reference for the EPR spectra.

3. Results and discussion

3.1. Effects of low temperature irradiation of commercial $CaSO_4$:Dy

To evaluate the crystal capacities of irradiated commercial $CaSO_4$:Dy (0.2 mol%), the integral TL (area under the glow) was measured at three different temperatures, chilled (0 ± 3 °C), frozen (−10 ± 4 °C) and liquid nitrogen temperature (−196 °C) with two different doses 0.4 and 1.0 kGy. Recently, Hernandez-Medina et al., 2010 showed that annealed (400 °C, 1 h) samples of $CaSO_4$:Dy exhibited a considerable decrease in response with the decrease of irradiation temperature. But, in our study with commercial phosphor, no significant difference in integral TL was observed with a maximum variation within ±5% (Fig. 1). Fig. 2 shows the glow curve structure of $CaSO_4$:Dy (0.2 mol%) irradiated at 0 ± 3 °C temperature. The low temperature and high temperature peaks were observed at 142 °C and 245 °C, respectively, without any structural changes in the glows with respect to the phosphor irradiated at ambient temperature. Low temperature peak (142 °C) was observed to be broad in nature. In case of LiF: Mg,Cu,P phosphor, the shifting of intensity maximum towards lower temperature with decreasing temperatures of irradiation was reported by Ramos-Bernel et al. (2002). No such shifting was observed in $CaSO_4$:Dy phosphor. However, the peak temperatures shifted towards lower values with the increasing dose.

$CaSO_4$:Dy (0.2 mol%) phosphor was irradiated at 0 ± 3 °C and responses of the low temperature (142 °C) and high temperature (245 °C) peak heights as a function of gamma dose were studied in the dose range 0.5–7.0 kGy. As shown in Fig. 3, both the peak heights increased with gamma dose. Both the peaks showed a linear response ($R = 0.99923$) in the range 0.5–1.0 kGy limiting the application of this phosphor to measure the radiation dose in the range 3.0–4.0 kGy which is normally used in irradiation of food at sub-ambient temperatures. In commercial phosphor supralinear responses were observed above 1.0 kGy with 76.5% increased slope with respect to the linear region. As per ISO/ASTM 51956, supralinearity refers to a region where the slope of the response versus dose is greater than that for the linear region. Chen and McKeever (1994) suggested that the term supralinearity was to describe the property of the measured quantity being above the continuation of the initial linear range. The production of significantly more number of defects at doses more than 0.1 kGy may be responsible for the supralinear dose response. Another possible reason of the supralinear response of the phosphor with increasing radiation dose could be the simultaneous contribution of the competition

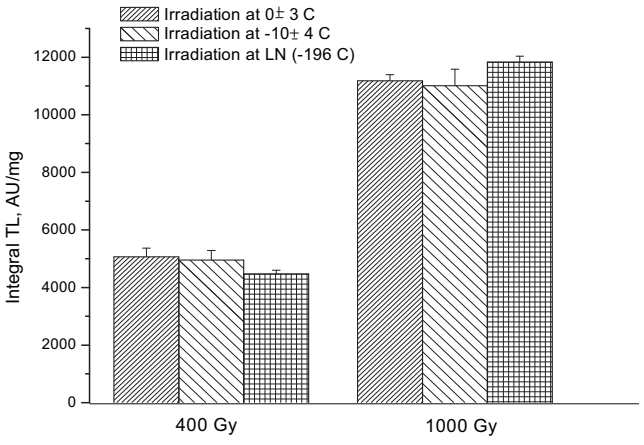

Fig. 1. Integral TL output of commercial $CaSO_4$:Dy (0.2 mol%) irradiated at chilled (0 ± 3 °C), Frozen (−10 ± 4 °C) and liquid nitrogen temperature (−196 °C).

Author's personal copy

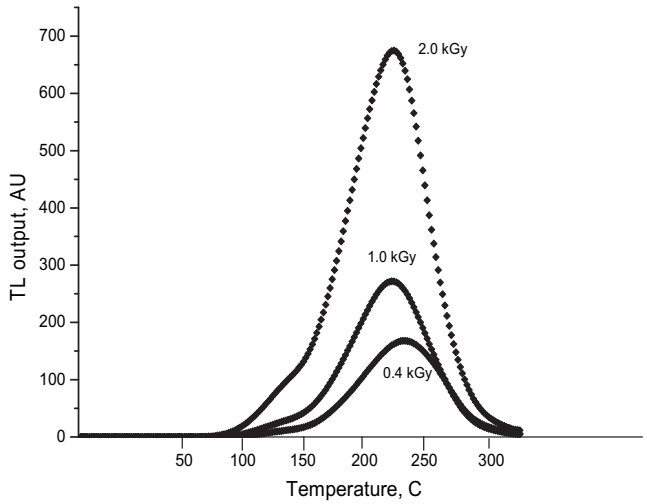

Fig. 2. TL response of $CaSO_4$:Dy (0.2 mol%) with increasing gamma dose at 0 ± 3 °C.

during excitation as well as heating. Accumulation of doses may produce trapped electrons and holes at existing impurities along with the defects produced by the process of irradiation itself.

3.2. TL and EPR studies of thermally sensitized phosphor

Pre-irradiation thermal sensitization technique was employed to enhance the linear response of the $CaSO_4$:Dy phosphor with increasing dose. Exact determination of TL intensity of the low temperature peak was difficult due to its broad nature. Therefore, use of low temperature peak, as the dosimetry peak was limited unless it is distinguishable and sharp. Bakshi et al. (2002) had shown that the thermal treatment of $CaSO_4$:Dy in the range 400–700 °C enhanced the response of high temperature peak for the use of the phosphor in the dosimetry of radiation protection level. However, phosphor subjected to thermal treatment beyond 800 °C had been reported to exhibit irreversible changes in the intensities of the low temperature and high temperature peaks. In view of this, commercially available $CaSO_4$:Dy (0.2 mol%) phosphor

Table 1
Peak height ratio of high temperature peak to low temperature peak at different annealing temperature.

Temperature of thermal treatment	Peak height ratio of high temp peak to low temp peak
Without thermal treatment	14.63 ± 0.49
700 °C, 2 h	9.91 ± 0.86
800 °C, 2 h	7.68 ± 0.50
900 °C, 2 h	1.29 ± 0.04

was subjected to pre-irradiation thermal treatment at 700, 800 and 900 °C for a period of 2 h. As shown in Table 1, the peak height ratios (ratio of high temperature peak to low temperature peak) were observed to be decreased sharply with increasing temperature of the thermal treatment, indicating sharp rise of the low temperature peak intensity. These results were well in conformity with the reported literature (Bakshi et al., 2006). The change in glow curve structures with the annealing temperatures is shown in Fig. 4. The glow curves recorded from room temperature to 300 °C exhibited high temperature peak at about 245 °C and low temperature peak at about 142 °C. In order to understand the above observations, EPR spectra of the untreated and annealed $CaSO_4$:Dy phosphor were recorded at room temperature 297 K (24 °C) and 77 K (−196 °C) as shown in Figs. 5A–D and 6A–D. All the spectra recorded at room temperature and 77 K exhibited three distinct radicals induced by ionizing radiation, centered around 3361 G, 3360 G and 3347 G with $g = 2.0031 \pm 0.001$, 2.0038 ± 0.0005 and 2.0113 ± 0.0006, respectively. These lines were attributed to and SO_3^-, SO_4^- and O_3^- radicals respectively. The g values obtained are compared well with those reported in the literature (Mauricio et al., 1996; Sharaf and Hassan, 2004; Gupta et al., 1974; Natarajan et al., 1988; Seshagiri et al., 1988; Bakshi et al., 2008). From Figs. 3 and 4, it can be observed that, with the increase of temperature of the pre-irradiation thermal treatment, the intensities of SO_4^- and O_3^- radicals were enhanced. However, the intensity of the SO_3^- did not exhibit any significant change.

In order to investigate the role of radiation induced paramagnetic centers in TL glow and the cause of sensitization of low temperature peak, the thermal behaviors of the EPR lines were studied from room temperature to 300 °C. Fig. 7A, shows the behavior of SO_3^- radical with increasing temperature for all the

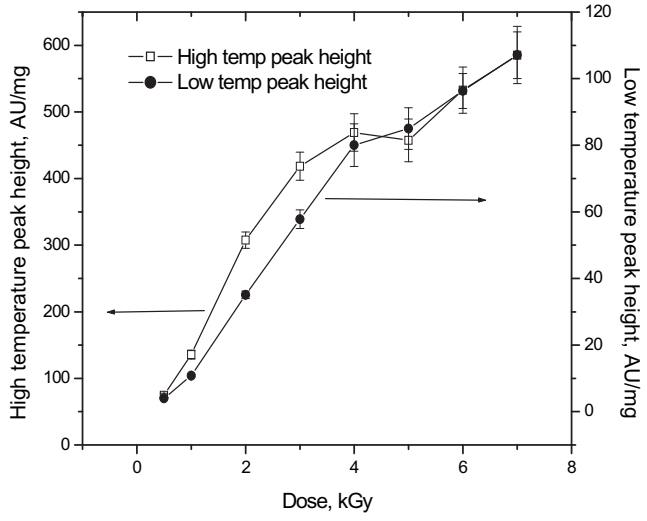

Fig. 3. Change in high temperature peak height and low temperature peak height with gamma dose at chilled temperature for commercial $CaSO_4$:Dy (0.2 mol%) without any sensitizing heat treatment prior to irradiation.

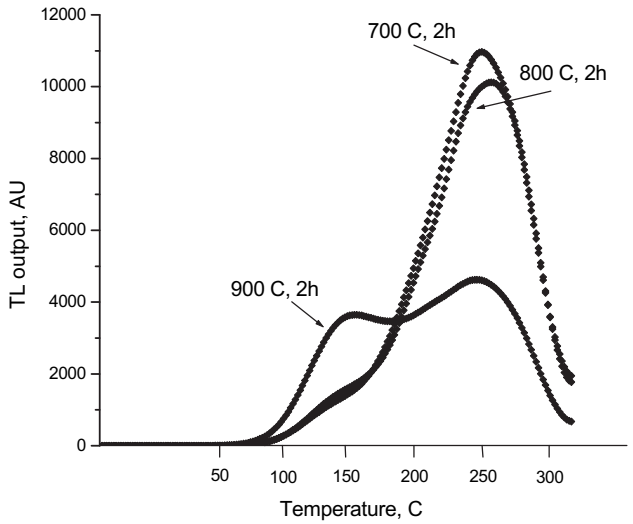

Fig. 4. Change in Glow curve structure of the commercial phosphor after pre-irradiation thermal treatments at 700, 800 and 900 °C.

Author's personal copy

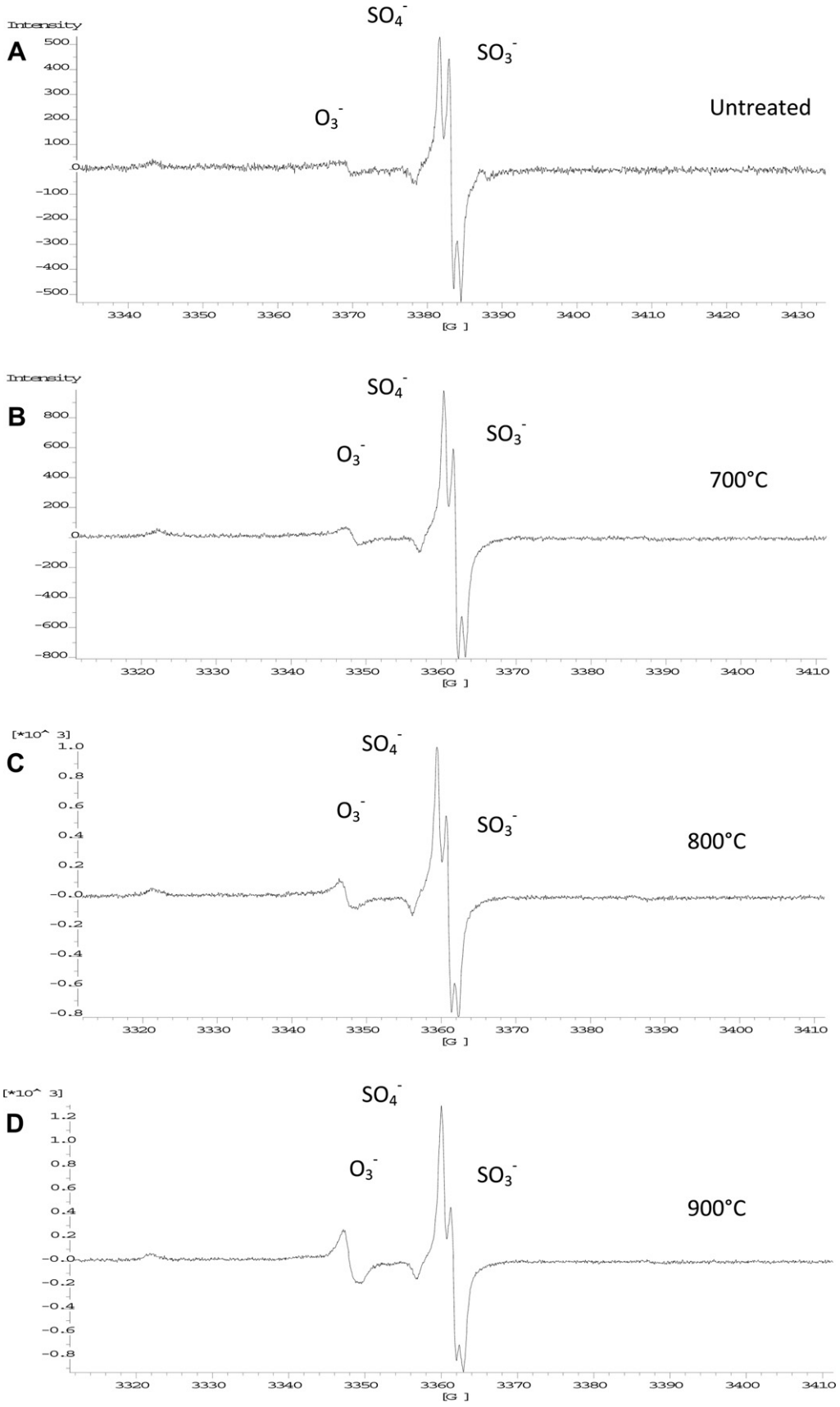

Fig. 5. EPR spectra recorded at room temperature with microwave power attenuation 15 db for (A) commercial $CaSO_4$:Dy (0.2 mol%) phosphor (B) annealed at 700 °C (C) annealed at 800 °C and (D) annealed at 900 °C.

Author's personal copy

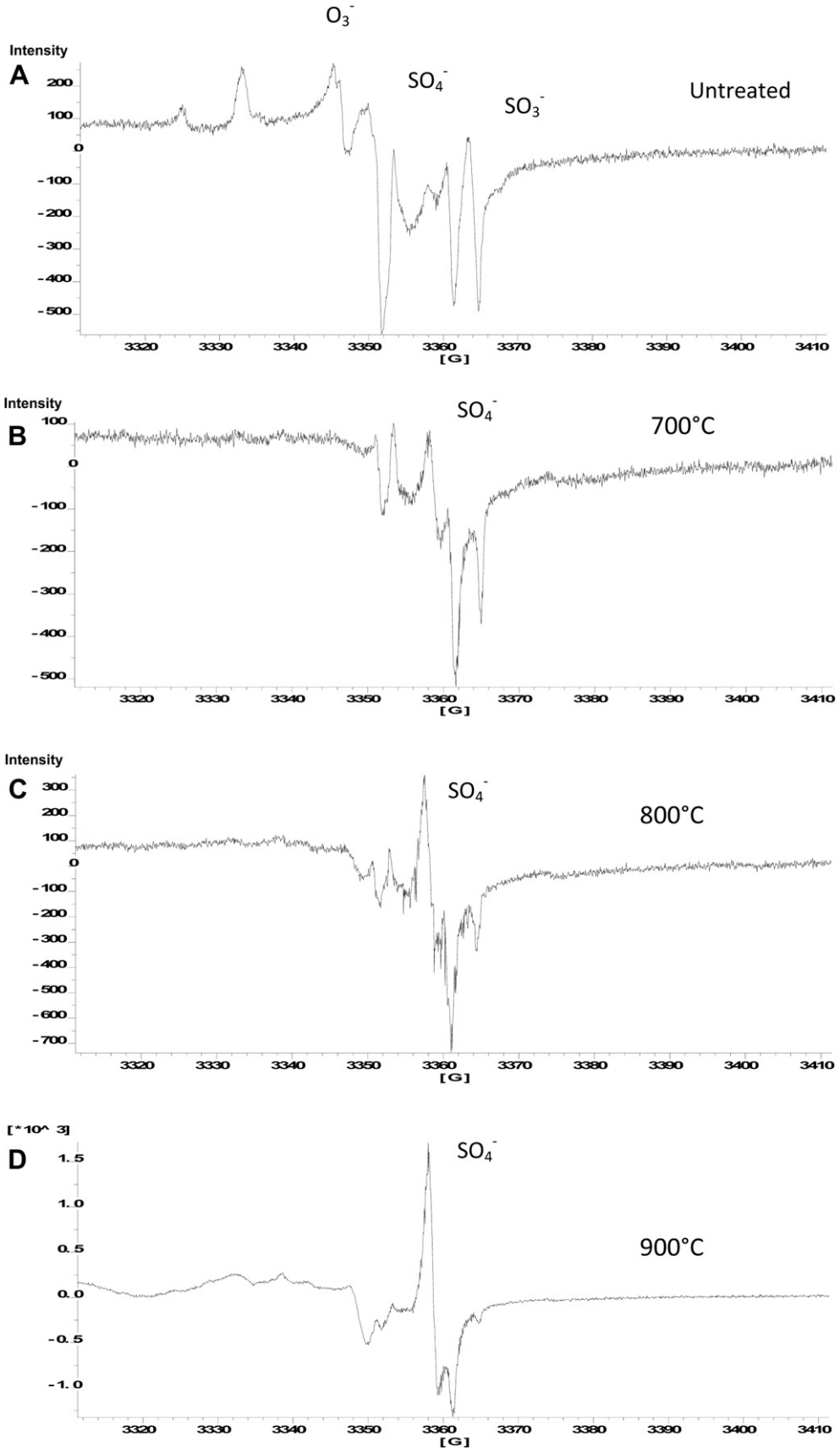

Fig. 6. EPR spectra recorded at 77 K (−196 °C) with microwave power attenuation 15 db for (A) commercial $CaSO_4$:Dy (0.2 mol%) phosphor (B) annealed at 700 °C (C) annealed at 800 °C and (D) annealed at 900 °C.

Author's personal copy

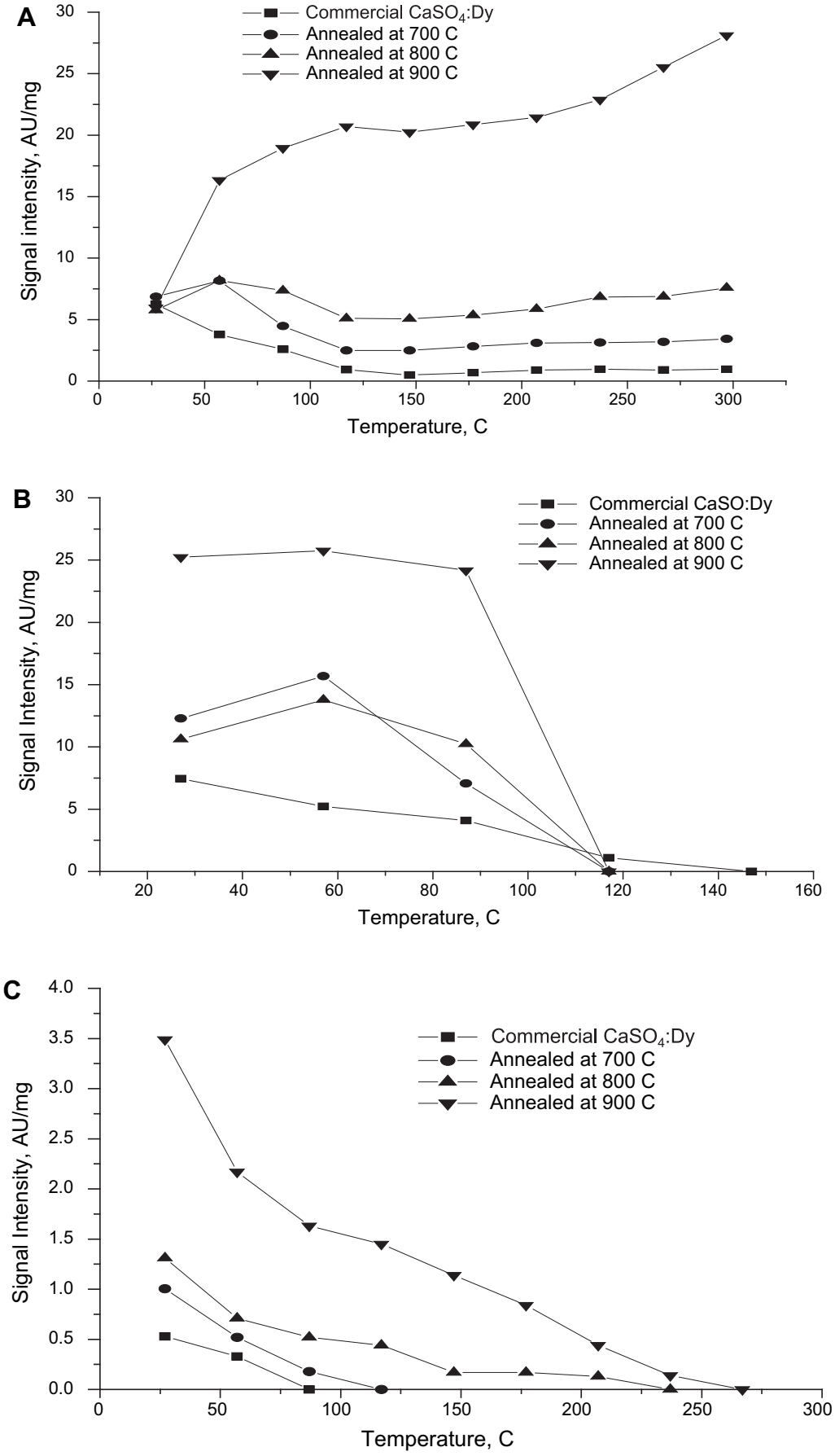

Fig. 7. Response of the EPR signal intensities of A. SO_3^-, B. SO_4^- and C. O_3^- of commercial and annealed at 700, 800, 900 °C $CaSO_4$:Dy phosphor with increasing temperature.

Author's personal copy

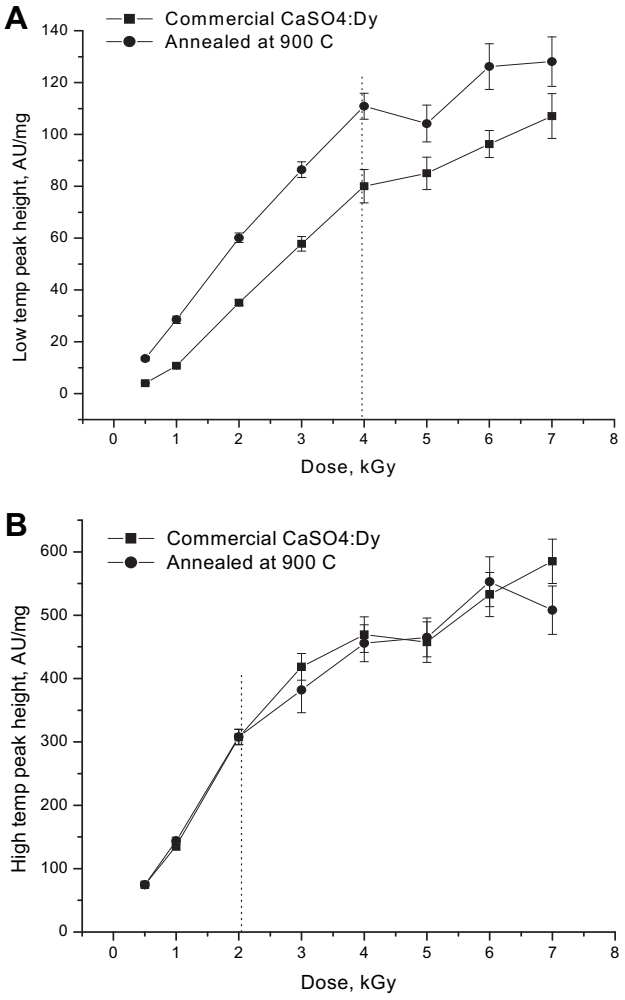

Fig. 8. Behavior of the TL response of the commercial and annealed (900 °C) $CaSO_4$:Dy phosphor with increasing radiation dose (at 0 ± 3 °C) of (A) low temperature peak height and (B) high temperature peak height.

three samples. In case of commercial phosphor a monotonous decrease up to a temperature of 150 °C was observed whereas, for the samples subjected to 700 and 800 °C annealing exhibited initial rise of the signal up to 60 °C followed by monotonous decrease. However, the phosphor annealed at 900 °C showed increasing trend throughout the temperature range and probably because of the development of Ca-vacancy defects $(Vca)^{2-}$ at the same position of SO_3^- radical. Similar observation has been reported by Danby et al. (1982), Morgan and Stoebe (1990), Mauricio et al. (1996), Bortolin and Onori (2005). These results suggest that the paramagnetic center at $g = 2.003$ either for SO_3^- or for Ca-vacancy defects may not be responsible for the enhancement of low temperature peak. Fig. 7B and C shows the behavior of SO_4^- and O_3^- radicals with increasing temperature. In case of phosphor annealed at 900 °C, the intensities of SO_4^- and O_3^- signals were more enhanced in comparison with the other samples. The SO_4^- line showed a sharp fall around 125 °C contributing to low temperature peak of the TL glow, whereas, O_3^- line exhibited a monotonous decrease in signal intensity up to 250 °C revealing its major contribution to high temperature peak of the TL glow. The behaviors of SO_4^- and O_3^- radicals were observed almost similar to that of phosphor annealed at 900 °C. The thermal characteristics of all the paramagnetic centers revealed that SO_4^- could be responsible for the enhancement of the low temperature peak intensity.Fig. 8A and B depicts the radiation dose response of the low and high temperature peak heights of the thermally annealed (900 °C) $CaSO_4$:Dy phosphor with respect to commercially available phosphor. An increased sensitivity of the low temperature peak with no significant deviation from its linear behavior with increasing dose up to 4 kGy was observed. However, post-preparation thermal treatment did not reveal any considerable change in the high temperature peak height with increasing dose.

4. Conclusion

$CaSO_4$:Dy phosphor exhibits reproducible dose response characteristics after irradiation at sub-ambient temperatures (0 and −16 °C) in the range 0.1–7.0 kGy with the onset of supralinearity above 1.0 kGy. Post-preparation thermal treatments revealed structural change in glow curve exhibiting increased sensitivity of the low temperature peak. Peak sensitization characteristics and the dose response behaviors of the peaks of annealed phosphor could be explained based on the observation from the EPR studies. Phosphor subjected to post-preparation thermal treatment of 900° C exhibited saturation of low temperature peak at more than 4.0 kGy and may be most suitable for the dosimetry of irradiated foods carried out at sub-ambient temperatures in the dose range 0.5–4.0 kGy.

References

ASTM standard, ISO/ASTM 51607:2004 E. Standard practice of use of an Alanine-EPR dosimetry system.
ASTM Standard, 51956. 2005 (E). Standard practice for use of thermoluminescence dosimetry (TLD) systems for radiation processing.
ASTM Standard, E 1026. Standard practice for using Fricke reference standard dosimetry system.
Bakshi, A.K., Pradhan, A.S., Srivastava, K., Kolambe, D.H., 2002. New parameters of annealing and re-use of TLDs based on $CaSO_4$:Dy phosphor. Radiat. Prot. Dosimetry 100, 293–296.
Bakshi, A.K., Pradhan, A.S., Tyagi, A.K., Kher, R.K., Bhatt, B.C., 2006. Correlation of phase transition with the change in TL characteristics in $CaSO_4$:Dy phosphor – effect of thermal treatment. Radiat. Prot. Dosimetry 119, 139–142.
Bakshi, A.K., Patwe, S.J., Bhide, M.K., Sanyal, B., Natarajan, V., Tyagi, A.K., Kher, R.K., 2008. Thermoluminescence, ESR and X-ray diffraction studies of $CaSO_4$:Dy phosphor subjected to post preparation high temperature thermal treatment. J. Phys. D. Appl. Phys. 41, 025402 (8 pp.).
Bortolin, E., Onori, S., 2005. Features of EPR dosimetry with $CaSO_4$:Dy phosphor. Appl. Radiat. Isot. 62, 349–352.
Campos, L.L., Lima, M.F., 1986. Dosimetric properties of $CaSO_4$:Dy teflon pellets produced at IPEN. Radiat. Prot. Dosimetry 14, 333–335.
Chen, R., McKeever, S.W.S., 1994. Characterization of nonlinearities in the dose dependence of thermoluminescence. Radiat. Meas. 23, 667–673.
Danby, R.J., Boas, J.F., Calvert, R.L., Pilbrow, J.R., 1982. ESR of thermoluminescence centres in $CaSO_4$ single crystals. J. Phys. C. Solid State Phys. 15, 2483–2493.
Gupta, N.M., Luthra, J.M., Shankar, J., 1974. Trapping and emission centres in thermoluminescent barium sulphate. Radiat. Eff. 21, 151–156.
Hernandez-Medina, A., Negron-Mendoza, S., Ramos-Bernal, 2010. Temperature effect during the gamma irradiation of $CaSO_4$:Dy. Radiat. Meas. 45, 586–588.
Mathur, V.K., Lewandowski, A.C., Guardala, N.A., Price, J.L., 1999. High dose measurements using thermoluminescence of $CaSO_4$:Dy. Radiat. Meas. 30, 735–738.
Mauricio, C.L.P., Bortolin, E., Onori, S., 1996. ESR study of $CaSO_4$:Dy TLD. Radiat. Meas. 26, 639–644.
Morgan, M.D., Stoebe, T.G., 1990. The role of Dy in the thermoluminescence of $CaSO_4$. Radiat. Prot. Dosimetry 33, 31–33.
Natarajan, V., Dalvi, A.G.I., Sastry, M.D., 1988. Trap level spectroscopy of actinide-doped alkaline-earth sulphates: II. $CaSO_4$:^{241}Am. J. Phys. C: Solid State Phys. 21, 5913–5922.
Ramos-Bernel, S., Cruz, E., Negron-Mendoza, A., Bustos, E., 2002. Irradiation dose determination below room temperature. Radiat. Phys. Chem. 63, 813–815.
Sanyal, B., Chawla, S.P., Sharma, A., 2009. An improved method to identify irradiated rice by EPR spectroscopy and thermoluminescence measurements. Food Chem. 116, 526–534.
Seshagiri, T.K., Dalvi, A.G.I., Sastry, M.D., 1988. Trao level spectroscopy of actinide-doped alkaline-earth sulphates: I. $SrSO_4$:^{239}Pu and $CaSO_4$:^{239}Pu. J. Phys. C: Solid State Phys. 21, 5891–5912.
Sharaf, M.A., Hassan, G.M., 2004. Radiation induced radical in barium sulphate for ESR dosimetry: a preliminary study. Nucl. Instrum. Methods Phys. Res. B. 225, 521–527.
Stoebe, T.G., Morgan, M.D., 1984. Models of TL Trapping and Recombination Centers. In: Thermoluminescence and Thermoluminescent Dosimetry, vol. 1, pp. 19–47.

THE Society for Food Science & Technology

A New Electron Paramagnetic Resonance Method to Identify Irradiated Soybean

BHASKAR SANYAL AND ARUN SHARMA

ABSTRACT: Low-dose gamma irradiation causes minimal changes in food matrix making identification of radiation-processed foods a challenging task. In the present study, soybean samples were irradiated with commercially permitted gamma radiation dose in the 0.25 to 1.0 kGy range for insect disinfestations of food. Immediately after irradiation electron paramagnetic resonance (EPR) spectrum of the skin part of soybean showed a triplet signal ($g = 2.0046$, hyperfine coupling constant $hfcc = 3.0$ mT) superimposed on naturally present singlet. These signals were characterized as cellulose and phenoxyl radicals using EPR spectrum simulation technique. Kernel part of the samples exhibited a short-lived, radiation-induced singlet of carbon-centered radical superimposed on naturally present sextet signal of Mn^{2+}. A detailed study on relaxation and thermal behavior of induced radicals in skin part was carried out using EPR spectroscopy. These findings revealed that progressive saturation and thermal characteristics of the induced radicals may be the most suitable parameters to distinguish soybean subjected to radiation dose as low as 0.25 kGy from thermally treated and nonirradiated samples, even after a prolonged period of storage.

Keywords: detection method, EPR spectroscopy, food irradiation, soybean

Introduction

Soybean (Glycine max) is a rich source of nutrition and bioactive phytochemicals. The nutritional quality of soybean has long been ascribed to its high protein and oil content accounting for 40% and 20% of its dry weight, respectively. The remainder consists of carbohydrate 35% and ash 5%. (Oliveira and others 2007). Insect infestation during storage is a major problem, resulting in economic losses. Irradiation is increasingly being recognized as an effective technology to reduce postharvest losses and improve quality. Irradiation effects are minimum and similar to those produced by conventional food processing methods, such as heating and freezing (Raffi and others 2000). Moreover, a low radiation dose in the range of 0.25 to 1.0 kGy for insect disinfestations is delivered for commercial irradiation of soybean, making the identification of irradiated product an extremely challenging task.

Regulatory authorities require a reliable method to identify irradiated foods to facilitate trade in radiation-processed food products and checking compliance with the labeling requirements. Development of reliable methods to distinguish between irradiated and nonirradiated food commodities is essential in view of the growing interest of the food industry in irradiation technology. This in turn will increase the confidence of the consumers in the technology.

Several detection methods based on physical, chemical, and biological principles have been developed for identification of irradiated foods (Chung and others 2004; Sanyal and others 2008, 2009). Among them, physical method like electron paramagnetic resonance (EPR) spectroscopy is a unique technique for the detection of paramagnetic species that are found during the gamma irradiation process. Three European standards for detection of irradiated food by EPR spectroscopy have been released by European Committee of Normalization (CEN) and adopted by Codex Alimenterius Commission as Codex Standards. These pertain to foods containing bone (European Standard EN 1786, 1997), crystalline sugar (European Standard EN 13708, 2001), and cellulose (European Standard EN 1787, 2000). The irradiated foods exhibiting radiation-specific EPR signal of cellulosic origin have been validated for various foods like, pistachio shells, paprika powder, and fresh strawberries (Raffi and others 1992; Desrosiers 1996). The application of EPR spectroscopy to identify irradiated foods is limited by the lifetime of the radiolytically produced free radicals (Yordanov and Gancheva 2000; Bayram and Delincee 2004). The main problem lies in the instability of the relatively weak satellite lines of cellulose. In some cases, the satellite lines are not detectable immediately after irradiation. However, the main advantage of EPR technique lies in its nondestructive approach and the sample under test does not require any preparation. Development of new approaches based on EPR methodology to identify irradiated food containing radiation-specific EPR signals is of increasing interest (Yordanov and Gancheva 2000; Sanyal and others 2008).

The main objective of this study was to identify irradiated soybean with commercially approved radiation dose (0.25 to 1 kGy) for the purpose of insect disinfestations particularly after prolonged storage. Skin and kernel parts of soybean were studied separately using EPR spectroscopy. Stable radiation induced signal identified in the skin part was characterized by EPR spectrum simulation technique. In addition to that a detailed study of EPR saturation characteristics and thermal behavior of the induced radicals was carried out to distinguish between treated and nontreated samples, when the satellite lines due to cellulose have presumably disappeared due to prolonged storage.

Materials and Methods

Materials

Soybean was procured from a local market and repacked into polyethylene bags (250 g). The packets were subdivided into 3

MS 20090180 Submitted 3/2/2009, Accepted 7/8/2009. *Authors are with Food Technology Div., Bhabha Atomic Research Centre, Mumbai, India. Direct inquiries to author Sharma (E-mail: ksarun@barc.gov.in).*

© 2009 Institute of Food Technologists®
doi: 10.1111/j.1750-3841.2009.01314.x
Further reproduction without permission is prohibited

Journal of Food Science

A Publication of the Institute of Food Technologists

lots. One served as control and the other was irradiated at 0.25 to 1.0 kGy radiation dose range recommended for disinfestations. The 3rd lot was subjected to thermal treatment in a glass container before repacking. The commodity has a shelf life of 2 to 3 mo. The standard 2, 2, diphenyl-1-picrylhydrazyl (DPPH) with $g = 2.0032$ was purchased from Sigma Chemical Co. (St. Louis, Mo., U.S.A.).

Irradiation conditions and thermal treatment

Irradiation was carried out at ambient temperature (300 ± 2 °K) using a cobalt-60 irradiator (GC-5000, BRIT, Mumbai, India dose rate of 6.2 kGy/h) at BARC, Mumbai, India. The determination of the absorbed dose was carried out using Fricke reference standard dosimeters (ASTM Standard, E) in each location where the

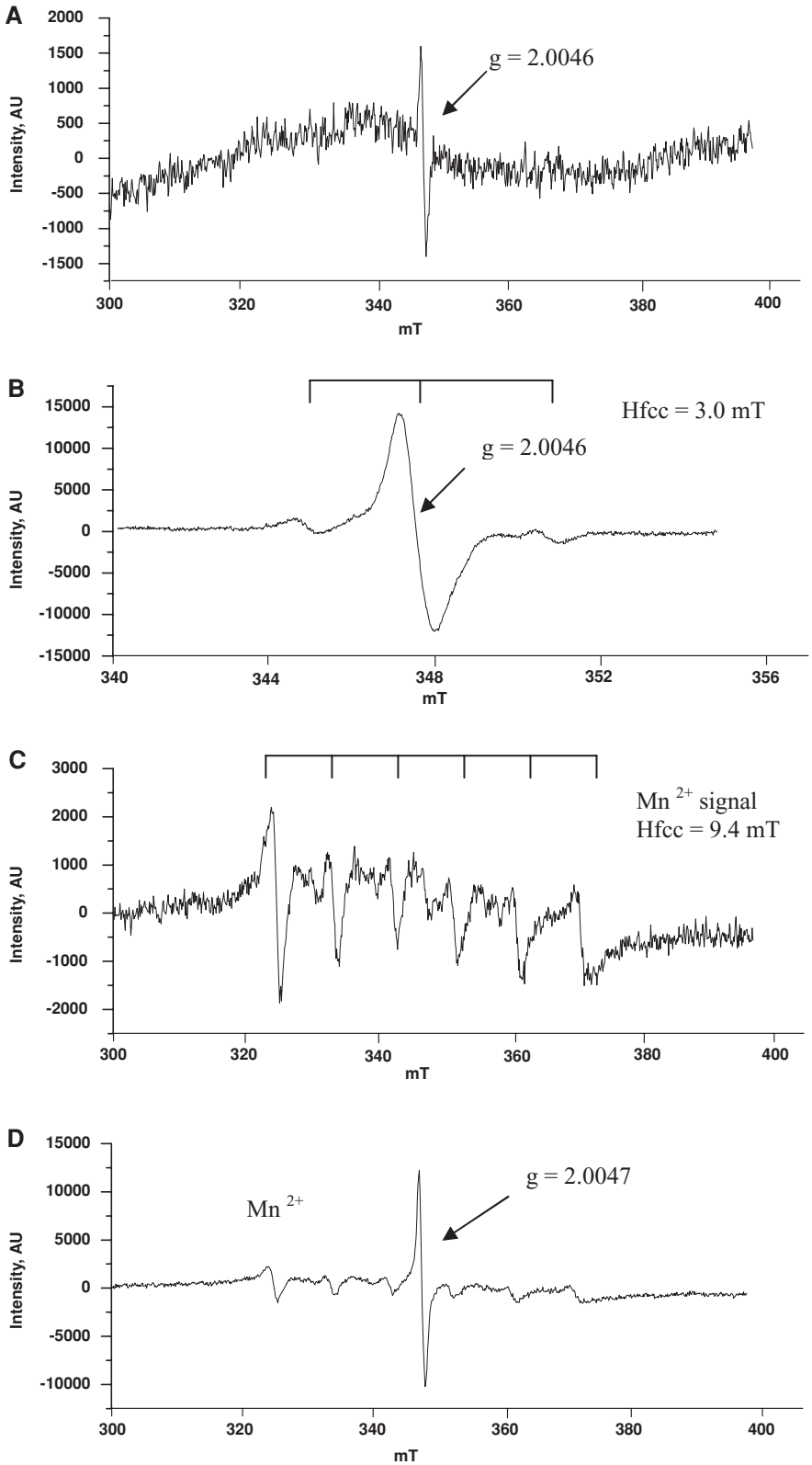

Figure 1—EPR spectra of soybean recorded at room temperature (A) nonirradiated skin part, (B) 1 d after radiation treatment (1 kGy) of the skin part, (C) nonirradiated kernel part, and (D) 1 d after radiation treatment (1 kGy) of the kernel part.

dosimeters were irradiated and a variation of 1.01% in absorbed dose was found out over the irradiation volume. Finally, the soybean samples packed in sealed polyethylene bags were irradiated in the dose range of 0.25 to 1 kGy, recommended for insect disinfestation. During irradiation the actual absorbed dose in the soybean samples was measured using two sets of chemical dosimeters. The first set was Fricke to measure the dose of 0.25 kGy and the second set was ceric-cerous sulphate dosimeters with concentration 0.003 M (ASTM Standard, ISO/ASTM 51205:2002 [E]) to measure the dose starting from 0.5 to 1.0 kGy. A variation in the absorbed dose with respect to the desired dose was observed within ± 2%.

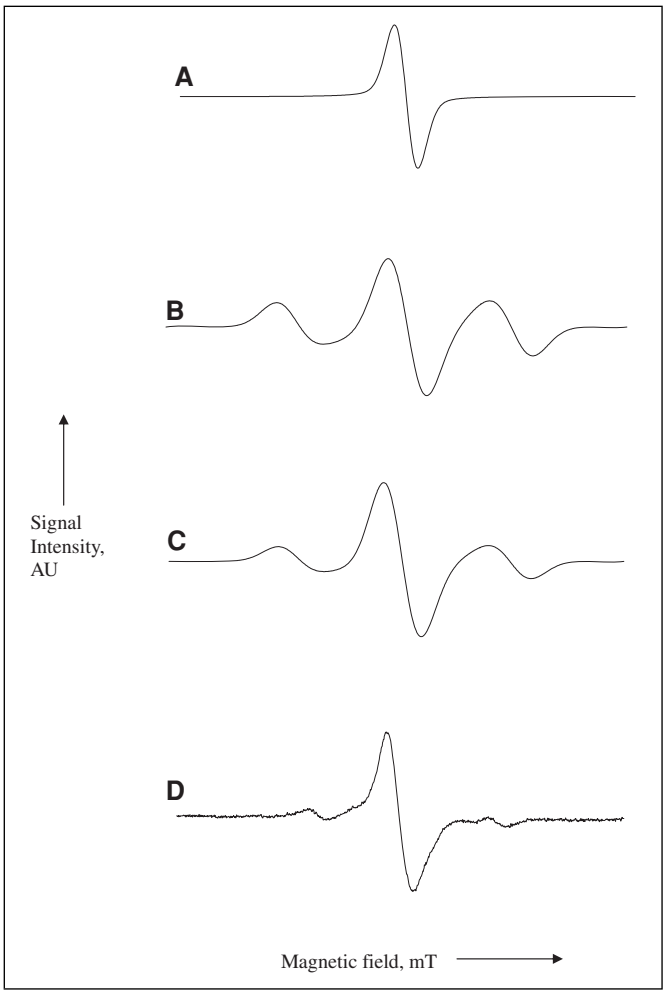

Figure 2—A scheme demonstrating a simulation analysis of experimental EPR spectrum of irradiated (1 kGy) soybean sample (A) simulation spectrum of phenoxyl ($C_6H_5O^-$) radical, (B) simulation spectrum of cellulose radical, (C) linear combination of the individual spectrum represented in a and b, and (D) experimental spectrum of irradiated sample.

Table 1—Spin Hamiltonian parameters of gamma irradiated induced EPR signals observed in soybean (skin part) treated with 1 kGy dose.

Origin of EPR signal	*g* value	Hyperfine splitting (Gauss)	ΔB_{pp} (Gauss)
Phenoxyl (O^-) radical	2.0040	0.00	9.2
Cellulose	$g_\perp = 2.0040$	$A_\perp = 30$	10
	$g_\parallel = 2.0032$	$A_\parallel = 18$	

To study the induced radicals by thermolysis, the samples were heated at 373 °K for 1 h using a laboratory oven (Roberto and others 2004).

Three replicates of each sample were evaluated. The irradiated, thermally treated, and nonirradiated soybean samples were stored inside EPR quartz tube under normal laboratory conditions at ambient temperature (298 ± 2 °K) throughout the time kinetics study of the paramagnetic species for a period of 60 d.

EPR spectroscopy

The skin and kernel parts of irradiated, thermally treated, and nonirradiated (control) soybean samples were separated. The skin part was chopped and the kernels were cut into fine pieces of an approximate length of 1.5 mm and transferred to 2-mm quartz capillary tubes and packed with gentle tapping to a length of 25.4 mm (active length) and the weight of the sample was determined in the range of 60 ± 4 mg. The results for the signal intensity of samples were normalized to the packing weight. EPR measurements were performed using Bruker EMX spectrometer (Bruker, Karlsruhe, Germany). All the spectra were recorded at ambient temperature (298 ± 2 °K) of EPR laboratory. All the spectra were recorded after 3 accumulated scans. EPR spectra simulation studies were carried out using WIN EPR and Simfonia programme (Bruker). The EPR spectrum having multiple components was evaluated as a linear combination of the individually simulated EPR spectra. The relative concentration of the individual paramagnetic species was evaluated from the contribution of the individual simulation to experimental spectrum by double integration. The correlation of the simulated and experimental spectra was determined by the respective correlation coefficient (R^2).

Operating conditions of the EPR spectrometer were as follows: Center field 348 mT, scan range 20 mT for narrow scan and 100 mT for wide scan, microwave power 0.253 mW, microwave frequency 9.66 GHz, modulation frequency 100 kHz, receiver gain 4×10^4 and time constant 20.48 s. The position of the radiation-induced EPR signal was compared with that of the standard 2, 2, diphenyl-1-picrylhydrazyl (DPPH) with $g = 2.0032$ (Sigma Chemical Co.).

EPR studies on progressive saturation and thermal characteristics of induced radicals

To determine the electron relaxation behavior of radicals in soybean samples using EPR spectrometer, the microwave field strength was varied between 0.06 and 50 mW to obtain progressive saturation behavior (PSB). Field modulation was operated at 100 kHz. All the EPR measurements were done at ambient temperature. Spin concentration was determined using DPPH (1, 1-diphenyl-2-picrylhydrazyl) as a standard sample.

In situ heat treatment from room temperature to 550 °K in a step of 20 °K was conducted using nitrogen gas for heating the samples within the EPR spectrometer using the BVT-3000 accessory of Bruker.

Results and Discussion

EPR spectral analysis of nonirradiated and irradiated soybean

Skin and kernel parts of nonirradiated and irradiated soybean were separated and EPR spectroscopy was carried out. Figure 1A shows the EPR spectra recorded using a broad magnetic field sweep width (100 mT) of skin part of soybean before radiation treatment. A singlet EPR signal at $g = 2.0046 \pm 0.0004$ centered around 347.8 mT was observed. This *g* value obtained compares well with those reported in the literature (Dodd and others 1985; Desrosiers

and McLaughlin 1989; Bortolin and others 2006). Several studies have suggested these free radicals to be those of semiquinones produced by the oxidation of plant polyphenolics (Scewartz and others 1972) or lignin (Maloney and others 1992; Tabner and Tabner 1994). Figure 1B shows the EPR spectrum 1 d after the radiation treatment with dose 1 kGy of the skin part with an increase in signal intensity of the existing weak singlet ($g = 2.0046$) by a factor of 7. Raffi and others (1992) also reported similar observations where an intense signal was noticed in the spectrum of irradiated spices. Irradiation was explained to be responsible for the relatively high intensity increase. The exposure to gamma radiation leads to another paramagnetic species (triplet signal) at the same g value as that of nonirradiated samples with hyperfine coupling constant (*hfcc*) 3 mT. To characterize the radiation induced signals in skin part of irradiated soybean, EPR spectra simulation studies were carried out using WIN EPR and Simfonia programme. The detailed simulation scheme of EPR spectra of the skin part of soybean irradiated with a dose of 1 kGy is depicted in Figure 2A to 2D and their spin Hamiltonian parameters ($g_\perp$, $g_\parallel$, $A_\perp$, $A_\parallel$; ΔB_{pp}) used in simulation are summarized in Table 1. The spectrum as depicted in Figure 2C was simulated as a linear combination of the individual signals represented in Figure 2A and 2B ($R^2 = 0.968$). Simulation of EPR spectra obtained from irradiated skin revealed the formation of 2 paramagnetic species, one was singlet signal attributed to phenoxyl radical ($C_6H_5O^-$) ion and the other was triplet signal of cellulose radicals. The signal attributed to cellulose radical was induced by the ionizing radiation as a consequence of the cleavage of cellulose polymer chain. Korkmaz and Polat (2001) have reported similar observation for gamma-irradiated red pepper.

EPR spectra of the kernel part of nonirradiated and irradiated soybean were carried out using similar experimental parameters as that of the skin part. Figure 1C shows the EPR spectrum of nonirradiated kernel depicting a sextet signal at $g = 2.0046$ with hyperfine interaction of $hfcc = 9.4$ mT. This signal was attributed to Mn^{2+} ion. Existence of Mn^{2+} has also been reported for ground black pepper and wheat flour (Polovka and others 2006).

Figure 1D shows the EPR spectrum of irradiated (1 kGy) soybean kernel part. A sharp and intense EPR singlet at $g = 2.0047$ was observed superimposed on the sextet signal of Mn^{2+}. This radiation-induced signal was attributed to carbon centered organic radical. Similar observation has been reported by Oliveira and others (2007) and proposed as a marker of radiation treatment. However, this radiation-specific signal observed in the matrix of kernel part was not particularly stable and disappeared after 10 to 12 d to a level that was similar to that of nonirradiated specimen exhibiting only the sextet signal of Mn^{2+}. The instability in signal intensity indicates that the detection of irradiated soybean by EPR spectroscopy of kernel part is limited.

The effect of increasing radiation dose from 0.25 to 1.0 kGy on the spectra of skin part of soybean samples was studied. The triplet signal of cellulose for 1 kGy irradiated sample was more prominent in comparison with the sample received 0.25 kGy dose and visible up to 50 d of storage. But the sample irradiated with minimum dose of 0.25 kGy, the radiation-specific triplet was visible up to 35 d. The integral intensities of the EPR signals were obtained by double integration of the spectrum and the integral intensity of the central line was observed to be significantly related to the radiation dose as shown in Figure 3. The measurement was performed 2 d after irradiation. The dotted line represents a polynomial fit, $Y = aD^2 + bD + c$ with $a = -2.55 \times 10^6$, $b = 3.49 \times 10^6$, and $c = 5.29 \times 10^5$, and each point is the mean value of 3 samples.

Characterizations of irradiated, thermally treated, and nontreated soybean by EPR saturation and thermal behavior

Characterization of the free radicals, naturally present or induced by radiation was essential for the investigation of radiation treatment. In view of this, 2 independent techniques based of EPR were employed, one was to study the electron relaxation behavior and the other was thermal characteristic of the EPR signals. To determine the electron relaxation behavior of the radicals in soybean, we varied the microwave field strength from 0.063 to 50 mW to

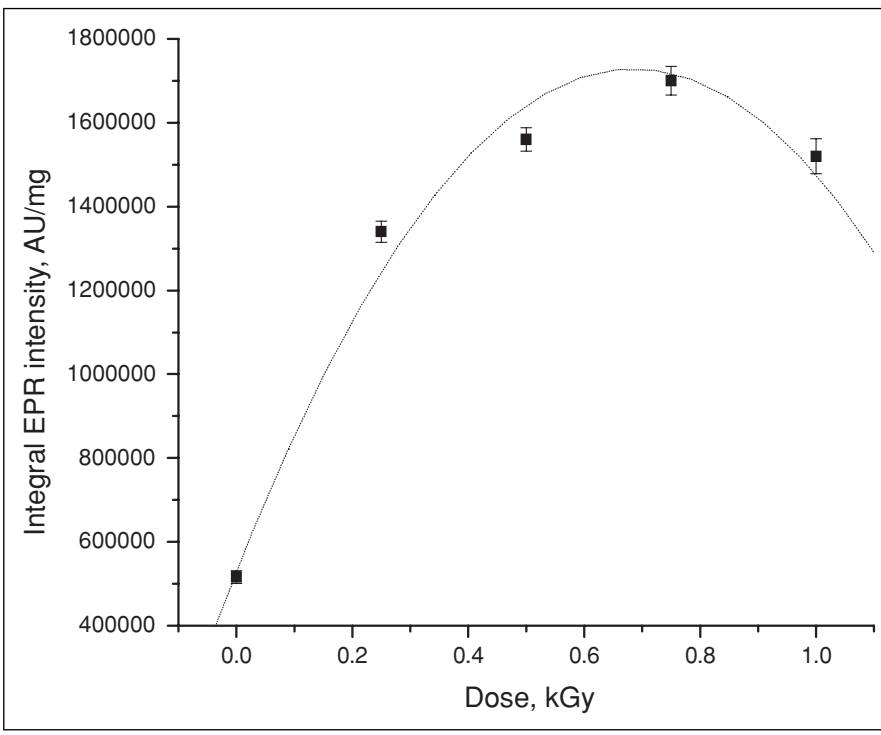

Figure 3—Response of the radiation induced signal ($g = 2.0046$) and the dependence of double integral EPR signal intensity evaluated with increasing dose after 2 d of radiation treatment.

obtain progressive saturation behavior (PSB). The effect of saturation is manifested by continuous nonlinear increase of EPR signal intensity with MWP $^{\frac{1}{2}}$, reaching a maximum followed by a decrease with the simultaneous increase of EPR line width.

Figure 4A shows the PSB of the central line (g = 2.0047) and Mn^{2+} signal of irradiated (1 kGy) soybean kernel part 5 d after radiation treatment. A comparatively faster saturation at microwave power around 6 mW followed by decrease in signal intensity by monotonic fashion was observed for the radiation induced signal in kernel. However, the PSB of Mn^{2+} signal showed a monotonous increase in signal intensity without any saturation confirming the characteristics of paramagnetic center of inorganic origin and short relaxation time. Figure 4B shows the behavior of the organic and inorganic signals in the matrix of kernel with increasing temperature from 300 to 450 °K. The intensity of the central singlet (g = 2.0047) exhibited a sharp fall in signal intensity up to 325 °K followed by almost unchanged behavior up to 400 °K. However, temperature increase beyond 400 °K led to an increase in signal intensity probably due to the decomposition of the samples as a result of phase transition of the organic matrix and formation of new thermally induced radicals. Whereas, in the case of inorganic signal of Mn^{2+}, the signal intensity showed a monotonous decrease in signal intensity up to 420 °K without further increase with temperature.

The most important objective of identification of irradiated food is to trace the signal, which is originated only because of radiation treatment. To validate a method for identifying irradiation, free radicals produced by other processing techniques such as heating (thermolysis) must be distinguished from those produced by irradiation. In view of this, whole soybean was subjected to thermal treatment at 373 °K for 1 h and EPR spectrum of skin part was recorded. The heat energy did not induce any specific change in the EPR spectrum. However, the intensity of the singlet (g = 2.0046) similar to that of nonirradiated sample was observed. To distinguish nonirradiated, irradiated, and thermally treated soybean samples, a detailed investigation of the paramagnetic centers of skin part was

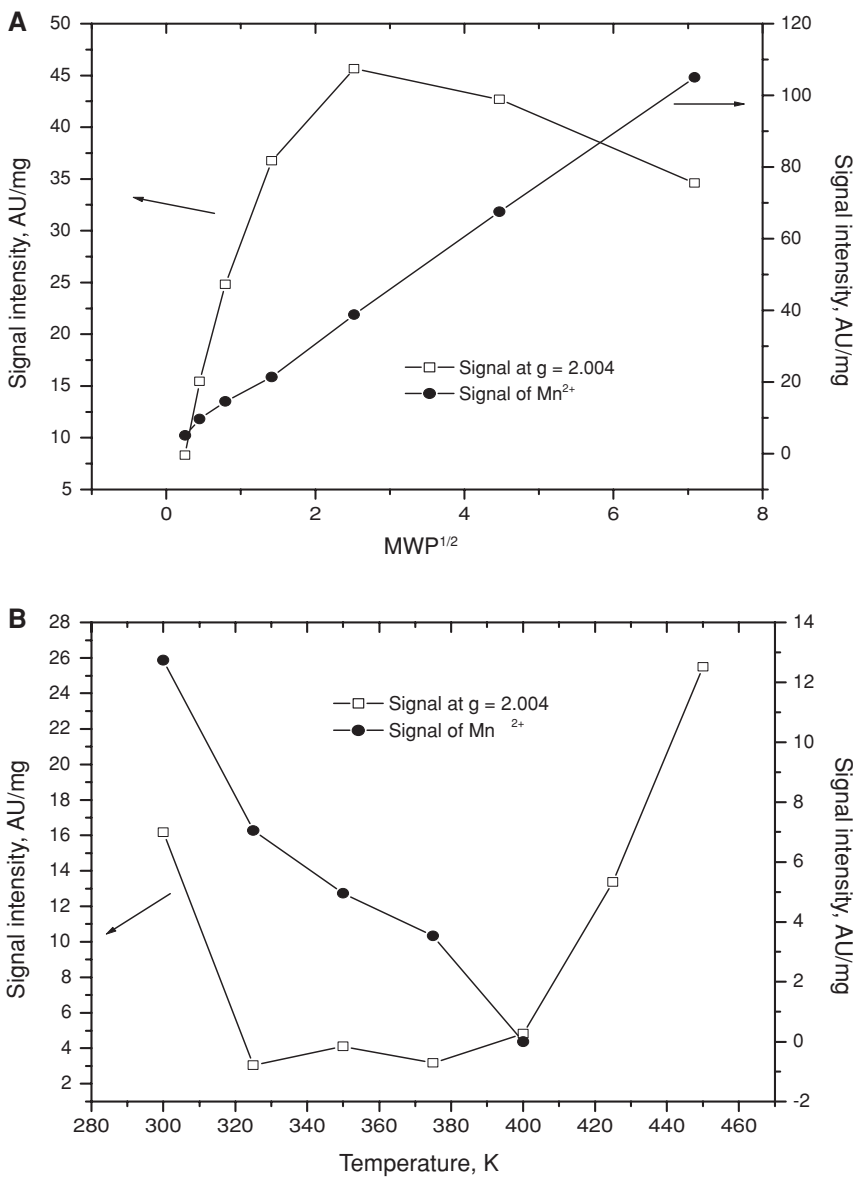

Figure 4—(A) Relaxation characteristics and (B) thermal behavior of the paramagnetic centers (g = 2.0047) in irradiated (1 kGy) kernel part of soybean after 5 d of radiation treatment.

carried out by PSB studies and thermal characteristics after storage period of 60 d. Figure 5 showed that a comparatively faster saturation at microwave power of 6 mW followed by a decrease in signal intensity in monotonic fashion was observed for thermally induced radicals. This saturation behavior revealed the characteristics of organic radicals with a large relaxation time. But both the nonirradiated and irradiated (0.25 and 1.0 kGy) samples exhibited a similar behavior of microwave saturation at around 20 mW. Improvement of the EPR detection of irradiated dry food using microwave saturation and thermal treatment has been proposed by Yordanov and others (2005). In this method, curves of saturation of nonirradiated and irradiated plants compared with $MWP^{1/2}$ were studied and nonirradiated samples showed saturation at microwave power higher than 15 mW, whereas, irradiated sample exhibited early saturation with microwave power of 8 mW. But in the case of soybean samples both the nonirradiated and irradiated samples exhibited similar relaxation characteristics with no significant difference in saturation behaviors. Therefore, EPR analysis by the progressive saturation behavior of the radicals may not be a useful method to distinguish irradiated soybean sample. However, faster EPR saturation of thermally induced radicals in comparison with the radiation-induced radicals could be used as a tool to distinguish between irradiated and heated soybean.

To address the problem of detection of irradiated soybean thermal behavior of the EPR signal was investigated. Nonirradiated, irradiated, and thermally treated samples were subjected to *in situ* heating from 300 to 450 °K. Figure 6A shows the thermal behavior of the central singlet for nonirradiated, irradiated, and thermally treated samples 1 d after heat and radiation treatments. With the increase in temperature from 300 to 400 °K, the central lines of nonirradiated and thermally treated samples exhibited a slow fall, but, that of irradiated samples showed a sharp fall of about 84%. However, temperature increase beyond 425 °K led to an increase in EPR signal intensities in all the cases. This could probably be due to the decomposition of the sample and formation of new thermally induced radicals. Similar observations on irradiated and nonirradiated spices have recently been reported by Polovka and others (2007). Figure 6B shows the thermal characteristics of the same samples after a storage period of 60 d. Samples irradiated with doses 1 and 0.25 kGy exhibited a sharp fall in signal intensities of 60% and 55%, respectively. Whereas, nonirradiated sample showed a slower fall in signal intensity of around 34% up to a temperature of 425 °K. Our results are well in agreement with the proposal of Yordanov and Gancheva, that, EPR analysis of the central peak of spices that had undergone thermal treatment before and relatively long time after irradiation could be used as a tool for detection of irradiation. The application of Protocol EN 1787 was not possible as the EPR signals of cellulose required by the European Standards were not visible in soybean sample after a prolonged storage. Therefore, temperature profiles of the respective samples depicting the thermal behavior of the gamma induced EPR signal represented a valuable tool for the assessment of previous radiation treatment.

Kinetic study

Different factors, including humidity, temperature, light intensity, exposure to air, and structure of the food matrix influence the behavior of the induced radicals during the storage of the sample before and after irradiation and thereby, restrict the time interval after irradiation during which detection is possible. The time interval after which identification of the irradiated samples is possible was evaluated by the fading kinetics of the radiation induced radicals. To avoid atmospheric variations all the samples were kept inside the EPR measurement tube in normal laboratory condition. Figure 7 showed the time kinetics of nonirradiated, irradiated, and thermally treated samples monitored up to 60 d after radiation treatment. In the case of kernel part, the EPR singlet at $g = 2.0047$ was visible with a marked decrease in intensity up to 15 d of radiation treatment. However, for skin part of the sample received 1 kGy dose, the radiation-specific triplet signal of cellulose was visible almost throughout the storage time. But for the sample irradiated with 0.25 kGy dose, triplet signal was distinguishable only for

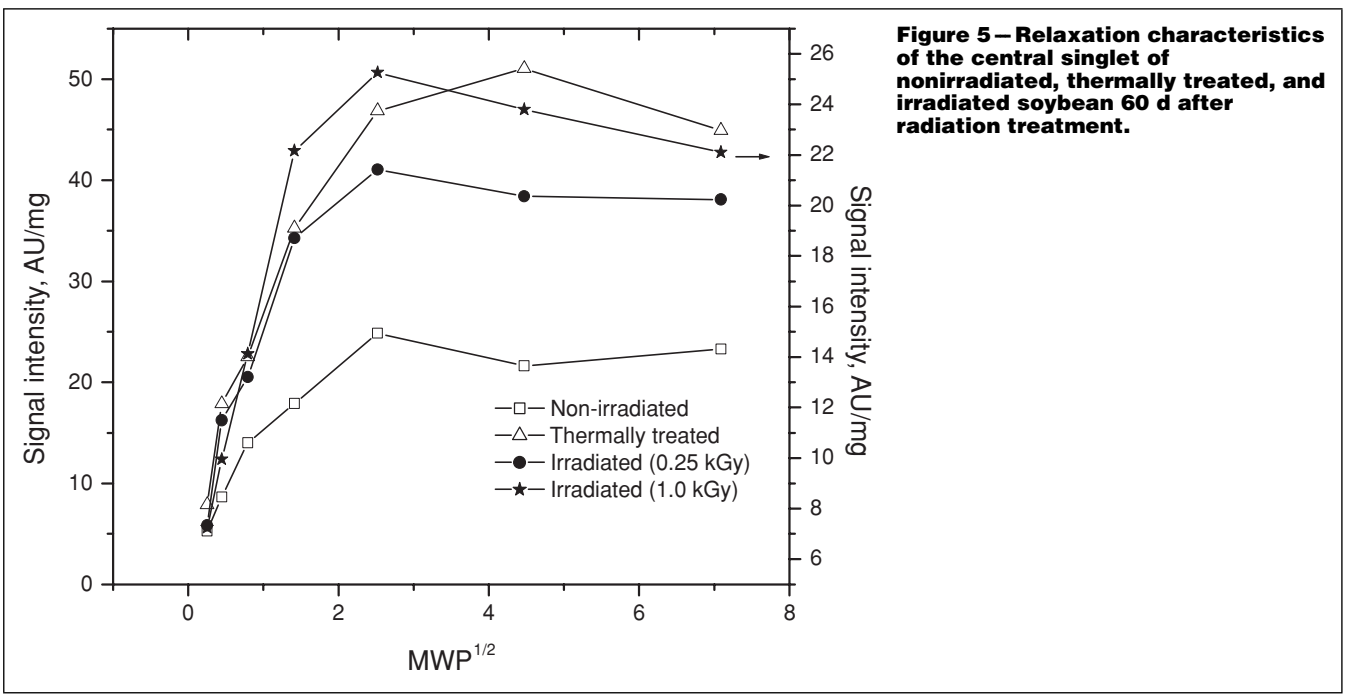

Figure 5—Relaxation characteristics of the central singlet of nonirradiated, thermally treated, and irradiated soybean 60 d after radiation treatment.

a time period of about 30 d. Decrease in the concentration of free radicals in irradiated spices with time has been reported by many researchers (Delincee 1998; Raffi and others 2000; Yordanov and Gancheva 2000). Therefore, application of EN 1787 Standard was not possible as a method of detection for the samples irradiated with a minimum dose of 0.25 kGy and stored beyond 30 d.

Conclusions

Identification of gamma-irradiated soybean was carried out by investigating free radicals using EPR spectroscopy. The skin part of nonirradiated, commercially available soybean exhibited a weak singlet signal, but in kernel part, a sextet signal of Mn^{2+} was identified. Immediately after radiation treatment, a triplet signal was observed in skin part and characterized by simulation technique as cellulose radicals. Kernel part exhibited a singlet after irradiation and observed to be stable for 15 d. EPR spectra of kernel and skin parts of the samples were monitored for a period of 60 d and it was concluded that EPR analysis of the skin part of the samples is most suitable for the detection of irradiated soybean. It was also found that sample irradiated with a maximum dose of 1 kGy could be identified by the cellulose radical signal as per the European Standard EN 1787 up to a period of 50 d. But the sample irradiated with a minimum dose of 0.25 kGy could be differentiated from nonirradiated (control) only up to a period of 30 d. These observations clearly revealed that application of EN 1787 was not possible to identify soybean samples irradiated with this minimum dose of 0.25 kGy after a prolonged storage. To address this limitation, relaxation and thermal behaviors of the radicals were studied. A full thermal profile of the radicals after a prolonged storage time exhibited an important clue to radiation treatment. The relaxation characteristics of the radicals were revealed as a useful technique to identify thermally treated samples from nonirradiated and irradiated soybean.

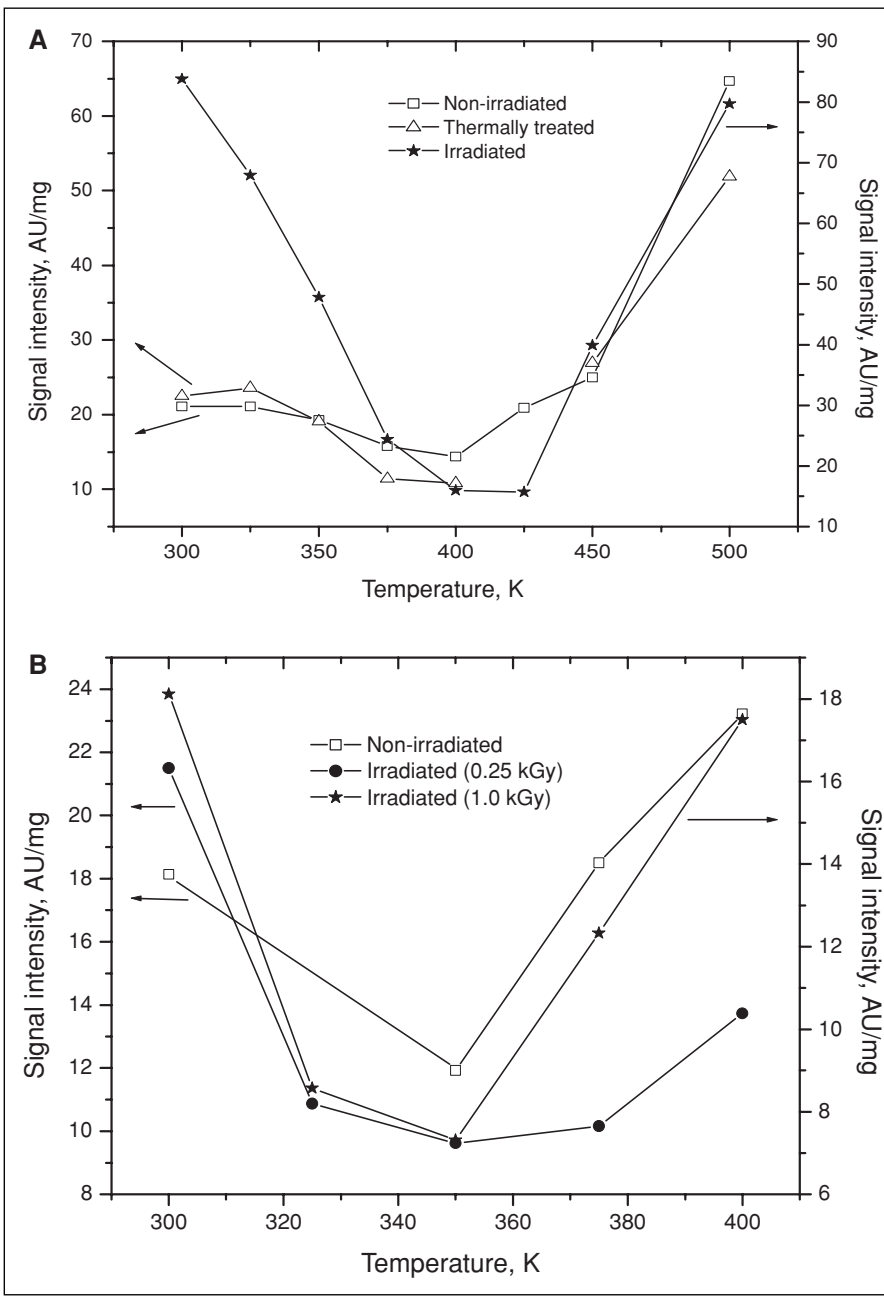

Figure 6—Thermal behaviors of nonirradiated, irradiated, and thermally treated skin part of soybean (A) 1 d after the treatments and (B) 60 d after the treatments.

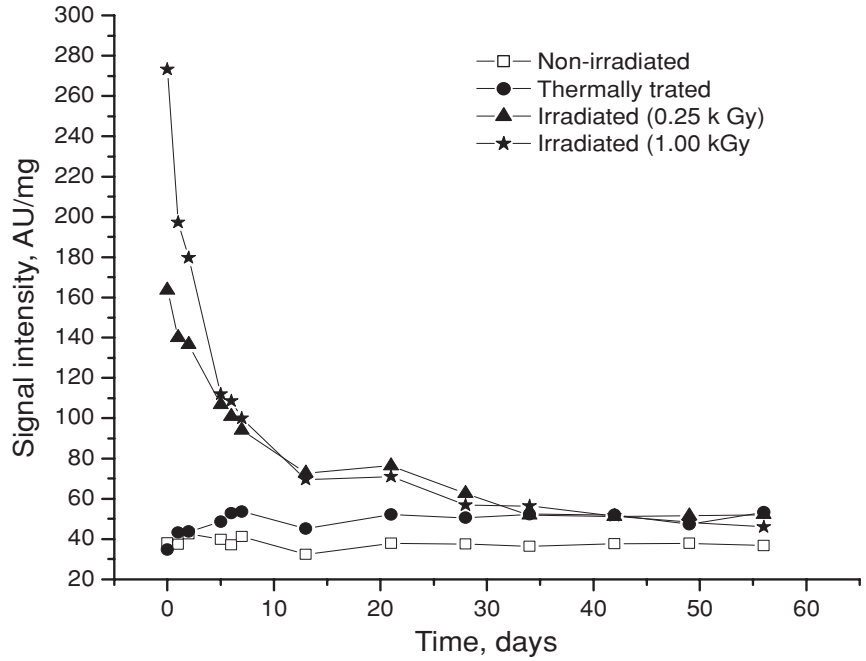

Figure 7—Kinetics of nonirradiated, irradiated (1.0 and 0.25 kGy), and thermally treated skin part of soybean sample throughout the storage period of 60 d.

References

ASTM Standard, E. 1026. 2004. Standard practice for using Fricke reference standard dosimetry system.

ASTM Standard, ISO/ASTM 51205:2002 (E). 2002. Standard practice for use of a ciriccerous sulphate dosimetry system.

Bayram G, Delincee H. 2004. Identification of irradiated Turkish foodstuffs combining various physical detection methods. Food Control 15:81–91.

Bortolin E, Griffin EB, Cruz-Zaragoza E, De Coste V, Onori S. 2006. Electron paramagnetic resonance detection of Mexican irradiated spices. Int J Food Sci Technol 41:375–82.

Chung HW, Delincee H, Han S, Hong J, Kim H, Kim M, Byun M, Kwon J. 2004. Trials to identify irradiated chestnut (*Castanea bungena*) with different analytical techniques. Radiat Phys Chem 71:179–82.

Delincee H. 1998. Detection of food treated with ionizing radiation. Trends Food Sci Technol 9:73–82.

Desrosiers MF. 1996. Current status of EPR method to detect irradiated food. Appl Radiat Isotopes 47:1621–8.

Desrosiers MF, McLaughlin WL. 1989. Examination of gamma irradiated fruits and vegetables by electron spin resonance spectroscopy. Radiat Phys Chem 34:895–8.

Dodd NJF, Swallow AJ, Ley FJ. 1985. Use of ESR to identify irradiated food. Radiat Phys Chem 26:451–3.

European Standard EN 1786. 1997. Foodstuffs-detection of irradiated food containing bone: analysis by electron paramagnetic resonance. Brussels, Belgium: European Committee for Standardization.

European Standard EN 1787. 2000. Foodstuffs-detection of irradiated food containing cellulose: analysis by EPR. Brussels, Belgium: European Committee for Standardization.

European Standard EN 13708. 2001. Foodstuffs-detection of irradiated food containing crystalline sugar: analysis by EPR. Brussels, Belgium: European Committee for Standardization.

Korkmaz M, Polat M. 2001. Radical kinetics and characterization of the free radicals in the gamma irradiated red pepper. Radiat Phys Chem 62:411–21.

Maloney DR, Tabner BJ, Tabner VA. 1992. An electron spin resonance study of gamma-irradiated fruits. Radiat Phys Chem 39:309–14.

Oliveira MRR, Quadrado MGO, Mastro NL. 2007. Analysis of gamma irradiated soybean components by electron paramagnetic resonance. Proceedings IJM Cancum, Mexico.

Polovka M, Brezova V, Stasko A, Mazur M, Suhaj M, Simko P. 2006. EPR investigation of gamma-irradiated ground black pepper. Radiat Phys Chem 75:309–21.

Polovka M, Brezova V, Simko P. 2007. EPR spectroscopy: a tool to characterize gamma irradiated foods. J Food Nut Res 46:75–83.

Raffi J, Stevenson MH, Kent M, Thiery JM, Belliardo JJ. 1992. Intercomparison on electron spin resonance identification of irradiated foodstuffs. Int J Food Sci Technol 27:111–24.

Raffi J, Yordanov ND, Chabane S, Douifi L, Gancheva V, Ivanova S. 2000. Detection of irradiated aromatic herbs and spices by electron paramagnetic resonance and thermoluminescence, spectrochim. Acta 56A:409–16.

Roberto WAF, Ladislau M, Maria SAK, Gilberto RF, Julio MMW, Luiz AC. 2004. Identification of irradiation treatment in black pepper by electron paramagnetic resonance. Int J Food Sci Technol 39:395–401.

Sanyal B, Sajilata MG, Chatterjee S, Singhal RS, Variyar PS, Kamat MY, Sharma A. 2008. Identification of irradiated cashew nut by electron paramagnetic resonance spectroscopy. J Agric Food Chem 56:8997–1.

Sanyal B, Chawla SP, Sharma A. 2009. An improved method to identify irradiated rice by EPR spectroscopy and thermoluminescence measurements. Food Chem 116:526–34.

Scewartz HM, Bolton JR, Brog DC, editors. 1972. Biological applications of electron spin resonance. New York: Wiley.

Tabner BJ, Tabner VA. 1994. Electron spin resonance spectra of gamma-irradiated citrus fruits skin, skin components and stalks. Int J Food Sci Technol 29:143–52.

Yordanov ND, Gancheva V. 2000. A new approach for the extension of the identification period of irradiated cellulose containing foodstuffs by EPR spectroscopy. Appl Radiat Isotopes 52:195–8.

Yordanov ND, Aleksieva K, Mansour I. 2005. Improvement of the EPR detection of irradiated dry plants using microwave saturation and thermal treatment. Radiat Phys Chem 73:55–60.

Provided for non-commercial research and education use.
Not for reproduction, distribution or commercial use.

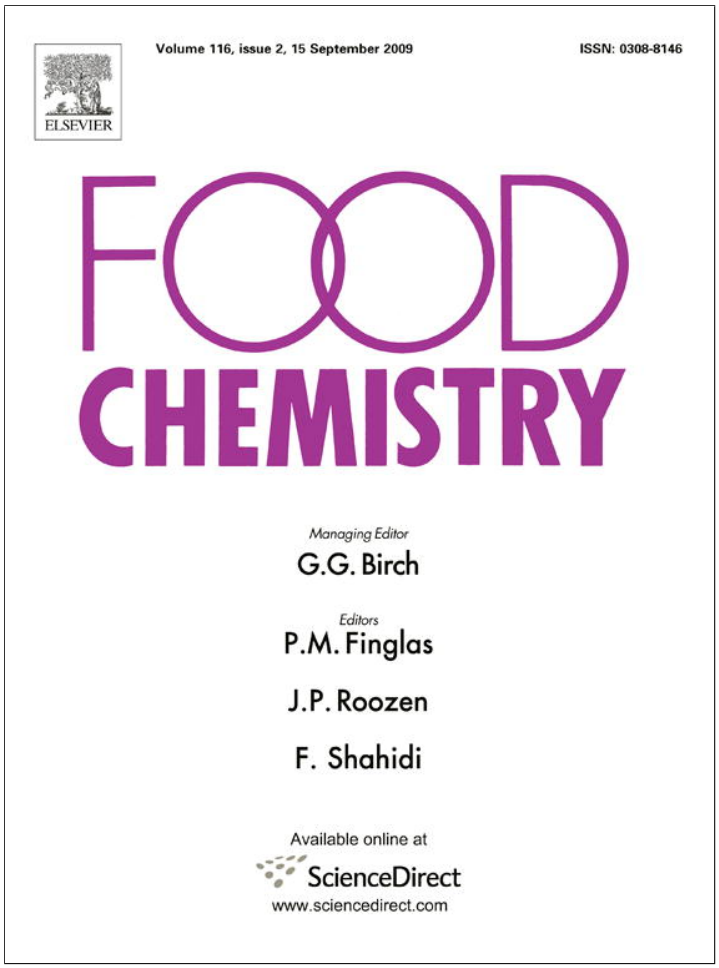

This article appeared in a journal published by Elsevier. The attached copy is furnished to the author for internal non-commercial research and education use, including for instruction at the authors institution and sharing with colleagues.

Other uses, including reproduction and distribution, or selling or licensing copies, or posting to personal, institutional or third party websites are prohibited.

In most cases authors are permitted to post their version of the article (e.g. in Word or Tex form) to their personal website or institutional repository. Authors requiring further information regarding Elsevier's archiving and manuscript policies are encouraged to visit:

http://www.elsevier.com/copyright

Author's personal copy

Food Chemistry 116 (2009) 526–534

Contents lists available at ScienceDirect

Food Chemistry

journal homepage: www.elsevier.com/locate/foodchem

Analytical Methods

An improved method to identify irradiated rice by EPR spectroscopy and thermoluminescence measurements

Bhaskar Sanyal *, S.P. Chawla, Arun Sharma

Food Technology Division, Bhabha Atomic Research Centre, FIPLY, Trombay, Mumbai, Maharashtra 400 085, India

ARTICLE INFO

Article history:
Received 3 October 2008
Received in revised form 5 January 2009
Accepted 22 February 2009

Keywords:
Food irradiation
Detection of irradiated foods
EPR
TL
Rice

ABSTRACT

Minimal change in irradiated foods with low dose treatment makes the identification process a difficult task. Two independent physical methods, electron paramagnetic resonance (EPR) spectroscopy and thermoluminescence (TL) detection were employed for detection of irradiation treatment on Basmati rice. EPR investigation of 0.5–2.0 kGy irradiated rice samples showed a short lived, asymmetric, dose dependent spectrum ($g = 2.005$), characterised by the radicals of irradiated starch. However, this signal disappears with time. The present work explores the possibility to identify irradiated rice by the relaxation characteristics and thermal behaviour of the radicals. This study reports for the first time that the different microwave saturation behaviours of the signal ($g = 2.004$) in irradiated and non-irradiated rice samples provide an important clue to identify radiation treatment beyond the period when the radiation specific EPR spectral lines have disappeared. TL investigation involving scanning electron microscopy/energy dispersive X-ray analysis (SEM/EDX) of the poly-minerals isolated from the rice samples allowed to discriminate clearly between irradiated and non-irradiated samples even after a prolonged period of storage.

© 2009 Elsevier Ltd. All rights reserved.

1. Introduction

Rice is an important cash crop and staple food for many countries. It has high nutritive value and the quality is governed by variety and climatic conditions. The eating quality of rice has long been ascribed to its starch. Starch accounts for 95% of the dry matter in milled rice grain (Martin & Fitzgerald, 2002). Insect infestation during storage is a major problem of rice, resulting in economic losses. Irradiation is increasingly being recognised as an effective technology to reduce post-harvest losses and improve quality. Irradiated (0.25–1.0 kGy) Basmati rice, a high value fragrant rice of India, did not exhibit insect infestation during a storage period of 6 months, at room temperature that varied between 27 °C and 33 °C and relative humidity between 59% and 87%, while the control (non-irradiated) samples were spoiled due to infestation. During sensorial evaluation, no significant difference was found between the acceptability of irradiated and non-irradiated (control) rice (Sudha Rao, Gholap, Adhikari, & Madhusudanan, 2000). These results are significant in view of the high export potential of Basmati rice and the losses attributed to infestation.

To facilitate trade in irradiated foods, regulatory authorities need a reliable method to detect irradiated foods and consequently check compliance with the labelling requirements. In view of the growing interest in irradiation technology of the food industry, development of reliable methods to distinguish between irradiated and non-irradiated food stuffs is essential for the benefit of enforcement agencies as well as consumers to increase confidence in radiation processing technology.

Several detection methods have been developed for identification of irradiated foods (Chung et al., 2004). Among them, EPR spectroscopy and thermoluminescence detection are the two leading techniques. For use in detection, radiation induced EPR signals in food must fulfil several requirements, i.e. they must be stable or fairly stable during the usual storage period of the foodstuff and must be clearly distinguishable from the background signals of the non-irradiated sample (Raffi, Agnel, Buscarlet, & Martin, 1988). Three European standards for detection of irradiated food by EPR spectroscopy have been released by European Committee of Normalisation (CEN) and adopted by Codex Alimenterius Commission as Codex Standards. These pertain to food containing bone (EN 1786, 1997), cellulose (EN 1787, 2000) and crystalline sugar (EN 13708, 2001). This last standard has been validated for irradiated skin of raisins and figures containing considerable amount of polysaccharides in the form of sugar. EPR is a user friendly technique, as the measurement is easy and the sample under test does not require any preparation. There is an increasing interest in extending the EPR methodology to various types of food. The main problem lies in the instability of the relatively weak radiation specific signals. Recently, in order to extend the applicability of EPR for identification of irradiated food, a new approach, based on thermal treatment and EPR saturation have been used when the radiation

* Corresponding author. Tel.: +91 22 25592533; fax: +91 22 25505151/255 19613.
E-mail addresses: bhaskar_sanyal@rediffmail.com, sanyal@barc.gov.in, bhaskar_barc@yahoo.com (B. Sanyal).

0308-8146/$ - see front matter © 2009 Elsevier Ltd. All rights reserved.
doi:10.1016/j.foodchem.2009.02.067

Author's personal copy

induced signals have disappeared due to long period of time elapsed after treatment (Yordanov, Aleksieva, & Mansour, 2005; Yordanov & Gancheva, 2000).

A negligible change in food commodities after radiation treatment makes the identification of irradiated food an extremely challenging task and the statistical safety margin is rather small for a reliable verdict to be given. Therefore, one method alone is not reliable enough for the detection of a treatment by ionizing radiation. In view of this, in present work, two independent physical methods were employed. Such a combined approach may be suitable for overcoming certain limitations with detection of irradiated foods. Thermoluminescence (TL) is a radiation specific phenomenon that arises due to energy stored by trapped charge carriers following irradiation (Sanderson, Carmichael, Spencer, & Naylor, 1996). TL has been tested for detection of spices and herbs and was adopted as a standard method for detecting irradiated foods from which silicate minerals can be isolated (EN 1788, 2001).

In this present work a detailed study of the radical species produced by gamma irradiation of rice has been carried out by EPR saturation and thermal behaviour to distinguish between treated and non-treated samples. In addition, characterisation of the extracted minerals from the rice sample and the possibility of TL technique to identify irradiated and non-irradiated samples have been examined.

2. Experimental

2.1. Materials

Rice (Basmati) samples were procured from a local market. The standard 2,2,diphenyl-1-picrylhydrazyl (DPPH) with $g = 2.0032$ was purchased from Sigma Chem. Co. USA. Pure starch was procured from Himedia, India. Sodium polytungstate ($Na_6W_{12}O_{39} * H_2O$) was purchased from Fluka, Germany to prepare a high density solution.

2.2. Irradiation conditions

Irradiation was carried out at ambient temperature (27 ± 2 °C) using a cobalt-60 irradiator (GC-5000, BRIT, Mumbai, dose rate of 6.2 kGy/h) at BARC, Mumbai. The doses were applied in the range of 0.5–2 kGy in order to cover the recommended doses for insect disinfestations. Dosimetry was performed using aqueous Fricke dosimeter (ASTM Standard, E 1026).

2.3. EPR spectroscopy

Rice samples were ground into fine granules and transferred to 2-mm quartz capillary tubes and packed with gentle tapping to a length of 25.4 mm (active length) and the weight of the sample was determined. The results for the signal intensity of samples were normalised to the packing weight. EPR measurements were performed using Bruker EMX spectrometer (Bruker, Germany). All the spectra were recorded at the ambient temperature of EPR laboratory (27 °C).

Operating conditions of the EPR spectrometer were as follows:

Centre field 3480 G, scan range 200 G, microwave power 0.253 mW, microwave frequency 9.66 GHz, modulation frequency 100 kHz, receiver gain 4×10^4 and time constant 20.48 s. The position of the irradiation – induced EPR signal was compared with that of the standard 2,2,diphenyl-1-picrylhydrazyl (DPPH) with $g = 2.0032$ (Sigma Chem. Co. USA).

The irradiated and non-irradiated rice samples were stored inside EPR quartz tube in the normal laboratory conditions at ambient temperature (27 ± 2 °C) until further use.

2.4. Thermal and progressive saturation behaviour of radicals

In situ heat treatment from room temperature to 250 °C in a step of 25 °C was conducted using nitrogen gas for heating the samples within the EPR spectrometer using BVT-3000 accessory of Bruker, Germany. To study the induced radicals by thermolysis, heat treatment before and after irradiation of the samples was carried out at 100 °C for 1 h using a laboratory oven. Four replications were made for the evaluation of each sample.

In order to determine the electron relaxation behaviour of radicals in rice samples, the microwave field strength was varied between 0.06 and 50 mW to obtain progressive saturation behaviour (PSB). Field modulation was operated at 100 kHz. All the EPR measurements were carried out at ambient temperature. Spin concentration was determined using DPPH (1,1-diphenyl-2-picrylhydrazyl) as a standard sample.

2.5. Thermoluminescence analysis

For separation of minerals and organic materials from the rice sample, European Standards EN 1788, 2001 was followed. The important procedures involved in sample preparation for TL analysis were as follows.

The solution of sodium polytungstate ($Na_6W_{12}O_{39} * H_2O$) was added to double distilled water to prepare a high density solution (2 g/ml). The samples were subjected to ultrasonication in a bath sonicator for 5 min followed by centrifugation at 1000*g* for 2 min. The organic material floating on the top of the polytungstate solution was removed. The bottom layer was washed three times with deionised water. After total removal of water, 2 ml of acetone was added. The minerals in acetone were transferred to clean and weighed aluminium discs (diameter 9.0 mm; thickness 0.4 mm) with the help of Pasteur pipette. The discs containing minerals were stored overnight at 50 °C.

The discs containing minerals from control and irradiated samples were weighed to determine the quantity of minerals deposited. Thermoluminescence analysis was carried using TL 1009I Reader (Nucleonix Systems, India). Nitrogen was flushed in the heating chamber to reduce spurious TL arising due to the presence of oxygen. The initial temperature was 40 °C, which was increased to 300 °C by linear heating at a rate of 5 °C/s. After measurement of glow 1, the discs with the deposited mineral were irradiated with a normalisation radiation dose of 1 kGy followed by TL measurement of glow 2 with the similar instrumental settings as described above. The samples were separated and analysed in triplicate under similar laboratory and instrumental conditions. The irradiated and non-irradiated rice samples were stored in dark in the normal laboratory conditions at ambient temperature (27 ± 2 °C) until further use.

Scanning electron microscopy and energy dispersive X-ray spectrometer analysis (SEM/EDX) were carried out to determine the poly mineral composition of the isolated minerals from rice samples. The electron microscopic analysis was done with TESCAN, Czechoslovakia and EDX, INCA x – sisht, Oxford, UK with secondary electron detector.

3. Results and discussion

3.1. Effects of gamma irradiation

Fig. 1a, shows the EPR signal of non-irradiated rice samples exhibiting a weak singlet characterised by $g = 2.0049 \pm 0.0004$ and $\Delta B_{pp} = 13$ G, centered around 3461 G. DPPH with $g = 2.0032$ was used as a reference to calculate the *g-values* of the radicals. Similar singlet EPR line has been reported for other food

Author's personal copy

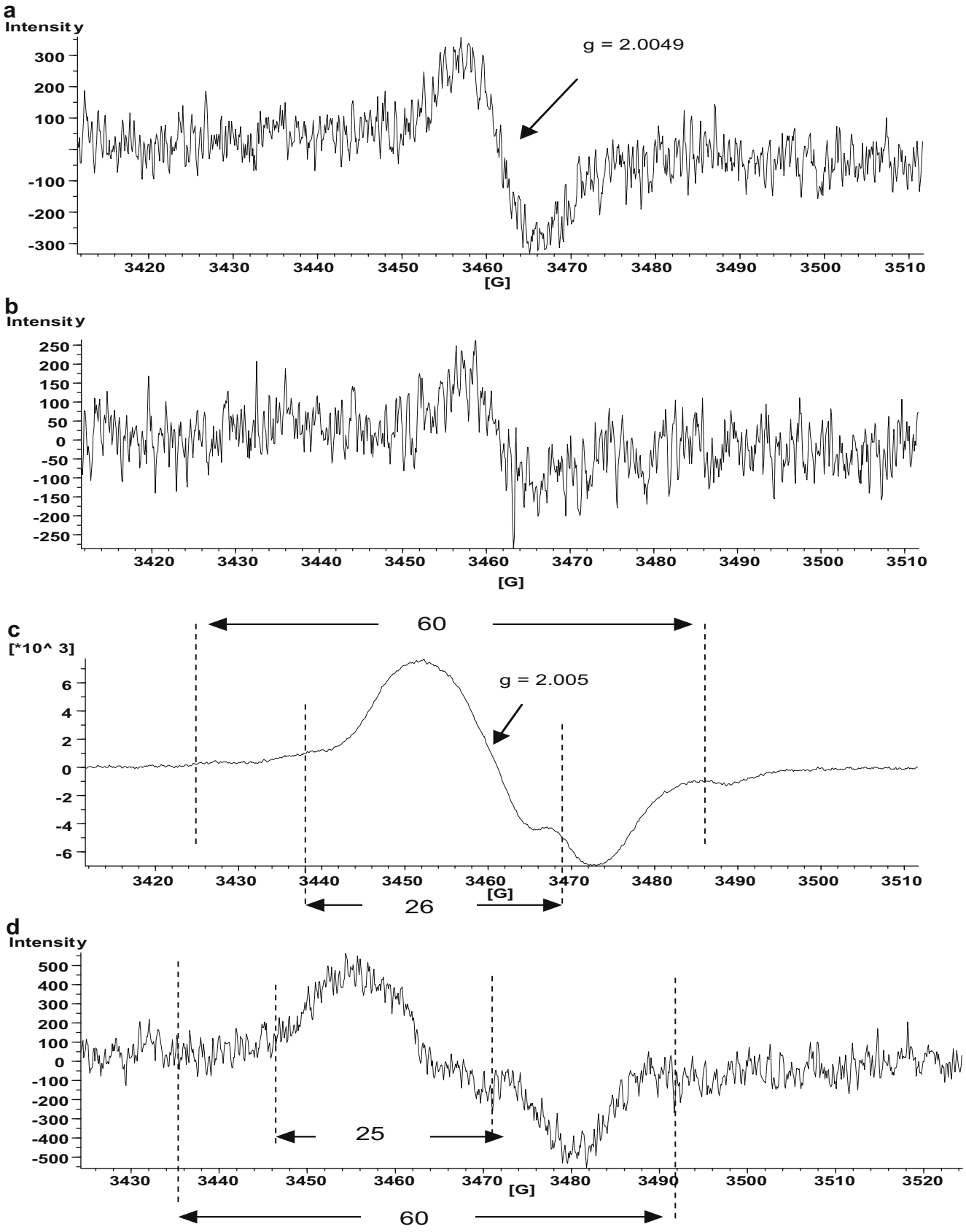

Fig. 1. EPR spectra of (a) non-irradiated (control), (b) heat treated at 100 °C, 1 h, (c) irradiated (1 kGy) rice samples and (d) EPR spectrum of irradiated pure starch.

commodities such as fresh strawberry (Desrosiers & McLaughlin, 1989; Dodd, Swallow, & Ley, 1985), grapes (Goodman, McPhail, & Duthie, 1989) and black pepper (Franco et al., 2004). The *g-value* obtained for non-irradiated rice sample compares well with those

Author's personal copy

reported in literature (Marchioni, Horvatovich, Charon, & Kuntz, 2005; Yordanov & Pachova, 2006). The origin of these free radicals responsible for the EPR signal is not clear. Several reports have suggested these free radicals to be those of semi-quinones produced by the oxidation of plant polyphenolics (Scewartz, Bolton, & Brog, 1972) or lignin (Maloney, Tabner, & Tabner, 1992; Tabner & Tabner, 1994).

In order to validate a method for identifying irradiation, free radicals produced by other processing techniques such as heating (thermolysis) must be distinguished from those produced by irradiation. Fig. 1b shows the EPR signal of the rice sample subjected to thermal treatment at 100 °C for 1 h. The heat energy did not induce any specific change in the EPR spectrum. However, the intensity of the singlet (g = 2.0049) was observed to reduce by about 20%.

Fig. 1c shows complex spectrum immediately after irradiation (1 kGy) of rice samples with an increase in signal intensity of the existing weak singlet (g = 2.005). Similar observations were also reported by Raffi et al. (1988), where the intense signal was noticed in the spectrum of irradiated spices. Irradiation was explained to be responsible for the relatively high intensity increase. As depicted in spectrum c, the exposure to gamma irradiation leads to change in rice matrix, producing two new types of paramagnetic species. One pair of intense satellite lines at a distance of 60 G from each other and the other less intense pair of lines situated at a distance of 26 G from each other. The starch accounts for 95% of the dry matter in milled rice grain (Martin & Fitzgerald, 2002). In order to characterise this radiation specific signal, EPR spectrum of pure starch sample irradiated with 1 kGy dose of gamma radiation was

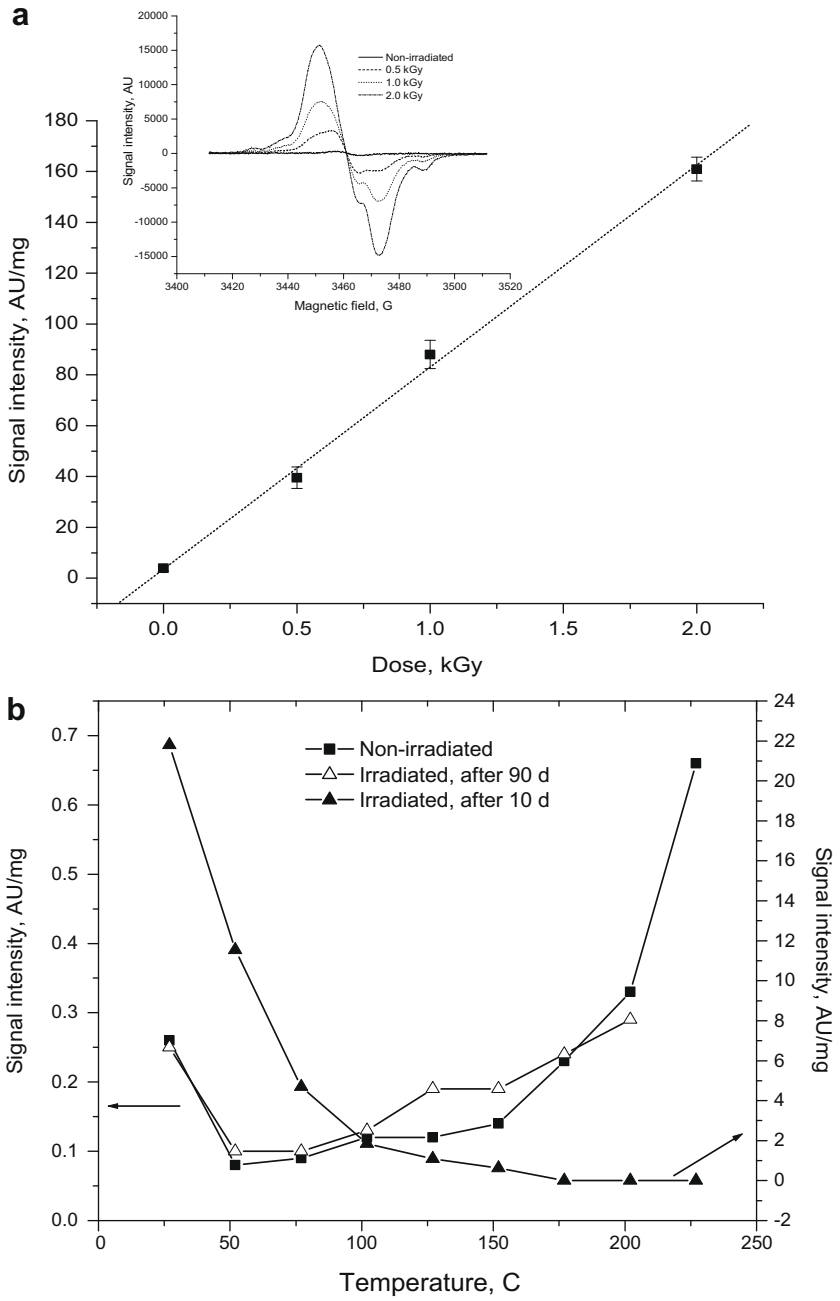

Fig. 2. (a) Response of the radiation induced signal intensity of the central line (g = 2.005) with increasing radiation dose and inset figure depicts the superposed EPR spectra of increasing radiation doses and (b) thermal behaviour of the central line of EPR spectrum for non-irradiated (control), irradiated (after 10 and 90 days) rice samples.

Author's personal copy

investigated as depicted in Fig. 1d. Irradiated starch exhibited similar signals as that of irradiated rice. This 'sugar-like' spectrum, originated from the radiation treatment of polysaccharides is considered to be an unambiguous evidence of the radiation treatment of the sample under investigation and recommended for the detection of irradiated foods in EN 13708 standards. The same has been validated for irradiated skin of raisins and figures containing considerable amount of polysaccharides in the form of sugar (EN 13708, 2001). These radiation specific signals observed in the rice matrix were not particularly stable and disappeared after 3–4 days with considerable decrease in intensity of the central singlet ($g = 2.005$) to a level that was similar to that of non-irradiated specimen. The instability in signal intensity means that the detection of irradiated rice by EPR spectroscopy is limited.

The effect of increasing radiation dose from 0.5 to 2.0 kGy on the spectra of rice samples was studied. The relative intensity of the central line was observed to be significantly related to the radiation dose as shown in Fig. 2a. The measurement was performed 2 days after irradiation. The dotted line represents a linear fit, $Y = aD + b$ with $a = 79.5$, $b = 3.5$ and each point representing the mean value of four samples.

3.2. Characterisations of non-irradiated and irradiated rice by thermal behaviour

The small life time of the radiation induced signals such as cellulose and 'sugar-like' strongly limits the applicability of the EPR analysis to detect irradiated food. This is the case with rice samples under investigation where the procedure based on EPR sugar-like signal (EN 13708, 2001) cannot be used beyond 2–3 days of radiation treatment. Therefore, alternative methods based on EPR are desirable. Thermal behaviour of the EPR signal was investigated in order to identify the irradiated rice samples from natural samples. Non-irradiated and irradiated samples were subjected to in situ heating from 27 to 275 °C. Fig. 2b shows the thermal behaviour of the non-irradiated and irradiated rice samples after a storage period of 10 and 90 days. The intensity of the central singlet of the irradiated rice after 10 days of storage exhibited a monotonous

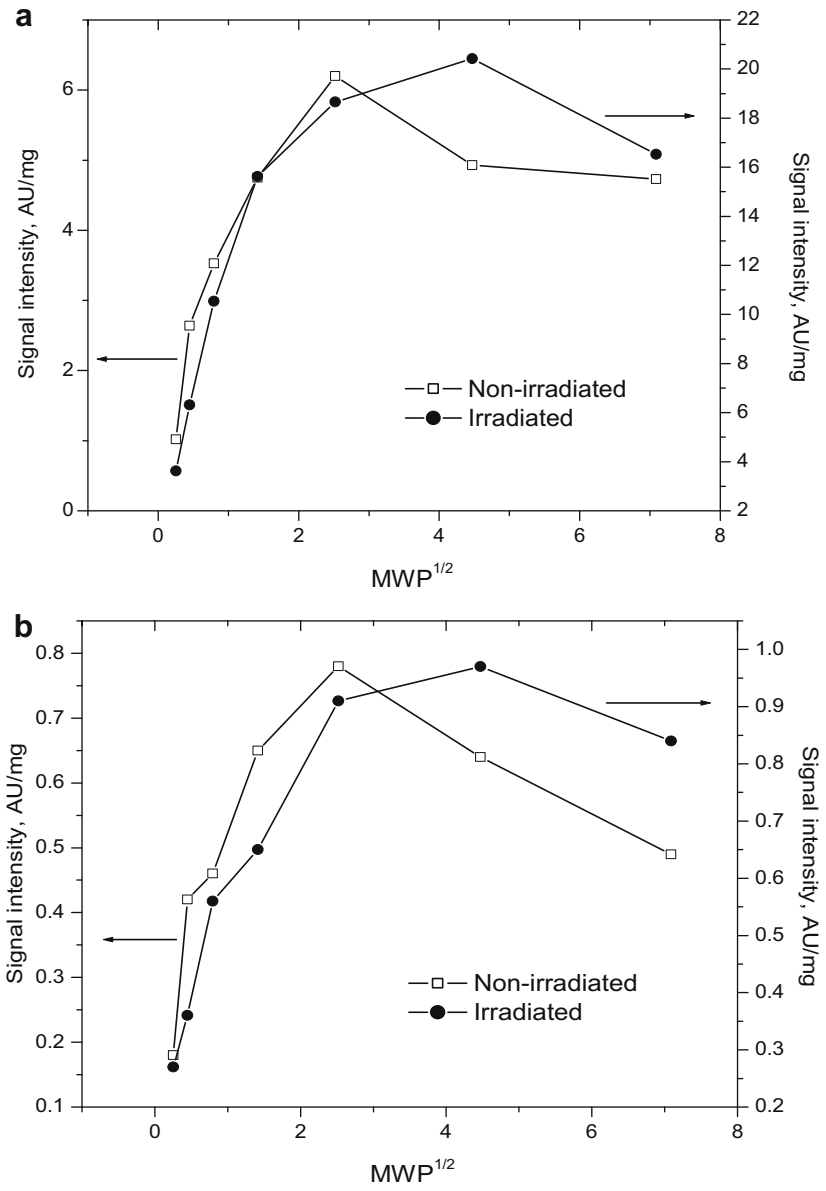

Fig. 3. Relaxation behaviour of main line of non-irradiated (control) and irradiated (1 kGy) rice sample (a) 10 days after irradiation and (b) 90 days after irradiation.

Author's personal copy

decrease in signal intensity up to 125 °C followed by almost unchanged behaviour up to 275 °C. Whereas, 90 days stored samples, both non-irradiated and irradiated (90 days) showed sharp fall in intensity of the central singlet up to 50 °C followed by slow increase up to 150 °C. However, temperature increases beyond 150 °C lead to an increase in signal intensities in both the cases. This could probably be due to the decomposition of the samples and formation of new thermally induced radicals. A decline of EPR signal of irradiated allspice sample has recently been reported by Polovka, Brezova, and Simko (2007). Yordanov and Gancheva (2000) proposed that EPR analysis of the central peak of spices that had undergone thermal treatment before and relatively long time after irradiation could be a tool for detection of irradiation. But, the present investigation revealed that a complete thermal behaviour of the singlet signal of rice samples can give a clue of radiation processing only after a storage period of 10 days. The thermal behaviours of the singlet of irradiated and non-irradiated rice samples after a long period of storage exhibited similar characteristics making the identification of irradiated rice sample difficult.

3.3. Characterisations of non-irradiated and irradiated rice by EPR saturation

The electron relaxation behaviours of radicals in the rice were studied. We varied the microwave field strength from 0.063 to 50 mW to obtain progressive saturation behaviour (PSB). The effect of saturation is manifested by continuous non-linear increase of EPR signal intensity with $P_{MW}^{\frac{1}{2}}$, reaching a maximum followed by a decrease with the simultaneous increase of EPR line width. Fig. 3a shows the PSB of the central line of non-irradiated and irradiated (1 kGy) samples 10 days after radiation treatment. For the radicals of non-irradiated rice sample a comparatively faster saturation at microwave power around 6 mW followed by a decrease in signal intensity in a monotonic fashion was observed. This saturation behaviour revealed the characteristics of organic radicals with large relaxation time. Whereas, the radicals of irradiated rice sample exhibited saturation at microwave power at around 20 mW. As depicted in Fig. 3b, even after a storage period of 90 days, the relaxation behaviour of non-irradiated rice sample exhibited early saturation of central singlet in comparison with the irradiated sample, similar to their behaviours noticed 10 days after radiation treatment. The EPR detection of irradiated dry food using microwave saturation has been proposed by Yordanov et al. (2006). In this method curves of saturation of non-irradiated and irradiated plants vs. $P_{MW}^{\frac{1}{2}}$ were studied and non-irradiated samples showed saturation at microwave power higher than 15 mW, whereas, irradiated sample exhibited early saturation at microwave power of around 8 mW. But, in the present study, non-irradiated rice samples exhibited early saturation even after a storage period of 90 days and revealed a significant difference in saturation behaviour from irradiated rice samples. As the EPR signals of cellulose or 'sugar-like' signals required by the European Standards were not visible in rice samples after prolonged storage, the application of Protocol EN 1787 or EN 13708 was not possible. However, faster EPR saturation of natural radicals in non-irradiated rice in comparison with the radiation induced radicals could be a tool to identify irradiated rice.

3.4. Kinetic study of the EPR singlet

Different factors, including humidity, temperature, light intensity, exposure to air and structure of the food matrix influence the behaviour of the induced radicals during storage of the sample

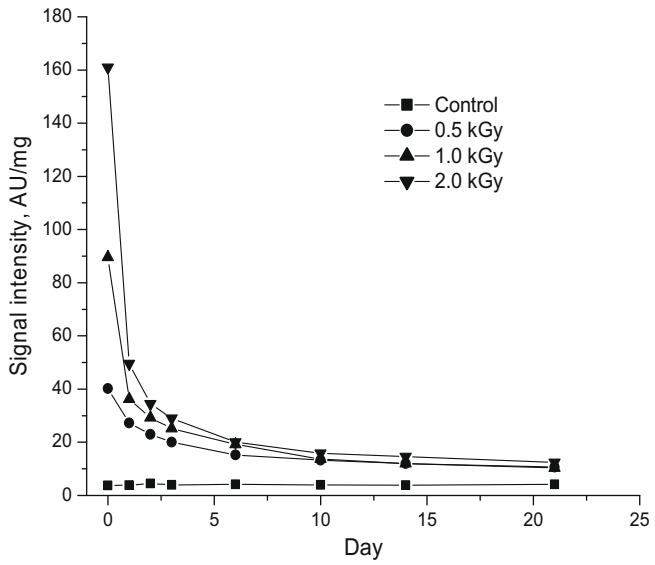

Fig. 4. Kinetics of the central line of the EPR signal of non-irradiated (control) and irradiated rice samples

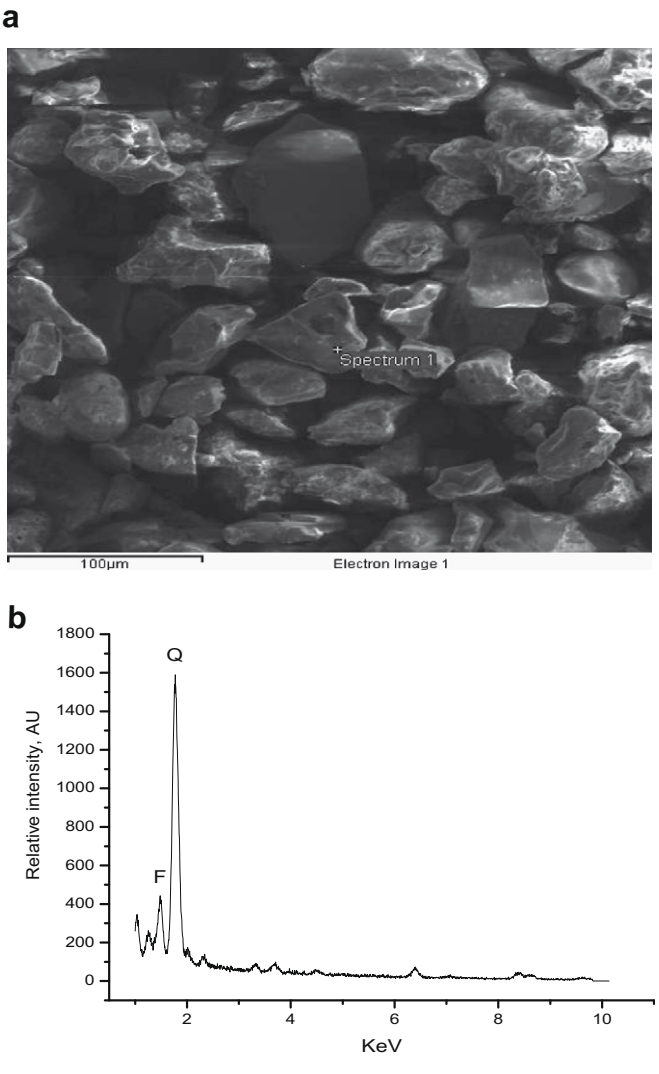

Fig. 5. (a) Scanning electron microscopy (SEM) image and (b) energy dispersive X-ray (EDX) spectrum of the poly-minerals extracted from rice. Feldspar: F and Quartz: Q.

Author's personal copy

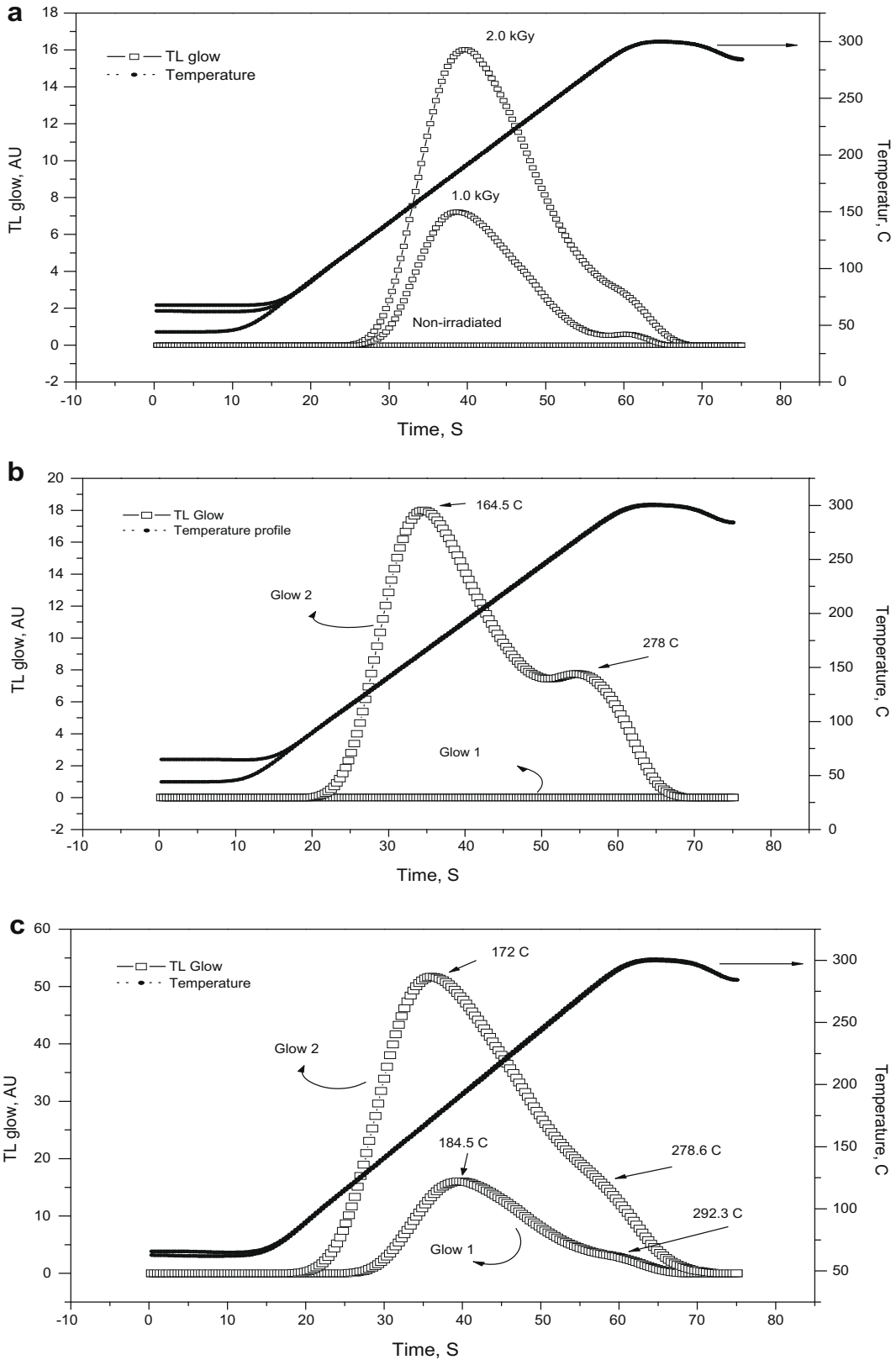

Fig. 6. (a) TL glows of isolated minerals from non-irradiated (control) and irradiated rice, (b) glow 1 and glow 2 of non-irradiated (control) sample and (c) glow 1 and glow 2 of irradiated sample.

before and after irradiation and thereby, restrict the time interval after irradiation during which detection is possible. The fading kinetics of the radiation induced radicals give information on the time interval after which identification of the irradiated samples is possible. Marked decreases in the concentration of free radicals in irradiated foods with time have been reported by many authors (Delincee, 1998; Raffi et al., 2000; Yordanov & Gancheva, 2000). In order to avoid these variations all the samples were kept inside the

Author's personal copy

EPR measurement tube under normal laboratory condition. Kinetics of non-irradiated and irradiated samples was monitored up to 12 weeks after radiation treatment. The radiation induced paramagnetic species identified as starch radical was observed to be stable up to 48–72 h after irradiation in the matrix of rice. Therefore, application of EN 1787 and EN 13708 Standards were not possible as a method of detection. Fig. 4 shows the fading characteristics of non-irradiated and irradiated rice samples throughout the storage period of 90 days. The results can be well fitted by a bi-exponential decay described by the following:

$$y = y_0 + A_1 \exp(-t/T_1) + A_2 \exp(-t/T_2)$$

where y represents the EPR signal intensity of the central line. Typical parameter values of the curve for the sample treated with 1 kGy radiation dose obtained with a non-linear least squares fitting procedure were $y_0 = 10.35$, $A_1 = 38.5$, T_1(days) = 3, $A_2 = 19.25$ and T_2 (days) = 15.

3.5. Thermoluminescence studies

TL method is applicable for the detection of irradiated foods, from which silicate minerals can be isolated (EN 1788, 2001). Therefore, investigation on the composition of the isolated minerals from the rice sample was of paramount importance to asses the possibility of employing TL method for the identification of the irradiated rice sample. In view of this, the composition of the separated poly-minerals from the rice sample was studied using scanning electron microscopy (SEM) and energy dispersive X-ray spectrometer (EDX) analysis. The results of these qualitative studies were interesting to examine the relative abundance of poly-minerals. Fig. 5a shows the SEM image of the extracted poly-minerals from the rice sample revealing the morphology. Fig. 5b shows the EDX spectrum which was mainly composed of quartz (SiO_2) and K-feldspars ($KAlSi_3O_8^-$) with a higher abundance of quartz (about 59.6%) than K-feldspars (20.7%). Apart from quartz and feldspar, traces of FeO (4.0%), Na_2O (4.1%), CaO (11.1%) were also identified. Similar patterns of mineral composition by X-ray diffraction (XRD) have been reported on herbs and spices such as oregano, mint and sage (Calderon et al., 1995), paprika (Correcher, Muniz, & Gomez-Ros, 1998), potato (Kwon, Jaeyoung, & Chung, 2002). TL response after radiation treatments is mainly responsible for quartz and feldspar component of the poly-minerals isolated from the food samples (Autio & Pinnoja, 1990).

Fig. 6a shows the TL intensities of glow curves for separated poly-minerals from the non-irradiated and irradiated rice samples 10 days after radiation treatment. In case of irradiated sample the glow curve was characterised by a low temperature peak at about 184 ± 4 °C and a high temperature peak at about 282 ± 5 °C. The position of glow peak for non-irradiated sample through all temperature ranges was not clear. However, low level natural radioactivity exhibited TL signal because of deep traps around 295 °C. The yield of the poly-minerals on each discs were in the range of 0.5–0.6 mg. The areas of glow curves for irradiated samples were 190–300 times more than the area from the non-irradiated samples. Higher values of TL glow (glow 1) in irradiated samples have been reported in previous studies on spices and herbs (Sanderson et al., 1996); chestnut (Chung et al., 2004). Glow peak temperatures at about 207 °C for irradiated anchovy and 192 °C for irradiated chestnut have been reported (Chung et al., 2004). Therefore, discrimination between irradiated and non-irradiated rice samples was possible on the basis of the shape of the first glow curve from the separated poly-minerals. Normalisation of results by re-irradiation with a dose of 1 kGy enhanced the reliability of the detection results. Fig. 6b and c shows the comparison of re-irradiation glow curves (glow 2) with respect to first glow curves (glow 1) for non-irradiated and irradiated samples respectively. The re-irradiation glow curves (glow 2) were characterised by a glow peak at 168 ± 4 °C and a higher temperature shoulder at 278 °C. The differences of the peak temperatures observed between glows 1 and 2 attributed to the time difference elapsed between irradiation and analysis because low energy trapped electrons were released during storage. Glow 2 was recorded 1 day after the normalisation doses whereas; samples were stored for several days after irradiation prior to the analysis of glow 1. The ratio of areas for first glow curve to second glow curve (glow 1/glow 2) determined for non-irradiated samples was 0.002 ± 0.023, while for irradiated sample 0.69 ± 0.085. Higher values of ratio of areas for glow 1/glow 2 in irradiated rice samples are in good agreement with the European Standard EN, 1788, 1997. TL glow of the irradiated samples were recorded after 65 days of storage in dark with normal laboratory condition and around 20% fading in TL glow intensity was observed with clear discrimination from the TL glow of the non-irradiated samples. Therefore, it was possible to discriminate clearly between irradiated and non-irradiated rice samples by the shape of the first TL glow and comparing the TL ratios (glow 1/glow 2).

4. Conclusions

Identification of gamma-irradiated Basmati rice was carried out by investigating free radicals using electron paramagnetic resonance (EPR) spectroscopy, and studying Thermoluminescence (TL) properties of the isolated poly-minerals. In case of EPR spectroscopy, a weak singlet was found in the commercially available rice sample. However, a short lived, complex spectrum was observed after radiation treatment attributed to radicals originating from starch. The change in free radical concentration showed a proportional increase with irradiation dose. By increasing the microwave power, the line shape of the EPR spectra altered and in saturation curves, it was possible to identify the irradiated and non-irradiated samples. However, thermal behaviour of the EPR signals was unable to identify irradiated rice samples. TL investigation of the poly-minerals isolated from the rice samples were carried out. SEM/EDX analysis revealed the maximum abundance of quartz (SiO_2) in the isolated minerals. TL glow curve structure of irradiated samples showed about 300 times increase in intensity than that of non-irradiated samples. Normalisation dose and ratio of the first and second glows (glow 1/glow 2) confirmed the identification of irradiated samples even after a long period of storage.

Identification of radiation treatment after storage of the sample under investigation was not possible by application of any of the European Standards (EN 13708; EN 1787) for EPR spectroscopy. TL technique provided promising results even after a long period of storage but, involved tedious sample preparation protocol (EN 1788, 2001; Carmichael & Sanderson, 2000). However, the microwave saturation characteristics of EPR signals of irradiated and non-irradiated rice can be a very useful tool to identify the irradiated sample from non-irradiated one even after prolonged period of storage.

References

ASTM Standard, E 1026. Standard practice for using fricke reference Standard Dosimetry System.

Autio, T., & Pinnoja, S. (1990). Identification of irradiated foods by the thermoluminescence of mineral contamination. *Zeitschrift fur Lebensmittel-Untersuchung und – Forschung, 191*, 177–180.

Calderon, T., Correcher, V., Millan, A., Beneitez, P., Rendell, H. M., Larrson, M., et al. (1995). New data on thermoluminescence of inorganic dust from herbs and spices. *Journal of Physics D: Applied Physics, 28*, 415–423.

Carmichael, L. A., & Sanderson, D. C. W. (2000). The use of acid hydrolysis for extracting minerals from shellfish for thermoluminescence detection of irradiation. *Food Chemistry, 68*, 233–238.

Chung, H. W., Delincee, H., Han, S., Hong, J., Kim, H., Kim, M., et al. (2004). Trials to identify irradiated chestnut (*Castanea bungena*) with different analytical techniques. *Radiation Physics and Chemistry, 71*, 179–182.

Author's personal copy

Correcher, V., Muniz, J. L., & Gomez-Ros, J. M. (1998). Dose dependence and fading effect of the thermoluminescence signal in ν-irradiated paprika. *Journal of Science and Food Agriculture, 76*, 149–158.

Delincee, H. (1998). Detection of food treated with ionizing radiation. *Trends in Food Science and Technology, 9*, 73–82.

Desrosiers, M. F., & McLaughlin, W. L. (1989). Examination of gamma irradiated fruits and vegetables by electron spin resonance spectroscopy. *Radiation Physics and Chemistry, 34*, 895–898.

Dodd, N. J. F., Swallow, A. J., & Ley, F. J. (1985). Use of ESR to identify irradiated food. *Radiation Physics and Chemistry, 26*, 451.

European Standard EN 1786 (1997). Foodstuffs-detection of irradiated food containing bone: Analysis by electron paramagnetic resonance. Brussels, Belgium: European Committee for Standardization.

European Standard EN 1788 (2001). Foodstuffs-detection of irradiated food from which silicate minerals can be isolated: Method by thermoluminescence. Brussels, Belgium: European Committee for Standardization.

European Standard EN 1787 (2000). Foodstuffs-detection of irradiated food containing cellulose: Analysis by EPR. Brussels, Belgium: European Committee for Standardization.

European Standard EN 13708 (2001). Foodstuffs-detection of irradiated food containing crystalline sugar: Analysis by EPR. Brussels, Belgium: European Committee for Standardization.

Franco, R. W. A., Martin-Neto, L., Kato, M. S. A., Furlan, G. R., Walder, J. M. M., & Colnago, L. A. (2004). Identification of irradiation treatment in black pepper by electron paramagnetic resonance. *International Journal of Food Science and Technology, 39*, 395–401.

Goodman, B. A., McPhail, D. B., & Duthie, D. M. L. (1989). Electron spin resonance spectroscopy of some irradiated foodstuff. *Journal of Science and Food Agriculture, 47*, 101.

Kwon, J. H., Jaeyoung, J., & Chung, H. (2002). Thermoluminescence characteristics of minerals from irradiated potatoes of different origin of production. *Radiation Physics and Chemistry, 63*, 415–418.

Maloney, D. R., Tabner, B. J., & Tabner, V. A. (1992). An electron spin resonance study of gamma-irradiated fruits. *Radiation Physics and Chemistry, 39*, 309–314.

Marchioni, E., Horvatovich, P., Charon, H., & Kuntz, F. (2005). Detection of irradiated ingredients included in low quantity in non-irradiated food matrix. 1. Extraction and ESR analysis of bones from mechanically recovered poultry meat. *Journal of Agriculture and Food Chemistry, 53*, 3769–3773.

Martin, M., & Fitzgerald, M. A. (2002). Proteins in rice grains influence cooking properties. *Journal of Cereal Science, 36*, 285–294.

Polovka, M., Brezova, V., & Simko, P. (2007). EPR spectroscopy: A tool to characterize gamma irradiated foods. *Journal of Food and Nutrition Research, 46*, 75–83.

Raffi, J. J., Agnel, J. L., Buscarlet, L. A., & Martin, C. C. (1988). Electron spin resonance identification of irradiated strawberries. *Journal of Chemical Society, Faraday Transactions, 84*(10), 3359–3362.

Raffi, J., Yordanov, N. D., Chabane, S., Douifi, L., Gancheva, V., & Ivanova, S. (2000). Detection of irradiated aromatic herbs and spices by electron paramagnetic resonance and thermoluminescence. *Spectrochimica Acta, 56A*, 409–416.

Sanderson, D. C. W., Carmichael, L. A., Spencer, J. Q., & Naylor, J. (1996). Luminescence detection of shell fish. In C. H. McMurray (Ed.), *Detection methods of irradiated foods* (pp. 139–148). Cambridge: The Royal Society of Chemistry.

Scewartz, H. M., Bolton, J. R., & Brog, D. C. (Eds.). (1972). *Biological applications of electron spin resonance*. New York: Wiley.

Sudha Rao, V., Gholap, A. S., Adhikari, H., & Madhusudanan, N. P. (2000). Disinfestation of Basmati rice by the use of γ-radiation. *International Journal of food Science and Technology, 35*, 533–540.

Tabner, B. J., & Tabner, V. A. (1994). Electron spin resonance spectra of gamma-irradiated citrus fruits skin, skin components and stalks. *International Journal of food Science and Ttechnology, 29*, 143–152.

Yordanov, N. D., & Pachova, Z. (2006). Gamma-irradiated dry fruits an example of wide variety of long-time dependent EPR spectra. *Spectrochimica Acta, 63*, 891–895.

Yordanov, N. D., Aleksieva, K., & Mansour, I. (2005). Improvement of the EPR detection of irradiated dry plants using microwave saturation and thermal treatment. *Radiation Physics and Chemistry, 73*, 55–60.

Yordanov, N. D., & Gancheva, V. (2000). A new approach for the extension of the identification period of irradiated cellulose containing foodstuffs by EPR spectroscopy. *Applied Radiation and Isotopes, 52*, 195–198.

JOURNAL OF AGRICULTURAL AND FOOD CHEMISTRY

Identification of Irradiated Cashew Nut by Electron Paramagnetic Resonance Spectroscopy

BHASKAR SANYAL,*,† M. G. SAJILATA,‡ SUCHANDRA CHATTERJEE,† REKHA S. SINGHAL,‡ PRASAD S. VARIYAR,† M. Y. KAMAT,‡ AND ARUN SHARMA†

Food Technology Division, Bhabha Atomic Research Centre, Mumbai- 400 085, India, and Food & Fermentation Technology Division, University Institute of Chemical Technology, Mumbai- 400 019, India

Cashew nut samples were irradiated at γ-radiation doses of 0.25, 0.5, 0.75, and 1 kGy, the permissible dose range for insect disinfestation of food commodities. A weak and short-lived triplet ($g = 2.004$ and hfcc = 30 G) along with an anisotropic signal ($g_{\perp} = 2.0069$ and $g_{||} = 2.000$) were produced immediately after irradiation. These signals were assigned to that of cellulose and CO_2^- radicals. However, the irradiated samples showed a dose-dependent increase of the central line ($g = 2.0045 \pm 0.0002$). The nature of the free radicals formed during conventional processing such as thermal treatment was investigated and showed an increase in intensity of the central line ($g = 2.0045$) similar to that of irradiation. Characteristics of the free radicals were studied by their relaxation and thermal behaviors. The present work explores the possibility to identify irradiated cashew nuts from nonirradiated ones by the thermal behaviors of the radicals beyond the period, when the characteristic electron paramagnetic resonance spectral lines of the cellulose free radicals have essentially disappeared. In addition, this study for the first time reports that relaxation behavior of the radicals could be a useful tool to distinguish between roasted and irradiated cashew nuts.

KEYWORDS: Food irradiation; detection of irradiated foods; EPR; cashew

INTRODUCTION

The cashew nut of the plant, *Anacardium occidentale*, is an important cash crop for many countries. It has high nutritive value; however, climatic conditions and variety govern quality (*1*). The kernel contains approximately 21% protein, 46% fat, and 25% carbohydrates. Cashew nut is an important export commodity for India, contributing about 7% to the national treasury. Insect infestation during storage is a major problem of cashew nut, resulting in economic losses. Irradiation is increasingly being recognized as an effective technology to reduce postharvest losses and improve quality. Cashew nuts, irradiated at 0.25 kGy and higher doses and stored under ambient conditions, showed no insect infestation during storage, while the control nonirradiated samples were spoiled due to infestation (*2*).

To facilitate trade in irradiated foods, regulatory authorities are interested in having a reliable method to detect irradiated foods and consequently check compliance with the labeling requirements. Methods to distinguish between irradiated and nonirradiated food stuffs are useful to both enforcement agencies and consumers to increase confidence in radiation processing technology.

Several detection methods have been developed for the identification of irradiated foods (*3*). Among them, electron paramagnetic resonance (EPR) spectroscopy is a leading technique. For use in detection, the radiation-induced EPR signals in food must fulfill several requirements; that is, they must be stable or fairly stable during the usual storage period of the foodstuff and must be clearly distinguishable from the background signals of the nonirradiated sample, even after a long storage period (*4*). Three European standards for the detection of irradiated food by EPR spectroscopy have been released by the European Committee of Normalization (CEN) and adopted by Codex Alimenterius Commission as Codex Standards. These pertain to food containing bone (*5*), crystalline sugar (*6*), and cellulose (*7*). This last standard has been validated for pistachio shells, paprika powder, and fresh strawberries (*8*−*11*). EPR is a user friendly technique, as the measurement is easy and the sample under test does not require any preparation, and there is increasing interest in extending the EPR methodology to other types of food containing cellulose. The main problem lies in the instability of the relatively weak satellite lines of cellulose. In some cases, the satellite lines are not detectable immediately after irradiation. Recently, to extend the applicabil-

* To whom correspondence should be addressed. E-mail: bhaskarsanyal@rediffmail.com.
† Bhabha Atomic Research Centre.
‡ University Institute of Chemical Technology.

10.1021/jf8016089 CCC: $40.75 © 2008 American Chemical Society
Published on Web 09/04/2008

ity of EPR for the identification of irradiated food, a new approach, based on thermal treatment and EPR saturation, has been used when the satellite lines due to cellulose have presumably disappeared due to long periods of time elapsed after treatment (*12, 13*).

In the present work, a detailed study of the radical species produced by γ-irradiation of cashew has been carried out. In addition, the EPR saturation and thermal behaviors to distinguish between treated and untreated samples by EPR spectroscopy have been examined.

EXPERIMENTAL PROCEDURES

Materials. Cashew nuts were procured from a local market. The standard 2,2-diphenyl-1-picrylhydrazyl (DPPH) with $g = 2.0032$ was purchased from Sigma Chem. Co. (United States).

Irradiation Conditions. Irradiation was carried out at ambient temperature (27 ± 2 °C) using a cobalt-60 irradiator (GC-5000, BRIT, Mumbai, dose rate of 6.2 kGy/h) at BARC, Mumbai. The doses were applied in the range of 0.25−1 kGy, recommended for insect disinfestation. Dosimetry was performed using an aqueous Fricke dosimeter (*14*). The irradiated, roasted, and nonirradiated cashew nut samples were stored inside EPR quartz tubes in the normal laboratory conditions at ambient temperature (27 ± 2 °C) until further use.

EPR Spectroscopy. Cashew nut kernels were cut into fine pieces and transferred to 2 mm quartz capillary tubes and packed with gentle tapping to a length of 25.4 mm (active length), and the weight of the sample was determined. The results for the signal intensity of samples were normalized to the packing weight. EPR measurements were performed using a Bruker EMX spectrometer (Bruker, Gemany). All of the spectra were recorded at ambient temperature of the EPR laboratory (27 °C).

Operating conditions of the EPR spectrometer were as follows: center field, 3480 G; scan range, 200 G; microwave power, 0.253 mW; microwave frequency, 9.66 GHz; modulation frequency, 100 kHz; receiver gain, 4×10^4; and time constant, 20.48 s. The position of the irradiation-induced EPR signal was compared with that of the standard DPPH with $g = 2.0032$ (Sigma Chem. Co.).

Progressive Saturation and Thermal Behavior of Radicals. To determine the electron relaxation behavior of radicals in cashew nut samples, the microwave field strength was varied between 0.06 and 50 mW to obtain progressive saturation behavior (PSB). The field modulation was operated at 100 kHz. All of the EPR measurements were done at ambient temperature. The spin concentration was determined using DPPH as a standard sample.

In situ heat treatment from room temperature to 187 °C in a step of 20 °C was conducted using nitrogen gas for heating the samples within the EPR spectrometer using BVT-3000 accessory of Bruker (Germany). To study the induced radicals by thermolysis, heat treatment before and after irradiation of the samples was carried out at 100 °C for 1 h and roasting at 180 °C using a laboratory oven. Three replications were made for the evaluation of each sample.

RESULTS AND DISCUSSION

Effect of γ-Irradiation. Figure 1, spectrum **a**, shows the EPR signal of cashew nut samples before irradiation exhibiting a weak and broad singlet characterized by $g = 2.0056 \pm 0.0004$ centered around 3475 G. This g value obtained compares well with those reported in literature (*13, 15*). The origin of these free radicals responsible for the EPR signal is not clear. Several reports have suggested these free radicals to be those of semiquinones produced by the oxidation of plant polyphenolics (*16*) or lignin (*17, 18*). To characterize the natural signal, EPR spectra of irradiated (1 kGy) pure quinone (hydroquinone) were recorded under a similar experimental setup. A weak singlet was observed with $g = 2.0032$ and was different from the signal observed in nonirradiated sample. This suggests that, in cashew nut, where the lipid content is more than 40%, the origin of the singlet could possibly be due to the oxidation of fatty acids (*19*).

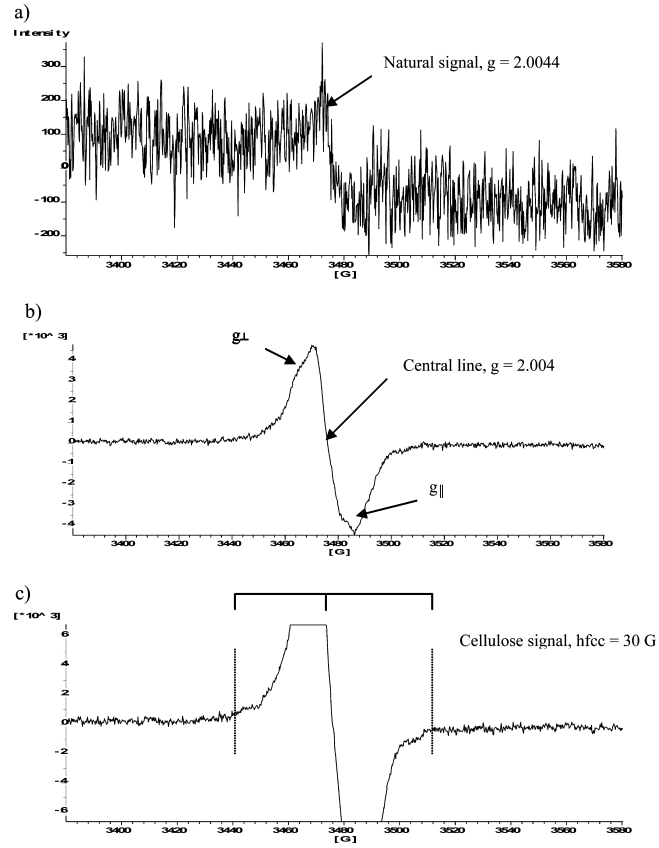

Figure 1. Ambient EPR spectra of cashew nut sample (**a**) before irradiation, (**b**) 1 day after irradiation (1 kGy), and (**c**) irradiated (1 kGy) and magnified.

Figure 1, spectrum **b**, shows a complex spectrum immediately after irradiation (1 kGy) of cashew samples with an increase in signal intensity of the existing weak singlet by a factor of 11. Similar observations were also reported by Raffi et al. (*15*), where the intense signal was noticed in the spectrum of irradiated spices. Irradiation was explained to be responsible for the relatively high intensity increase. The exposure to γ-irradiation leads to a change in the cashew matrix, producing two new types of paramagnetic species. One was identified as a very weak triplet signal probably because of crystalline cellulose (*20, 21*) superimposed on the natural singlet with a hyperfine coupling constant (hfcc) of 30 G (**Figure 1**, spectrum **c**). This signal is considered to be unambiguous evidence of the radiation treatment of sample under investigation and recommended for the detection of irradiated foods in EN 1787 standard (*7*). The same has been validated for pistachio shells by Raffi et al. (*9*). Another short-lived paramagnetic species with an axially symmetric spectrum (**Figure 1**, spectrum **b**) was characterized by an anisotropic g tensor ($g_\perp = 2.0069$ and $g_{||} = 2.0000$). This signal could possibly be of CO_2^- radical formed during the breakdown of fatty acid. DPPH with $g = 2.0032$ was used as a reference to calculate the g values of the radicals. The g values obtained compared well with those reported in the literature (*22, 23*). This component was not particularly stable and, after 2 days, had decreased in intensity to a level that was similar to that of nonirradiated specimen. The instability in signal intensity means detection of fat component by EPR spectroscopy is limited after irradiation.

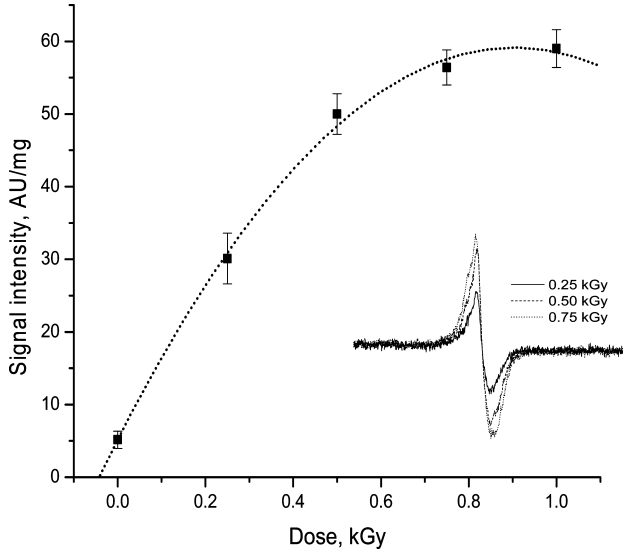

Figure 2. Response of the radiation-induced signal intensity of the central line ($g = 2.0044$) with increasing radiation dose.

The effects of increasing radiation dose from 0.25 to 1.0 kGy on the spectra of cashew samples were studied. The radiation-induced signal due to CO_2^- radical started developing at a minimum dose of 0.25 kGy, whereas the signal of cellulose radical was identified at 1.0 kGy dose. However, the relative intensity of the central line was observed to be significantly related to the radiation dose as shown in **Figure 2**. The measurement was performed 3 days after irradiation. The dotted line represents a second order polynomial curve $D = aD^2 + bD + c$ with $a = -66.19$, $b = 119.56$, and $c = 5.15$ and each point representing the mean value of three samples.

Effect of Thermal Treatment. Radiation-induced radicals formed from fat components of the cashew matrix are highly unstable. EPR spectra of irradiated and nonirradiated samples after storage showed similar patterns except for a significant enhancement in the natural signal intensity after irradiation. To validate a method for identifying irradiation, free radicals produced by other processing techniques such as heating (thermolysis) must be distinguished from those produced by irradiation. **Figure 3**, spectra **a**−**c** show the EPR spectra of cashew nut samples subjected to various thermal treatments before and immediately after heating. Only a weak singlet (**Figure 3**, spectrum **b**) similar to the natural signal was observed after thermal treatment of the whole sample at 100 °C for 1 h. Radicals originated due to thermolysis characterized by $g = 2.0045 \pm 0.0005$, centered around 3476 G. No satellite lines like cellulose and CO_2^- radicals were observed. The samples subjected to roasting at 180 °C showed increased signal intensity (**Figure 3**, spectrum **c**) similar to that of irradiated samples, making detection of radiation treatment of cashew difficult.

Characterizations of Nonirradiated, Irradiated, and Heat-Treated Cashew Nuts by EPR Saturation and Thermal Behavior. The applicability of the EPR analysis to detect irradiated food is strongly limited by the lifetime of the radiation-induced free radicals such as cellulose radicals. This is the case with cashew nut under investigation where the procedure based on EPR cellulose signal (*7*) cannot be used beyond 1 day of radiation treatment. Therefore, alternative methods proposed in the European Standard EN 1787 (*7*) and based on EPR are desirable. Characterization of the free radicals, naturally present, induced by radiolysis or by thermolysis was essential for the investigation to identify different techniques of processing. To determine the electron relaxation behavior of radicals in the

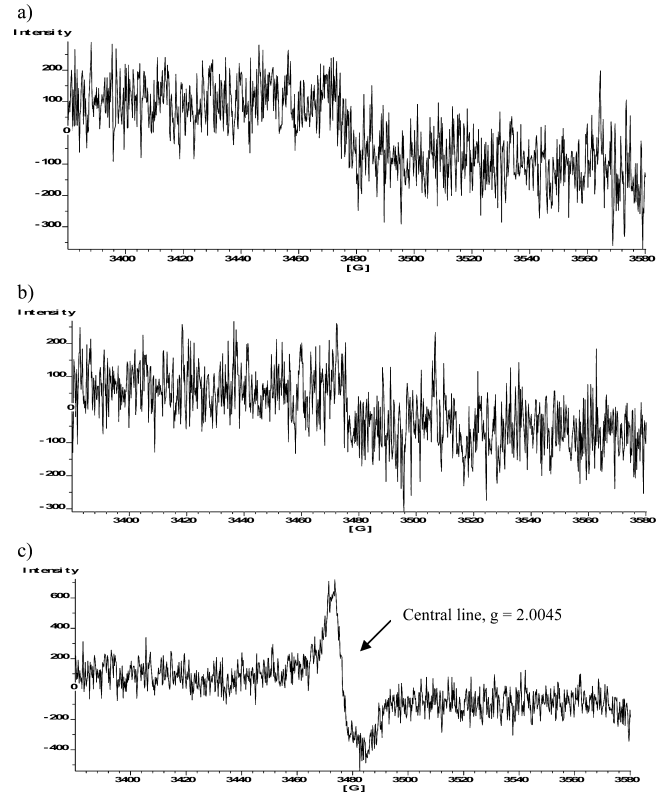

Figure 3. EPR spectra after 1 day of various thermal treatments (**a**) without thermal treatment, (**b**) subjected to 100 °C for 1 h, and (**c**) roasted at 180 °C.

cashew, we varied the microwave field strength from 0.063 to 50 mW to obtain PSB. The effect of saturation is manifested by a continuous nonlinear increase of EPR signal intensity with $P_{MW}^{1/2}$, reaching a maximum followed by a decrease with the simultaneous increase of EPR line width. **Figure 4a** shows the PSB of the central line of irradiated (1 kGy), roasted (180 °C), and nonirradiated samples 1 day after radiation and heat treatments. A comparatively faster saturation at microwave power around 6 mW followed by a decrease in signal intensity by monotonic fashion was observed for the radicals formed after roasting. This saturation behavior revealed the characteristics of organic radicals with large relaxation time. Improvement of the EPR detection of irradiated dry food using microwave saturation and thermal treatment has been proposed by Yordanov et al. (*12*). In this method, curves of saturation of nonirradiated and irradiated plants vs $P_{MW}^{1/2}$ were studied, and nonirradiated samples showed saturation at microwave power higher than 15 mW, whereas an irradiated sample exhibited early saturation at microwave power of around 8 mW. In the present study, no significant difference of saturation behaviors of nonirradiated and irradiated cashew nut was observed. The central line of the spectra for both nonirradiated and irradiated samples exhibited similar saturation at microwave power around 20 mW, revealing shorter relaxation time. As depicted in **Figure 4b**, the relaxation behaviors of nonirradiated, irradiated, and roasted samples, even after a storage period of 45 days, were almost similar to that of behavior noticed immediately after irradiation and heat treatment. Therefore, EPR analysis by the saturation behavior of the signals could not be used to distinguish irradiated cashew sample. However, faster EPR saturation of thermally induced radicals in comparison with the radiation-induced radicals could be a tool to distinguish between irradiated and roasted cashew.

To identify the irradiated cashew sample from natural and roasted samples, the thermal behavior of the EPR signal was

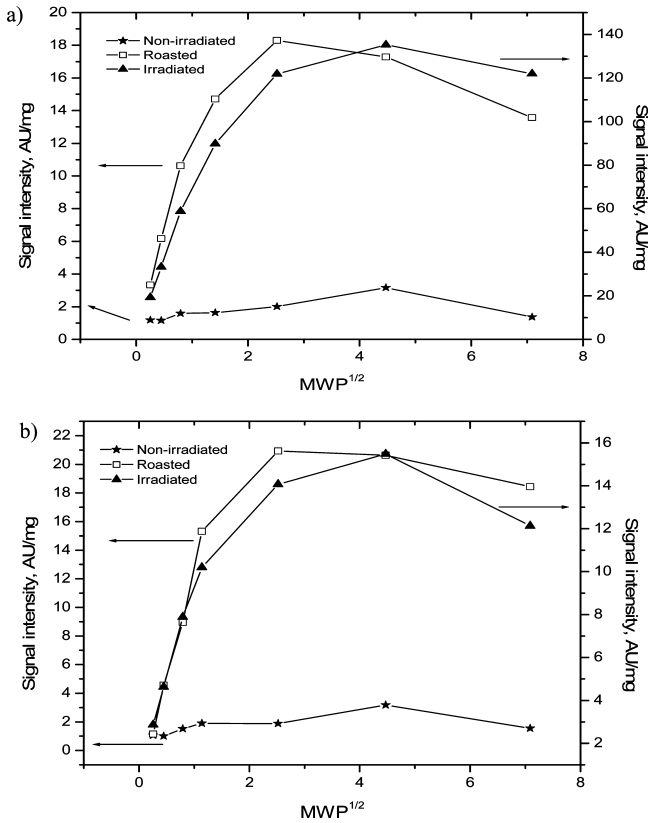

Figure 4. Relaxation behavior of main line of nonirradiated, irradiated (1 kGy), and roasted cashew (**a**) 1 day after irradiation and (**b**) after 45 days of storage.

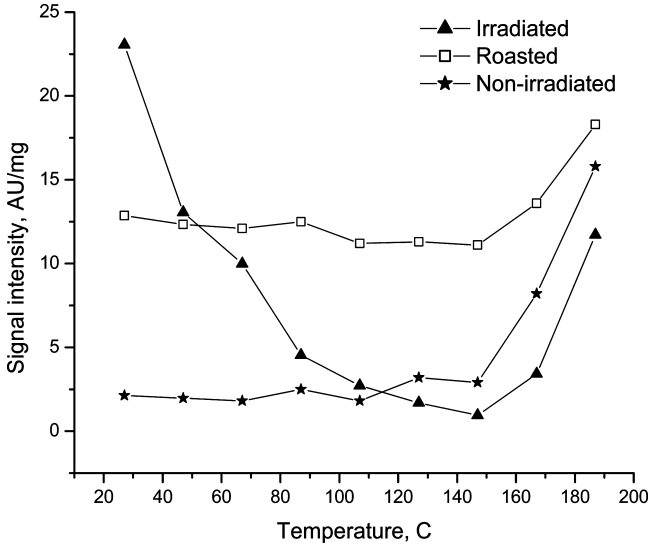

Figure 5. Thermal behavior of the central line of EPR spectrum for nonirradiated, irradiated (1 kGy), and roasted (180 °C) cashew nut samples.

investigated. Nonirradiated, irradiated, and roasted samples were subjected to in situ heating from 27 to 187 °C. As depicted in **Figure 5**, with the increase of temperature from 27 to 97 °C, signal intensities of the central lines of nonirradiated and roasted samples were observed to be almost unchanged, but that of irradiated samples showed a fast fall of about 50%. However, a temperature increase beyond 152 °C lead to an increase in signal intensities in all of the cases. This could probably be due to the decomposition of the samples and the formation of new thermally induced radicals. Polovka et al. (*24*) have recently

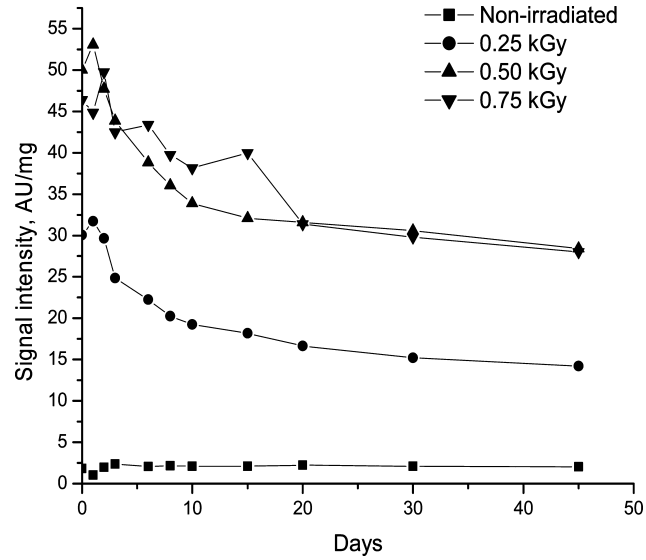

Figure 6. Kinetics of the central line of the EPR signal of nonirradiated and irradiated cashew nut samples.

investigated the thermal behavior of irradiated and nonirradiated spices. A decline of EPR signal of irradiated allspice sample was reported. Yordanov and Gancheva (*13*) proposed that EPR analysis of the central peak of spices that had undergone thermal treatment before and a relatively long time after irradiation could be a tool for detection of irradiation. To establish this method, thermal behaviors of the samples were investigated after a storage period of 6 weeks. Nonirradiated, roasted, and irradiated samples were subjected to thermal treatment of 100 °C for 1 h. Irradiated samples showed 39% reduction in signal intensity, whereas nonirradiated and roasted samples did not exhibit any significant change in signal intensity. Our results are well in agreement with the proposal of Yordanov and Gancheva (*13*). As the EPR signals of cellulose required by the European Standards were not visible in cashew samples after a long period of storage, the application of Protocol EN 1787 (*7*) was impossible. Therefore, the thermal behavior of the γ-induced EPR signal represented a valuable tool for the assessment of previous radiation treatment.

Kinetic Study. The fading kinetics of the radiation-induced radicals give information on the time interval after which identification of the irradiated samples is possible. Marked decreases in the concentration of free radicals in irradiated spices with time have been reported by many authors (*13, 15, 25*). Different factors, including humidity, temperature, light intensity, exposure to air, and structure of the food matrix influence the behavior of the induced radicals during storage of the sample before and after irradiation and, thereby, restrict the time interval after irradiation during which detection is possible. To avoid these variations, all of the samples were kept inside the EPR measurement tube in normal laboratory conditions. Kinetics of nonirradiated, irradiated, and roasted samples were monitored up to 6 weeks after radiation treatment. Both of the radiation-induced paramagnetic species identified as cellulose radicals and CO_2^- radical were observed to be stable up to 24−40 h after irradiation in the matrix of cashew nut. Therefore, application of EN 1787 Standard (*7*) was not possible as a method of detection. However, increased intensity of the central line of the irradiated samples was observed even after several days of irradiation with a clear distinction with respect to nonirradiated samples (**Figure 6**).

In conclusion, investigation of free radicals in γ-irradiated cashew nuts by EPR spectroscopy showed a proportional

increase in free radical concentration with an increase of irradiation dose. A weak singlet was found in the commercially available cashew nuts. However, two distinct but short-lived signals were identified as cellulose and CO_2^- radicals in irradiated sample. By increasing the microwave power, the line shape of EPR spectra altered, and from the saturation curves, it was possible to identify the irradiated and roasted samples. However, radicals present naturally were not distinguishable from the irradiated signal by the respective relaxation behavior. The thermal behavior of the radicals after storage clearly showed the distinction between naturally present and radiation-induced radicals. Identification of radiation treatment after storage of the sample under investigation was not possible by the application of protocol EN 1787 (*7*). However, irradiated cashew nut can be distinguished from nonirradiated samples after a long period of storage by the thermal behavior of the EPR signals. In addition, this report for the first time proposes a method to distinguish between irradiated and roasted sample by studying the relaxation characteristics of the induced radicals.

LITERATURE CITED

(1) Ohler, J. G. *Cashew*; Department of Agricultural Research, Royal Tropical Institute: Amsterdam, 1979.

(2) Bhattacharjee, P.; Singhal, R. S.; Gholap, A. S.; Variyar, P. S.; Bongirwar, D. R. Compositional profiles of γ-irradiated cashew nuts. *Food Chem.* **2003**, *80* (2), 151–157.

(3) Chung, H. W.; Delincee, H.; Han, S.; Hong, J.; Kim, H.; Byun, M.; Know, J. Trials to identify irradiated chestnut (*Castanea bungena*) with different analytical techniques. *Radiat. Phys. Chem.* **2004**, *71* (1−2), 181–184.

(4) Raffi, J. J.; Agnel, J. L.; Buscarlet, L. A.; Martin, C. C. Electron spin resonance identification of irradiated strawberries. *J. Chem. Soc. Faraday* **1988**, *84* (10), 3359–3362.

(5) Detection of Irradiated Food Containing Bone: Analysis by Electron Paramagnetic Resonance; Protocol EN 1786; European Committee for Standardization: Brussels, 1997.

(6) Detection of Irradiated Food Containing Crystalline Sugar: Analysis by EPR; Protocol EN 13708; European Committee for Standardization: Brussels, 2001.

(7) Detection of Irradiated Food Containing Cellulose: Analysis by EPR; Protocol EN 1787; European Committee for Standardization: Brussels, 2000.

(8) Desrosiers, M. F. Current status of EPR method to detect irradiated food. *Appl. Radiat. Isot.* **1996**, *47*, 1621–1628.

(9) Raffi, J.; Stevenson, M. H.; Kent, M.; Thiery, J. M.; Belliardo, J. J. European intercomparison on electron spin resonance identification of irradiated food stuffs. *Int. J. Food Sci. Technol.* **1992**, *27*, 111–124.

(10) Schreiber, G. A.; Helle, N.; Schulzki, G. Intercomparisons to evaluate the suitability of gas chromatographic, electron spin resonance spectrometric and thermoluminescence methods to detect irradiated foods in routine control. *Radiat. Phys. Chem.* **1993**, *43*, 391–396.

(11) Schreiber, G. A.; Helle, N.; Schulzki, G. Interlaboratory tests to identify irradiation treatment of various food stuffs via gas chromatographic detection of hydrocarbons, ESR spectroscopy and TL analysis. *Detection Methods for Irradiated Foods—Current Status*; Royal Society of Chemistry: Cambridge, United Kingdom, 1996; pp 98−107.

(12) Yordanov, N. D.; Aleksieva, K.; Mansour, I. Improvement of the EPR detection of irradiated dry plants using microwave saturation and thermal treatment. *Radiat. Phys. Chem.* **2005**, *73*, 55–60.

(13) Yordanov, N. D.; Gancheva, V. A new approach for the extension of the identification period of irradiated cellulose containing foodstuffs by EPR spectroscopy. *Appl. Radiat. Isot.* **2000**, *52*, 195–198.

(14) ASTM Standard, E 1026. Standard Practice for Using Fricke Reference Standard Dosimetry System.

(15) Raffi, J.; Yordanov, N. D.; Chabane, S.; Douifi, L.; Gancheva, V.; Ivanova, S. Detection of irradiated aromatic herbs and spices by electron paramagnetic resonance and thermoluminescence. *Spectrochim. Acta* **2000**, *56A*, 409–416.

(16) Scewartz, H. M., Bolton, J. R., Brog, D. C., Eds. *Biological Applications of Electron Spin Resonance*; Wiley: New York, 1972.

(17) Maloney, D. R.; Tabner, B. J.; Tabner, V. A. An electron spin resonance study of gamma-irradiated fruits. *Radiat. Phys. Chem.* **1992**, *39*, 309–314.

(18) Tabner, B. J.; Tabner, V. A. Electron spin resonance spectra of gamma-irradiated citrus fruits skin, skin components and stalks. *Int. J. Food Sci. Technol.* **1994**, *29*, 143–152.

(19) Ikeya, M.; Baffa, O. F.; Mascarenhas, S. Quality assessment of coffee beans with ESR and gamma- irradiation. *Appl. Radiat. Isot.* **1989**, *40*, 1219–1222.

(20) Raffi, J.; Agnel, J. P. L. Electron spin resonanace identification of irradiated fruits. *Radiat. Phys. Chem.* **1989**, *34*, 891–894.

(21) Bortolin, E.; Butos Griffin, E.; Cruz-Zaragoza, E.; De Coste, V.; Onori, S. Electron paramagnetic resonance detection of Mexican irradiated spices. *Int. J. Food Sci. Technol.* **2006**, *41*, 375–382.

(22) Geoffroy, M.; Tochon-Danguy, H. J. ESR identification of radiation damage in synthetic apatites: a study of the carbon-13 hyperfine coupling. *Calcif. Tissue Int.* **1982**, *34*, S99–S102.

(23) Marchioni, E.; Horvatovich, P.; Charon, H.; Kuntz, F. Detection of irradiated ingredients included in low quantity in non-irradiated food matrix. 1. Extraction and ESR analysis of bones from mechanically recovered poultry meat. *J. Agric. Food Chem.* **2005**, *53*, 3769–3773.

(24) Polovka, M.; Brezova, V.; Simko, P. EPR spectroscopy: A tool to characterize gamma irradiated foods. *J. Food Nutr. Res.* **2007**, *46*, 75–83.

(25) Delincee, H. Detection of food treated with ionizing radiation. *Trends Food Sci. Technol.* **1998**, *9*, 73–82.

Received for review May 23, 2008. Revised manuscript received July 4, 2008. Accepted August 1, 2008.

JF8016089

Provided for non-commercial research and education use.
Not for reproduction, distribution or commercial use.

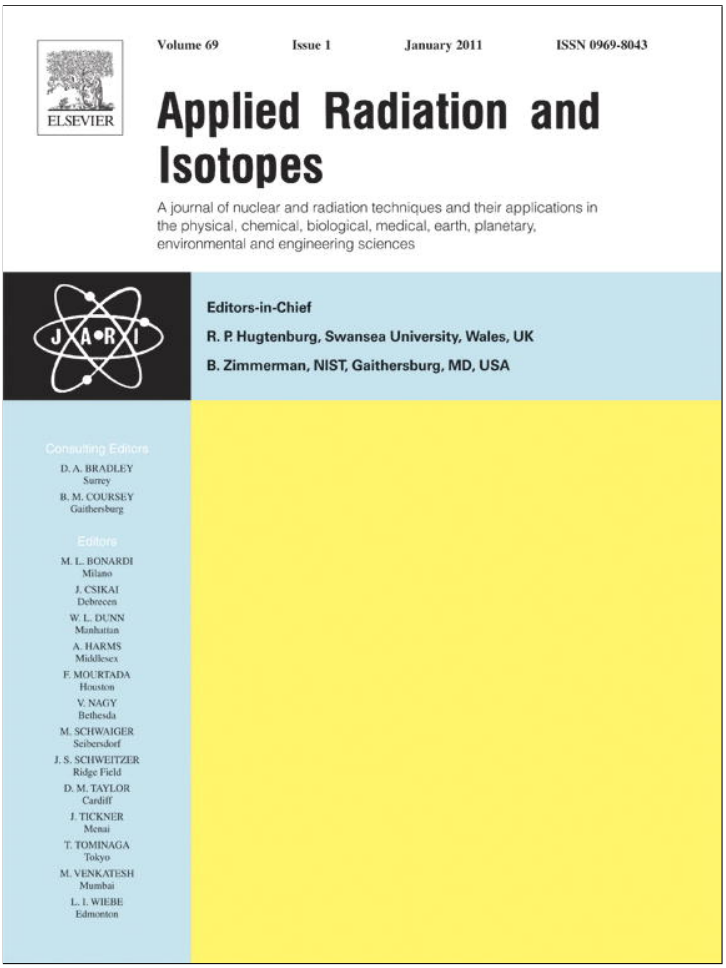

This article appeared in a journal published by Elsevier. The attached copy is furnished to the author for internal non-commercial research and education use, including for instruction at the authors institution and sharing with colleagues.

Other uses, including reproduction and distribution, or selling or licensing copies, or posting to personal, institutional or third party websites are prohibited.

In most cases authors are permitted to post their version of the article (e.g. in Word or Tex form) to their personal website or institutional repository. Authors requiring further information regarding Elsevier's archiving and manuscript policies are encouraged to visit:

http://www.elsevier.com/copyright

Author's personal copy

Applied Radiation and Isotopes 69 (2011) 254–260

Contents lists available at ScienceDirect

Applied Radiation and Isotopes

journal homepage: www.elsevier.com/locate/apradiso

EPR-TL correlation studies on Bi co-doped $CaSO_4$:Dy phosphor

A.K. Bakshi [a], Bhaskar Sanyal [b,*], V.J. Joshi [a], M.K. Bhide [c], V. Natarajan [c], Arun Sharma [b]

[a] Radiological Physics and Advisory Division, Bhabha Atomic Research Centre, Mumbai 400 085, India
[b] Food Technology Division, Bhabha Atomic Research Centre, Mumbai 400 085, India
[c] Radio Chemistry Division, Bhabha Atomic Research Centre, Mumbai 400 085, India

ARTICLE INFO

Article history:
Received 7 May 2010
Received in revised form
8 September 2010
Accepted 20 September 2010

Keywords:
Thermoluminescence (TL)
Electron paramagnetic resonance (EPR)
Phosphor
Food irradiation

ABSTRACT

$CaSO_4$:Dy, $CaSO_4$:(Dy, Bi) and $CaSO_4$:Bi phosphors were prepared through re-crystallization method. Thermoluminescence (TL) characteristics of these phosphor samples were investigated. The radiation induced radical ions formed in these phosphors were investigated using electron paramagnetic resonance (EPR) spectroscopy. The main signals observed in both $CaSO_4$:(Dy, Bi) and $CaSO_4$:Bi were identified as SO_4^- (II), SO_4^- ($\perp$) and SO_3^- (isotropic) with "g" values 2.023, 2.0089 and 2.004, respectively. In order to understand the TL mechanism, $CaSO_4$:(Dy, Bi) phosphor samples were annealed between 100 and 250 °C and their EPR spectra were studied. It was observed that EPR signal intensities reduce drastically in 250 °C annealed phosphor confirming the role of SO_4^- and SO_3^- types of defect centers in the dosimetric peak. The reduction in the TL sensitivity with increase in Bi^{3+} co-dopant in the phosphor samples was correlated with quenching of TL by Bi^{3+} ions rather than the reduction in the concentration of the above defect centers. An effort was also made to use the Bi^{3+} co-doped $CaSO_4$:Dy phosphor for dosimetry of chilled or frozen food irradiation.

© 2010 Elsevier Ltd. All rights reserved.

1. Introduction

$CaSO_4$:Dy phosphor is well known for its high thermoluminescence (TL) sensitivity and stability to environmental variation. This phosphor is used both in personnel and environmental monitoring. In India, this phosphor is used as the detector material in TLD badges used for countrywide personnel monitoring programme for the last 30 years (Vohra et al., 1980).

Energy transfer mechanism from one dopant (sensitizer) to another (luminescent center) is sometimes used to enhance the sensitivity of a phosphor. Earlier several researchers have tried to sensitize this phosphor by co-doping with different rare earth metals (Lin et al., 1996). The most important co-doped phosphor is $CaSO_4$:Dy^{3+}, Ce^{3+}, wherein it is reported that the emission from Ce^{3+} in the region 306–324 nm overlaps with the Dy^{3+} excitation and in turn, it enhances its TL emission. Bi^{3+} is a heavy metal with $7s^2$ electronic configuration and is known for its fluorescence properties (Moncorge et al., 1979; Murata and Mouri, 2007). It is an interesting co-dopant ion, capable of transferring energy to rare earth ions such as Eu^{3+} (Qiang et al., 1983). It displays broad intense ultraviolet absorption bands in the wavelength range 230–330 nm and broad emission band, generally in the region 400–600 nm. However the emission band varies from one host lattice to another. In $CaSO_4$:Bi^{3+}, violet emission around 380 nm ($^3P_0 \rightarrow {}^1S_0$) has been reported at room temperature, while its absorption maximum is around 345 nm (Van der Voort and Blasse, 1992). Therefore, it is of interest to examine the TL characteristics of Bi and Dy co-doped $CaSO_4$ phosphor. In the present study, we have reported the TL and photoluminescence (PL) properties of Bi^{3+} co-doped $CaSO_4$:Dy in different proportions. Further, we have reported the results of electron paramagnetic resonance (EPR) studies on gamma irradiated $CaSO_4$:Bi^{3+} and $CaSO_4$:(Dy^{3+}, Bi^{3+}) and tried to correlate EPR results with the observed TL characteristics for possible explanation. Measurement of high radiation dose using TL phosphor has several advantages. These phosphors can be used for dose measurement during food irradiation using simple read out methods (Lewandoski and Mathur, 1996; Ramos-Bernal et al., 2002). A large number of food materials namely perishable foods such as fish, meat and shrimps are permitted for commercial radiation processing in the dose range of 3.0–4.0 kGy. In view of this, the efficacy of the Bi^{3+} co-doped $CaSO_4$:Dy phosphor to measure the food irradiation dose in the range of 1.0–5.0 kGy was also studied.

2. Experimental

2.1. Preparation of the phosphor

$CaSO_4$:Bi^{3+}, $CaSO_4$:(Dy^{3+}, Bi^{3+}) and $CaSO_4$:Dy^{3+} phosphors were prepared by recrytallisation method following the recipe of

* Corresponding author. Tel.: +91 22 25592533.
E-mail addresses: bhaskar_sanyal@rediffmail.com, sanyal@barc.gov.in (B. Sanyal).

0969-8043/$ - see front matter © 2010 Elsevier Ltd. All rights reserved.
doi:10.1016/j.apradiso.2010.09.014

Author's personal copy

Yamahashita et al. (1968). The raw materials, $CaSO_4{:}2H_2O$, Bi_2O_3 and Dy_2O_3, were used in sulphuric acid medium. The concentration of Dy was 0.05 mol%, while the concentrations of Bi in $CaSO_4$:(Dy, Bi) sample were 0.05, 0.2 and 0.5 mol%. After the preparation, phosphors were washed with de-ionized water and dried at 100 °C. The phosphors were further annealed at 700 °C for 2 h in presence of N_2 in a furnace capable to attain a maximum temperature of 1100 °C.

2.2. TL measurements

Phosphor samples were irradiated to a dose of 1 Gy of Cobalt 60 gamma from teletherapy machine and the TL glow curves were recorded 24 h after irradiation on a research reader having a photo multiplier tube (PMT) with S-11 response supplied by M/s Nucleonix, Hyderabad. The glow curve was recorded at 40–300 °C with a heating rate of about 5 °C/s. Fluorescence spectra were recorded on a Spectrophotometer model F-4500 procured from Hitachi, Japan.

2.3. EPR spectroscopy

EPR study was carried out using an EMX model EPR spectrometer (BRUKER, Germany) with a microwave frequency of 9.42 GHz. EPR spectra were obtained at liquid nitrogen temperature (−196 °C) and at room temperature (25 °C). The samples were irradiated at 2.0 kGy gamma dose before recording their EPR spectra. Recording parameters were 3382 G central field, 1.0 G modulation amplitude and 10.2 ms time constant with microwave power attenuation of 15 dB. EPR sensitivity was measured

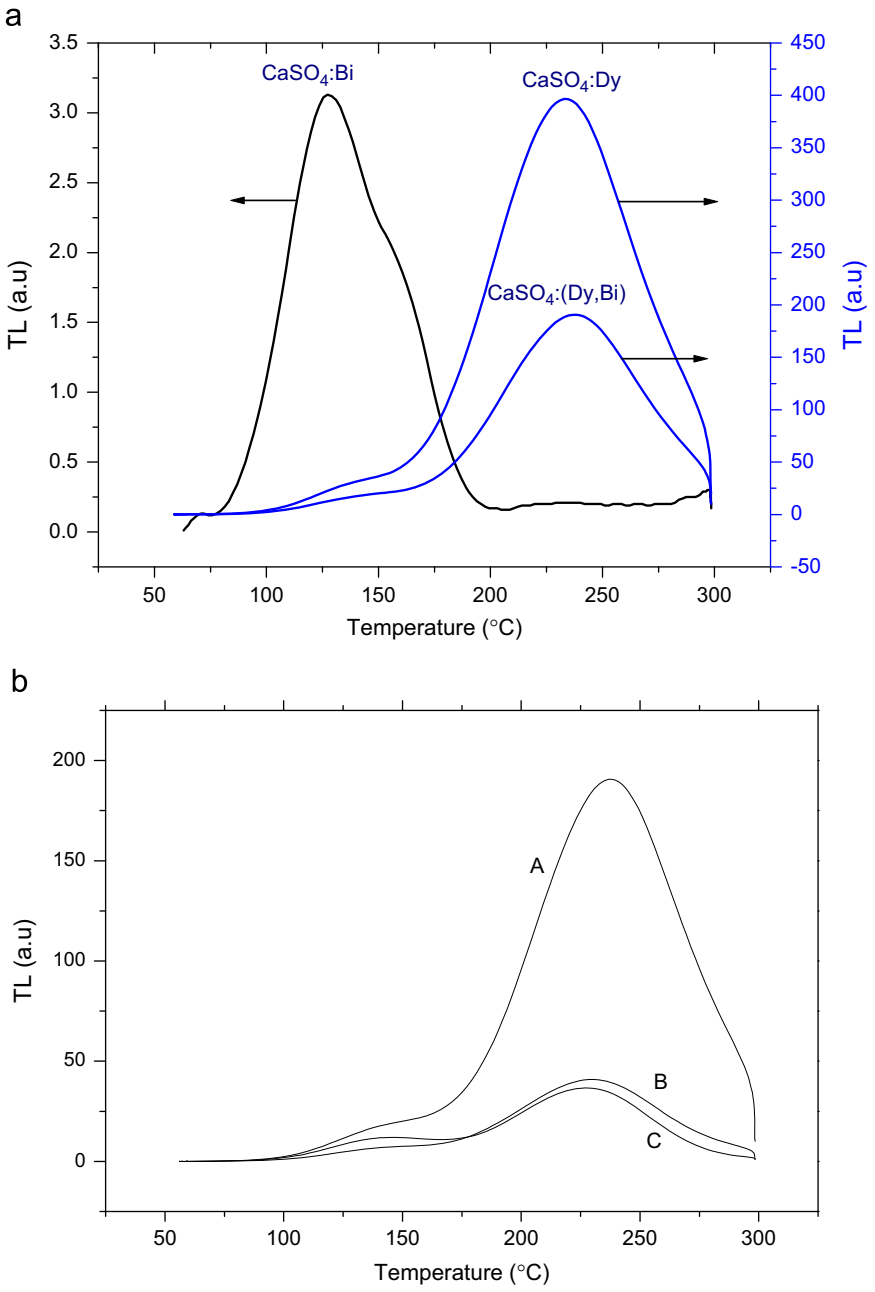

Fig. 1. (a) TL glow curves of $CaSO_4$:Dy (0.05 mol%), $CaSO_4$:Dy (0.05) Bi (0.05 mol%) and $CaSO_4$:Bi (0.05 mol%). The right hand *Y* axis is used to specify the glow peaks of $CaSO_4$:Dy and $CaSO_4$:(Dy, Bi). (b) Glow curves of $CaSO_4$:Dy, Bi with different concentrations of Bi; (A) Bi: 0.05 mol%, (B) Bi: 0.2 mol% and (C) Bi: 0.5 mol%.

Author's personal copy

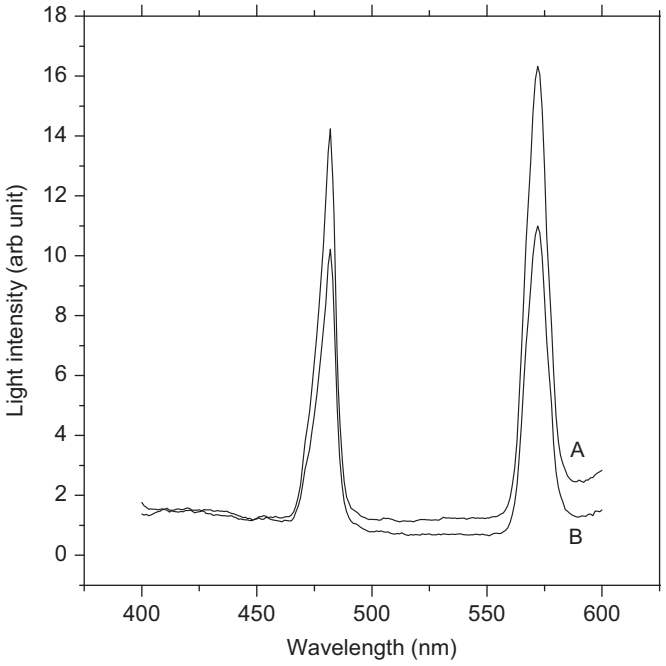

Fig. 2. Flourescence spectrum: (a) $CaSO_4$:Dy and (b) $CaSO_4$:(Dy, Bi).

by peak to peak amplitude (ASTM standard, 51607:2004 E; Sanyal et al., 2009; Sharaf and Hassan, 2004). 2,2-diphenyl-1-picrylhydrazyl (DPPH) with *g* value 2.0036 was taken as reference for the EPR spectra.

2.4. Food irradiation dosimetry

For the purpose of high dose dosimetry $CaSO_4$:(Dy, Bi) (Bi concentration 0.2 and 0.5 mol%) was chosen due to its lower TL sensitivity. The phosphor in powder form was irradiated in a glass tube inside a Dewar flask with Cobalt 60 gamma radiation in a gamma chamber (GC 5000, Board of Radiation Isotope Technology, India, dose rate 6.5 kGy/h). The dose was calibrated with a Fricke reference standard dosimeter (ASTM Standard, E 1026, 2005). The phosphors were irradiated in the dose range of 1–5 kGy, which is recommended for commercial irradiation of chilled or frozen food for preservation. The irradiation response was analyzed by a TL reader as stated in the earlier paragraph. Neutral density filters (Melles Griot BV, Netherland) of optical densities 3.0 and transmittance 0.01% were used to avoid saturation of PMT. The peak height is vertical length of the peak tip from the temperature axis measured directly from the glow curve (Bakshi et al., 2008; Mathur et al., 1999). Control and irradiated phosphors were stored in dark place at normal laboratory condition, when they were not in use. Entire study

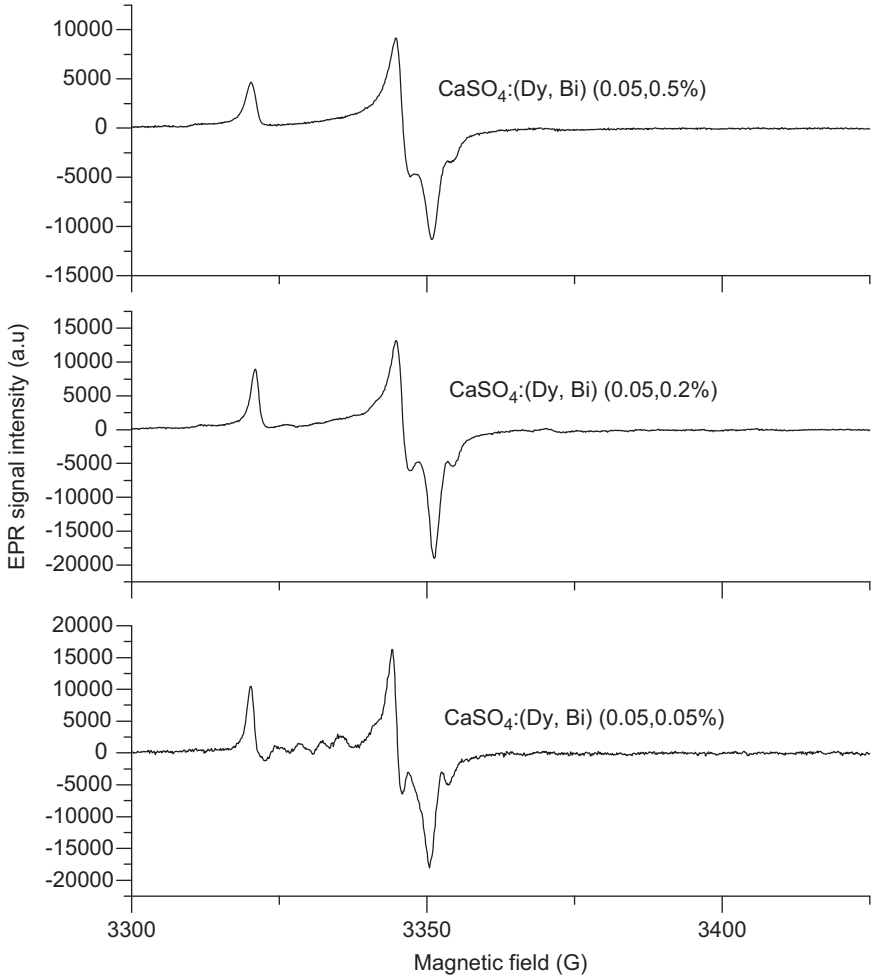

Fig. 3. EPR spectra of $CaSO_4$:(Dy, Bi) at −196 °C with a fixed concentration of Dy (0.05 mol%) and different concentrations of Bi such as 0.05, 0.2 and 0.5 mol%.

Author's personal copy

was carried out using the same batch of the phosphor to avoid inter-batch uncertainty.

3. Results and discussion

3.1. TL studies

Fig. 1a shows the TL glow curve of $CaSO_4$:Dy, $CaSO_4$:(Dy, Bi) and $CaSO_4$:Bi phosphors, which had undergone annealing treatment in N_2 atmosphere at 700 °C for 2 h. As such, there is no change in the TL glow curve (peak temperature and shape) of $CaSO_4$:Dy and $CaSO_4$:(Dy, Bi). Glow curve consists of a dosimetric peak at around 236 °C with a lower temperature satellite peak at around 140 °C for both $CaSO_4$:Dy and $CaSO_4$:(Dy, Bi) (0.05 mol%) phosphors. It is clear from Fig. 1a that the TL sensitivity reduced in the presence of Bi co-dopant for $CaSO_4$:Dy phosphor. The TL intensity of $CaSO_4$:Bi was significantly lower than that of $CaSO_4$:Dy as well as $CaSO_4$:(Dy, Bi) phosphors. Its glow curve shape is also different from the other two phosphors. The glow curve has a prominent peak at 130 °C and a hump at around 160 °C. Fig. 1b shows the glow curve of $CaSO_4$:(Dy, Bi) with varying concentration of Bi. It can be seen that with increase in concentration of Bi, the peak intensities have reduced and peak temperature of the dosimetric peak shifted towards lower temperature side. This indicated that with increase in Bi concentration either Bi^{3+} acts as a quencher of dosimetric TL peak or the concentration of defect center related to dosimetric peak gets reduced. In case of $CaSO_4$:Bi, it seems Bi is not creating any additional defect centers. The glow curve is characteristic of host lattice (Manam and Das, 2008). $CaSO_4$:Dy and CaSO4:(Dy, Bi) with Bi concentration 0.05, 0.2 and 0.5 mol% were subjected to thermal treatment at 700 °C for 2 h in the inert atmosphere of nitrogen to study the relative TL sensitivity of $CaSO_4$:(Dy, Bi) with varying concentration of Bi with respect to that of $CaSO_4$:Dy phosphor. The relative sensitivity of $CaSO_4$:(Dy, Bi) with Bi concentration 0.05% exhibited maximum sensitivity of 0.72 with respect to $CaSO_4$:Dy (considering sensitivity 1). Phosphors having Bi concentrations of 0.2 and 0.5 mol% revealed relative sensitivities of 0.26 and 0.13, respectively.

The fluorescence spectra of both $CaSO_4$:Dy and $CaSO_4$:(Dy, Bi) phosphors are shown in Fig. 2. It shows that fluorescence

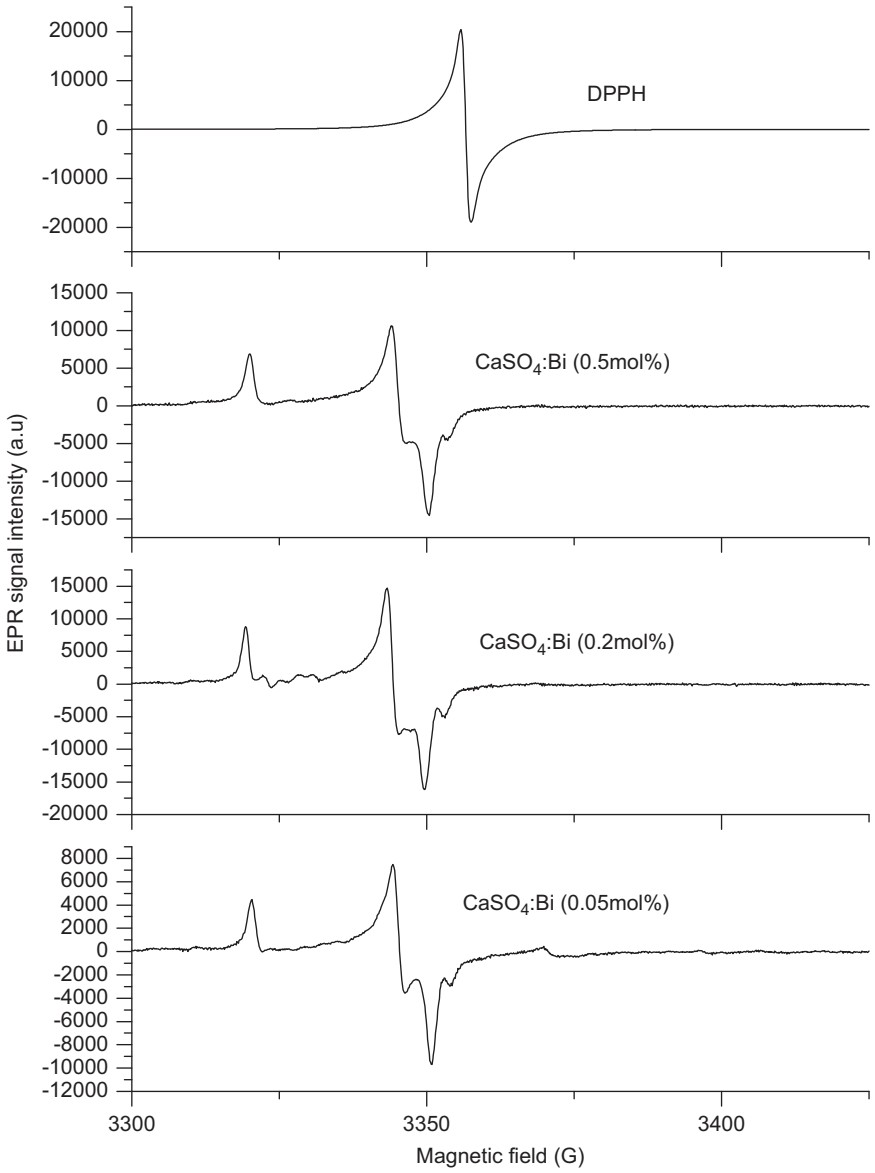

Fig. 4. EPR spectra of $CaSO_4$:Bi at −196 °C with different concentrations of Bi such as 0.05, 0.2, 0.5 mol% along with DPPH.

Author's personal copy

emission peaks occur at exactly same wavelengths (473 and 582 nm) for $CaSO_4$:(Dy, Bi) and $CaSO_4$:Dy. However the intensities of the peaks in the former case are less than those of $CaSO_4$:Dy, which is in the same line as observed in TL.

3.2. EPR studies

Fig. 3 shows the EPR spectra of $CaSO_4$:(Dy, Bi) with different concentrations of Bi and irradiated to a gamma dose of 1.0 kGy. Three prominent peaks were observed with g values 2.023, 2.0089 and 2.004. Fig. 4 shows the ESR spectra of $CaSO_4$:Bi phosphor samples with different concentration of Bi. In this case also, three peaks with g values 2.024, 2.009 and 2.004 were observed. On the basis of earlier reports (Gupta et al., 1974; Natarajan et al., 1988; Mauricio et al., 1996), the three lines were identified as follows: line 1: SO_4^- ($\parallel$), line 2: SO_4^- ($\perp$) and line 3: SO_3^- (isotropic). The g values of the signals compared well with those reported in the literature. The concentration of these radical ions [SO_4^- (II) and SO_4^- ($\perp$)] decreased with increase in concentration of Bi (Fig. 3). This indicates that the lowering of TL sensitivity (dosimetric peak) with increase in Bi concentration is attributable to quenching of TL by Bi^{3+} ions rather than reduction in defect concentration.

In order to understand the TL mechanism, $CaSO_4$:(Dy, Bi) phosphor samples were subjected to post-irradiation annealing from 150 to 250 °C for 5 min in air oven and their EPR spectra were recorded. Fig. 5a–c shows the EPR spectra of $CaSO_4$:(Dy, Bi) samples annealed between 150 and 250 °C. EPR signals from

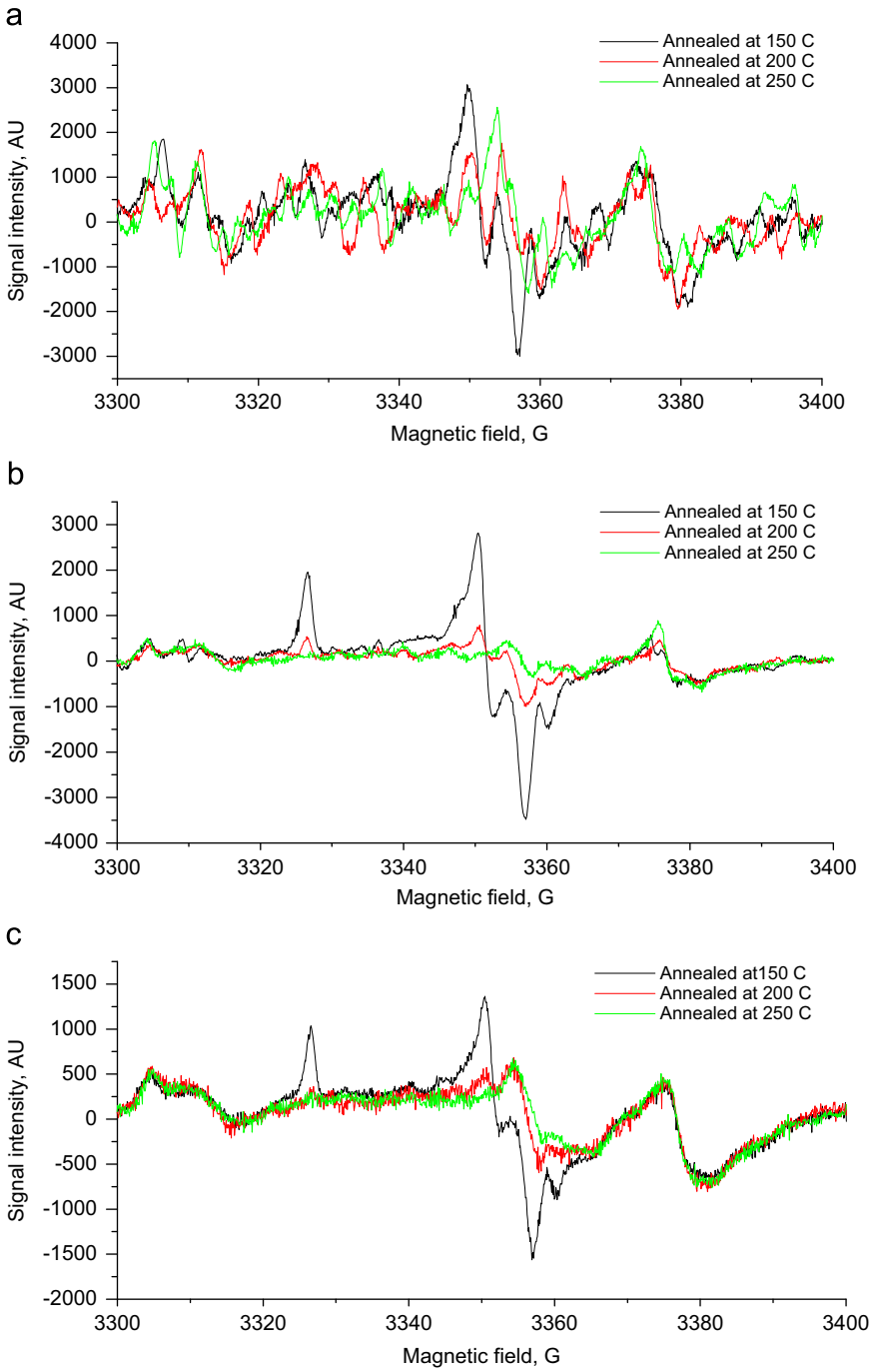

Fig. 5. EPR spectra of $CaSO_4$:(Dy, Bi) undergone annealing at different temperatures: (a) Bi—0.05 mol%, (b) Bi—0.2 mol% and (c) Bi—0.5 mol%.

Author's personal copy

traces of Mn^{2+} were also seen in these spectra around the signals from SO_4^- and SO_3^- ions. Mn^{2+} is an unintentional trace impurity from the starting material used for the preparation of the phosphor. The changes in the EPR line intensities of the radical ions observed in $CaSO_4$:(Dy, Bi) with increase in annealing temperature are depicted in Fig. 6a–c. It may be noted that with increase in annealing temperature, the intensities of both SO_4^- and SO_3^- signals are reduced. The temperature of 250 °C was chosen, considering the peak temperature of the dosimetric peak of $CaSO_4$:(Dy, Bi). From these figures, it is evident that EPR line intensities of SO_4^- ions reduced drastically in 250 °C annealed phosphor as compared to those in un-annealed samples.

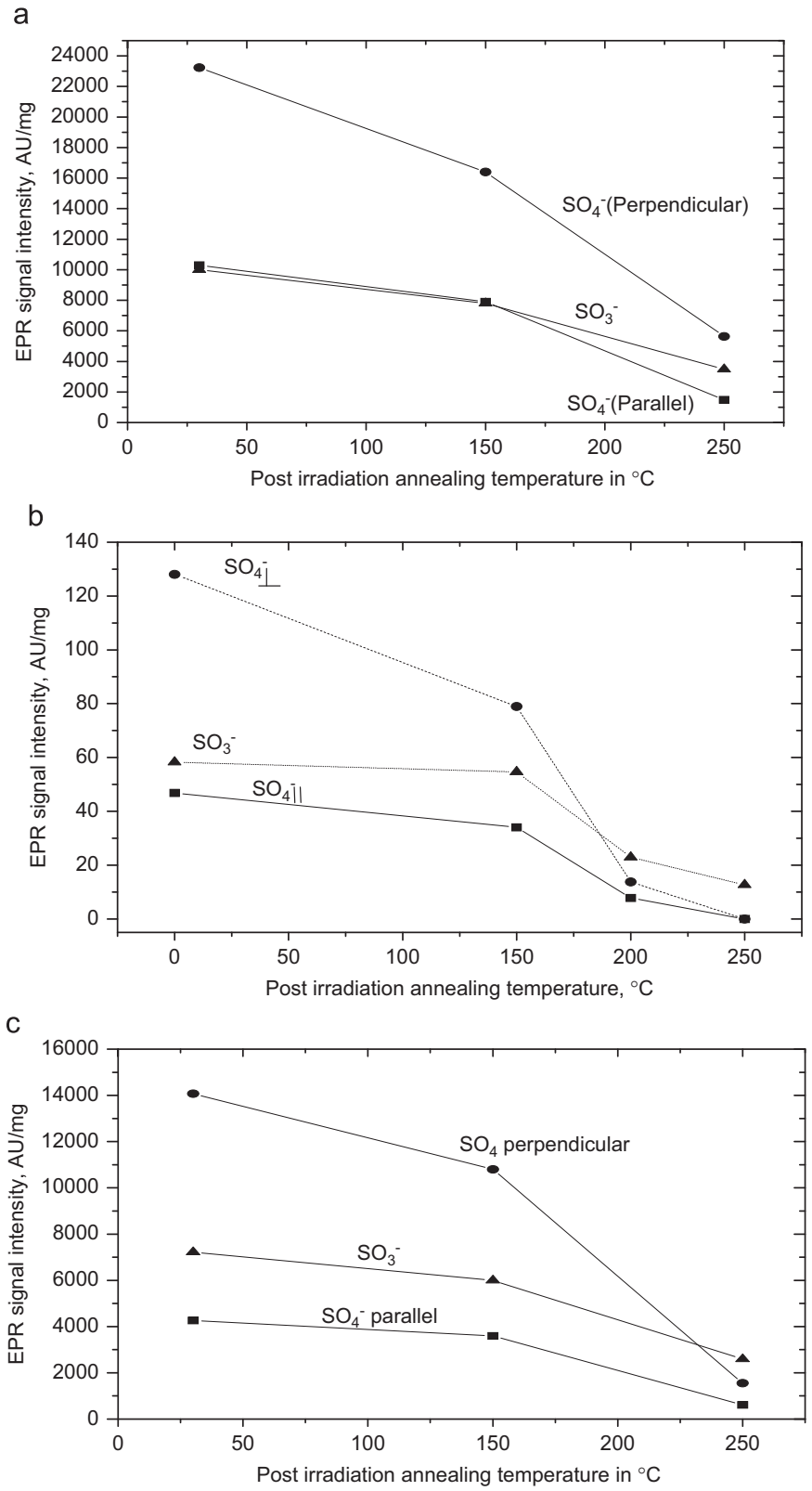

Fig. 6. Variation in peak intensities of sulphoxy radical ions with temperature for $CaSO_4$:(Dy, Bi): (a) Bi—0.05 mol%, (b) Bi—0.2 mol% and (c) Bi—0.5 mol%.

Author's personal copy

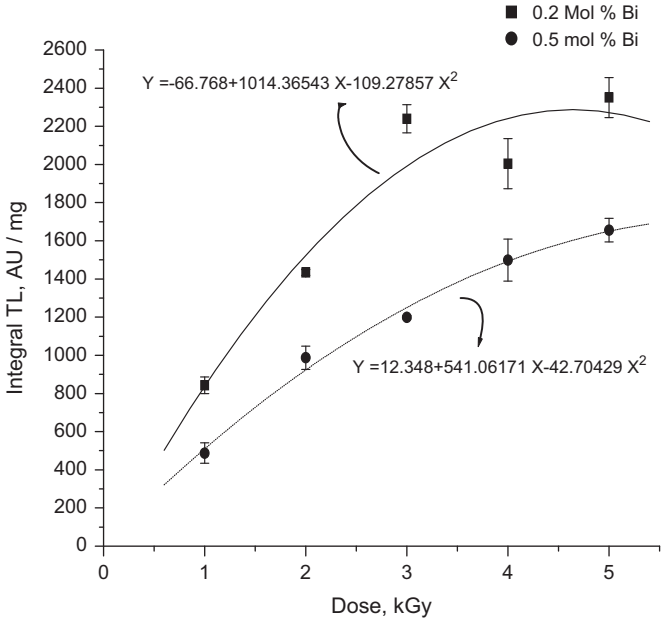

Fig. 7. Dose response of $CaSO_4$:(Dy, Bi) with Bi concentrations 0.2 and 0.5 mol% in the dose range of 1–5 kGy.

These results confirmed the role of sulphoxy radical ions, especially SO_4^- ion, in the dosimetric peak.

3.3. Food irradiation dose measurements

Though different high dose measurement techniques such as Alanine-EPR dosimetry system (ASTM Standard, ISO/ASTM 51607:2004 E), ceric-cerous sulphate dosimetry system (ASTM Standard, ISO/ASTM 51205 2002 E) are available, they are either expensive and cumbersome or not suitable for low temperature dosimetry, which is required for dosimetry of perishable food commodities like chilled or frozen foods. In this context, thermoluminescence dosimeters are useful as they are cheaper with simple method of measurement. The present investigation showed that the TL sensitivity of $CaSO_4$:(Dy, Bi) phosphor reduced with increase in concentration of Bi^{3+} ion. This property of the phosphor was exploited in our present study of measurement of food irradiation dose. For the purpose of measurement of high dose, $CaSO_4$:(Dy, Bi) phosphors (Bi concentration 0.2 and 0.5 mol%) were chosen due to their lower TL sensitivity. The phosphors were irradiated using Cobalt 60 gamma irradiator in the dose range of 1–5 kGy, which is recommended to be used for irradiation of chilled or frozen food.

Fig. 7 shows the dose response of $CaSO_4$:(Dy, Bi) phosphor samples in the dose range of 1–5 kGy. The dose response of the phosphor with Bi (0.2 mol%) did not reveal well defined relation with increasing radiation dose. However, the dose response of the $CaSO_4$:(Dy, Bi) (0.5 mol%) was well fitted using a second order polynomial ($R^2=0.99129$). The defined response of thermoluminescence characteristics of $CaSO_4$:Dy phosphor with increase in radiation dose in the range of radiation processing of food has already been reported in literature (Mathur et al., 1999). The response of $CaSO_4$:(Dy, Bi) (0.5 mol%) with increase in dose exhibited saturation beyond 3 kGy. However, the preliminary study revealed a clear trend in the dose response in the higher dose range. Therefore adequately calibrated $CaSO_4$:Dy phosphors co-doped with 0.5 mol% Bi could be used as a potential dosimeter for food irradiation dosimetry.

4. Conclusions

EPR studies on gamma irradiated $CaSO_4$:(Dy, Bi) and $CaSO_4$:Bi phosphor samples revealed the presence of SO_4^- and SO_3^- defect centers. The reduction in TL sensitivity and glow curve structure with increase in Bi concentration in $CaSO_4$:(Bi, Dy) is attributed to the quenching action of Bi^{3+} ions on TL rather than the change in concentration of SO_4^- and SO_3^- related defect centers. The role of SO_4^- and SO_3^- ions was identified by analyzing the EPR of $CaSO_4$:(Dy, Bi) samples subjected to post-irradiation annealing up to 250 °C. The study also suggested that $CaSO_4$:(Dy, Bi) (0.5 mol%) can be used as a suitable dosimeter in food irradiation dosimetry.

Acknowledgements

The authors are thankful to Dr. Y.S. Mayya, Head, RPAD, BARC, Dr. M.P. Chougaonkar, Head, S&QAS, RPAD, BARC, and Mr. H.S. Kushwaha, Director HS&E Group, BARC, for their encouragement in the work.

References

ASTM Standard, E 1026, 2005. Standard practice for using Fricke reference standard dosimetry system.
ASTM Standard, ISO/ASTM 51607,2004 E. Standard practice of use of an alanine-EPR dosimetry system.
ASTM Standard, ISO/ASTM 51205,2002 (E). Standard practice for use of a ceric-cerous sulphate dosimetry system.
Bakshi, A.K., Patwe, S.J., Bhide, M.K., Sanyal, B., Natarajan, V., Tyagi, A.K., Kher, R.K., 2008. Thermoluminescence, ESR and X-ray diffraction studies of $CaSO_4$:Dy phosphor subjected to post preparation high temperature thermal treatment. J. Phys. D: Appl. Phys 41 (025402), 8.
Gupta, N.M., Luthra, J.M., Shankar, J., 1974. Trapping and emission centres in thermoluminescent barium sulphate. Radiat. Eff 21, 151–156.
Lewandoski, A.C., Mathur, V.K., 1996. High dose and phototransferred thermoluminescence in $CaSO_4$, $CaSO_4$:Dy and $CaSO_4$:Tm. Radiat. Prot. Dosim. 66, 213–216.
Lin, J., Su, Q., Wang, S., Zhang, H., 1996. Influence of crystal structure on the luminescence properties of bismuth (III), europium (III) and dysprosium (III) in Y_2SiO. J. Mater. Chem. 6, 265–269.
Manam, J., Das, S., 2008. Thermally stimulated luminescence studies of undoped, Cu- and Mn-doped $CaSO_4$ compounds. Radiat. Eff. Defects Solids 163, 955–965.
Mathur, V.K., Lewandowski, A.C., Guardala, N.A., Price, J.L., 1999. High dose measurements using thermoluminescence of $CaSO_4$:Dy. Radiat. Meas. 30, 735–738.
Mauricio, C.L.P., Bortolin, E., Onori., S., 1996. ESR study of $CaSO_4$:Dy TLD. Radiat. Meas. 26, 639–644.
Moncorge, R., Boulon, G., Denis, J.P., 1979. Fluorescence properties of bismuth doped $LaPO_4$. J. Phys. C: Solid State Phys 12, 1165–1171.
Murata, T., Mouri, T., 2007. Matrix effect on absorption and infrared fluorescence properties of Bi ions in oxide glasses. J. Non-Cryst. Solids 353, 2403–2407.
Natarajan, V., Dalvi, A.G.I., Sastry, M.D., 1988. Trap level spectroscopy of actinide-doped alkaline-earth sulphates: II. $CaSO_4$: ^{241}Am. J. Phys. C: Solid State Phys. 21, 5913–5922.
Qiang, Su., Barthou, C., Denis, J.P., Pelle, F., Blanzat, B., 1983. Luminescence and energy transfer in Y_2O_3 CO-doped with Bi^{3+} and Eu^3. J. Lumin 28, 1–11.
Ramos-Bernal, S., Cruz, E., Negron-Mendoza, A., Bustos, E., 2002. Irradiation dose determination below room temperature. Radiat. Phys. Chem. 63, 813–815.
Sanyal, B., Chawla, S.P., Sharma, A., 2009. An improved method to identify irradiated rice by EPR spectroscopy and thermoluminescence measurements. Food Chem 116, 526–534.
Sharaf, M.A., Hassan, G.M., 2004. Radiation induced radical in barium sulphate for ESR dosimetry: a preliminary study. Nucl. Instrum. Methods Phys. Res. B 225, 521–527.
Van der Voort, D., Blasse, G., 1992. Luminescence of $CaSO_4$:Bi^{3+}: a small-offset. J. Solid State Chem. 99 (2), 404–408.
Vohra, K.G., Bhatt, R.C., Chandra, Bhuwan, Pradhan, A.S., Lakshmanan, A.R., Sastry, S.S., 1980. A personal dosimeter TLD badge based on $CaSO_4$:Dy teflon TLD discs. Health Phys. 38, 193–197.
Yamahashita, T., Nada, N., Omishi, H., Katimura, S., 1968. Calcium sulphate phosphor activated by rare earth. In: Proceedings of the Second International Conference on Luminescence Dosimetry, Gatlinburg, NTIS; Springfield, VA, CONF 680920.